THE UNIVERSITY *of* EDINBURGH

Fruit softening: demonstration of *in-vivo* pectate lyase and rhamnogalacturonan lyase action

Thurayya Zahran Sulaiman Al Hinai

Doctor of Philosophy

The University of Edinburgh
School of Biological Sciences

2022

Declaration

This thesis has been composed by myself and the work, of which it is a record, has been carried out by myself. All sources of information have been specifically acknowledged by means of a reference.

Thurayya Zahran Sulaiman Al Hinai

Acknowledgments

The PhD journey was not easy, but I managed to succeed with the strength granted by Allah, the faith in my heart and the support I got from my family, friends and the team I worked with (Alhamdulellah).

Thanks to the Ministry of Higher Education, Oman, for sponsoring my studies and thanks to everyone at the Omani Embassy, London, and the University of Technology and Applied Sciences, Oman, for their support.

I would like to express my gratitude to my supervisor, Prof. Stephen C. Fry, for his guidance and endless support through the years. I would like to thank the ECWG members (previous and current) for their support and the nice times we had working together in the lab. Thanks to my thesis committee (Prof. Andrew Hudson, Dr Nakayama Naomi and Prof. Justin Goodrich) for their feedback and support. Thanks to Dr Sophie Haupt for the highly appreciated advices and for welcoming me in her office every time I needed to do my prayers. Thanks to the collaborators, Dr Sara Posé and Prof. Tatyana Gorshkova for the productive collaborations, valuable input to my project and sending their samples for me to process. Thanks to Dr Logan Mackay for helping with mass spectrometry and to Prof. Ian Sadler and Lorna Murray for helping with NMR.

Thanks to Iman Al Bahri for collecting and keeping my Omani date and mango samples. Thanks to Dr Khalid Al Shuaili for offering me his lab (at the Directorate General of Agricultural and Livestock Research, Oman) to prepare my samples before transporting them to Edinburgh.

Special thanks to my husband, my mother and the rest of my family for their continuous support throughout my journey.

Thanks to the lovely friends who made my life much easier in Edinburgh. Thanks for the time we spent together, hiking, walking, shopping, the long nights of talking and all the sleepovers we had over the years.

Last, but not least, thanks to my lovely little children (Mohammed and Dana) who have joined my journey mostly in Edinburgh and sometimes in Oman. “One day when you grow-up, I hope you will be proud of your mom.”

List of abbreviations

$^{\bullet}OH$: hydroxyl radical

$AgNO_3$: silver nitrate

AGPs: arabinogalactan proteins

AIR: alcohol-insoluble residue

Ara: L-arabinose

BAW: butan-1-ol/acetic acid/water

Ca^{2+}: calcium ions

$CaCl_2$: calcium chloride

CAPS

COSY: correlation spectroscopy

DAMPs: damage-associated molecular patterns

EAW: ethyl acetate/acetic acid/water

EPAW: ethyl acetate/pyridine/acetic acid/water

EPG: endo-polygalacturonase

ESI FT-ICR: Electrospray ionization coupled to fourier transform ion cyclotron resonance

EtOH: ethanol

Exo-PG: exo-polygalacturonase

FT-ICR: Fourier-transform ion cyclotron resonance

Gal: L-galactose

GalA: L-galacturonic acid

Glc: D-glucose

H_2SO_4: sulphuric acid

H_3PO_4: phosphoric acid

HG: homogalacturonan

HMBC: heteronuclear multiple bond correlation

HOAc: acetic acid

HVPE: high-voltage paper electrophoresis

IP: isoprimeverose

Man: D-mannose

MS: mass spectrometry

Na^+: sodium ion

Na_2CO_3: sodium carbonate

$Na_2S_2O_3$: sodium thiosulfate

$NaAsO_2$: sodium arsenite

NaAc: sodium acetate

$NaBH_4$: sodium borohydride

$NaIO_4$: sodium periodate

NaOH: sodium hydroxide

NH_4OH: ammonium hydroxide

NMR: nuclear magnetic resonance

NOESY: nuclear overhauser effect spectroscopy

PC: paper chromatography

PL: pectate lyase

PME: pectin methylesterases

PNWA: propan-1-ol/nitromethane/water/acetic acid

PRRs: pattern recognition receptors

PyAW: pyridine/acetic acid/water

Pyr: pyridine

RG-I: rhamnogalacturonan-I

RG-II: rhamnogalacturonan-II

RGL: rhamnogalacturonan lyase

Rha: L-rhamnose

ROS: reactive oxygen species

TBA: Thiobarbituric acid

TFA: trifluoroacetic acid

TLC: thin-layer chromatography

XEH: xyloglucan endohydrolase

XET: xyloglucan endo-transglucosylase

XGA: xylogalacturonan

XTHs: xyloglucan endotransglucosylase/hydrolases

α-AFase: α-L-arabinofuranosidase

β-Gase: β-galactosidase

ΔUA: 4-deoxy-β-L-*threo*-hex-4-enopyranuronose residue

Abstract

The programmed softening that occurs during fruit development requires scission of wall and/or middle lamella polysaccharides, especially pectin. Proposed mechanisms include the action of cell-wall enzymes [e.g. pectate lyase (PL), endo-polygalacturonase (EPG) or rhamnogalacturonan-I lyase (RGL)] or hydroxyl radicals (˙OH). Sometimes PL, EPG, RGL and ˙OH may all occur simultaneously, and it may be difficult to distinguish which play(s) the predominant role *in vivo*.

Recent evidence has highlighted a role for PL and RGL gene expression in softening. In addition, PL and RGL activities have been reported in certain fruit extracts when assayed *in vitro*. However, no evidence had demonstrated the *in-vivo* action of PL or RGL. This project focused on finding evidence for PL and RGL *in-vivo* action in several softening fruits at three ripening stages (unripe, turning and ripe) by detecting their diagnostic reaction-products ('fingerprints') during fruit development.

PL cleaves the non-methylesterified homogalacturonan domains of pectin by an elimination reaction, leaving a 4-deoxy-β-L-*threo*-hex-4-enopyranuronose residue (ΔUA) residue as the newly formed non-reducing end. This product distinguishes PL action from EPG action, which generates a simple galacturonic acid (GalA) residue as the new non-reducing terminus. RGL cleaves the α-(1,4) glycosidic bond between rhamnose and galacturonic acid of the RG-I backbone by β-elimination, producing a new rhamnose reducing end and ΔUA as the new non-reducing end. To detect the ΔUA termini (in both PL and RGL products) in cell walls of softening fruits, cell walls (in the form of alcohol-insoluble residue; AIR) were digested with Driselase to release the smallest possible products, which were then resolved by high-voltage paper electrophoresis to reveal any products with a ΔUA residue (very low pK_a) and then by thin-layer chromatography to resolve PL from RGL products. In addition to large

amounts of free Driselase-generated GalA, which quantified the total pectin, appreciable amounts of both PL (ΔUA–GalA) and RGL (ΔUA–Rha-GalA-Rha) fingerprints were detected in almost all the tested fruits including date, strawberry and mango at the three ripening stages. The ΔUA–GalA:GalA ratio from ripe date AIR was ~1:20, mol/mol, indicating approximately one PL-cleaving event per 20 GalA units of homogalacturonan. This is the first biochemical evidence of PL and RGL being in action in healthy fruits. The methodology clearly distinguishes the PL product from the RGL product and in future can be used to investigate other plant tissues as well.

Lay summary

Fruits undergo different chemical changes during ripening including changes in color, odour and texture from hard, green, acidic tissue to soft, attractive, fragranced and tasty fruit. During the process of ripening, the cell wall, which is responsible for the cell's rigidity, gets disassembled reducing the firmness of the fruit. This can be accompanied by cell growth like in grape and strawberry or with no growth like in peach and tomato.

The plant cell wall is a complex structure made of different polysaccharides (mainly cellulose, hemicellulose and pectin), proteins, and aromatic and aliphatic compounds that surround the plant cells. It determines the cell size and shape. It is essential for the cells' survival and has limited mobility which helps plants to withstand different harsh environmental conditions and acts as a defence against pathogens and herbivores.

There are different mechanisms that lead to fruit softening including action of some enzymes that catalyze the degradation of the fruit cell walls. This project demonstrates the role of two cell wall-degrading enzymes known as pectate lyase and rhamnogalacturonan lyase. These two enzymes have different substrates to degrade and they both leave a unique fingerprint in their action products, which I have developed methods to detect and quantify. Here I demonstrate the first evidence of the action of these two enzymes by detecting their unique fingerprints confirming their contribution in fruit softening.

Understanding the process of fruit softening can help in modifying fruit shelf-life after harvesting. Some fruits, such as tomato and strawberry, have short shelf-life and that have always been an economical challenge. Modification of cell wall properties (by genetic modification of cell wall-degrading enzymes) can prolong the fruit shelf-life, reduce the waste and give a better understanding of fruit ripening.

List of figures

List of tables

Table of contents

Results

Chapter 1

Introduction

1.1. Fruit development

Fruits are plant organs that originate from the plant's reproductive organs, the flowers. Plants produce fruits as a way of protection and distribution for their seeds. Fruits that are developed from the ovary-walls (Fig. 1.1) are regarded as true fruits, such as plums and cherries. Non-ovarian floral parts including receptacles, sepals, petals and stamens can also be involved in fruit development producing what are regarded as false or accessory fruits, such as strawberries and apples.

In true fruits, a single ovary or a fusion of multiple ovaries on one flower gives rise to what is regarded as a simple fruit, the most common kind. Fusion of separate carpels gives rise to aggregate fruits, such as raspberries. Individual fruits can also fuse during development giving rise to what are called multiple fruits, such as figs and pineapples (Mauseth 2009).

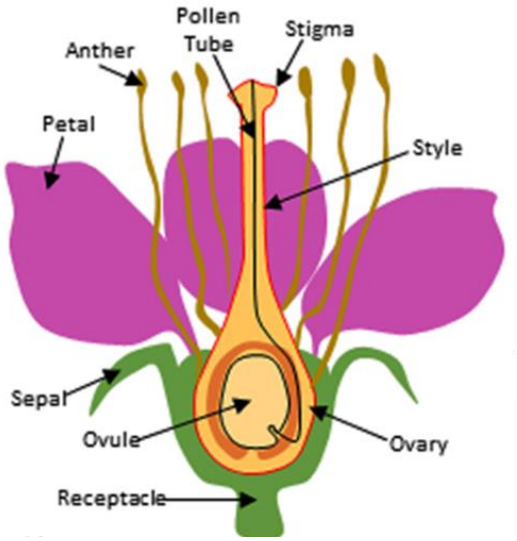

Fig. 1.1. Basic structure of a flower. A drawing of a longitudinal section through the ovary showing the different floral parts. Adapted from Dardick and Callahan (2014).

Fruits usually have three distinct layers throughout their development: exocarp, mesocarp and endocarp. The exocarp is the outer layer, the skin or peel. In true fleshy fruits, the mesocarp is the middle, edible layer or flesh. The endocarp is the innermost layer that can be fleshy like in watermelon, or hard (known as drupes) like in peach, mango, date and plum. The fruit fleshiness and thickness varies with fruit type and often one or two of their layers are absent (Mauseth 2009; Dardick and Callahan 2014).

1.1.1. Fruit Ripening

The fruits undergo different chemical and physical changes during ripening including changes in colour, odour and texture from hard, green, acidic tissue to soft, attractive, fragranced and tasty fruit (Seymour and Gross 1996; Fig. 1.2). This can be accompanied by cell growth like in grape and strawberry or with no continuing growth like in peach and tomato.

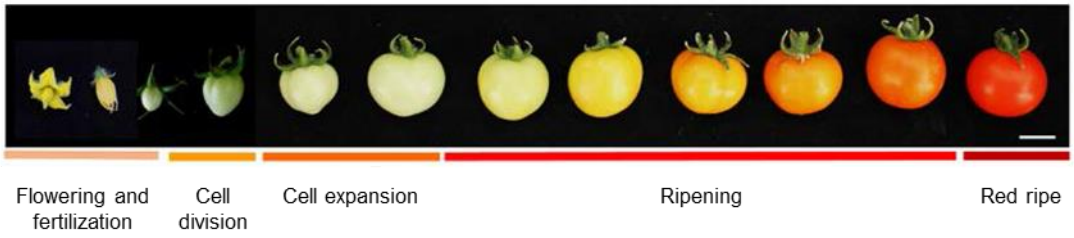

Fig. 1.2. Overview of tomato fruit development. The different stages of the tomato fruit development from flower to red-ripe fruit. Adapted from Rosas Cárdenas *et al.* (2017).

The programmed softening that occurs during the ripening of many fruit species requires cell-wall loosening and a reduction in cell–cell adhesion as a result of dissolution of the pectin-rich middle lamella (Jarvis *et al.* 2003; Brummell 2006). Characteristic modifications include solubilisation and depolymerisation of pectin,

loss of neutral sugars from pectic side-chains, cell-wall swelling, and disassembly of the xyloglucan–cellulose network (Paniagua *et al.* 2017) resulting in up to 80% softer fruits (Harker and Sutherland 1993; Brummell 2006; Airianah *et al.* 2016). In fleshy fruits, softening is associated with a reduced proportion of large wall polymer molecules, reduced level of polysaccharide branching and shorter polysaccharide side-chain length (Wang *et al.* 2018). These modifications are partly due to non-enzymic reactions with reactive oxygen species (especially the hydroxyl radical $^{\bullet}OH$; Dumville and Fry 2000; Airianah *et al.* 2016) or expansins (Brummell *et al.* 1999), and partly the result of wall-modifying enzymes secreted into the apoplast during ripening (Wang *et al.* 2018).

Expression analysis of hundreds of genes with changing expression profiles during fruit development has been correlated with ripening. For example, expression of some enzymes involved in carotenoid synthesis, sugar metabolism, generation of flavour and aroma compounds and cell wall modifications has been characterized (Hirschberg 2001; Chen *et al.* 2004; Tieman *et al.* 2006; Wang *et al.* 2018). However, the signalling pathways that trigger these changes are less well defined. Multiple approaches investigating mutations in certain genes involved in fruit ripening began unveiling the mystery of these complicated phenomena, some of which include plant hormones (such as auxin and ethylene) as promoting agents for the ripening process in various species (Given *et al.* 1988; Manning *et al.* 2006; Barry and Giovannoni 2007; Sun *et al.* 2013).

Fruit species (including tomato, apple, peach, and banana) with elevated levels of ethylene and respiration accompanying the ripening process are categorized as climacteric, whereas fruit species that do not exhibit high ethylene levels (including citrus, grape, and strawberry) are non-climacteric (Barry and Giovannoni 2007).

Although ethylene levels do not usually rise much during ripening of non-climacteric fruits, it is still required for normal development. In strawberry, ethylene affected the expression of genes involved in aroma production and cell wall degradation (Merchante *et al.* 2013). Down-regulation of several cell wall-modifying enzymes related to fruit softening including β-galactosidase and pectin methylesterase caused by ethylene was reported in strawberry (Trainotti *et al.* 2001; Castillejo *et al.* 2004). In addition, chemical inhibition of ethylene action caused down-regulation of polygalacturonase genes (Villarreal *et al.* 2009). On the other hand, application of exogenous ethylene to peach fruits induced the expression of softening-related proteins including pectate lyase, pectin methyl esterase and expansins, which was correlated with rapid softening (Zhu *et al.* 2019). These reports suggest a role of ethylene (and probably other hormones) in signalling pathways of such enzymes not only in climacteric fruits but in non-climacteric fruits as well.

Plant growth regulators other that ethylene can also affect the ripening process. In strawberry, the application of auxin, abscisic acid and gibberellic acid altered the expression and/or activity of cell wall-modifying enzymes including polygalacturonases, pectate lyase and rhamnogalacturonan lyase (Medina-Escobar *et al.* 1997; Villarreal *et al.* 2009; Molina-Hidalgo *et al.* 2013; Sénéchal *et al.* 2014)

1.1.2. Fruit cell walls

The plant cell wall is a complex structure made of different polysaccharides, proteins, and aromatic compounds that surround the plant cell. It determines the cell size and shape (Vogler *et al.* 2015). It is essential for the cells' survival and has limited mobility

which helps plants to withstand different harsh environmental conditions and acts as a defence against pathogens and herbivores (Collmer and Keen 1986).

The primary cell wall has more pectic polysaccharides and less cellulose than the secondary cell wall and it gives the plant cells their specific size and fixes the area of the cell surface upon which the secondary wall may be formed. The secondary cell wall is a thicker wall layer where most of the plant biomass occurs and commonly has an additional component, the lignin polymer (Lerouxel *et al.* 2006; Keegstra 2010; Fig. 1.3).

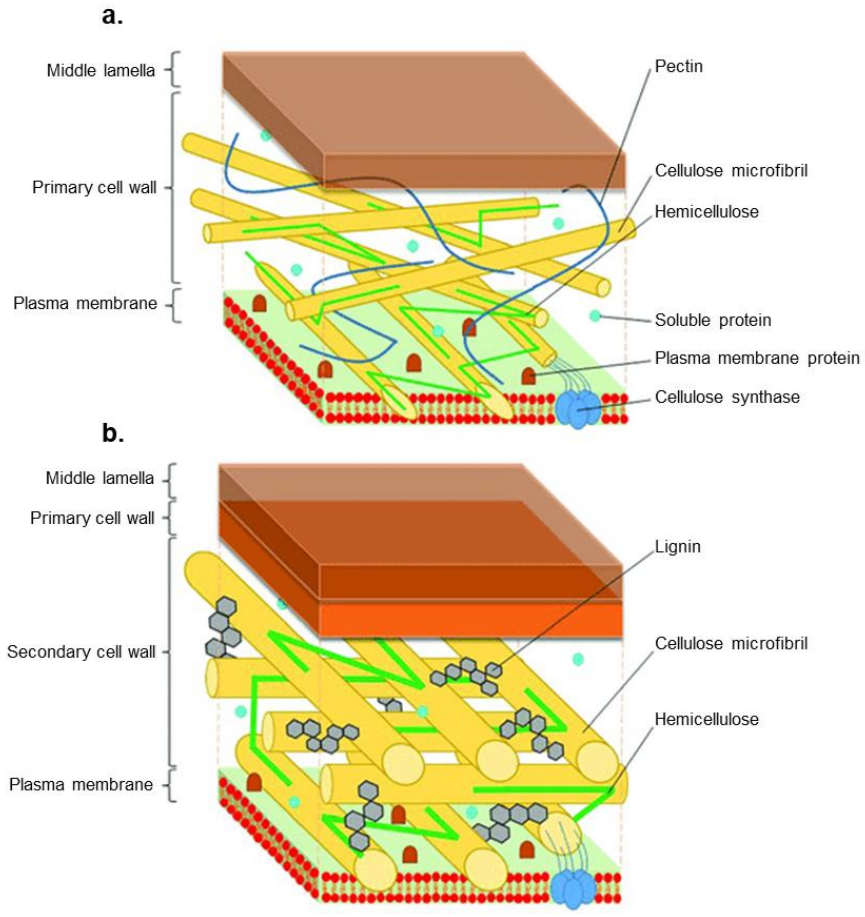

Fig. 1.3. Structure of primary and secondary plant cell walls. (a) The primary cell wall consists of cellulose microfibrils (synthesised by cellulose synthase complexes) tethered by hemicelluloses (including xylans, mannans, xyloglucans, and mixed linkage β-glucans) and embedded in a matrix of hemicelluloses and pectin (including the domains homogalacturonan (HG), xylogalacturonan, rhamnogalacturonan I (RG-I), and rhamnogalacturonan II (RG-II) in addition to proteins. **(b)** The secondary cell wall consists of cellulose microfibrils, often impregnated with lignin molecules in addition to hemicelluloses and proteins. Adapted from Loix *et al.* (2017). A simplified model to which details have been added by Cosgrove (2018).

Fruit primary cell walls are composed of cellulose microfibrils surrounded by a matrix of non-cellulosic polysaccharides (mainly hemicelluloses and pectin; Fig. 1.3). This is different from the primary cell walls of commelinid monocots (such as grasses), which are rich in glucuronoarabinoxylans and hydroxycinnamates and poor in pectin and structural proteins (Vogel 2008).

Cellulose consists of β-(1–4)-D-glucan chains made within the plasma membrane by cellulose synthase proteins and packed into crystallized microfibrils (Fig. 1.4). Cellulose microfibrils are tethered by hemicelluloses via hydrogen bonds and embedded in a matrix of pectin and additional hemicellulose (Fry 2004; Fry 2010).

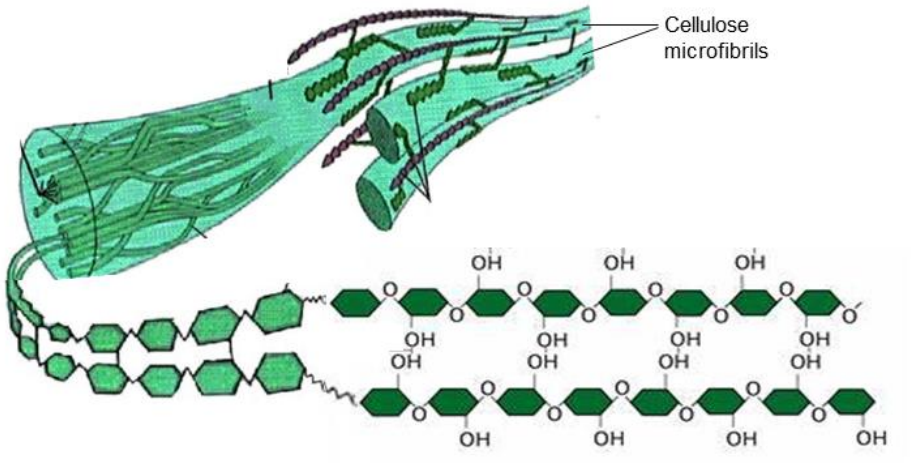

Fig. 1.4. Schematic representation of the cellulose in plant cell walls. Cellulose microfibrils are made from β-(1–4)-D-glucan chains linked by hydrogen bonds. Adapted from Chattopadhyay and Patel (2016).

Hemicelluloses are composed of neutral sugar chains with β-(1–4)-linked backbones, which bind with the cellulose microfibrils (sometimes also with lignin), enhancing the strength of the cell wall. Hemicelluloses are synthesized by glycosyltransferases located at the Golgi membranes. Xyloglucan is the most abundant glycan in primary cell walls of dicots with a backbone of β-(1–4)-D-glucopyranose residues. A single α-D-xylopyranose residue is attached at *O*-6 of about 75% of the backbone

glucopyranose residues. Some of the α-D-xylopyranose are β- D-galactopyranosylated at *O*-2, which in turn can be α-L-fucopyranosylated at *O*-2 (Fry *et al.* 1992; Fig. 1.5a). Other hemicelluloses include xylans, mannans and mixed-linkage glucans. Xylans consist of a backbone of β-(1–4)-xylose residues and are the major hemicellulose in commelinid monocot primary walls. Their xylose residues can be substituted with α-(1–2)-linked glucuronosyl and 4-*O*-methyl glucuronosyl producing glucuronoxylans (common in secondary walls of dicots). Arabinose side chains are also commonly attached to xylans producing what are known as arabinoxylans or glucuronoarabinoxylans (Fig. 1.5b). Mannans have a backbone consisting of β-(1–4)-linked mannose, as in mannans and galactomannans, or β-(1–4)-linked mannose and glucose (in a non-repeating pattern) as in glucomannans and galactoglucomannans (Scheller and Ulvskov 2010; Fig.1.5c). Mixed-linkage glucans consist of β-(1–3,1–4)-linked glucans and are major non-cellulosic polysaccharides in the Poales (Fry *et al.* 2008; Fig.1.5d).

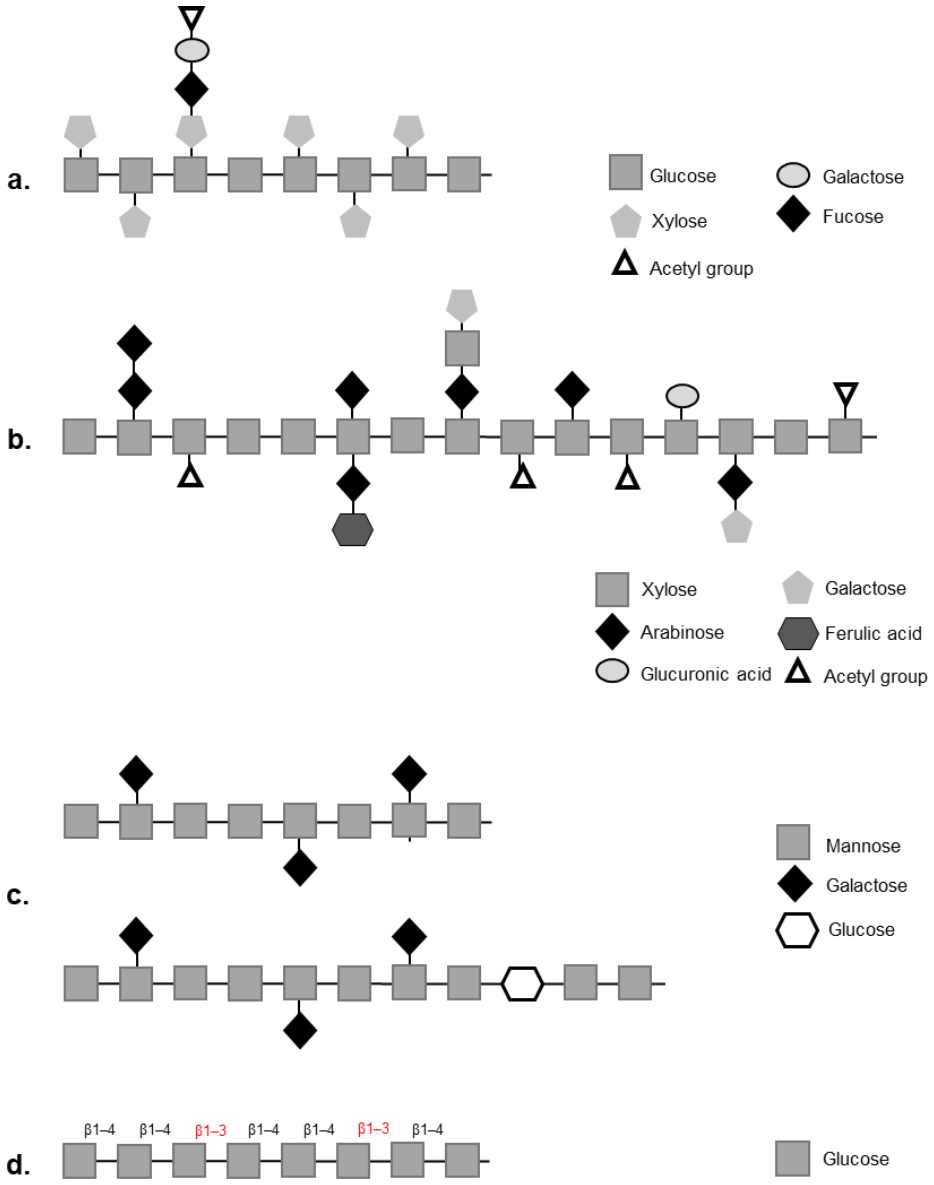

Fig. 1.5. Schematic representation of the hemicelluloses in plant cell walls. (a) Xyloglucan with a backbone of β-(1–4)-D-glucopyranose residues. **(b)** Xylan with a backbone of β-(1–4)-xylose residues. **(c)** Mannans including galactomannan (upper structure) and galactoglucomannan (lower structure). **(d)** Mixed-linkage glucan with a backbone of consists of β-(1–3, 1–4)-linked glucans. Adapted from de Vries and Visser (2001).

Pectin is the most complicated polysaccharide in plant cell walls. It has three major covalently-linked domains: homogalacturonan (HG), rhamnogalacturonan-I (RG-I) and rhamnogalacturonan-II (RG-II), which are synthesised in Golgi vesicles by several enzymes including glycosyltransferases, methyltransferases, and acetyltransferases (Ridley *et al.* 2001; Mouille *et al.* 2007; Caffall and Mohnen 2009; Fry 2010; Harholt *et al.* 2010; Fig.1.6). Homogalacturonan ('pectate') constitutes

more that 60% of the pectin (Caffall and Mohnen 2009) and consists of a mainly unbranched chain of anionic (1–4)-α-D-galacturonic acid (GalA) residues plus neutral blocks of methyl-esterified (1–4)-α-GalA residues. Rhamnogalacturonan-I constitutes up to 35% of the pectin (Mohnen 2008) and has a backbone of repeating disaccharide units of (1–4)-α-D-GalA-(1–2)-α-L-Rha (where Rha = rhamnose), with neutral side chains of β-galactose and/or α-arabinose usually attached to ~50% of the rhamnose residues at their *O*-4 position. The GalA residues of the RG-I backbone are not methyl-esterified; however, they can be *O*-acetylated at C-2 and/or C-3 (Ishii 1997; Perrone *et al.* 2002; Yapo *et al.* 2007). Rhamnogalacturonan-II consists of eight or more (1–4)-α-D-GalA residues as a backbone to which five different side-chains are attached, making a highly complicated structure. In primary cell wall, RG-II is found predominantly as a dimer cross-linked by a 1:2 borate-diol ester (Kobayashi *et al.* 1996; Ishii *et al.* 1999). Another, often minor, domain of pectin is xylogalacturonan which has an α-D-GalA backbone (with or without methyl esters) with β-D-xylose and α-L-fucose side chains.

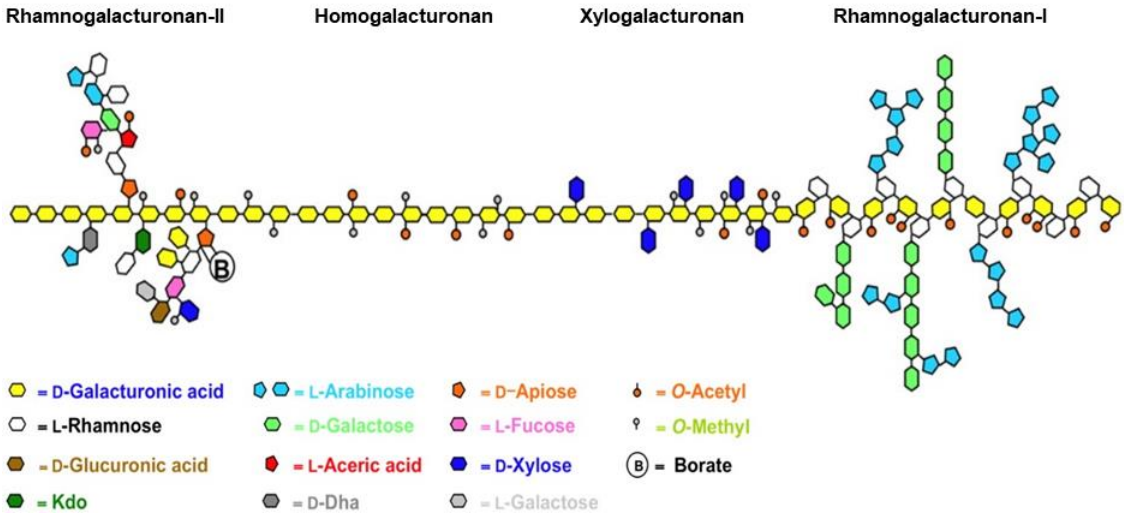

Fig. 1.6. A schematic representation of the pectic domains. The four pectic domains are homogalacturonan (HG), rhamnogalacturonan-I (RG-I), rhamnogalacturonan-II (RG-II) and xylogalacturonan (XG). GalA makes the backbone of HG, RG-II and XG while RG-I's backbone consists of repeated disaccharide of GalA-Rha. Adapted from Harholt *et al.* 2010.

The cell wall undergoes structural modifications in response to different stimuli to accommodate the needs for cell growth and development and environmental conditions (Caffall and Mohnen 2009).

1.1.3. Cell wall modifications during fruit ripening

Cell wall modifications during ripening can be non-enzymic and/or enzymic, requiring a range of reactions catalysed by various enzymes each with a specific substrate within the cell wall.

Non-enzymic modifications include pectic polysaccharide depolymerisation by reactive oxygen species (especially the hydroxyl radical $^{\bullet}OH$; Dumville and Fry 2000; Airianah *et al.* 2016). In addition, expansins, which are polysaccharide binding proteins lacking hydrolase and transglycosylase activities, act at the matrix–microfibril interface causing cell wall loosening (McQueen-Mason and Cosgrove 1995; Brummell *et al.* 1999). Roles of expansin gene expression in softening were reported in tomato where down-regulation of such genes reduced fruit softness and overexpression enhanced it (Brummell *et al.* 1999), while in strawberry such effects were not detected (Posé *et al.* 2011).

Many cell wall-modifying enzymes act by cleaving polysaccharides, resulting in mechanical weakening. There are three such types of enzyme activity: hydrolases, transglycosylases and lyases, requiring specific substrates (Moya-León *et al.* 2019). Cell wall-modifying enzymes studied in relation to fruit softening include cellulases, xyloglucan endotransglucosylase/hydrolases (XTHs), endo-polygalacturonases (EPGs), pectate lyases (PLs), rhamnogalacturonan lyases (RGLs), pectin methylesterases (PMEs), and exo-polygalacturonases.

Cellulases catalyse the hydrolysis of β-(1→4)-D-glucoside linkages in cellulose and sometimes also xyloglucan backbones (Fry *et al.* 1992; Dong *et al.* 2018; Fig. 1.7a). Roles of cellulase activity in fruit softening were reported in tomato (Hobson 1968), mango (Abu-Sarra and Abu-Goukh 1992), date (Hasegawa and Smolensky 1971) and strawberry (Abeles and Takeda 1990).

Xyloglucan endo-transglucosylase/hydrolases (XTHs) are known to exhibit transglucosylase (xyloglucan endo-transglucosylase (XET)) activity by catalysing the transfer of a xyloglucan fragment to another pre-existing xyloglucan molecule. Some XTHs exhibit hydrolase activity (xyloglucan endohydrolase; XEH) by hydrolysing xyloglucan chains, while others exhibit both activities (Fry *et al.* 1992; Nishitani 1997; Rose *et al.* 2002; Fig. 1.7b). A role of XTHs in fruit ripening was reported in tomatoes, where reduction of gene expression and extractable enzyme activities were correlated with softening (Saladié *et al.* 2006; Miedes and Lorences 2009).

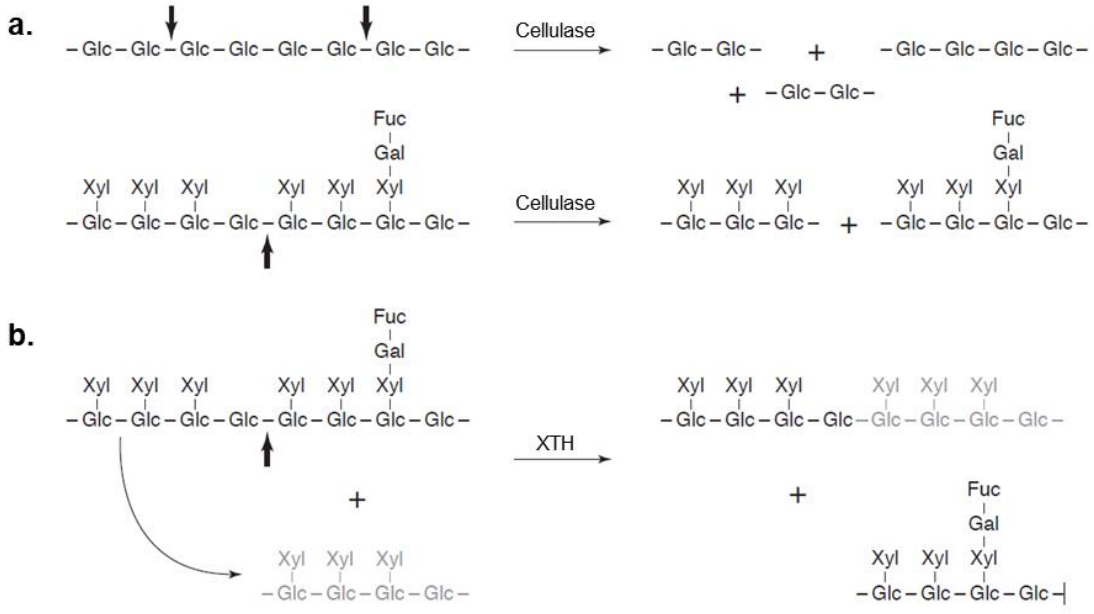

Fig. 1.7. Representation of the mode of action of cellulase and xyloglucan endo-transglucosylase (XET) on xyloglucan. (a) Cellulase catalyses the endo-hydrolysis of β-1,4-linked glucan residues in cellulose (upper) or xyloglucan (lower) backbones. **(b)** XET catalyses the cleavage of xyloglucan polymers (donor substrates) at mid-chain, grafting of the newly generated reducing end to another polymeric or oligomeric xyloglucan molecules (acceptor substrates). Thick arrows indicate the enzyme cleavage sites. Adapted from Rose and Bennett (1999).

Fruit-softening roles of pectin-modifying enzymes were reported (Wang *et al.* 2018; Fig. 1.8), which attack pectin domains in mid-chain, including endo-polygalacturonases (EPGs) (Wu *et al.* 1993; Asif and Nath 2005; Quesada *et al.* 2009), pectate lyases (PLs) (Marín-Rodríguez *et al.* 2003; Dong *et al.* 2018; Uluisik and Seymour 2020; Al Hinai *et al.* 2021) and rhamnogalacturonan lyases (Ochoa-Jiménez *et al.* 2018; Méndez-Yañez *et al.* 2020). In addition, pectin methylesterases (Tieman *et al.* 1992; Phan *et al.* 2007) and exo-polygalacturonases (Bartley 1978; Yang *et al.* 2018) attack pectin but not by mid-chain cleavage. Roles of β-galactosidase and α-L-arabinofuranosidase in the degradation of RG-I side chains were also reported (Goulao *et al.* 2007).

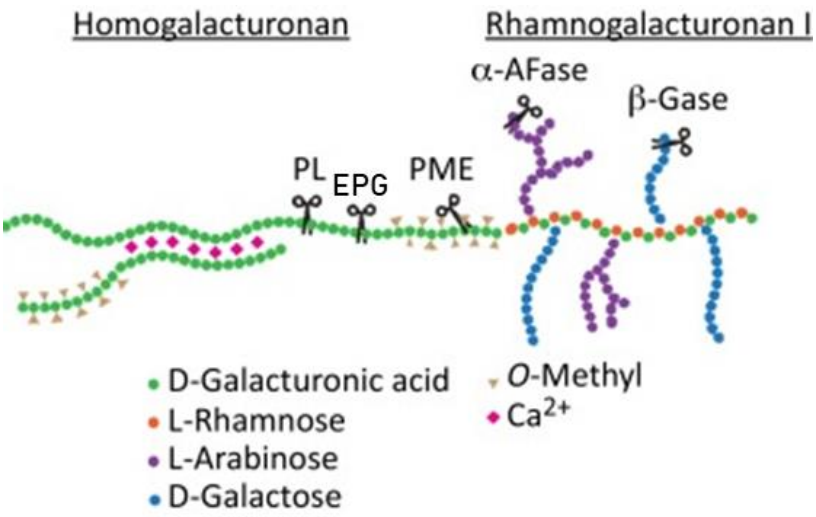

Fig. 1.8. Schematic representation of pectin-modifying enzymes' action sites. Endo-acting enzymes are PL, pectate lyase and EPG, endopolygalacturonases. Exo-acting enzymes are PME, pectin methylesterase; α-AFase, α-arabinofuranosidase; β-Gase, β-galactosidase. Adapted from Wang *et al.* (2018).

The link between enzyme activities (measured *in vitro* after extraction of the enzymes) and fruit softening was often contradictory. Each of the cell wall-modifying enzymes has a different expression pattern and suppression of its expression could lead to different effects on cell wall polymers and, therefore, fruit softening. For instance,

there was an increase in pectin degradation as a result of expression of endo-PG (EPG) in a *rin* (ripening inhibitor) mutant of tomato (Giovannoni *et al.* 1989) and there was a reduction in pectin depolymerisation as a result of suppression of the EPG expression (Smith *et al.* 1990). However, there was no effect of these on fruit softening. Silencing of PME had a minor effect on softening as well (Phan *et al.* 2007). These results indicate that the enzyme expression does not necessarily mean action and that there is no one enzyme responsible for fruit softening; it is a rather more complicated process that requires a coordinated action of many enzymes and other non-enzymatic substances as well.

1.2. Pectin modifications

Fruits have primary cell walls rich in pectin (Brummell 2006). In tomato, the most extensively studied model fruit, and in many other fleshy fruits, pectin modification is the most pronounced cell-wall change during ripening (Paniagua *et al.* 2014; Wang *et al.* 2018).

1.2.1. Non-enzymic pectin modification by hydroxyl radicals (•OH)

Reactive oxygen species (ROS) are intermediate products of the reduction of O_2 to H_2O which requires progressive addition of four single [H] atoms. The •OH is the most reactive ROS and is produced non-enzymatically by Fenton reactions in the apoplast where H_2O_2 reacts with a reduced Cu or Fe metal ion.

$$Cu^{+} + H_2O_2 \longrightarrow {}^{\bullet}OH + OH^{-} + Cu^{2+}$$

$$Fe^{2+} + H_2O_2 \longrightarrow {}^{\bullet}OH + OH^{-} + Fe^{3+}$$

It can cause damage to cellular DNA, structural carbohydrates and enzymes due to its high rate of reactivity with most organic compounds (Vreeburg and Fry 2005). However, it has a very short half-life of about 1 ns and therefore is only able to migrate to a maximum distance of 1 nm from its production site (Griffiths and Lunec 1996; Vreeburg and Fry 2005). The short half-life makes it unlikely for apoplastic $^{\bullet}OH$ to cause any damage to the protoplast but (if the $^{\bullet}OH$ is produced within the cell wall) it still can attack the cell wall polysaccharides causing their depolymerisation via oxidation reactions (Vreeburg *et al.* 2014 and Airianah *et al.* 2016). There was evidence for longer shelf-life of muskmelon fruits in cultivars that produced less $^{\bullet}OH$ (Lacan and Baccou 1998). Pectin solubilisation and depolymerisation were induced by $^{\bullet}OH$ treatment of tomato (Dumville and Fry 2003), banana (Cheng *et al.* 2008) and longan (Duan *et al.* 2011) i*n vitro*. Evidence for the *in-vivo* attack of pectin at mid chain by $^{\bullet}OH$ during ripening was reported by Airianah *et al.* (2016).

1.2.2. HG-modifying enzymes

Plants possess two enzyme activities capable of cleaving the backbone of anionic HG domains in mid-chain: EPG and PL. Both of these act only on anionic HG domains, and therefore prior de-methylesterification by pectin methylesterase (PME) may be necessary (Tieman *et al.* 1992; Dong *et al.* 2018). In addition, plants have exo-PG (α-galacturonidase), which removes GalA residues one at a time from the non-reducing end of HG, presumably having relatively little immediate effect on the cell wall's mechanical properties.

PME is an enzyme that exhibits hydrolase and/or (speculatively) trans-acylase activities. As a hydrolase, PME is responsible for the de-esterification (cleavage of the

ester bond between the methyl group and the carboxyl group at C6) of GalA residues within the HG chain (Fig. 1.9a). The C6 carboxyl group could therefore be transferred to water, fulfilling the de-esterification process (hydrolysis), releasing methanol and protons to the apoplast and changing the charge and pH of the cell wall (Reca *et al.* 2012; Dorokhov *et al.* 2018). Other acceptors have also been proposed, including other pectic polysaccharides (Lee *et al.* 2003; Wu *et al.* 2004) or polyamines (Lenucci *et al.* 2005), potentially resulting in higher molecular weight pectin (Fig. 1.9b & c).

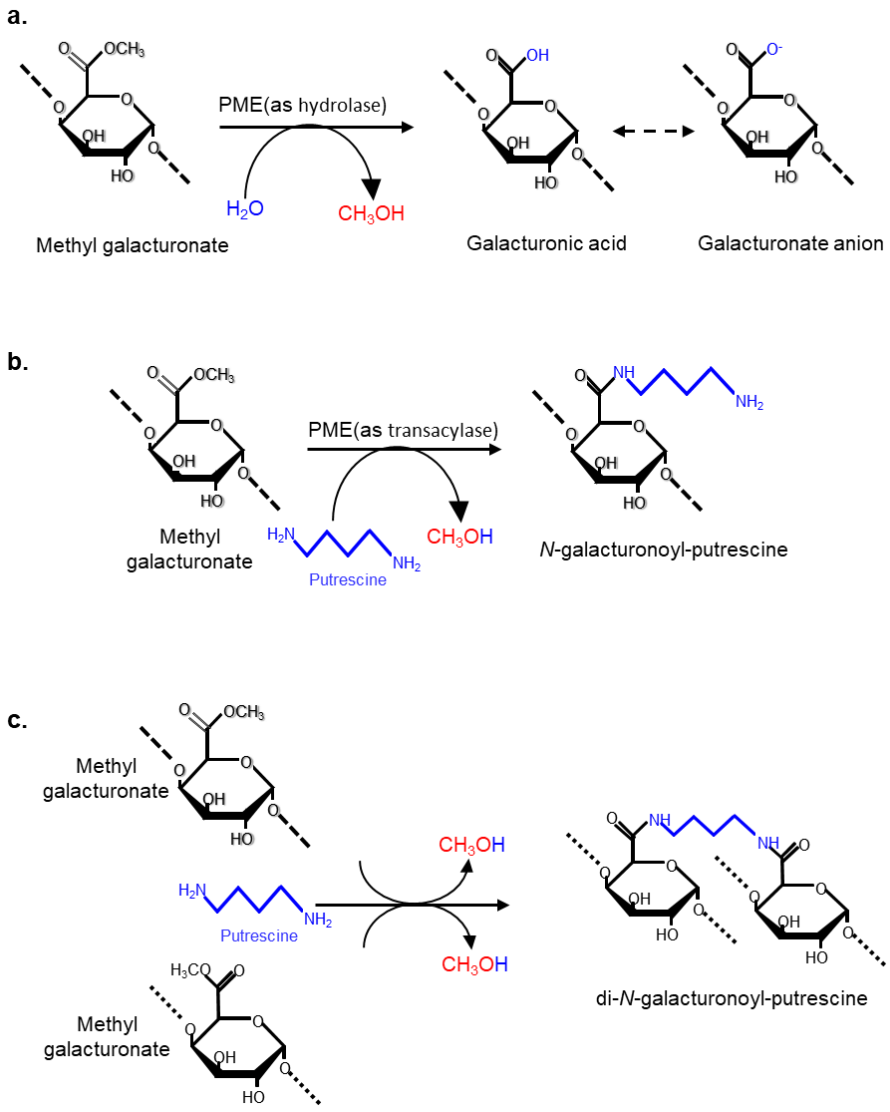

Fig. 1.9. Possible pectin methylesterase (PME) activities. (a) PME acting as a hydrolase cleaving the ester bond between the methyl group and the carboxyl group at C6 on GalA residues within the homogalacturonan domain. **(b)** PME acting as trans-acylase replacing the methyl group at C6 with putrescine (a polyamine). **(c)** PME acting as trans-acylase replacing the methyl group at C6 with putrescine facilitating the production of di-N-galacturonoyl-putrescine via joining two N-galacturonoyl-putrescine polymers. Adapted from Fry 2017.

In tomato, the degree of HG esterification dropped from 90% in mature green fruit to 35% in red-ripe fruit (Koch and Nevins 1989). De-esterification of the pectic HG domain increases its accessibility to pectin degrading enzymes such as PL and EPG (Limberg *et al.* 2000; Wakabayashi *et al.* 2003). In addition, it allows the formation of cross bridges between HG chains via Ca^{2+} forming what are known as the egg-box structures (Jarvis *et al.* 2003).

Increased PME expression and activity was correlated to fruit softening. In tomato, mRNA accumulation peaked at the mature green stage and protein activity reached its maximum after that. Transgenic fruits with antisense PME had a 15–40% increase in the degree of methyl-esterification and a reduced polyuronide degree of polymerization compared with wild type fruits; however, no effect on fruit softening was observed (Brummell and Harpster 2001). On the other hand, silencing PME genes in strawberry caused a significant decrease in fruit softness while overexpression had the opposite effect (Xue *et al.* 2020).

EPG, which catalyses endo-hydrolysis of HG (Fig. 1.10), is the most studied pectin-cleaving enzyme, yet its effect on fruit softening may be low (Wang *et al.* 2018). Genes encoding EPGs are often upregulated during fruit ripening (Tucker and Grierson 1982), suggesting that this enzyme may be produced during softening. This is supported by reports of PG (polygalacturonases where reports did not specify whether it was the endo- or exo- enzyme) activity extractable from fruit (Wu *et al.* 1993; Orr and Brady 1993; Villarreal *et al.* 2008; Zhang *et al.* 2020). However, many such reports have not satisfactorily distinguished between EPG and PL, and even exo-PG, activities. For example, EPG activity in strawberry extracts was often assayed as *in-vitro* production of new reducing termini (i.e., as total reducing groups) from pure HG (Villarreal *et al.* 2009; Figueroa *et al.* 2010; Zhou *et al.* 2015, based on an influential

paper by Gross 1982); however, reducing groups are generated from HG by endo-PG, exo-PG and PL, and also by certain •OH reactions, so these three enzyme activities and the reactive oxygen species would not have been distinguished in such studies.

Transformation experiments with antisense PG genes in tomato and strawberry produced discrepant data. In tomato, PG expression (measured as mRNA levels by northern blotting) could be reduced to 1% of wild-type without affecting softening (Smith *et al.* 1990; Brummell and Harpster 2001), whereas in strawberry and apple, firmer fruits were produced when PG expression was reduced to 5–25% of wild-type (Quesada *et al.* 2009; Atkinson *et al.* 2012; Posé *et al.* 2015).

PL cleaves the anionic HG domain by a β-elimination reaction (non-hydrolytically) to give a product with a 4-deoxy-β-L-*threo*-hex-4-enopyranuronose residue (abbreviated as ΔUA, for 'unsaturated uronic acid') at the newly formed non-reducing end (Fig. 1.10) (Fuchs 1965; Shaligram and Singhal 2010; Nasuno and Starr 1967; Iqbal *et al.* 2016; Zhou *et al.* 2016; Al Hinai *et al.* 2021). [Note: rules of carbohydrate nomenclature dictate that a β-L-ΔUA residue is the product expected when a lyase catalyses an elimination reaction starting with a pectic α-D-GalA residue; this does not imply any change in the configuration at carbon-1.] Earlier work had reported a microbial pect**in** lyase (not PL) that acts on methylesterified HG (Albersheim *et al.* 1960). PL gene expression (monitored as mRNA accumulation) has been reported in ripening fruits including tomato (Uluisik *et al.* 2016), strawberry (Benítez-Burraco *et al.* 2003; Figueroa *et al.* 2008), banana (Dommguez-Puigjaner *et al.* 1997; Pua *et al.* 2001), mango (Chourasia *et al.* 2006; Deshpande *et al.* 2017) and grapes (Nunan *et al.* 2001). Despite early negative reports (e.g. Besford and Hobson 1972), recent studies have suggested a central role of PL genes in tomato fruit softening: tomato fruits with

silenced PL genes had reduced PL mRNA expression, reduced extractable PL enzyme activity and increased fruit firmness (Uluisik *et al.* 2016; Yang *et al.* 2017). A putative PL gene was ascribed a possible role in softening as firmer strawberry fruits were produced when PL genes were silenced (Jiménez-Bermúdez *et al.* 2002; Marín-Rodríguez *et al.* 2002). PL activity (assayed *in vitro*) is extractable from ripening strawberry (Zhou *et al.* 2016), banana (Marín-Rodríguez *et al.* 2003), and several other fruits (Wang *et al.* 2018; Uluisik and Seymour 2020).

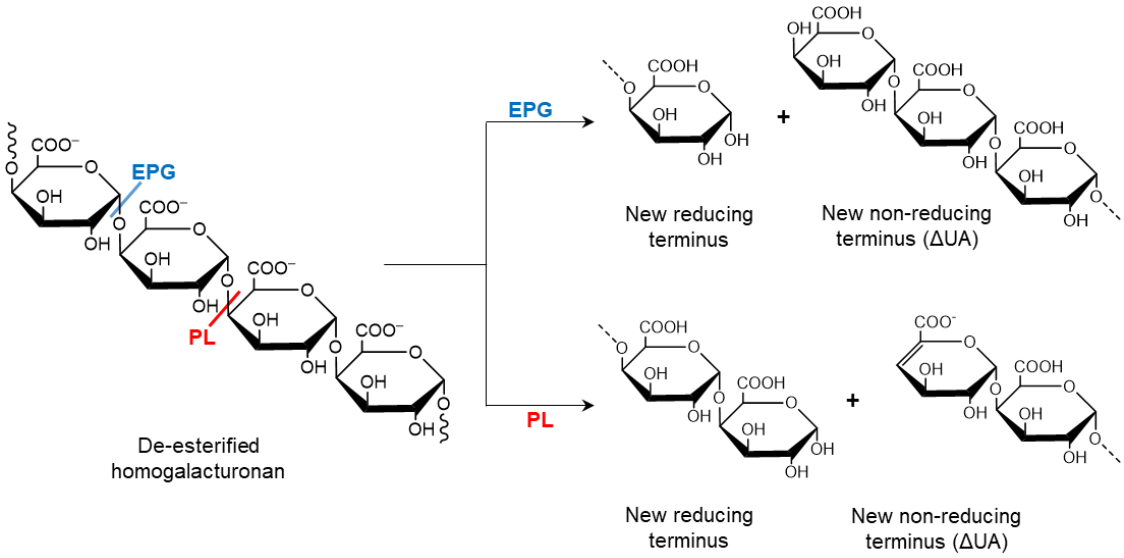

Fig. 1.10. Endo-polygalacturonase (EPG) and pectate lyase (PL) activities. EPG and PL enzymes act on methyl-de-esterified pectic HG domain. PL produces ΔUA-$GalA_n$s with one unsaturated non-reducing terminus (ΔUA) and one new reducing terminus. EPG produces $GalA_n$s with one new reducing terminus (the same as in PL products) and one new saturated non-reducing terminus. The dash lines indicate longer chains of repeating GalA units.

The oligogalacturonides released from the degradation of the HG domain play a significant role not only in softening of fruits, but also as damage-associated molecular patterns (DAMPs) which activate specific receptors (pattern recognition receptors, PRRs) upon microbial infection or mechanical damage (Duran-Flores and Heil 2016).

1.2.3. RG-I-modifying enzymes

RG-I is the second most abundant pectic domain in plant cell walls known as the hairy region (Yapo 2011). During ripening, loss of galactose side chains from RG-I is one of the remarkable changes in the cell wall structure (Gross and Sams 1984). The expression of genes encoding β-galactosidase, which has an exo-galactanase activity cleaving β-D-galactose residues at the non-reducing terminus, was reported in several fruits including tomato (Smith and Gross 2000), strawberry (Trainotti *et al.* 2001) and pear (Tateishi *et al.* 2001). In tomato, the decrease in polymeric galactose and increase in the free galactose during ripening was related to a seven-fold increase in the activity of β-galactosidase (Seymour *et al.* 1990; Smith and Gross 2000; Brummell and Harpster 2001). Transformation with antisense β-galactosidase genes reduced softness of tomato and strawberry fruits (Smith *et al.* 2002; Paniagua *et al.* 2016). Over-expression of endo-galactanase in potato tubers decreased the galactan content and enhanced the accessibility of homogalacturonan to PME and EPG (Sørensen *et al.* 2000), suggesting that degradation of RG-I side chains can increase the porosity of the cell wall, which in-turn increases the accessibility of other pectic domains to pectin-degrading enzymes including PME, EPG, PL and RGL (Brummell and Harpster 2001).

Loss of arabinose (from pectic and/or hemicellulosic cell wall polysaccharides) was also commonly observed during ripening of several fruit species (Gross and Sams 1984), although the extent of its loss varies between species (Brummell 2006). For instance, extensive loss of arabinose was reported in blueberry and pear; however, it was absent in plums and watermelon (Tateishi 2008; Chea *et al.* 2019). An increase in the extractable activity of α-L-arabinofuranosidase, which hydrolyses the arabinofuranose residues at the non-reducing terminus of matrix glycans (e.g. RG-I

side chains), was reported in tomato (Sozzi *et al.* 2002), peach (Brummell *et al.* 2004) and several other fruits (Tateishi 2008). The enzyme activity reports showed contradictory results among different species. A significant decrease in activity was reported in tomato (Takizawa *et al.* 2014) and Chilean strawberry (Figueroa *et al.* 2010), while an increase was reported in European strawberry (Rosli *et al.* 2009) and apple (Gwanpua *et al.* 2016).

Rhamnogalacturonan lyase (RGL) is an enzyme capable of cleaving the α-(1,4) glycosidic bonds between rhamnose and galacturonic acid of the RG-I backbone via β-elimination, producing a new (ordinary) rhamnose reducing end and a new unsaturated uronic acid (ΔUA) non-reducing end (Fig. 1.11; McKie *et al.* 2001; McDonough *et al.* 2004; Ochoa-Jiménez *et al.* 2018). RGL was first purified from *Aspergillus aculeatus* and tested on RG-I from apple fruits (Schols *et al.* 1990; Kofod *et al.* 1994). An RGL gene expressed in receptacles of ripening strawberry was reported and silencing this gene resulted in a more intact middle lamella and firmer fruits (Molina-Hidalgo *et al.* 2013). In addition, Dautt-Castro *et al.* 2015 reported a five-fold increase in the expression of an RGL gene in ripe mango compared with mature green fruit. RGL activity was reported in tomato (Ochoa-Jiménez *et al.* 2018) and Chilean strawberry fruits (Méndez-Yañez *et al.* 2020). In general, few data are available regarding the role of RGL in fruit ripening.

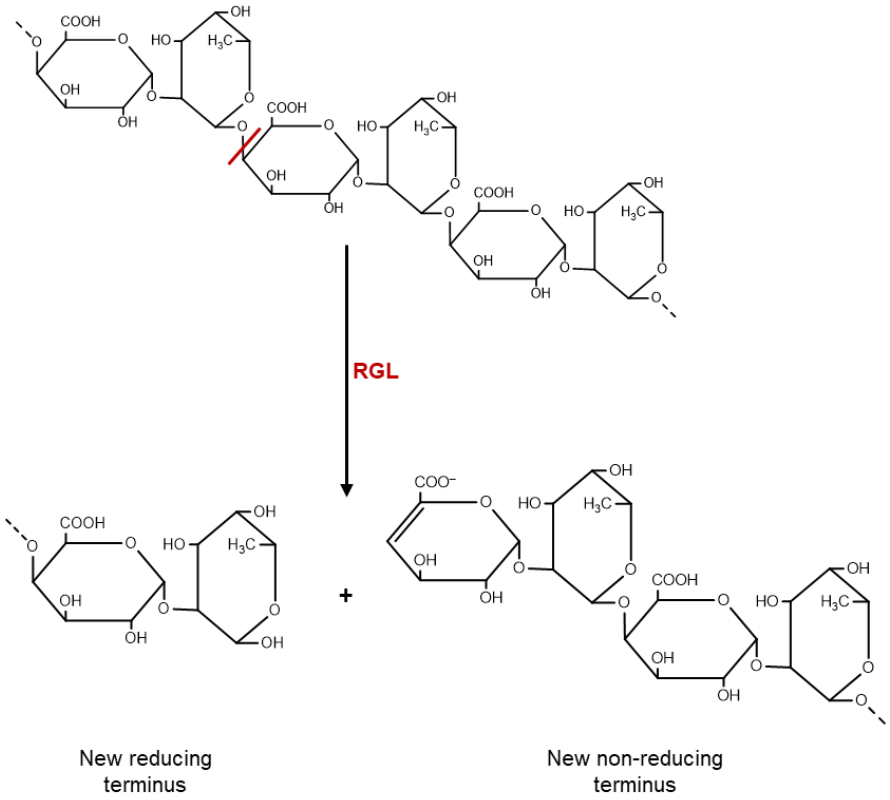

Fig. 1.11. Rhamnogalacturonan-lyase (RGL) activity. RGL acts on the RG-I backbone by cleaving the α-(1,4) glycosidic bond between rhamnose and galacturonic acid of the RG-I backbone via β-elimination producing a reducing end and an unsaturated uronic acid (ΔUA) at the non-reducing end. The wavy lines indicate longer chains of repeating GalA-Rha units.

1.2.4. Expression, activity and action

Fruit species clearly differ in the reactions modifying pectin during ripening, and in no species can it be precisely defined which reaction(s) contribute the key role in softening. Often, mRNA accumulation has been taken as evidence of 'contribution'. Fewer studies have assayed extractable enzyme activities, and very few have tested whether the enzymes exhibit action in the fruit *in vivo*. For instance, production of RGL mRNA did not correlate with extractable enzyme activity in tomato, suggesting that gene expression does not necessarily mean action (Ochoa-Jiménez *et al.* 2018).

Enzyme activity is measured in katals under optimised conditions *in vitro*. Enzymes are usually extracted from the plant tissue and applied to specific substrates and the products would then be analysed. For example, the presence of the unsaturated uronic acid in PL activity tests is usually detected by the absorbance at 235 nm. However, when these products are present in nanomole quantities, it is challenging to quantify them spectrophotometrically (Naran *et al.* 2007).

Enzyme action is what can be observed *in vivo*, in living fruit tissue. Direct evidence for enzyme action can be provided by analysis of changes in polysaccharide chemistry during ripening, which could also be challenging to detect when the changes are minimal.

There are several plausible reasons why an enzyme that exhibits *in-vitro* activity when extracted from the plant might not exhibit action within the living plant. For example (Fry 2004) the enzyme and its substrate may be spatially separated, specific inhibitors may be present, the apoplastic redox potential, pH or ionic strength may not be optimal, or the prior action of a necessary helper enzyme (PME in the case of EPG and PL) may not have occurred.

1.3. Project aim

Fruit softening has gained a lot of researchers' attention over the years. Many economically important fruits such as tomatoes and strawberries have a short shelf-life, causing the loss of a high percentage of the fruit harvest. Understanding the genetic and the biochemical mechanisms behind fruit softening is very important to achieve the best methods to control fruit softening and improve the fruit's shelf-life. Most of the genetic modifications used to slow the ripening and improve fruit shelf-

life caused also changes in fruit colour, flavour and nutritional values of the fruit. Studies of genes encoding enzymes involved in cell-wall modifications including EPG, PL and RGL revealed important roles in fruit softening; however, evidence that these enzymes are in action *in vivo* has never been reported.

1.3.1. Date and other fruits

This project aims to establish suitable methods to detect signs of PL and RGL attack on HG and RG-I respectively in cell walls of the date (*Phoenix dactylifera*) fruit as well as other fruit species. Date is a dioecious monocot in the commelinid family Arecaceae. It is widely cultivated in the Middle East and North Africa. Date ripening in many varieties is marked by a decrease in water content and increase in soluble sugar (Ahmed *et al.* 1995; El Arem *et al.* 2011). A remarkable decrease in the cell wall content of the fruit pulp (measured as g of alcohol-insoluble residue (AIR) per g fruit fresh weight) has also been reported in ripe date as well as other fleshy fruits (Vicente *et al.* 2007; Griba *et al.* 2013).

In date fruits, pectin is the major non-cellulosic cell-wall component, rather than hemicellulose. During date ripening, a decreased degree of HG methyl-esterification was reported (Gribaa *et al.* 2013), making it a potential substrate for hydrolysis by EPG and β-elimination by PL. Moreover, an increase in extractable cellulase, β-galactosidase (Rastegar *et al.* 2012) and EPG (Serrano *et al.* 2001) activities was reported in date. Extractable EPG and β-galactosidase activities peaked at the full ripe stage, after which the EPG activity was reduced while β-galactosidase activity remained high. The increase in these two enzymes' extractable activities was correlated with fruit softness during ripening (Serrano *et al.* 2001). No data are

available about PL or RGL in dates — either their activities in extractable proteins or their actions *in muro*; however, PL genes were reported by the National Centre for Biotechnology Information (NCPI).

Other fruit species analysed in this project include strawberry, blackberry, plum, mango, and several other species from the families Rosaceae, Ericaceae and Taxaceae, some of which had PL and/or RGL genes expressed and their activities had been reported as mentioned earlier and summarized in Table 1.1.

Table 1.1. List of references where PL and RGL activities (extractable) or mRNA were detected in some of the fruit species studied in this project.

Fruit	Reports of PL activity or mRNA		Reports of RGL activity or mRNA	
	mRNA	Enzyme activity	mRNA	Enzyme activity
Date	No data, but genes were detected (NCPI)	No data	No data	No data
Strawberry	Jiménez-Bermúdez *et al.* (2002), Santiago-Doménech *et al.* (2008) and Youssef *et al.* (2009)	Zhou *et al.* (2016)	Molina-Hidalgo *et al.* (2013) and Méndez-Yañez *et al.* (2020)	Méndez-Yañez *et al.* (2020)
Mango	Chourasia *et al.* (2006b), Dautt-Castro *et al.* (2015) and Deshpande *et al.* (2017)	Chourasia *et al.* (2006a)	Dautt-Castro *et al.* (2015)	No data
Apple	Harb *et al.* (2012)	Goulao *et al.* (2007) and Manzocco *et al.* (2009)	No data	No data
Yew aril	No data	No data	No data	No data

1.3.2. Strategy for detecting PL and RGL actions

Each of the proposed mechanisms of homogalacturonan and rhamnogalacturonan-I endo-cleavage leaves a fingerprint on the fruit's pectin which may be used as a tool to examine the *in-vivo* contribution of each mechanism to ripening. Oxidation by •OH leaves mid-chain oxo groups (Airianah *et al.* 2016), hydrolysis by EPG leaves a new non-reducing terminal GalA residue, and β-elimination by PL and RGL leaves a new non-reducing terminal ΔUA residue. It had not been tested whether PL or RGL exhibit action *in vivo* — in the fruit of any species, or indeed in any other plant organs. This project provides the first evidence of PL and RGL *in-vivo* actions by detecting their unique fingerprints (containing ΔUA) in fruits of several species at different stages of ripening.

Chapter 2

Materials and methods

2.1. Materials

2.1.1. Enzymes

Pectate lyase (PL) provided in ammonium sulphate suspension (from *Cellvibrio japonicus*, Megazyme) was centrifuged at 14500 g for 3 minutes and the pellet was re-dissolved in water at 10 U/ml.

Endo-polygalacturonase (EPG) provided in ammonium sulphate suspension (from *Aspergillus aculeatus*, Megazyme) was dialysed using standard 12 kDa dialysis membrane against a buffer of pyridine/acetic acid/H_2O (1:1:98 by vol., pH ≈ 4.7, containing 0.5% chlorobutanol) for 16 hours stirring at 4°C (cold room). Dialysis was used to get rid of the ammonium sulphate as EPG would not precipitate when centrifuged.

Driselase (from *Basidiomycetes* sp., Sigma product D9515), was purified by ammonium sulphate precipitation and gel-permeation chromatography (Fry, 2000), dried and re-dissolved in pyridine/acetic acid/H_2O (1:1:98 by vol., containing 0.5% chlorobutanol).

Rhamnogalacturonan lyase (RGL) was provided in 35 mM Na-Hepes buffer, pH 7.5, 750 mM NaCl, 200 mM imidazole, 3.5 mM $CaCl_2$ and 25% (v/v) glycerol (from *Dickeya dadantii*, Nzytech).

2.1.2. Other materials and chemicals

Chemicals used in his project were from Sigma–Aldrich (https://www.sigmaaldrich.com/united-kingdom.html), Fisher scientific

(https://www.fishersci.co.uk/gb/en/home.html) or Megazyme (https://www.megazyme.com).

Aluminium-backed F254 silica-gel (1.05554.0001) and plastic-backed (1.05748.0001) silica-gel TLC plates were from Merck (https://www.merckgroup.com/uk-en).

2.2. *In-vitro* digestion of polysaccharides

2.2.1. TFA hydrolysis

Hot TFA was used to hydrolyse di-, oligo- and polysaccharides (e.g. ΔUA-GalA, ΔUA-$GalA_n$ and HG) to their monosaccharides. TFA hydrolysis was done by adding 10 vol of 2 M TFA to samples of these saccharides. The reaction tubes were incubated in hot sand at 120ºC for 1h. After cooling, the products were dried in a SpeedVac (SPD140DDA), re-dissolved in H_2O and analysed by TLC.

2.2.2. Alkaline hydrolysis

Alkaline hydrolysis was conducted on fruit cell walls to remove methyl-ester groups prior to digestion with EPG. This was done within the fruit AIR preparation process after the second ethanolic wash of the fruit homogenate (§2.9) by adding aqueous 0.2 M Na_2CO_3 followed by shaking and incubation at 4°C for 16 h. After that, acetic acid was added to bring the pH down to < 5 and EtOH was added to make a final concentration of 75%. The tube was incubated on a wheel for 1 h and then, the mixture

was centrifuged at 3220 *g* for 5 min. The supernatant was discarded and the pellet was washed with 75% EtOH as described for preparing AIR.

In fruit AIR preparations for studying products of endogenous PL and RGL action at three ripening stages, the alkaline hydrolysis was done after the first Driselase digestion. The non-saponified AIR was digested with 0.05% Driselase and the products were freeze-dried and re-suspended in 75% EtOH. The products were centrifuged at 3220 *g* for 5 min and the supernatant was collected and dried in a SpeedVac. Alkaline hydrolysis was conducted by addition of 200 µl of 0.2 M Na_2CO_3 and incubation at 4°C for 16 h. After that, acetic acid was added to bring the pH down to < 5.

2.2.3. PL digestion

PL digestion was conducted on commercial de-esterified HG to create markers and standardise the methods to be used for detecting PL products in fruit cell walls *in vivo*. A reaction mixture containing 6.6 mg/ml HG, 50 mM CAPS (or 50 mM ammonia) buffer, 1 mM $CaCl_2$ (pH 10 adjusted by acetic acid) and 3.3 U/ml of PL was prepared. At specific time points, 5 µl of the reaction mixture was added to 35 µl of 26% formic acid to stop the reaction. Products of this reaction were stored at −20℃ and used as markers for chromatographic analysis of PL products.

2.2.4. EPG digestion

EPG digestion was conducted on a variety of samples, e.g. HG, PL products from incomplete digestion of HG, RG-I and fruit-AIR (the latter routinely after freeing of ester groups by alkaline hydrolysis (as in §2.2.2). Samples were digested with 10 U/ml EPG in pyridine/acetic acid/H_2O (1:1:98 by vol., pH 4.7) containing 0.5% chlorobutanol. The reaction mixture was incubated on a wheel at 20°C overnight. The products were stored at −20℃.

2.2.5. Driselase digestion

Driselase digestion was conducted on HG, PL products from incomplete digestion of HG, RG-I and fruit-AIR. Samples were either dry (fruit-AIR) or dissolved in H_2O at specific concentrations. The reaction was buffered by pyridine/acetic acid/H_2O (1:1:98 by vol., pH 4.7) containing 0.5% chlorobutanol and Driselase was used at 0.05% concentration. The reaction mixture was incubated on a shaker at 37°C typically for 3 days. After that, the reaction was stopped by the addition of 0.2 vol of formic acid and the products were dried in a SpeedVac. After drying, the products were re-dissolved in H_2O and stored frozen at −20°C.

2.2.6. RG-I digestion

RGL digestion was conducted on commercial RG-I. The potato RG-I was dissolved in 60 mM NaOH and dialysed against 0.5% chlorobutanol for 16 hours. After dialysis, RG-I was dried and washed 3 times in 65% EtOH to precipitate the polymer and wash-

off any small oligomers. The pellet was then dried in freeze-dryer and weighed as a pure stock of RG-I. A reaction mixture containing of 2.9 mg/ml RG-I, 14.7 mM of lutidine buffer (pH 6 adjusted by acetic acid) and 0.03 mg/ml of RGL was prepared. The reaction was conducted at 37°C on a shaker for 16 h. The reaction was stopped by addition of 0.2 volumes formic acid. Products were dried and digested with Driselase (§2.2.5) to release the smallest unsaturated products, which were then resolved by HVPE.

2.3. Ethanol precipitation of polymeric products of enzyme digestion

Ethanol precipitation was conducted to avoid contamination of the monomeric and/or oligomeric products with un-digested polymers. This was done by the addition of ethanol (enough to reach a final concentration of 75%) to the polysaccharide/enzyme digestion products followed by shaking and incubation in fridge (4°C) for 16 h. After that, the products were centrifuged at 3220 *g* for 5 min, and the supernatant was collected, dried in a SpeedVac and re-dissolved in H_2O.

2.4. Chromatography and electrophoresis methods

2.4.1. Markers for chromatographic analysis

Marker monosaccharides (mainly purchased from Sigma–Aldrich) were prepared as 0.5% w/v solutions in 0.5% chlorobutanol and stored at 4°C. An oligo-galacturonide mixture ($GalA_{1–3}$) was prepared by EPG digestion of 20 mg/ml HG (§2.2.4). A mixture of unsaturated oligogalacturonides ($\Delta UA\text{-}GalA_{1–3}$) was prepared by PL digestion of HG (§2.2.3). An Orange G stock solution (10 mM) was stored at room temperature.

2.4.2. Thin-layer chromatography (TLC)

Thin-layer chromatography (TLC) was used to separate different saccharides from different reactions based mainly on their molecular weight. Two types of TLC plates were tested for the best separation of PL products: aluminium-backed F254 TLC plates (Merck, 1.05554.0001) and plastic-backed TLC plates (Merck, 1.05748.0001). Samples and markers were loaded as a 0.8-cm streak of 2.5 µl at a time followed by drying. A space of 0.2 cm was kept between samples. The plate was run in volatile solvent (usually butan-1-ol/acetic acid/water, BAW 2:1:1 for 7 hours) and then dried overnight in a fume hood. After drying, the plate was stained using thymol (§2.5.1) to view the spots and scanned using an Epson A3 scanner. Other solvents used in TLC were butan-1-ol/acetic acid/water (BAW) 4:1:1, propan-1-ol/nitromethane/ water/acetic acid (PNWA) 5:2:3:2, PNWA 5:2:3:0.25, PNWA 5:2:3:0.5 and Ethyl acetate/pyridine/acetic acid/water (EPAW) 6:3:1:1.

2.4.3. Paper chromatography (PC)

Paper chromatography (PC) was used to separate saccharides based partly on their molecular weight. Samples and markers were loaded as 10-µl spots at a time followed by drying (with or without a hair dryer) on Whatman paper No. 1. A space of 2 cm was kept between the spots, 2.5 cm from the paper edge and 9 cm from the bottom. The routine solvent used was ethyl acetate/acetic acid/water (EAW) 10:5:6 for 30 h. The apparatus and methods are described by Fry (2000). After drying, the paper was exposed to 254-nm UV to visualise any unsaturated products (ΔUA-GalA_ns) and photographed using a Doc-It system fitted with UV lamps and operated by Doc-It

software. The paper was then stained using the $AgNO_3$ method (§2.5.3) and scanned using an Epson A3 scanner.

2.4.4. High-voltage paper electrophoresis (HVPE)

High-voltage paper electrophoresis was used to separate saccharides on paper according to their mass and charge using volatile solvents at specific pH values. Samples and markers were loaded as 10-µl spots at a time followed by drying (with a hair dryer) on Whatman paper No. 3. A space of 2 cm was kept between the spots, 2.5-3.0 cm from the paper edge and 12 cm from the bottom. Electrophoresis was conducted on the paper (usually at pH 2 in a volatile solvent of formic acid/acetic acid/water 1:3.5:35.5 by vol. at 3 kV for 4 h). The apparatus and methods are described by Fry (2020). Papers were dried and viewed under a 254-nm UV lamp to visualise any unsaturated products (ΔUA-GalA_ns) and photographed using Doc-It system. The paper was then stained using the $AgNO_3$ method (§2.5.3) and scanned using an Epson A3 scanner.

2.4.5. Preparative PC and HVPE

Preparative PC and HVPE were conducted as methods to pull out specific sugars. Products were loaded as a 20-cm streak (200 µl/cm) in addition to marker spots on Whatman No. 3 paper. Preparative paper chromatograms were run in EAW 10:5:6 for 30 h. Preparative paper electrophoretograms were run at pH 2 (as in §2.4.4).

After running, the paper chromatograms and electrophoretograms were dried and viewed under a 254-nm UV lamp to help locate any UV-absorbing unsaturated sugars. A small part of each paper (including a fringe of the preparative streak-loading and the neighbouring markers) was cut and stained with $AgNO_3$. The remaining part of the streak (un-stained) was cut as 1-cm strips starting from the line of origin (Fig. 2.1a). Each strip was rolled and inserted into 5-ml plastic syringe barrel and each barrel was placed inside a 15-ml Falcon centrifuge tube (Fig. 2.1b). The paper strips were wetted with 400 µl of the eluent (usually 75% ethanol), incubated on the bench for 5 min to let the sugars dissolve and then centrifuged at 3220 *g* for 5 min. Wetting and centrifugation was repeated five more times with a lower eluent volume (200 µl) to ensure that all the sugars in each paper strip were dissolved in the ethanol, giving a maximum recovery of products. Eluates were then dried in a SpeedVac, re-dissolved in H_2O and stored frozen at –20°C. Other eluents tested were de-ionised H_2O, 96, 85, 65 and 55% ethanol.

2.5. Staining methods

2.5.1. Thymol staining for TLC plates

Thymol stain solution was prepared as a mixture of 1.5% w/v thymol and 5% H_2SO_4 v/v in EtOH. TLC plates were dipped quickly and evenly into the thymol solution and then left to dry for 15 min in a fume hood. The plates were then incubated in an oven at 105℃ for 5 min. Plates were then scanned immediately (using an EPSON A3 scanner connected to a computer) as the stain fades with time.

2.5.2. Fluorescent sulforhodamine B staining for TLC plates

The fluorescent sulforhodamine B was tested for staining the TLC plates with the unsaturated PL products. A 2.5-fold serial dilution from 0.1mg/ml to 0.00256 mg/ml sulforhodamine B in 90% acetone was tested. PL products were loaded as spots of 10 µl on five small pieces of aluminium backed (F254) TLC plates. After drying, each TLC plate piece was dipped in a different concentration of sulforhodamine B, dried and then exposed to 254-nm UV light. After showing the best staining intensity, 0.00256 mg/ml sulforhodamine B was then tested for staining a TLC plate with samples of PL products which had been run in a solvent of butano1-ol/acetic acid/water (BAW, 2:1:1). A Doc-It system fitted with UV lamps was used to visualise and capture photos of the stained TLC plates.

2.5.3. Silver nitrate ($AgNO_3$) staining for paper chromatograms and paper electrophoretograms

The silver nitrate ($AgNO_3$) staining requires passing the paper chromatogram or paper electrophoretogram through three different solutions with a 15-min gap between each, allowing the paper to dry. The first solution consists of 25 ml saturated aqueous $AgNO_3$ in 500 ml acetone with a little extra H_2O to fully dissolve. The second solution consists of 0.125 M aqueous NaOH in ethanol and the paper can be dipped in this solution up to 3 times to get darker spots (though this also gives a darker background). The third solution consists of 10% w/v aqueous $Na_2S_2O_3$ (Fry, 2000). Staining was carried out in near-darkness because of the light sensitivity of $AgNO_3$.

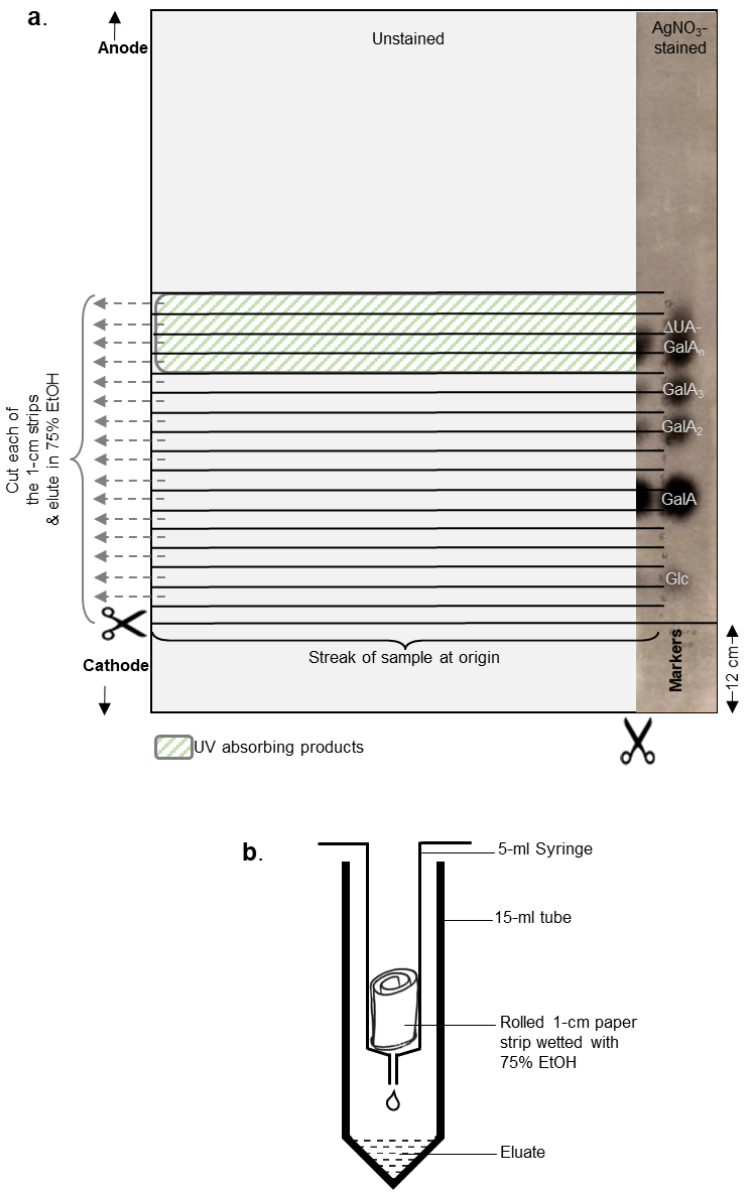

Fig. 2.1. Layout of the preparative paper electrophoretograms and tools for eluting the samples from them. (a) A diagram of a paper electrophoretogram with a 20-cm streak of sample loaded and run in pH 2 volatile buffer at 3 kV for 4 hours. The paper was dried and a portion of the right-side containing markers and a fringe of the sample streak was cut, stained with $AgNO_3$ and used as a guide for the expected unsaturated products from PL and RGL actions. On the left-hand un-stained part of the paper (i.e., the majority), 1-cm lines from the origin were marked with pencil and cut for eluting the samples. **(b)** A 5-ml syringe barrel with the rolled paper strip put inside a 15-ml Falcon centrifuge tube. The paper was wetted with 400 µl of the eluent (usually 75% ethanol), incubated on the bench for 5 min and then centrifuged at 3220 *g* for 5 min. Wetting and centrifugation were repeated for five more times with lower eluent volume (200 µl).

2.6. Investigating PL products' (ΔUA-GalA$_n$s) properties

2.6.1. Thiobarbituric acid (TBA) assay for ΔUA residues

The ΔUA residues (including those in di-, tri- and tetra-saccharides) were assayed by a TBA assay according to Iqbal *et al*. (2016). Samples from the PL digest (40 µl) were mixed with 20 µl of 0.2 M $NaIO_4$ and incubated for 40 min at 20°C, then 40 µl of 7.5 M H_3PO_4 was added followed immediately by 200 µl of 0.77 M $NaAsO_2$. The solution was shaken until the brown colour disappeared and then 600 µl of 0.04 M 2-thiobarbituric acid (pH 2 adjusted by 1M NaOH) was added. The solution was incubated in a boiling water bath for 15 min. After cooling, 400 µl dimethyl sulfoxide was added and the solution was centrifuged at 14500 *g* for 3 min. The absorbance of the clear pink supernatant was read at 540 nm in a plate reader (Perkin Elmer, VICTORTM X3). A standard curve was prepared with 0–1 mM malondialdehyde as the sample.

2.6.2. Stability of PL products in different pH and ethanol treatments

To test the stability of PL products (ΔUA-GalA$_n$s) in different pH environments, 20 µl of purified ΔUA-GalA$_3$ (concentration not determined, but sufficient for $AgNO_3$ staining on a PC) were dried into each of twelve small Eppendorf tubes in a SpeedVac. Then, 5 µl of solutions with pH 0–11.3 were added to the dry samples (Table 2.1) and incubated at 20°C for 30 h In the case of pH 11.3 (Na_2CO_3), 5 µl of 0.3 M acetic acid was added to neutralize the alkali. After that, the whole 25 µl from each tube was run by PC.

The effect of NaOH on PL products was also tested by incubating 2.5 µl of ΔUA-$GalA_2$ in each of three small Eppendorf tubes with 3 µl of 0, 0.1 and 1 M NaOH (dissolved in 75% ethanol) at 20°C for 16 h. The whole mixture was then neutralised with acetic acid and run by TLC.

The effect of ethanol on PL products was tested by individual treatment of 2.5 µl of each of purified ΔUA-$GalA_3$, ΔUA-$GalA_2$ and ΔUA-GalA (dried in a SpeedVac) with 3 µl of each of 0, 75 and 96% ethanol at 20°C for 16 h. After that, 3 µl of H_2O was added to each tube to fully dissolve the sugars and the whole solution was run by TLC.

The effect of Na_2CO_3 was tested by individually treating 40 µl of ΔUA-$GalA_3$ (dried in a SpeedVac) with 10 µl of 0, 0.1, 0.2 and 0.5 M Na_2CO_3 and incubating at 4℃ for 16 hours. Then, acetic acid was added to neutralize the Na_2CO_3. The whole solution was run by PC.

Table 2.1. List of buffers used to prepare the specific pH environments. A list of the substances and their concentrations used to prepare different pH environments ranging from pH 0 to pH 11.3 for testing the stability of ΔUA residues *in vitro*.

Buffer pH	Prepared by:
0.0	1.5 M TFA
1.5	0.05 M TFA
2.0	Formic acid/acetic acid/water (1:4:45)
3.0	0.5 M formic acid (adjusted with pyridine)
4.0	0.5 M formic acid (adjusted with pyridine)
5.0	0.5 M acetic acid (adjusted with pyridine)
6.0	0.1 M acetic acid (adjusted with pyridine)
7.0	0.5 M collidine (adjusted with acetic acid)
8.0	0.5 M collidine (adjusted with acetic acid)
9.0	0.5 M ammonia (adjusted with acetic acid)
10.0	0.5 M ammonia (adjusted with acetic acid)
11.3	0.1 M Na_2CO_3

2.6.3. Detecting the ΔUA moiety of PL products by thymol staining on TLC plates

A side experiment was conducted to test whether thymol is suitable to detect the ΔUA moiety of ΔUA-GalA$_n$s. Dried samples of each of ΔUA-GalA and ΔUA-GalA$_3$ (purified from preparative PC) were incubated with freshly prepared 0.5% $NaBH_4$ in 1 M NH_4OH at 20°C for 16 h to reduce the reducing terminal D-GalA moiety to an L-galactonic acid moiety (which does not stain with thymol). After that, the products were dried in a SpeedVac, re-dissolved in 1% acetic acid and analysed by TLC followed by thymol staining.

2.7. Collection of fruit samples

Date (*Phoenix dactylifera*, Khalas cultivar), and mango (*Mangifera indica*) samples were collected at three ripening stages: unripe (green), turning/mid-ripe (yellow) and ripe (brown and yellow-red, respectively) from three different randomly selected trees from a farm in Oman in June 2018. The samples were stored at –80°C for further processing. Alcohol-insoluble residue (AIR) of date and mango fruits was prepared at the food processing laboratory, The Directorate General of Agriculture and Livestock Research, Oman. Date and mango AIR were then transferred as dry powder to our laboratory.

Raspberries (*Rubus idaeus*), blackberries (*Rubus fruticosus*) and plums (*Prunus domestica*) were randomly collected at 3 ripening stages: unripe (green), turning (pale pink and red) and ripe (pink and black) from an orchard in Edinburgh, Scotland.

Ripe rowan berries (*Sorbus aucuparia*), cranberries (*Vaccinium macrocarpon*), yew arils (*Taxus baccata*), sea buckthorn (*Hippophae rhamnoides*), apple (*Malus domestica*) and pear (*Pyrus communis*) were selected randomly from different sites in and near Edinburgh, Scotland. Details of the fruit stages, source and supply condition are summarised in Table 2.2.

Samples of three lines of mutant strawberries (*Fragaria* × *ananassa*) were sent to our laboratory by Dr Sara Posé, University of Malaga, Spain, as part of a collaboration to analyse them for PL *in-vivo* action. Strawberry C1.1 was a control while strawberry A14.1.1 and A39.1.1 were transgenic lines expressing the antisense sequence of *njjs25* PL gene (Jiménez-Bermúdez *et al.* 2002).

2.8. Fruit softness measurements

Fruit softness was measured using a penetrometer (Force Gauge, PCE-FM200) with a flat 5-mm diameter probe (Fig. 2.2). The penetrometer was pushed onto the fruit against a stationary hard wall and the force (in newtons, N) required to cause 20% (of the fruit diameter) deformation on the fruit surface was recorded. Measurements were repeated three times for each fruit for 3 individually selected fruits. Measurements were taken for dates, raspberries, blackberries and plums at the 3 stages of fruit development (unripe, turning and ripe).

Table 2.2. List of fruits analysed for PL action *in vivo*. A list of all fruits used in the experiments for detecting PL *in-vivo* action products with details of their binomial names, source, developmental stage, and supply conditions.

Fruit common name	binomial nomenclature	source	Stage of development	Supply condition
Date*	*Phoenix dactylifera*	Oman	Unripe, turning & ripe	Fresh
Mango*	*Mangifera indica*	Oman	Unripe, turning & ripe	Fresh
Plums	*Prunus domestica*	Scotland	Unripe, turning & ripe	Fresh
Raspberry	*Rubus idaeus*	Scotland	Unripe, turning & ripe	Fresh
Blackberry	*Rubus fruticosus*	Scotland	Unripe, turning & ripe	Fresh
Strawberry	*Fragaria × ananassa*	Scotland	Unripe, turning & ripe	Fresh
Sea buckthorn	*Hippophae rhamnoides*	Scotland	Ripe	Fresh
Cranberry	*Vaccinium macrocarpon*	USA	Ripe	Frozen (commercial)
Yew arils	*Taxus baccata*	Scotland	Ripe	Fresh
Apple	*Malus domestica 'Bramley's Seedling'*	Scotland	Ripe	Fresh
Pear	*Pyrus communis*	Scotland	Ripe	Fresh
Rowan berry	*Sorbus aucuparia*	Scotland	Ripe	Fresh
Strawberry C1.1	*Fragaria × ananassa*	Spain	Ripe	Freeze-dried
Strawberry A14.1.1**	*Fragaria × ananassa*	Spain	Ripe	Freeze-dried
Strawberry 39.1.1**	*Fragaria × ananassa*	Spain	Ripe	Freeze-dried

*Fruit processed in Oman and then transported to our laboratory as dry AIR. Thanks to Iman Al Bahri for collecting and storing the samples and thanks to Dr. Khalid Al Shuaili at the Directorate General of Agricultural and Livestock Research (Oman) for giving access to his lab for sample processing. **Transgenic fruits with PL genes silenced.

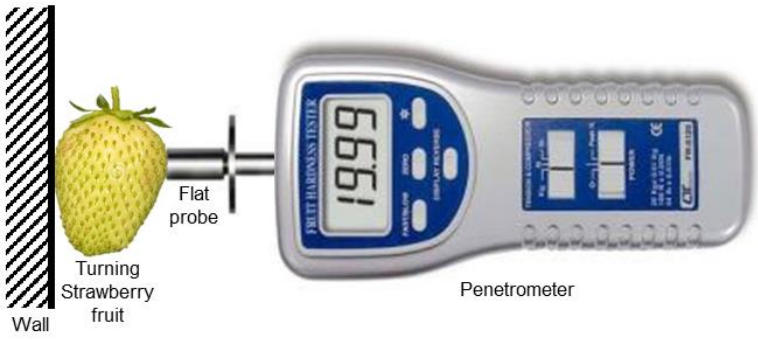

Fig. 2.2. Penetrometer used for measuring fruit softness. A penetrometer with a 5-mm flat probe was used for measuring the fruit softness. The probe was pushed against the fruit supported by a hard stationary wall behind. Readings (in newtons) were taken of the force required to cause 20% (of the total fruit diameter) surface deformation.

2.9. Preparation of alcohol-insoluble residue (AIR) from fruits

Alcohol-insoluble residue from each fruit sample was prepared as the source of cell walls. Fruit skin and seeds were removed when possible. Then, 9 g of fresh fruit was homogenised with 5% formic acid and ethanol (enough to reach final ethanol concentration of 75% considering the fruit water content). The homogenate was incubated on a wheel for 16 h and then centrifuged at 3220 *g* for 5 minutes. The supernatant (alcohol-soluble fraction) was kept for further analysis. The pellet was washed with 75% ethanol on a wheel for 1 hour, then centrifuged at 3220 *g* for 5 minutes. The supernatant was discarded. As a preparation for the AIR to be digested with EPG, the pellet (approximately 0.3 g dry weight) was de-esterified in 10 ml aqueous 0.2 M Na_2CO_3 followed by shaking and incubation at 4°C for 16 h. After that, acetic acid was added to bring the pH down to < 5. Pure ethanol was added to make a final concentration of 75% and the tube was incubated on a wheel for 1 h. The mixture was centrifuged at 3220 *g* for 5 min. The supernatant was discarded and the pellet was washed in 75% ethanol 3 times on a wheel for 1 h each as done previously. The pellet was then washed twice in acetone each for 1 h on a wheel. The pellet (AIR) was dried

and stored at room temperature. The AIR was ground using pestle and mortar before using to enhance enzyme accessibility and therefore, get maximum products. In fruit AIR preparations for studying PL and RGL action at three ripening stages, the de-esterification step with Na_2CO_3 was skipped, so the resulting AIR was not pre-saponified. Fig. 2.3 summarises the general AIR preparation procedure.

A modified method of AIR preparation was made for sea buckthorn because of its high water content which made the fruit burst when trying to remove the skin and seed. The fruit (about 22 g) was homogenised in 10 ml H_2O and containing 5% formic acid. The homogenate (about 27 ml) was filtered using a plastic sieve. Four volumes of 96% ethanol were added and the solution was incubated with stirring at 4°C for 16 h. The solution was centrifuged at 3220 *g* for 5 min. The supernatant was kept as the ethanol-soluble fraction for further analysis. The pellet was washed four times in 75% ethanol and twice in acetone all on a wheel for 1 h each as done previously. The pellet was then dried and kept as AIR.

For the mutant and wild-type strawberry AIR preparations, the first wash was done with 75% ethanol instead of the pure ethanol because the fruits were supplied freeze-dried. The number of ethanol washes was also increased to ensure getting rid of all remaining ethanol-soluble carbohydrates.

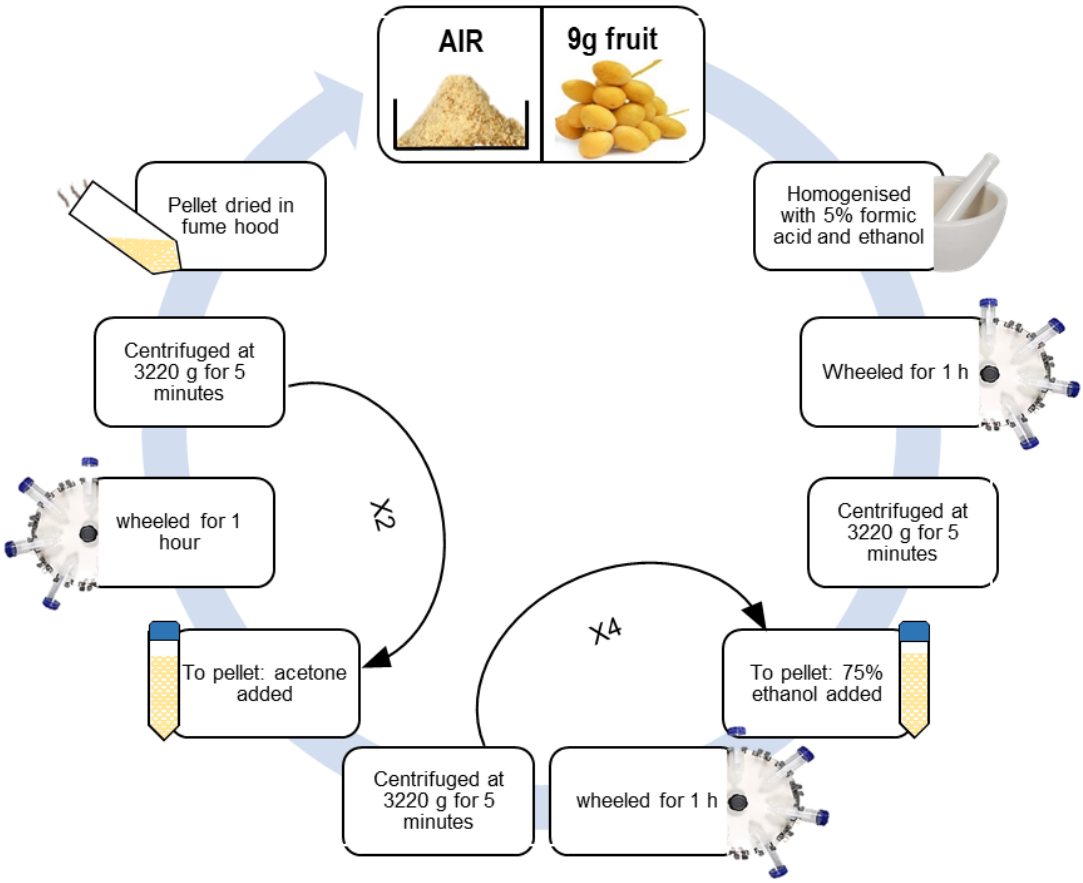

Fig. 2.3. Alcohol-insoluble residue (AIR) preparation procedure. A diagram with detailed steps of the process of AIR preparation from fruits (date as example) used in this project.

2.10. Mass spectrometry (MS)

Samples were prepared for electrospray MS analysis at a concentration of ~10 µM in acetonitrile/water (1:1). Analysis was performed on a 12-tesla SolariX 2XR Fourier-transform ion cyclotron resonance (FT-ICR) mass spectrometer (Bruker Daltonics) operating in negative mode. Each spectrum was the sum of 20 scans, with a data set size of 2 M words. Fragmentation was performed by collision-induced dissociation (CID) with argon as a neutral gas. The collision voltage was 10 V. Data interpretation was achieved with DataAnalysis 5.0 (Bruker Daltonics). Thanks to Dr. Logan Mackay for help.

2.11. Nuclear magnetic resonance (NMR) spectroscopy

A sample of putative ΔUA-GalA was prepared by complete digestion of 6.6 mg/ml HG in 3.3 U/ml PL in 50 mM CAPS (Na^+, pH 10) and 1 mM $CaCl_2$. The resulting ΔUA-GalA was purified by a preparative high-voltage paper electrophoresis, eluted in 75% ethanol and then dried. The 1D and 2D proton and carbon-13 NMR spectra were recorded on a Bruker AVANCE NEO instrument (18.8 T; 800 MHz for protons) using d_4-methanol as solvent. Proton spectra were referenced to the residual $CD_2\underline{H}OD$ signal at 3.33 ppm and carbon-13 spectra were referenced to $\underline{C}D_3OD$ at 49.0 ppm. Chemical shifts were given in ppm (δ) relative to tetramethylsilane, and scalar coupling constants (*J*) were given in Hz. Thanks to Ian Sadler and Lorna Murray for help.

2.12. Analysing the ethanol-soluble fraction of fruits

In the fruit AIR preparation methods (§2.9), the supernatant after the first ethanol wash was stored at room temperature as the source of the ethanol-soluble fraction expected to contain the monosaccharides and small oligosaccharides of the fruit. This fraction was analysed to look for possible low-molecular-weight PL and RGL action products. To start with, 10 ml of the ethanol-soluble fraction from fruits was transferred to small petri dishes, which were left open inside a fume hood for drying. After drying, the residue was re-dissolved in 1 ml H_2O and transferred to an Eppendorf tube. The solution was centrifuged at 14500 *g* for 3 min. The supernatant (~1 ml) was run by preparative HVPE (pH 2 solvent at 2.5 kV for 288 min) as a 6-cm streak on Whatman paper No. 3. After drying, the products were eluted from the paper in 75% EtOH and analysed by TLC.

2.13. Quantification of sugars from TLC plates using ImageJ software

Sugar samples run on TLC plates were quantified by reading the "intensity density" (as defined in ImageJ software) of their spots. Immediately after thymol staining, TLC plates were scanned and saved in high-resolution format (e.g. tiff; Fig. 2.4a). Using the software, the background of the TLC plate picture was inverted to black to facilitate accurate band selection (Fig. 2.4b). A rectangular area was selected covering the biggest band of interest on the plate and the same area was maintained to read the intensity density of all spots, even the faint ones. The intensity density of the background was also recorded, which was then subtracted from the intensity densities of all the bands on the same plate. For each band, the intensity density was recorded (Fig. 2.4c) and used as a measurement for estimating the amount of sugar in each band after comparing with markers of known amounts loaded on the same TLC plate.

a.

b.

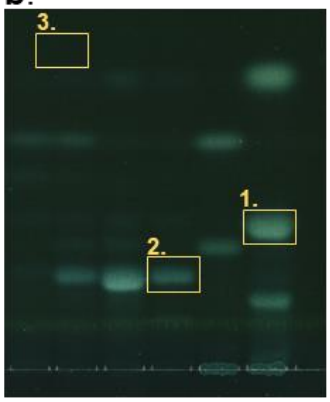

c.

	ImageJ arbitrary unit area	Intensity density	Corrected intensity density
1	0.135	8.166	4.611
2	0.135	5.979	2.424
3 (background)	0.135	3.555	—

Fig. 2.4. Quantification of products on TLC using ImageJ software. The amount of sugars (including PL and RGL products) extracted from fruit cell walls as a result of enzymic or non-enzymic hydrolysis was estimated by comparing their spots' intensity density with marker spots of known amounts using ImageJ software. **(a)** Original TLC plate stained with thymol. **(b)** The same TLC plate image after being inverted using the software; background ("3") and sugar spots selected for measurements ("1", "2") are shown. **(c)** The table created by the software reading the area selected, intensity density and corrected intensity density (subtracted from the background) of each spot. The intensity density of the background would be subtracted from the intensity density of each spot.

Chapter 3

Results

3.1. PL activity *in vitro*

3.1.1. Distinguishing PL products from EPG products

3.1.1.1. Paper and thin-layer chromatography

As PL and EPG activity both cleave de-esterified HG, it was essential to find suitable methods for distinguishing them. PL was expected to produce a range of unsaturated galacturonides with the dimeric ΔUA-GalA as the smallest product depending on the reaction duration. EPG was expected to produce a range of saturated galacturonides with GalA as the smallest product (Fig. 3.1).

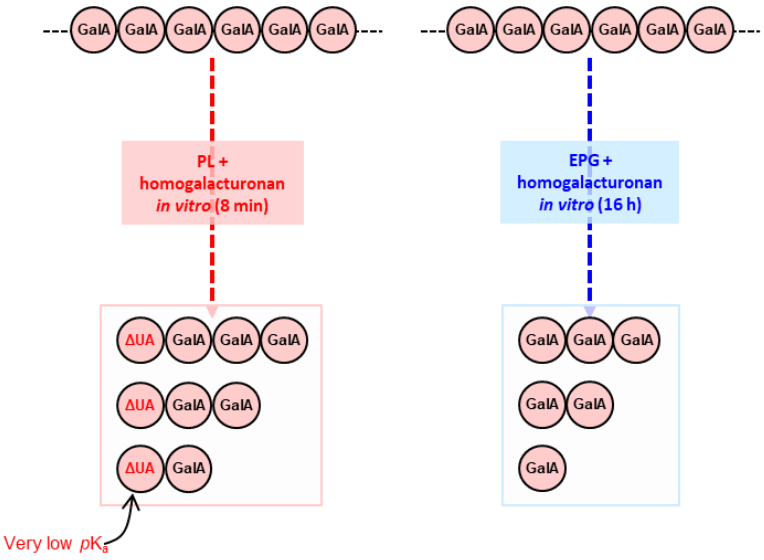

Fig. 3.1. Illustration of PL and EPG *in-vitro* products expected from de-esterified homogalacturonan (HG). PL (*left*) is expected to produce a range of unsaturated oligogalacturonides with ΔUA-GalA as the smallest product. EPG (*right*) is expected to produce a range of saturated oligogalacturonides with GalA as the smallest product.

Acting on commercial de-esterified homogalacturonan (HG), PL produced dimeric, trimeric and tetrameric ΔUA-GalAs after eight minutes as visualised on a thymol-stained TLC plate (Fig. 3.2a). On the other hand, EPG produced saturated monomeric,

dimeric and trimeric GalAs after 16 hours reaction with commercial HG. These products were later used as markers for detecting PL and EPG *in-vivo* products.

PL and EPG products were run on two types of silica-gel TLC plates: aluminium-backed F254 (with fluorescent indicator) and plastic-backed (without fluorescent indicator). PL products, especially ΔUA-GalA and ΔUA-$GalA_2$ were very well resolved from each other and from GalA and $GalA_2$ on the F254 TLC plates (Fig. 3.2a), whereas in normal plastic-backed plates, PL products were less separated from each other and from EPG products (Fig. 3.2b). Therefore, the F254 plates were used for separating oligogalacturonides throughout this project. No enzyme controls were run in this experiment.

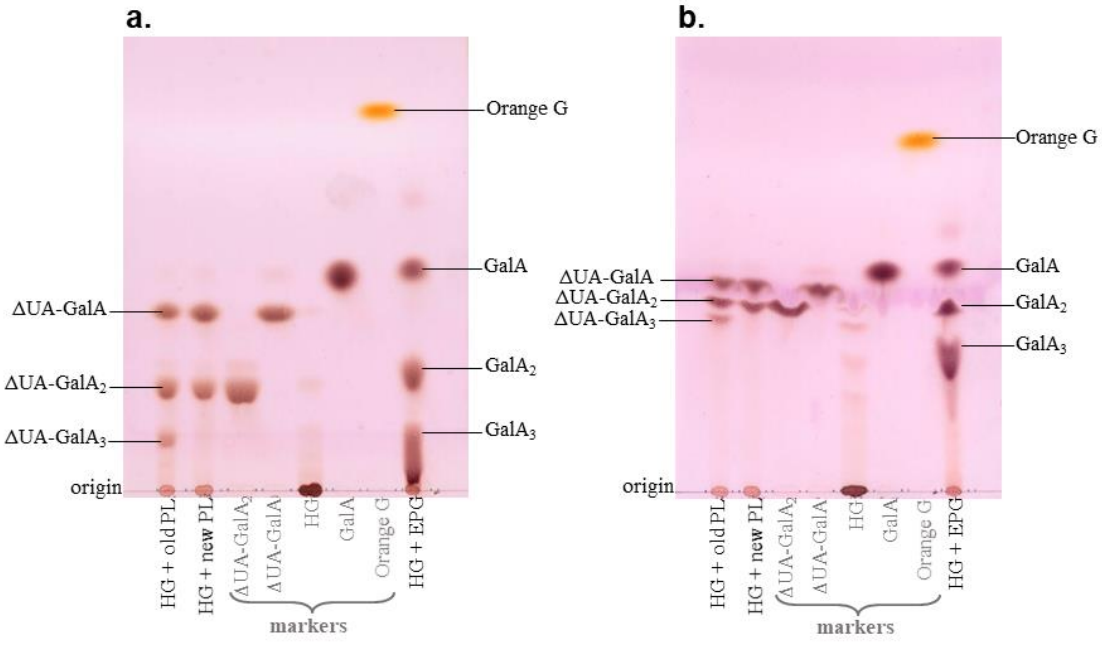

Fig. 3.2. PL and EPG *in-vitro* products from commercial (de-esterified) HG. The PL reaction mixture contained PL at 3.3 U/ml and the substrate HG at 6.6 mg/ml, in 50 mM CAPS buffer (Na^+, pH 10.0) with 1 mM $CaCl_2$. The reaction was stopped after 8 min by addition of 0.2 volumes of formic acid. The EPG reaction contained EPG at 10 U/ml in PyAW (1:1:98, pH 4.7) with 0.5% chlorobutanol and 20 mg/ml HG. The reaction mixture was incubated with rotation on a wheel at 20°C for 16 h. **(a)** Aluminium-backed 'F254' silica-gel TLC plate of PL and EPG products from commercial (de-esterified) HG. **(b)** The same products and markers as in (a) but loaded on a plastic backed silica-gel TLC plate. Old and new PL refer to expired and new stock of PL tested in this experiment, respectively. Both plates were stained by thymol.

On the other hand, both PL and EPG products with the same number of GalA residues co-migrated on paper chromatography (PC) after 30 h in EAW (10:5:6) regardless of the presence of the ΔUA residues in PL products (Fig. 3.3a). However, PL and EPG products were very well resolved by TLC (Fig. 3.3b). These results confirmed that TLC is better for separating PL products (unsaturated oligogalacturonides, ΔUA-$GalA_n$s) from EPG products ($GalA_n$s).

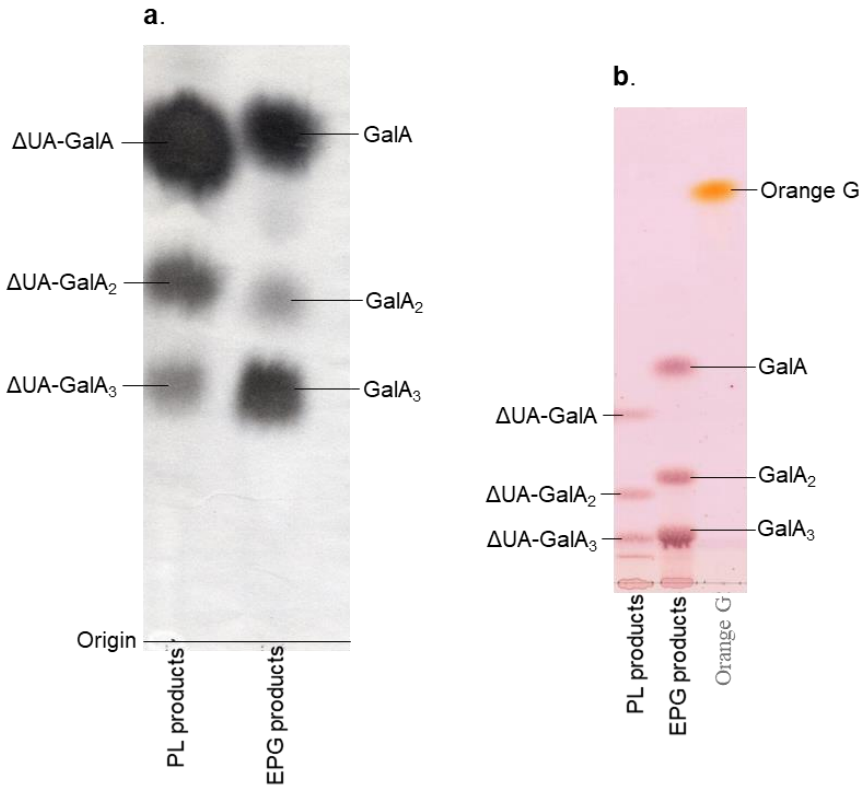

Fig. 3.3. Paper and thin-layer chromatograms of pectate lyase and EPG products from commercial (de-esterified) HG. PL products were from 6.6 mg/ml HG, after incubation in presence of 50 mM ammonium acetate (pH 10) 1mM $CaCl_2$ and 3.3 U PL at room temperature for 8 minutes. EPG products were from 20 mg/ml HG after incubation with 10 U/ml EPG in PyAW (1:1:98, pH 4.7, containing 0.5% chlorobutanol) at 20°C for 16 h. **(a)** PC run in EAW (10:5:6) for 30 hours and stained by $AgNO_3$. **(b)** TLC run in BAW (2:1:1) and stained by thymol.

3.1.1.2. Paper electrophoresis separates the acidic PL products from EPG products

Paper electrophoresis at pH 2.0 showed a good discrimination between PL and EPG products, providing an efficient method to distinguish these two enzymes' products. PL products ran faster than EPG products owing to the low pK_a of the ΔUA residue (Fig. 3.4a). The pK_a value for the monomeric GalA is reported to be 3.51, but no data about the pK_a value of monomeric ΔUA was found (Kohn and Kováč 1978). A pK_a values of 3.51 for GalA Me-glycoside and a value of 3.10 for ΔUA Me-glycoside were reported (Kohn and Kováč 1978), which seemed to be more relevant, modelling the residue in ΔUA-GalA and GalA-GalA) than free ΔUA and GalA. Regardless of the number of GalA residues (ΔUA-$GalA_{1–3}$), PL products ran to a specific region of the electrophoretogram, giving a UV-absorbing spot (short-wavelength (254 nm) UV, characteristic of the ΔUA residue), while EPG products ran slower, with monomeric GalA being the slowest-migrating acidic product. Electrophoresis at pH 2.0 thus effectively gave a group separation of saturated from unsaturated oligogalacturonides. In contrast, during electrophoresis at pH 6.5 (at which pH all –COOH groups are almost fully ionised; Fry, 2020), $GalA_2$ and ΔUA-GalA (which both possess two –COOH groups and are of similar molecular weight) were not well separated (Fig. 3.4b). Therefore, electrophoresis at pH 2.0 is recommended as the preferred method for isolating PL 'fingerprints'.

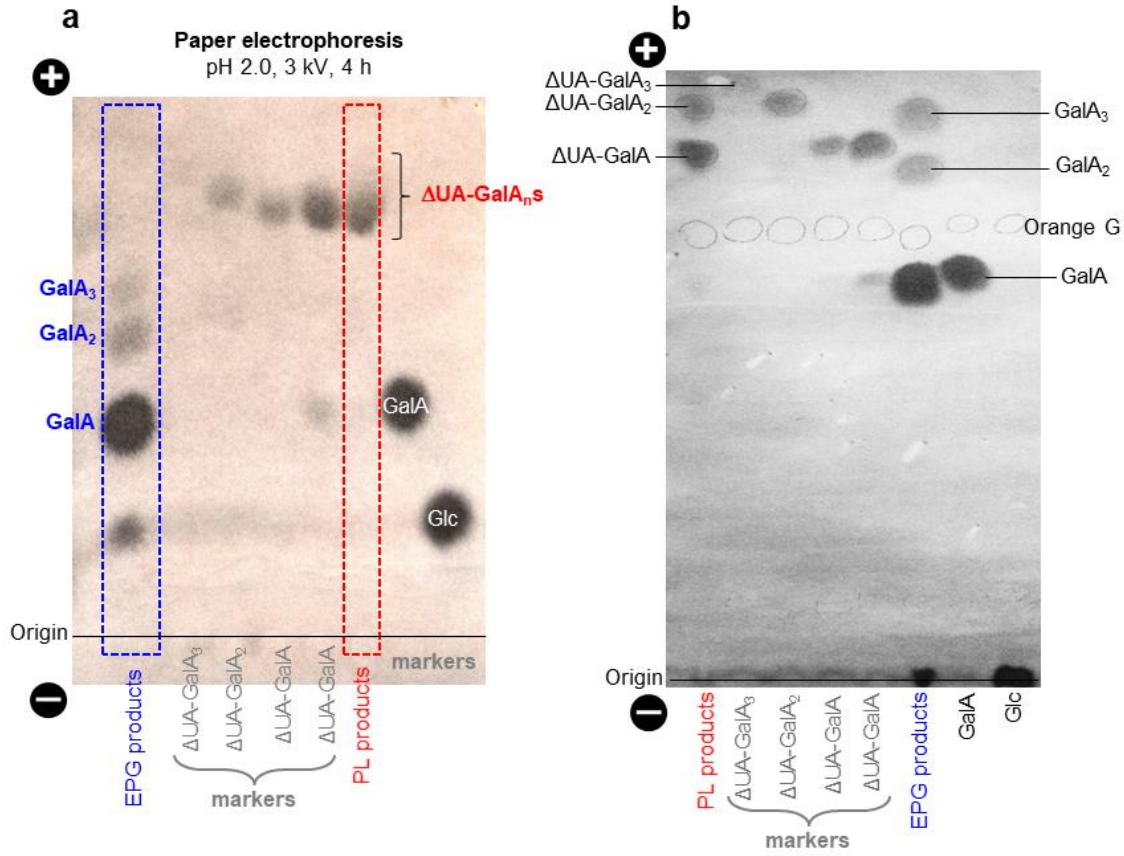

Fig. 3.4. Paper electrophoresis for separating PL products from EPG products. Products formed from HG by EPG digestion and PL digestion. EPG (10 U/ml) was incubated at 20°C for 16 h with HG (20 mg/ml) in pyridine/acetic acid/water (1:1:98 by vol., containing 0.5% chlorobutanol), pH 4.7, yielding $GalA_3$, $GalA_2$ and GalA. PL (3.3 U/ml) was incubated at 20°C for 10 min with HG (6.6 mg/ml) in 50 mM CAPS buffer (Na^+, pH 10) containing 1 mM $CaCl_2$, yielding $\Delta UA\text{-}GalA_3$, $\Delta UA\text{-}GalA_2$ and ΔUA-GalA. **(a)** Products were electrophoresed at pH 2.0 (3 kV, 4 h), alongside markers. **(b)** Electrophoresis at pH 6.5 (4 kV, 68 min) of comparable markers. Each sample contained an internal marker (Orange G), which was marked in pencil prior to staining as it got washed out during staining. Both electrophoretograms were stained with $AgNO_3$.

3.1.2. Investigating PL products from commercial HG

3.1.2.1. Thiobarbituric acid assay for detecting PL products in vitro

The thiobarbituric acid (TBA) assay was conducted to estimate the molar concentration of the ΔUA residues produced as a result of PL activity on commercial HG *in-vitro* using a malondialdehyde-equivalent standard curve (Fig. 3.5a). The estimated concentration of ΔUA residues increased with time up to at least 128 minutes

(Fig. 3.5b). After reaction completion, (four hours as observed in Fig. 3.8 where all HG was converted to ΔUA-GalA), the concentration of ΔUA was estimated (using the standard curve) to be 0.03 mM.

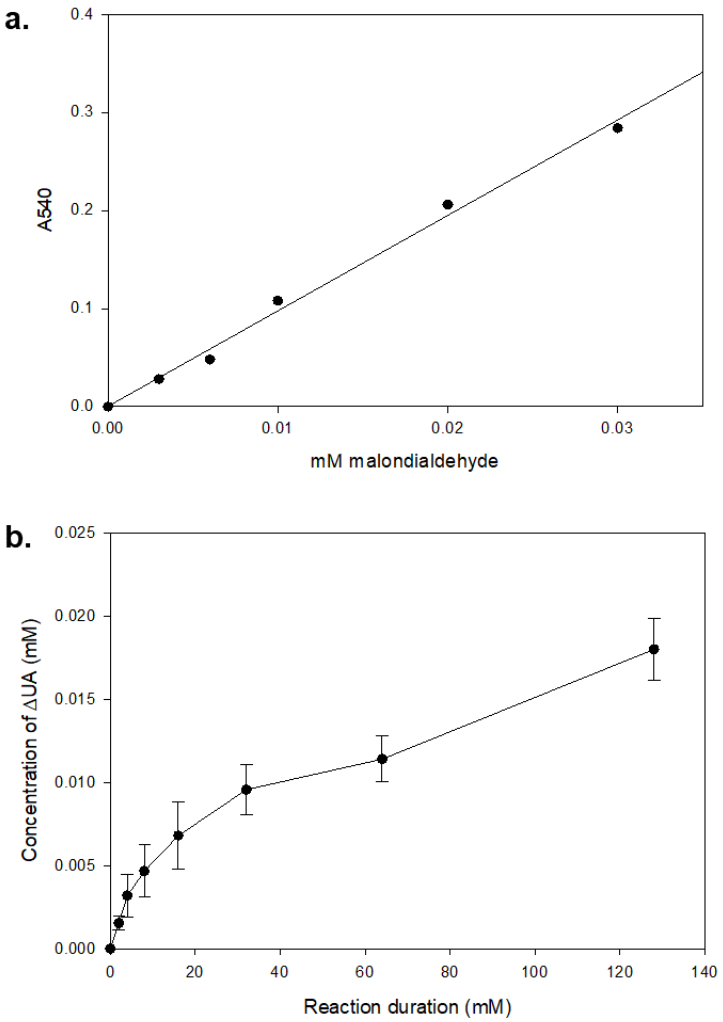

Fig. 3.5. Formation of ΔUA residues as a result of PL action on commercial HG *in vitro*. The reaction mixture contained 6.6 mg/ml HG, 50 mM CAPS, 1 mM $CaCl_2$ and 3.3 U PL and incubated at 20°C. The reaction was stopped at intervals by addition of 0.2 volumes formic acid. The TBA assay was then conducted on 5 µl of PL products from each time-point. **(a)** A standard curve of the measured absorbance at 540 nm of 0–1 mM malondialdehyde following a TBA assay. **(b)** The estimated concentration of ΔUA (mM of malondialdehyde-equivalent) in PL products at each time point.

3.1.2.2. Fluorescent sulforhodamine B versus thymol for TLC staining

As the unsaturated PL products (containing the ΔUA residues) absorb UV light and appear as dark spots when exposed to short wavelength (254 nm) UV light, it was

worth trying to stain the TLCs with a fluorescent stain and test their sensitivity to UV light. The fluorescent dye incorporated on the F254 TLC plates was partially washed up by the BAW (2:1:1) solvent usually used for running the samples on the TLC plates, so it was hard to rely on the dark spots seen in this method by exposing the plates to UV light. In addition, UV light seemed to be a less sensitive detection method for low concentrations of the PL products (Fig. 3.6a and b).

Sulforhodamine B was tested as a fluorescent stain instead of the fluorescent dye incorporated on the F254 TLC plates. After running 2 TLC plates with identical samples of PL products on BAW (2:1:1) in the same tank for 7 hours, one plate was stained with thymol (Fig. 3.6c), the other with sulforhodamine B (Fig. 3.6d). The sulforhodamine B stain seemed less sensitive to low concentrations of samples compared to thymol, which clearly stained the spots with equivalent concentrations. It was less sensitive than the fluorescent dye incorporated on the F254 TLC plates. Therefore, thymol is used to stain the TLC plates throughout this project.

3.1.2.3. Different sizes of ΔUA-GalA$_n$s produced at different PL concentrations and reaction durations

In order to understand PL activity, it was important to test different enzyme concentrations and reaction durations. The size of PL products (from commercial de-esterified HG) was highly dependent on both parameters. Keeping the reaction duration constant, lower enzyme concentrations produced bigger unsaturated oligo-galacturonides compared to higher concentrations (Fig. 3.7). On the other hand, keeping the enzyme concentration constant, longer reaction durations produced smaller unsaturated products. The smallest PL product was the unsaturated dimer

(ΔUA-GalA) which was the only product detected after 4 hours of reaction (Fig. 3.8). Producing a range of ΔUA-GalA$_n$s was helpful to use them as markers and to further investigate how EPG and Driselase would hydrolyse them. No enzyme controls were run in this experiment.

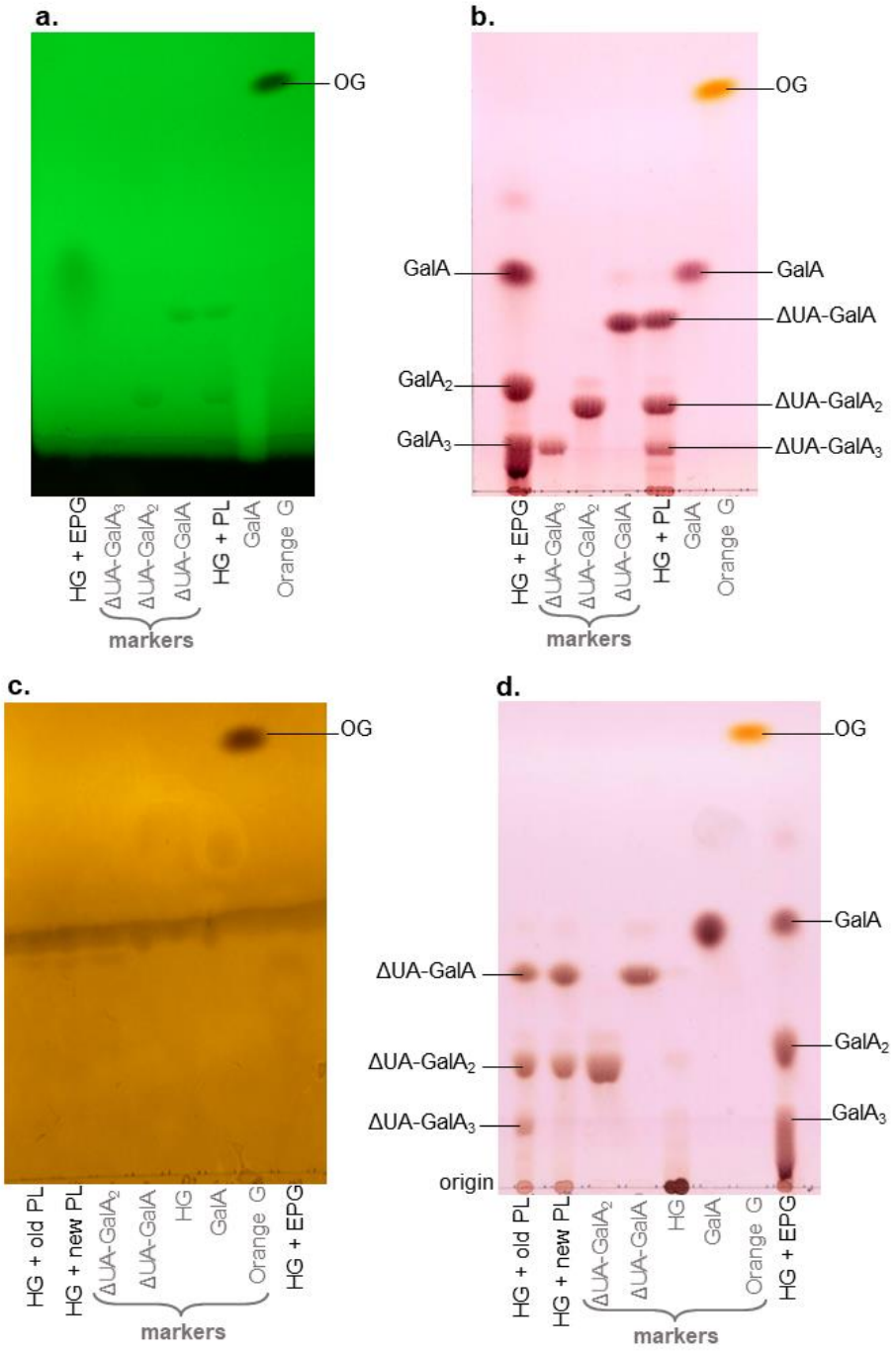

Fig. 3.6. Thymol and sulforhodamine stained TLCs of PL and EPG products from commercial (de-esterified) HG. PL and EPG products were prepared as in Fig. 3. **(a)** and **(b)** are scans of the same TLC plate where in (a) the plate was exposed to short wavelength UV and in (b) it was stained with thymol. **(c)** and **(d)** are duplicate plates where (c) was stained with sulforhodamine B and (d) was stained with thymol. Both TLCs were run in BAW (2:1:1).

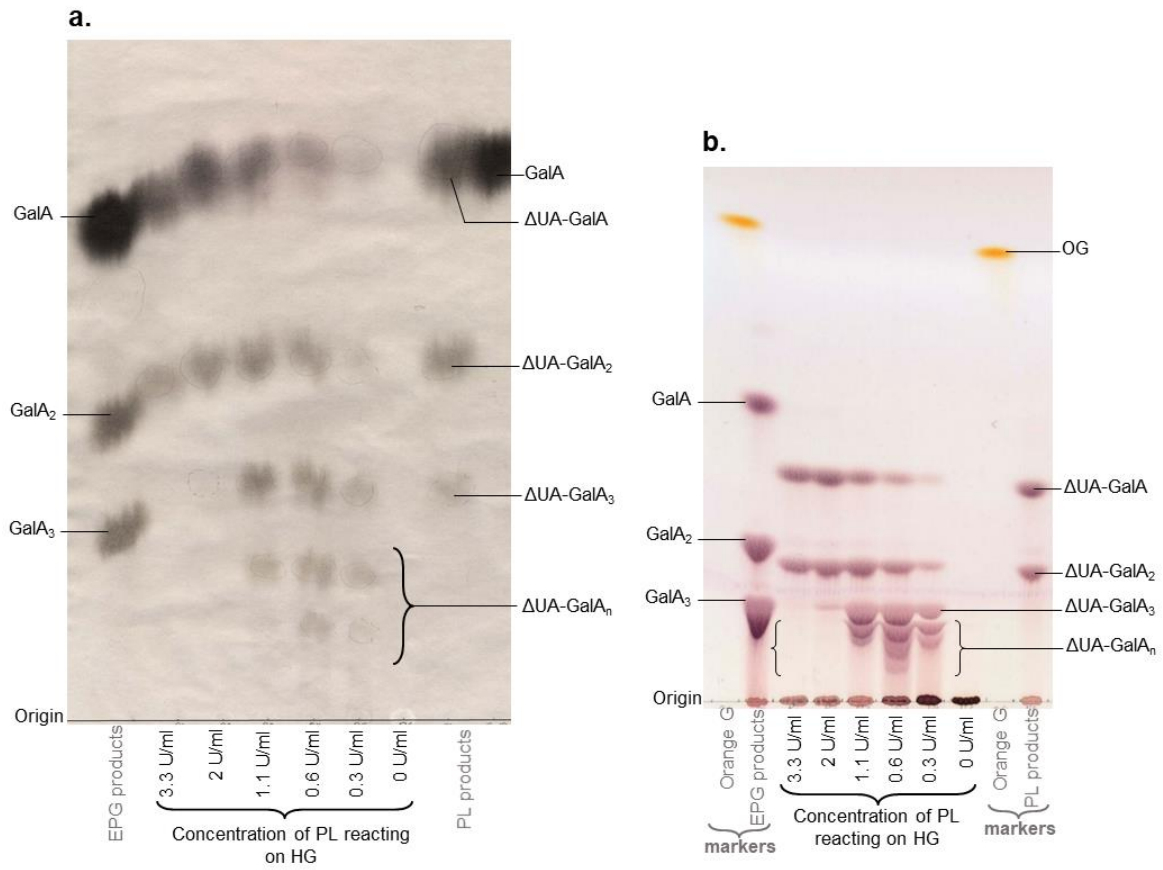

Fig. 3.7. Paper and thin-layer chromatograms of pectate lyase products from incomplete digestions. PL products from reactions set with 3.3 down to 0 U/ml final enzyme concentrations on 6.6 mg/ml HG in presence of 50 mM ammonium acetate and 1mM $CaCl_2$. Reactions were stopped after 30 minutes by 0.2 volumes formic acid. **(a)** PC run in EAW 10:5:6 for 30 h and stained by $AgNO_3$. All spots of PL products and ΔUA-$GalA_n$s markers are UV absorbing (pencilled circles). **(b)** TLC run in BAW 2:1:1, 2 ascents and stained with thymol.

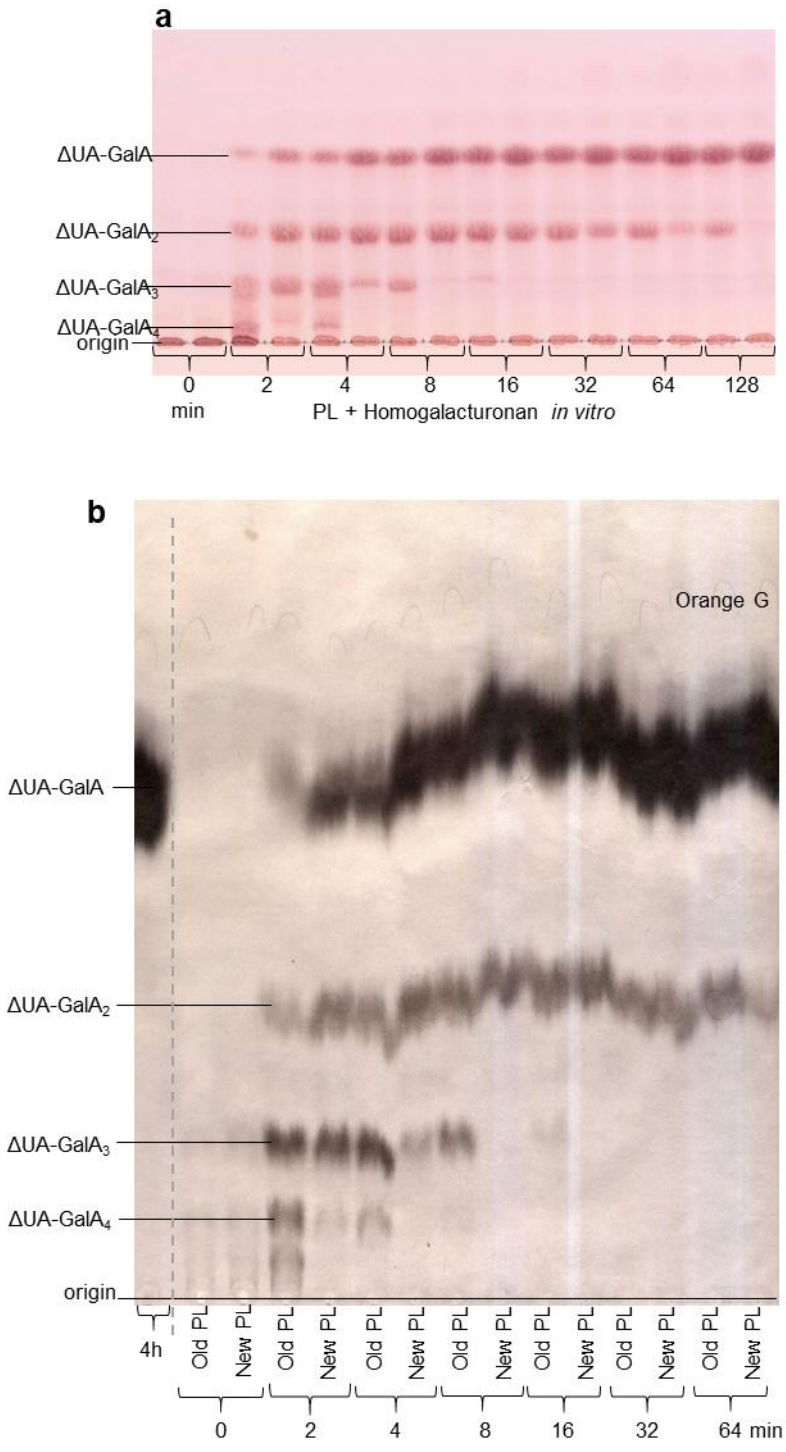

Fig. 3.8. Time-course of action of pectate lyase on commercial de-esterified HG *in vitro*. Products formed from HG by digestion with commercial PL for 0 min to 4 h. The reaction mixture was prepared as in Fig. 3.2. **(a)** TLC run in BAW 2:1:1 and stained with thymol. Each time-point is in duplicate, using old (expired) and new PL stocks. **(b)** Paper chromatogram run in ethyl acetate/acetic acid/water (10:5:6) for 30 h and stained with $AgNO_3$.

3.1.2.4. Purification of ΔUA-GalA$_3$, ΔUA-GalA$_2$ and ΔUA-GalA from PL digestion products

A pure stock of each of ΔUA-GalA$_3$, ΔUA-GalA$_2$ and ΔUA-GalA (all UV absorbing) was eluted from a preparative PC of PL products which appeared as dark streaks when exposed to short-wavelength (245 nm) UV light. (Fig. 3.9). The eluates were assayed by TBA, which detected the unsaturated products in each fraction. The data showed three peaks corresponding to ΔUA-GalA$_3$, ΔUA-GalA$_2$ and ΔUA-GalA (Fig. 3.10). The fractions with the same compound were pooled as a pure stock of each and used for further experiments.

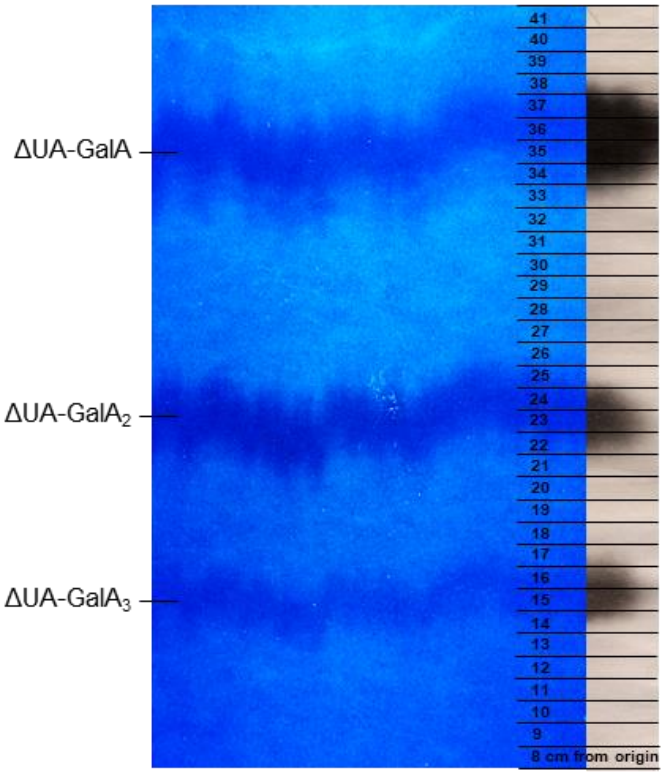

Fig. 3.9. Preparative paper chromatogram of pectate lyase products. Products from 6.6 mg/ml HG, after incubation in presence of 50 mM ammonium acetate, 1mM $CaCl_2$ and 3.3 U PL at 20°C for 15 min. The reaction was stopped by adding 0.2 volumes of formic acid. Products were loaded at 60 µl/cm and run in EAW (10:5:6) for 30 h. The right-hand fringe of the paper was stained with $AgNO_3$, visualising the products. The unstained paper (viewed under short-wave UV) was cut into 1-cm strips and solutes were eluted as a pure stock of each.

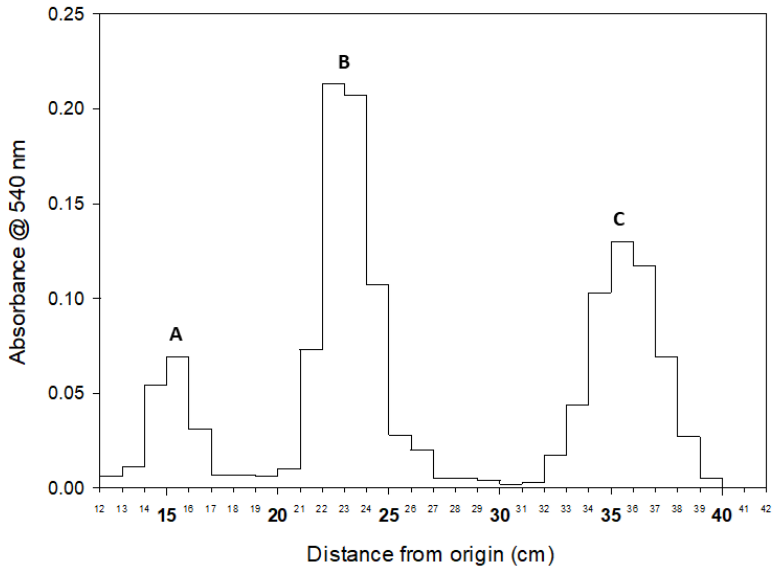

Fig. 3.10. Quantification of pectate lyase products eluted from a preparative paper chromatogram. Products from Fig. 10 were assayed by TBA and the absorbance was read at 540 nm. The three peaks, A, B and C, correspond to ΔUA-GalA$_3$, ΔUA-GalA$_2$ and ΔUA-GalA respectively.

3.1.2.5. Stability of ΔUA-GalA$_n$s at different pH and ethanol treatments

A few tests were conducted to study the stability of PL products under different conditions, which will help decide on the appropriate methods for extracting and handling them *in vivo*. Purified PL products (from the preparative PC) were found stable under treatments with 75 and 96% ethanol with no detectable signs of degradation as visualized on TLC (Fig. 3.11).

The ΔUA-GalA$_n$s also proved to be highly stable under various pH conditions. Samples of purified ΔUA-GalA$_3$ incubated in various buffers (pH 0-10) remained intact, confirming its stability under a wide range of acidic and alkali conditions. However, harsh alkali treatment at pH 11.3 could have caused a slight degradation creating a new spot, faintly stained with $AgNO_3$ (Fig. 3.12).

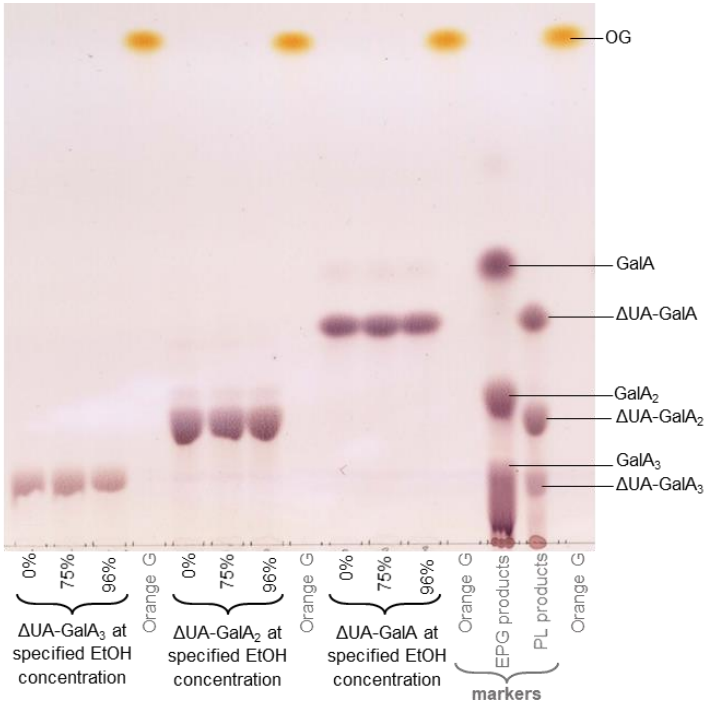

Fig. 3.11. Thin-layer chromatography of PL products treated with various ethanol concentrations. Samples of PL products (ΔUA-GalA$_3$, ΔUA-GalA$_2$ and ΔUA-GalA) previously purified from preparative PC (refer to Fig. 3.9) were dried in a SpeedVac, re-suspended in 0, 75 or 96% ethanol solutions, and incubated at 20°C for 16 h. The TLC was run in BAW 2:1:1 and stained with thymol.

Treatments with certain concentrations of NaOH and Na_2CO_3, routinely used to de-esterify sugars, seemed to cause partial degradation of PL products. Treatment with ≥ 0.1 M NaOH caused partial break-down of ΔUA-GalA$_2$ to ΔUA-GalA showed by clear reduction in $AgNO_3$ staining intensity on PC (Fig 3.13a). As the thymol stain seemed to be more sensitive, it was clear that even mild NaOH treatment (0.1 M) caused degradation of ΔUA-GalA$_2$ to ΔUA-GalA and maybe some other products undetectable by thymol as the amount of the resulting ΔUA-GalA seemed much less that the amount lost from the ΔUA-GalA$_2$ substrate shown on TLC (Fig. 3.13b). At 1 M NaOH, the substrate was almost completely degraded to unknown products (not detectable by thymol).

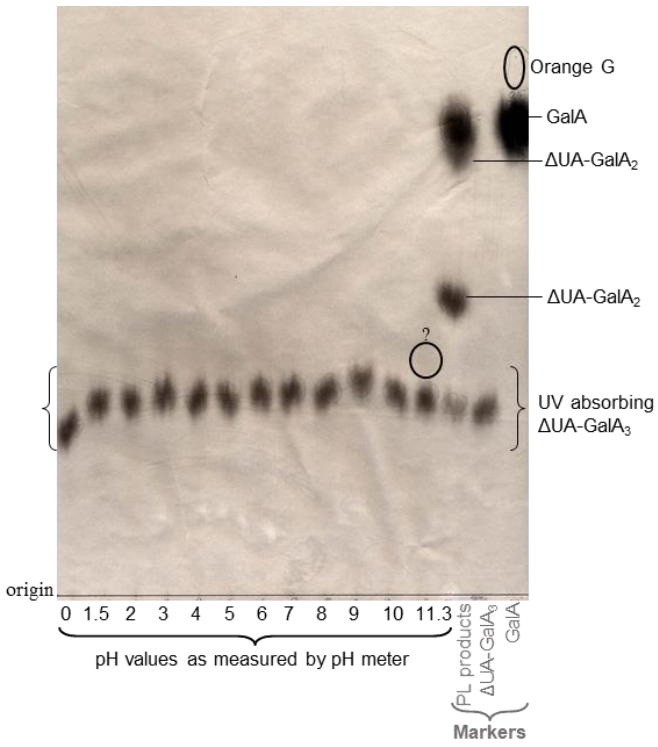

Fig. 3.12. Paper chromatogram of PL products incubated at various pH conditions. Samples of PL products (ΔUA-GalA$_3$) previously purified from preparative PC (refer to Fig. 3.9) were dried in a SpeedVac, re-dissolved in 20 µl of the specified pH buffers (0-11.3; refer to table 2.1 for buffer ingredients) and incubated at 20°C for 30 hours. PC was run in EAW (10:5:6) for 30 h and stained with $AgNO_3$. All the ΔUA-GalA$_3$ spots were UV absorbing (pencilled circles).

On the other hand, Na_2CO_3 seemed to be less destructive PL products. Treatments with 0.1-1 M Na_2CO_3 had no detectable effects on ΔUA-GalA$_3$ (Fig. 3.14). These results suggested that for future de-esterification experiments of pectin to study PL products, NaOH should be avoided because of its effects on them. Instead, 0.2 M Na_2CO_3 could be used. A previous study by Chormova *et al.* (2014) used 1 M Na_2CO_3 for pectin de-esterification prior to EPG digestion, however, a lower concentration (0.05 M) was used by Wakabayashi *et al.* (2003) which decreased the level of pectin-methylesters from 74% to 4% suggesting that a concentration of 0.2 M should be good enough to de-esterify the fruits' AIR.

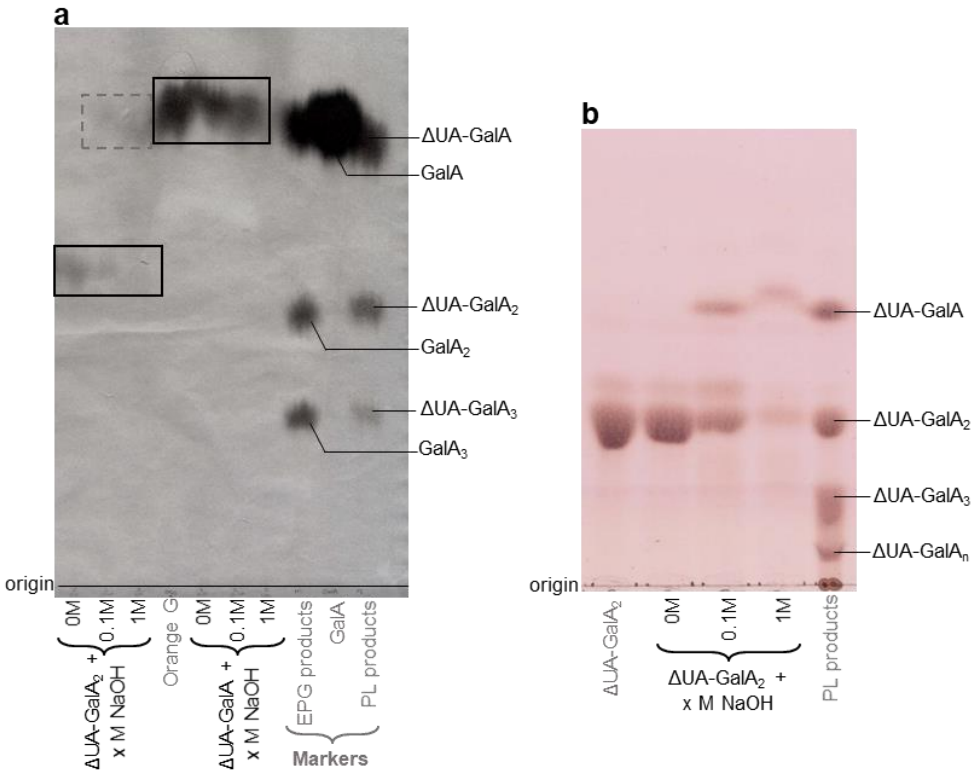

Fig. 3.13. PC and TLC of PL products treated with NaOH. Samples of PL products (ΔUA-GalA_2 or ΔUA-GalA) previously purified from preparative PC (refer to Fig. 3.9) were dried in a SpeedVac, re-dissolved in 0, 0.1 or 1 M NaOH at 20°C for 16 h **(a)** PC run in EAW (10:5:6) for 30 h and stained with $AgNO_3$. **(b)** TLC run in BAW 2:1:1 and stained with thymol.

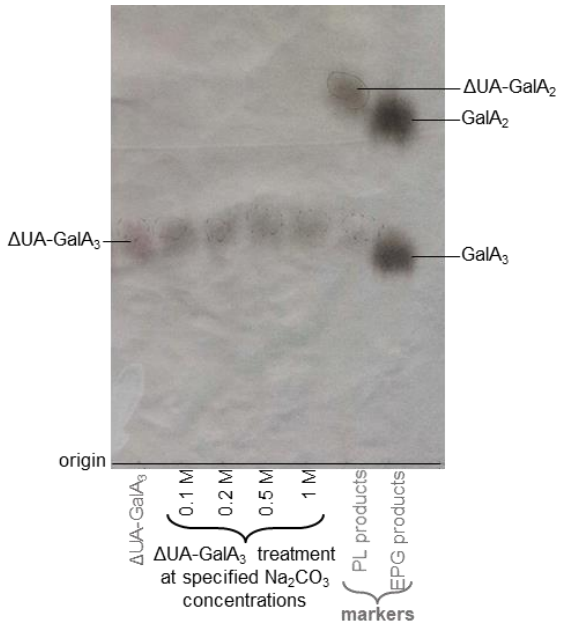

Fig. 3.14. Paper chromatography of PL products treated at various Na_2CO_3 concentrations. Samples of 20 µl of ΔUA-GalA_3 were dried in a Speed Vac, re-dissolved in 0.1–1.0 M Na_2CO_3 and incubated at 4˚C for 16 h. Acetic acid was added after that to neutralize the solution and samples were run by PC in EAW (10:5:6) for 30 h and stained with $AgNO_3$. All the ΔUA-GalA_3 spots (pencilled dotted lines) are UV absorbing.

In regards to the best concentration of Na_2CO_3 which could be used to de-esterify cell wall pectin, the amount of the resulting sodium acetate (CH_3COONa) from the neutralisation with acetic acid (CH_3COOH) could be detrimental to the quality of electrophoretic separation of the ΔUA-$GalA_n$s as it is a neutral salt that could prevent the movement of such acetic products. This was tested by loading various amounts of ΔUA-GalA (treated with 0.2 M Na_2CO_3 and neutralized by acetic acid) on Whatman number 3 paper and conducting electrophoresis at pH 2. The products containing 6.56 mg CH_3COONa ran nicely on the paper electrophoretogram (Fig. 3.15). Increasing the amount to 26 mg caused a smear of the ΔUA-GalA streak which would cause the spread of the ΔUA-GalA in more fractions (when the samples eluted) resulting in contamination with other products and inaccuracy of quantification in future experiments with fruit pectin.

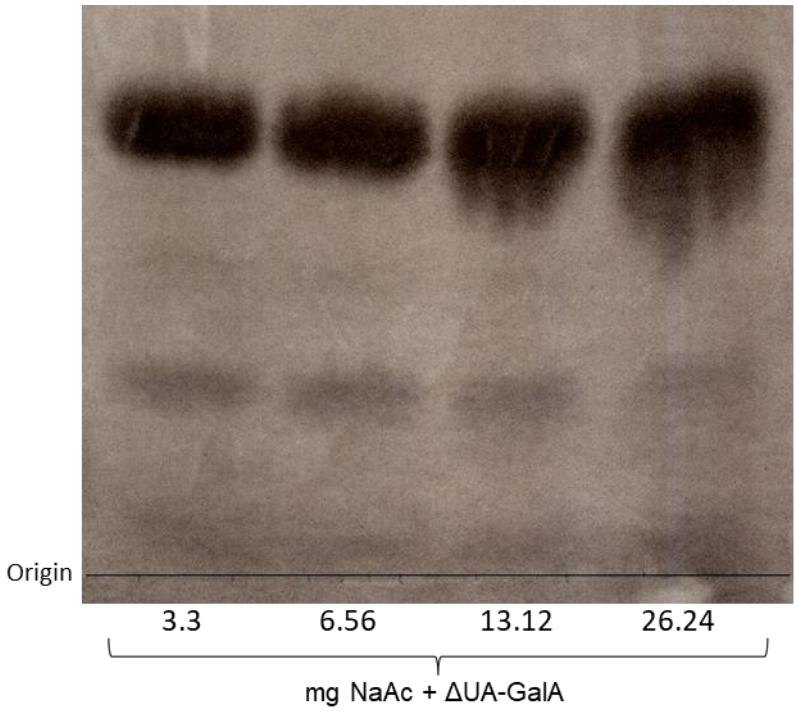

Fig. 3.15. Paper chromatography of ΔUA-GalA with various amounts of sodium acetate (NaAc). Four samples of 100 µl of ΔUA-GalA each were dried in a Speed Vac, re-dissolved in 100, 200, 400 or 800 µl of 0.2 M Na_2CO_3 and incubated at 4˚C for 16 h. Enough acetic acid was added after that to neutralize the solution and samples were run by PC as 3-cm streaks in EAW (10:5:6) for 30 h and stained with $AgNO_3$. The total amounts of NaAc resulted from the neutralization process are as indicated.

3.1.3. Endo-polygalacturonase (EPG) and Driselase digestion of PL products

3.1.3.1. EPG trims large PL products to a mixture of smaller products

It was important to understand how EPG would hydrolyse HG that had been briefly digested with PL to know the smallest product which will help to understand EPG's behaviour *in vivo*. In addition, this information will also help to decide whether to use EPG or Driselase prior to extracting PL fingerprint as an evidence of PL *in-vivo* action to make sure of getting a single, small, stable unsaturated PL product.

The larger PL products showed a high susceptibility to further digestion by EPG. PL products from a brief digestion (2 min) of commercial (de-esterified) HG with commercial PL (as in Fig. 3.8) followed by a time-course digestion with EPG showed a gradual appearance of the products and the best reaction time for the smallest products to be produced. EPG digestion for up to one week at 20°C produced a major spot of the unsaturated trimer (ΔUA-$GalA_2$) which was gradually degraded to the unsaturated dimer (ΔUA-GalA). In addition, the expected saturated GalA, $GalA_2$ and $GalA_3$ were detected as a result of the EPG hydrolysis in sites close to the reducing termini of PL products (Fig. 3.16a). The same products were observed after EPG digestion of PL products from HG using lower PL concentrations (Fig. 3.16b, using PL products showed in Fig. 3.7b). No enzyme controls were run in this experiment.

Paper electrophoresis was used to separate the highly acidic unsaturated products from the saturated GalA, $GalA_2$ and $GalA_3$. EPG products from HG that had been briefly digested with PL were electrophoresed at pH 2. The products were eluted (from the electrophoretogram) and analysed by TLC, in which all the products were confirmed by their fraction number (paper strip number, Fig. 3.17a) and position on TLC (Fig. 3.17b).

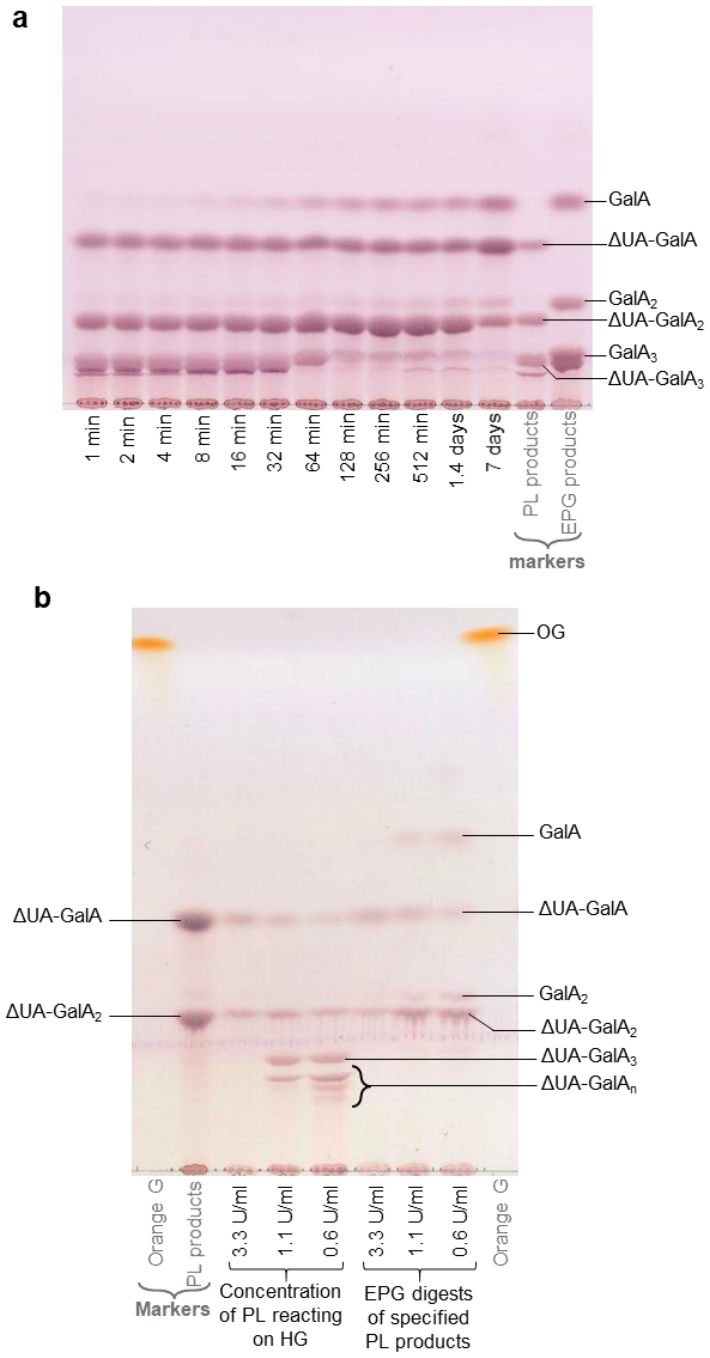

Fig. 3.16. EPG digestion of PL incomplete digestion products. (a) TLC of products formed by EPG (1 min – 7 days) from commercial (de-esterified) HG that had previously been digested with commercial PL for 2 min. The PL pre-treatment reaction was prepared as in Fig. 3.2. Products were then dried in a SpeedVac and digested in a time-course for up to 1 week with EPG at 10 U/ml in PyAW containing 0.5% chlorobutanol. TLC was run in BAW 2:1:1 and stained with thymol. **(b)** TLC of PL products from reactions set with 3.3 (standard), 1.1, or 0.6 U/ml final enzyme concentrations on 6.6 mg/ml HG in presence of 50 mM ammonium acetate and 1mM $CaCl_2$. Reactions were stopped after 30 min by addition of 0.2 volumes formic acid. Products were dried in a SpeedVac and then digested with EPG as in (a). TLC was run in BAW 2:1:1, two ascents.

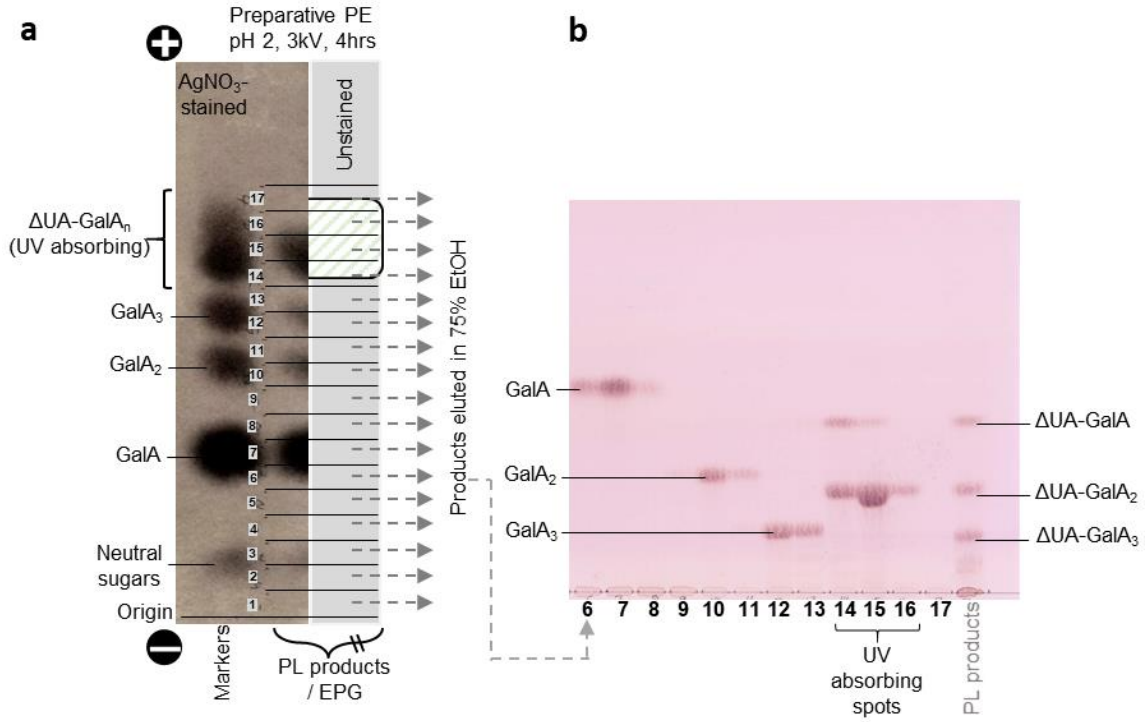

Fig. 3.17. Isolation of PL fingerprint from PL-pre-treated HG further digested with EPG. Products were formed from commercial (de-esterified) HG by digestion with commercial PL for 2 min as in Fig. 3.2. Products were then dried in a Speed Vac and digested for 16 h with EPG at 10 U/ml in PyAW containing 0.5% chlorobutanol. **(a)** The products were loaded as a 20-cm streak on Whatman No. 3 paper and electrophoresed at pH 2 (3 kV for 4 h). The left-hand fringe of the paper plus the markers were stained with $AgNO_3$, visualising the products. The major portion, only part of which is shown (in grey), was not stained; shading (/////) indicates a UV-absorbing band. The whole unstained portion was cut into seventeen 1-cm strips and products were eluted. **(b)** Eluates from strips 6–17 were run by TLC in BAW (2:1:1) alongside marker mixtures and stained with thymol.

3.1.3.2. Driselase trims PL products to the disaccharide (ΔUA-GalA)

A time-course digestion of PL products (from a brief digestion (2 min) of commercial HG with commercial PL; Fig. 3.8) with 0.05% Driselase at 37°C for one week showed the gradual appearance of hydrolysis products and the best reaction time for the smallest products to be produced. Driselase produced predominant spots of monomeric GalA and the unsaturated dimer (ΔUA-GalA) already after 8 hours, as visualised on TLC (Fig. 3.18). Bands of faster migrating products than GalA appeared with time

which might be a result of Driselase self-digestion or break-down of GalA or ΔUA-GalA after a long incubation with Driselase.

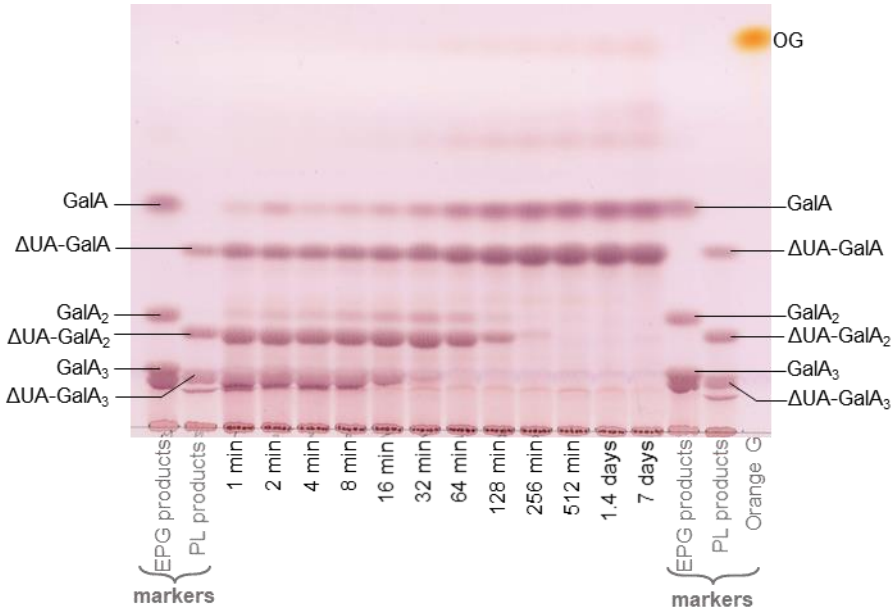

Fig. 3.18. Driselase time-course digestion of PL incomplete digestion products. Products were formed from commercial (de-esterified) HG by digestion with commercial PL for 2 min as in Fig. 3.2. Products were then dried in a Speed Vac and digested with 0.05% Driselase in PyAW (containing 0.5% chlorobutanol), pH 4.7, at 37°C for up to 1 week. The TLC was run in BAW 2:1:1 and stained with thymol.

As a major conclusion so far, Driselase, producing a single unsaturated product, is therefore the preferred agent for isolating a specific PL 'fingerprint' (ΔUA-GalA) from plant cell walls that had potentially been acted on *in vivo* by endogenous PL. Furthermore, the possibility that Driselase or even EPG may possess PL activity which would generate ΔUA-GalA_ns even from unmodified homogalacturonan, was proven not to be the case (Fig. 3.19). Driselase and EPG digestion of commercial HG generated only saturated products. Driselase produced a spot of GalA as the only final product visualised on TLC, and EPG digestion produced GalA, $GalA_2$ and $GalA_3$ (Fig. 3.19a). No enzyme controls were run in this experiment.

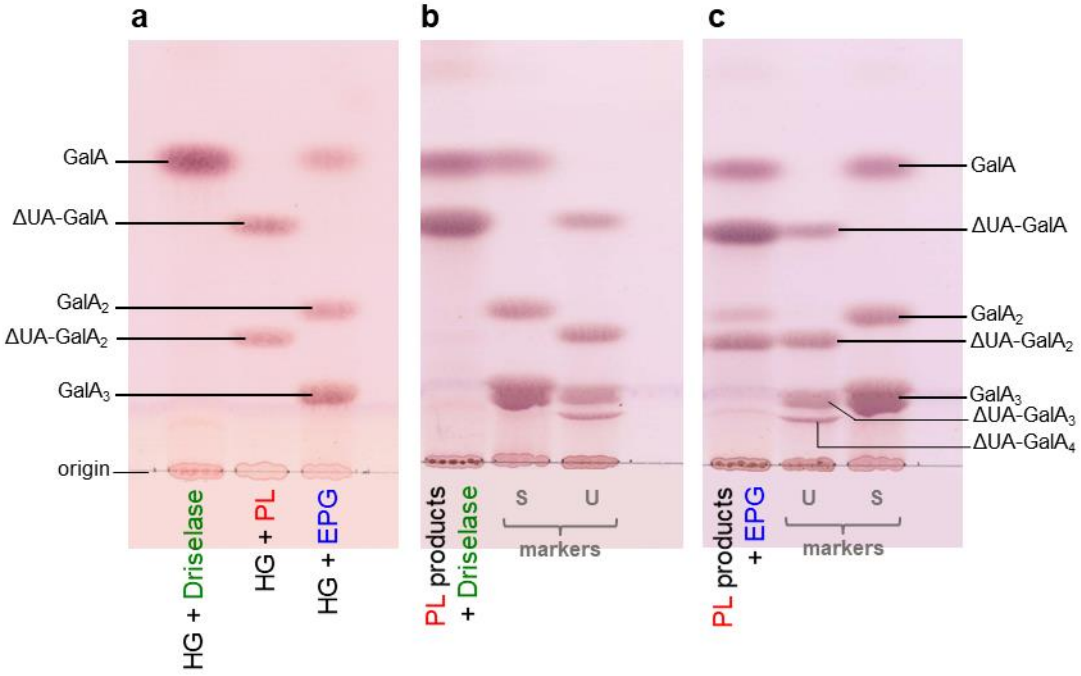

Fig. 3.19. Driselase or EPG digestion of HG or PL products from incomplete digestion of commercial HG. Products were formed from commercial (de-esterified) HG by digestion with commercial PL for 2 min as in Fig. 3.2. (a) Evidence that Driselase and commercial EPG lack pectate lyase activity. HG (20 mg/ml) was digested with Driselase (0.05%, in PyAW, pH 4.7) for 3 days, PL (3.3 U/ml, in CAPS/Ca^{2+} as above) for 30 min or EPG (10 U/ml, in PyAW, pH 4.7) for 16 h, then analysed by TLC. (b), (c) Driselase or EPG re-digestion of partial PL digestion products. HG was digested with PL for only 2 min, then the enzyme was denatured with formic acid and dried *in vacuo*, and the incomplete digestion products were re-digested for 1 week with (b) 0.05% Driselase at 37°C or (c) 10 U/ml EPG at 20°C, both in PyAW (1:1:98) containing 0.05% chlorobutanol. Marker mixtures were: S, saturated oligogalacturonides; U, unsaturated oligogalacturonides. In all cases: TLC solvent was BAW (2:1:1) with 1 ascent; stain, thymol.

3.1.4. Confirmation of PL fingerprint (ΔUA-GalA) identity

3.1.4.1. TFA hydrolysis of ΔUA-GalA

The smallest PL product (ΔUA-GalA) purified from a preparative paper chromatogram was hydrolysed by TFA to check if it is possible to get a known spot of GalA and a new (unfamiliar) spot of free ΔUA. ΔUA-GalA was largely broken-down by heat (120°C) even without TFA (Fig. 20), though mysteriously giving much less

ΔUA than GalA. At 120°C, 0.2 M TFA completely hydrolysed the ΔUA-GalA giving GalA (known from the marker) and a new unknown spot that could theoretically be ΔUA on a thymol-stained TLC (Fig. 3.20). The ratio of spot intensity of ΔUA:GalA (as a result of TFA hydrolysis) was 1:2 (measured using ImageJ).

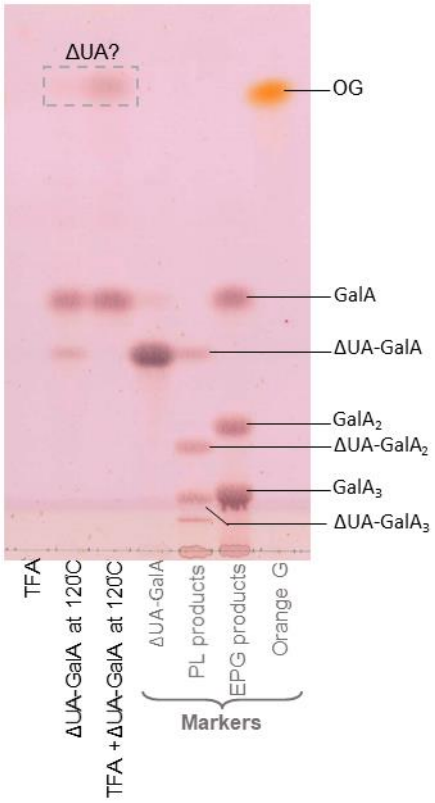

Fig. 3.20. TFA hydrolysis of the PL fingerprint (ΔUA-GalA). A sample of ΔUA-GalA was dried in a SpeedVac, re-dissolved in 0.2 M TFA and incubated in pre-heated oven at 120°C for 1 h. The products were analysed by TLC, run in BAW, 2:1:1 and stained with thymol.

3.1.4.2. NMR evidence for the structure of the proposed ΔUA-GalA

The identity of the proposed ΔUA-GalA, obtained from complete digestion (for 4 hours) of commercial HG with commercial PL and isolated by preparative high-voltage paper electrophoresis (Fig. 3.21), was tested by NMR spectroscopic analysis.

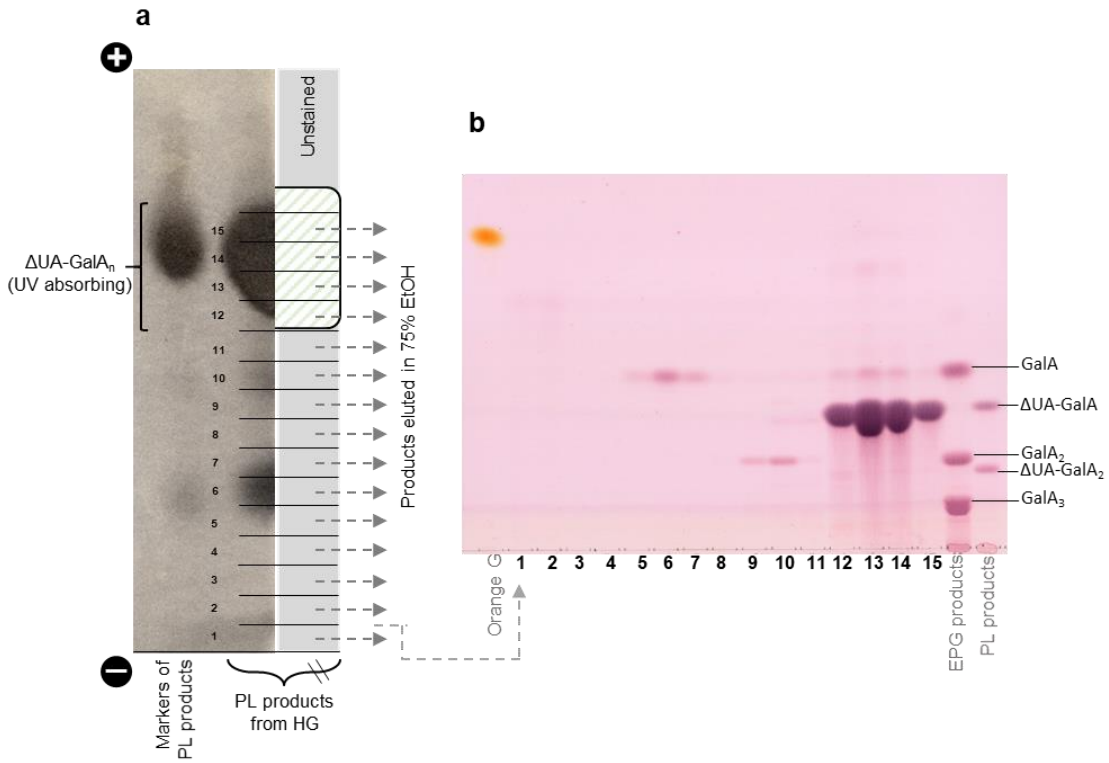

Fig. 3.21. Isolation of the PL 'fingerprint' compound from HG digested with PL. Products were formed from commercial (de-esterified) HG by digestion with commercial PL for 4 h as in Fig. 3.2. **(a)** The products were loaded as a 20-cm streak on Whatman No. 3 paper and electrophoresed at pH 2 (3 kV for 4 h). The left-hand fringe of the paper plus the markers were stained with $AgNO_3$, visualising the products. The major portion, only part of which is shown (in grey), was not stained; shading (/////) indicates a UV-absorbing band. The whole unstained portion was cut into 1-cm strips and products were eluted in 75%EtOH. **(b)** Eluates from strips 1–15 were run by TLC in BAW (2:1:1) alongside marker mixtures and stained with thymol.

The identity of the proposed ΔUA-GalA, obtained from complete digestion of commercial HG with commercial PL and isolated by preparative high-voltage paper electrophoresis, was tested by NMR spectroscopic analysis.

The proton spectrum (Fig. 3.22) showed dominant signals from the disaccharide (ΔUA-GalA) in addition to significant impurity signals and the ΔUA-GalA was a mixture of α and β anomers (60:40) at the GalA moiety.

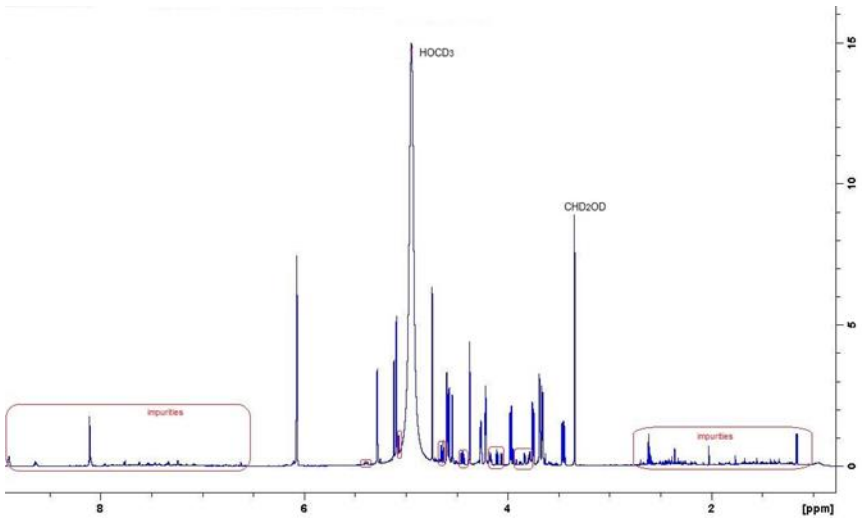

Fig. 3.22. Full proton NMR spectrum of ΔUA-GalA. ΔUA-GalA was produced by *in-vitro* action of commercial PL on commercial HG.

The proton COSY spectrum (Fig. 3.23) allowed the identification of the separate proton signals. The carbon-13 spectrum showed 24 signals as expected. These were assigned from the HSQC 1-bond CH correlation spectrum. Spectral data are given in Table 3.1. The proton–proton coupling constants confirm the stereochemistry of the GalA residue. The position of the linkage between the two rings is clear from the HMBC spectrum (Fig. 3.24) which showed 3-bond correlations between H-1 of ΔUA and C-4 of GalA and between H-4 of GalA and C-1 of ΔUA. All the other signals show correlations between protons and carbons in the same ring. In addition to the expected responses from di-axial protons (close in space), the proton NOESY spectrum (Fig. 3.25) also confirmed presence of the GalA fragment as there are responses between H-3 & H-4 and H-4 & H5, confirming that H-4 is equatorial (H-4 axial would be too far away to give these responses). The response between the ΔUA protons H1 and H2 demonstrates that the linkage there is β-L. If this were α-L-, these protons would be too far apart to give a response. There are also responses between the H1 of ΔUA and H4 of GalA supporting the position of linkage on GalA.

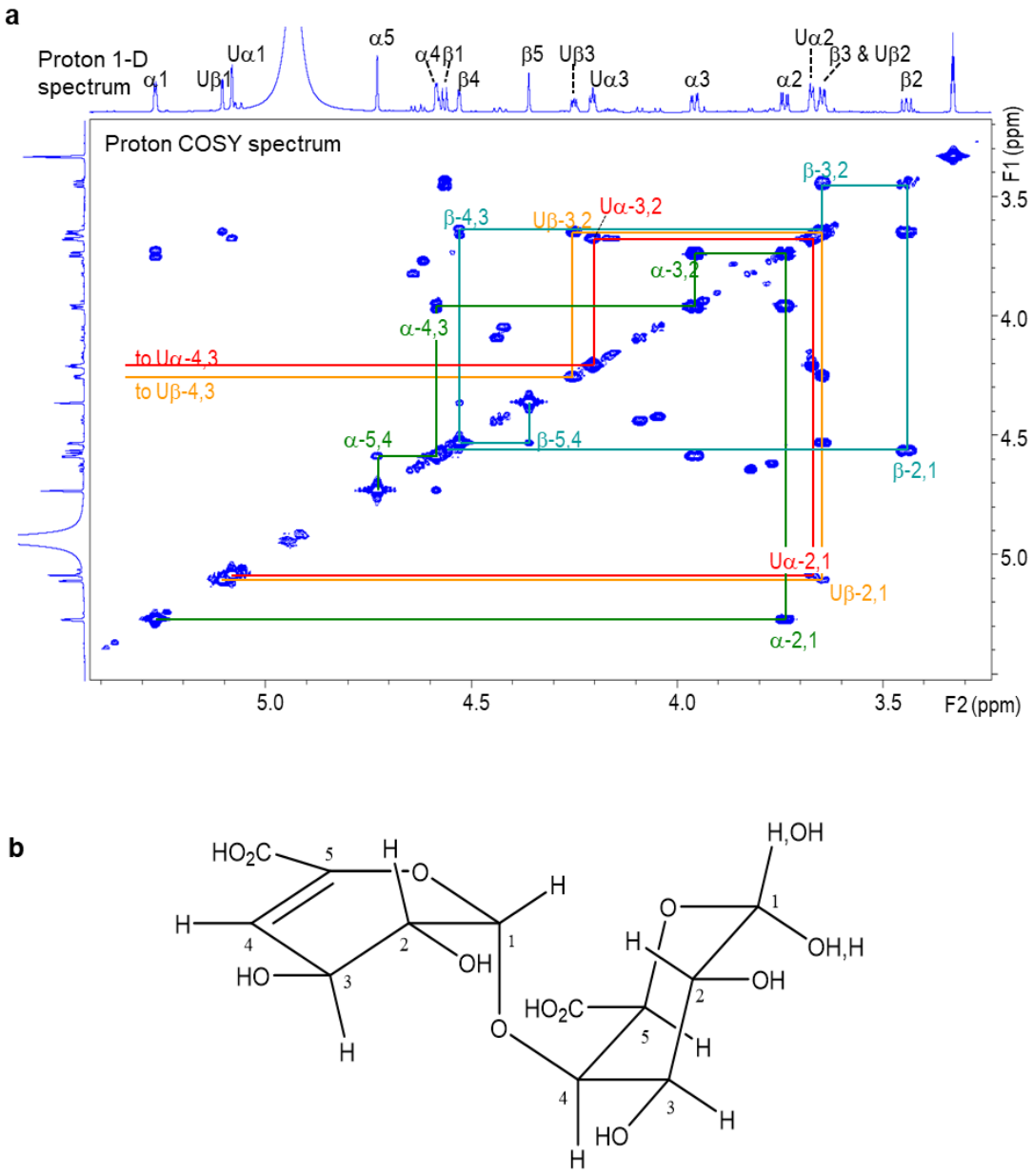

Fig. 3.23. NMR evidence for the structure of the proposed ΔUA-GalA. (a) Proton 1D and proton COSY NMR spectra (region 3.3–6.0 ppm) of ΔUA-GalA produced by *in-vitro* action of commercial PL on commercial HG. Signals labelled U arise from ΔUA; other 'α' and 'β' labelled signals arise from GalA. The signal at 3.33 ppm arises from CD_2HOD. **(b)** Proposed structure of ΔUA-GalA.

Table 3.1. Data from HSQC 1-bond CH correlation spectrum for ΔUA-GalA.

α-anomer (60%)				β-anomer (40%)			
	δ_H	J_{HH} (Hz)	δ_C		δ_H	J_{HH} (Hz)	δ_C
GalA-1α	5.279	3.6	94.4	GalA-1β	4.576	7.8	98.6
GalA-2α	3.75	3.6, 10.2	70.2	GalA-2β	3.454	7.8, 10.0	73.3
GalA-3α	3.969	3.2, 10.2	70	GalA-3β	3.658	obscured	73.7
GalA-4α	4.596	3.2, u	81.4	GalA-4β	4.541	3.1, u	80.2
GalA-5α	4.74	bs	70.7	GalA-5β	4.371	bs	74.3
GalA-6α			172.4	GalA-6β			171.4
ΔUA-1	5.093	1.9	101.5	ΔUA-1	5.116	2	101.5
ΔUA-2	3.984	1.9, 5.6	71.8	ΔUA-2	3.658	obscured	71.9
ΔUA-3	4.216	3.8, 5.6	67.2	ΔUA-3	4.262	3.6, 6.2	67.2
ΔUA-4	6.071	3.8	112.6	ΔUA-4	6.066	3.6	112.9
ΔUA-5			142.7	ΔUA-5			142.5
ΔUA-6			165.3	ΔUA-6			165.4

bs = broad singlet, u = unresolved

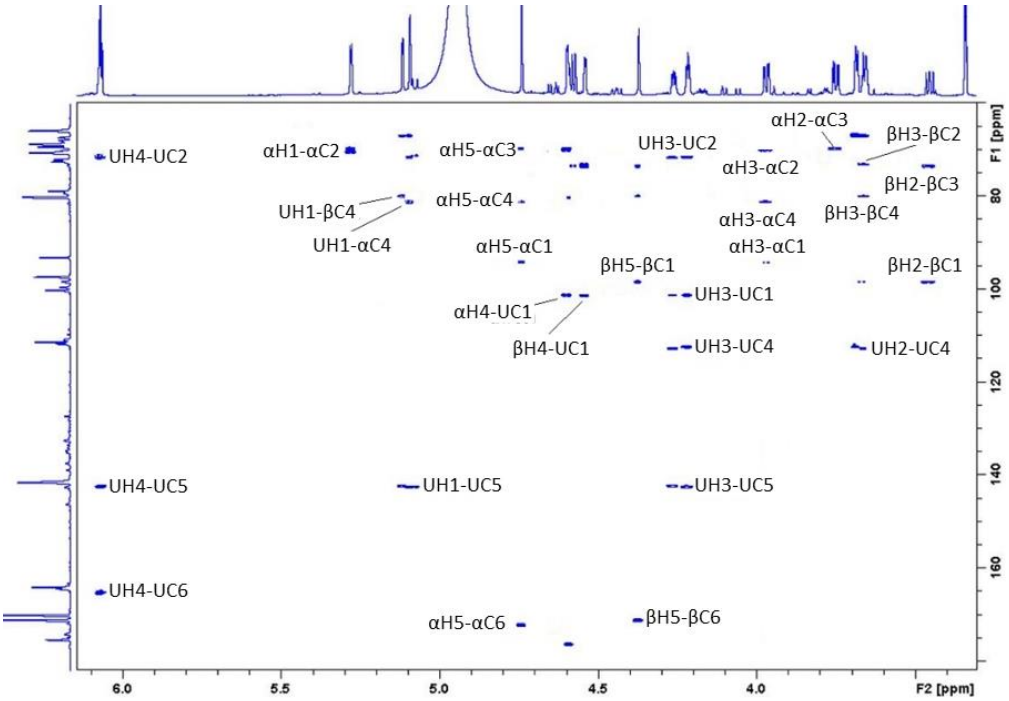

Fig. 3.24. Heteronuclear multiple bond correlation (HMBC) spectra of ΔUA-GalA. U refers to the ΔUA moiety; αC and βC refers to the α and β GalA moiety.

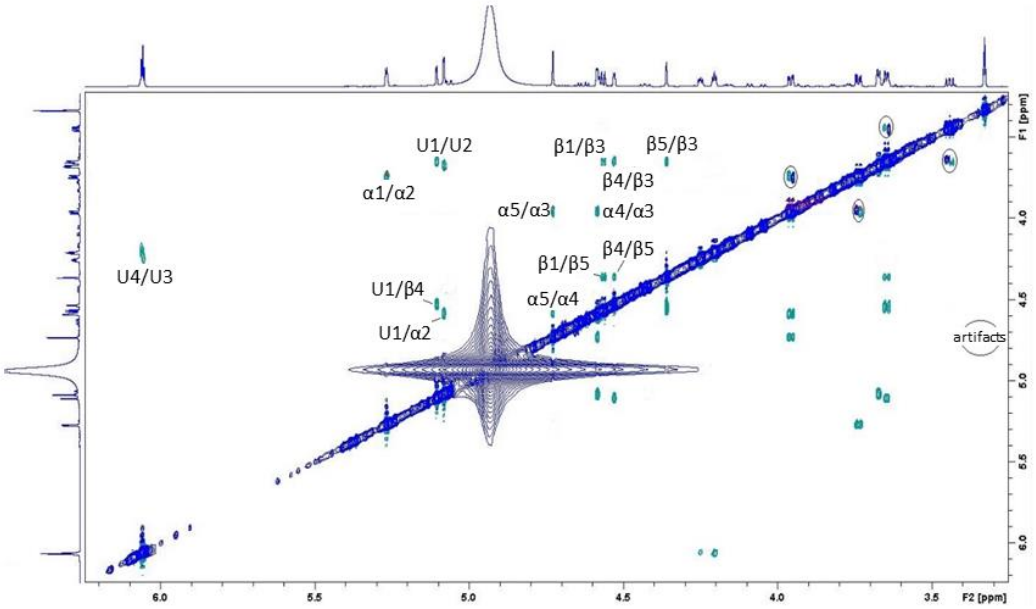

Fig. 3.25. Nuclear overhauser effect spectroscopy (NOESY) spectrum of ΔUA-GalA. α and β refers to the GalA moiety. U refers to the ΔUA moiety.

The sample of ΔUA-GalA seemed to be labile when stored at 4°C. The same sample as in the previous NMR spectra was run again after 2 months. The sample had probably rearranged or fallen apart as many more signals were detected than in the previous run when the sample had been freshly prepared (Fig. 3.26).

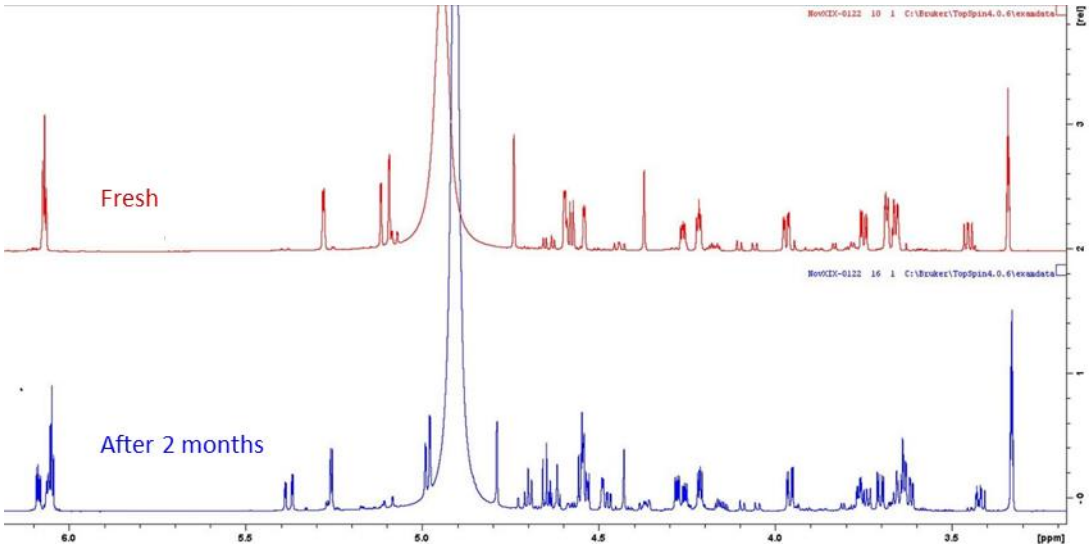

Fig. 3.26. Proton NMR spectrum of ΔUA-GalA after storage at 4°C for 2 months. The ΔUA-GalA sample was run immediately after purification from the paper electrophoretogram and then stored at 4°C for 2 months and re-run under the same conditions.

3.1.4.3. Mass spectrometry evidence for the mass of the proposed ΔUA-GalA

The identity of the proposed ΔUA-GalA, obtained from complete digestion of commercial HG with commercial PL and isolated by preparative high-voltage paper electrophoresis, was tested also by negative-mode electrospray-ionisation FT-ICR mass spectrometry (MS). The simulated *m/z* of the ΔUA-GalA anion is 351.05690 based on its formula of $C_{12}H_{15}O_{12}^-$. Experimentally, molecular-ion negative-mode MS measured the *m/z* at 351.05729, i.e. the value expected with 0.48 ppm error (Fig. 3.27).

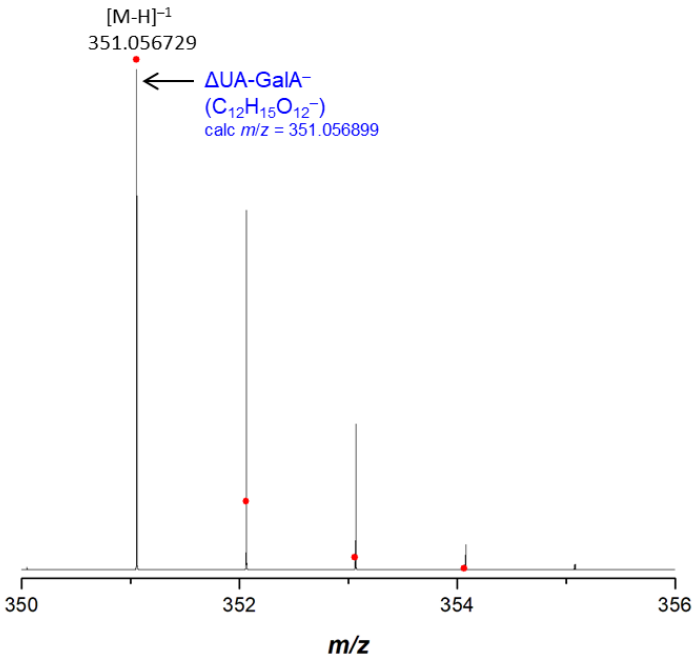

Fig. 3.27. Mass spectrometry of ΔUA-GalA obtained by Driselase digestion of commercial HG. Negative-mode ESI FT-ICR mass spectrum. The *in-silico* simulated isotope distribution (expected mass with 0, 1 or 2 ^{13}C atoms) is highlighted (red dots). The mass error is 4 ppm. The abundance of the measured values did not fully match the simulated isotope distribution due to the presence of some radicals.

3.2. RGL activity *in vitro*

3.2.1. Investigating RGL products from commercial RG-I

3.2.1.1. In-vitro digestion of potato RG-I with RGL with unknown properties

RGL is expected to cleave the α-(1,4) glycosidic bond between Rha and GalA in the RG-I backbone via β-elimination, creating a double bond between C4 and C5 in the GalA residue (making the unsaturated ΔUA) at the non-reducing terminus. RGL was not expected to release small unsaturated products which could be detected by TLC; therefore, Driselase was used after RGL treatment to release the smallest possible products. The smallest expected product after Driselase digestion of the RG-I was not yet known. It could be the dimer (ΔUA-Rha) known as lepidimoic acid (Iqbal *et al.*, 2016), the trimer (ΔUA-Rha-GalA), the tetramer (ΔUA-Rha-GalA-Rha) or an even bigger oligomer (Fig. 3.28), all of which are expected to be highly acidic owing to the presence of the acidic GalA and the highly acidic ΔUA residues.

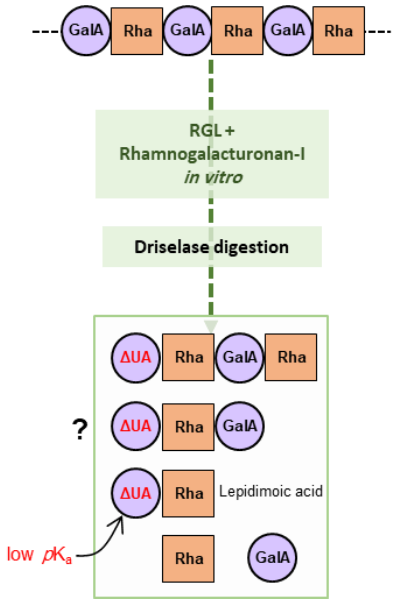

Fig. 3.28. Illustration of RGL *in-vitro* products expected from digestion of RG-I. RGL is expected to produce a range of unsaturated oligogalacturonides with ΔUA-Rha-[GalA-Rha]$_n$. After digestion with Driselase, RGL products are expected to include free GalA and Rha and unsaturated oligomers (could be a dimer (lepidimoic acid) or bigger) with ΔUA at the non-reducing end.

Initially, a promising preparation of RGL was kindly donated by Dr B. McCleary (Megazyme) with no specifications of source, enzyme concentration or optimal reaction conditions. The RGL was supplied in ammonium sulphate buffer. That RGL preparation was tested on commercial RG-I from potato and soy using various reaction conditions and buffers.

Acting *in vitro* on RG-I from potato, RGL produced a faint smear of products which migrated a short distance on TLC while most of the products remained at the origin indicating polymeric content (Fig. 3.29a). The RGL products were then digested with Driselase and produced a range of products including the expected rhamnose (Rha), galactose (Gal), and GalA in addition to four unknown products (labelled with numbers, Fig. 3.29b). Unknown 2 could be (but not expected) ΔUA-GalA as it lined up with the marker ΔUA-GalA on TLC. Unknowns 1, 3 and 4 (or some of them) could potentially be unsaturated oligomers produced by RGL.

To make sure that the source of these products was not Driselase, an experiment was conducted with Driselase acting on potato RG-I and HG. The batch of purified Driselase used in this experiment failed to fully hydrolyse the polymers (RG-I and HG), shown as a spot at the origin of the thymol-stained TLC (Fig. 3.30). The expected RG-I monomers (GalA, Rha, Ara and Gal) were detected in RG-I/Driselase products and GalA was detected in HG/Driselase products. The difference in the products observed in each case indicated that their source was the substrate (RG-I or HG) and not Driselase.

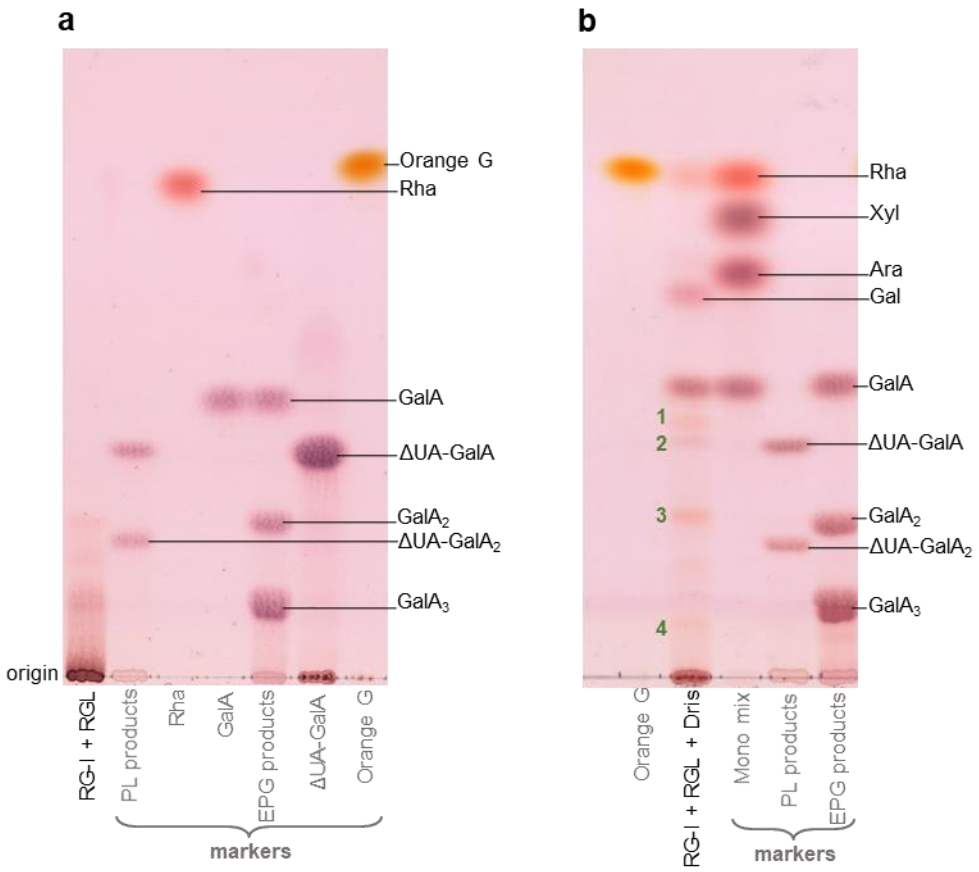

Fig. 3.29. Digestion of RG-I by RGL with and without subsequent Driselase treatment. The RGL reaction mixture contained RGL at 60 µl (no specified concentration) in a total of 300 µl reaction mixture and RG-I at 6.6 mg/ml, in 50 mM ammonium acetate buffer (pH 10.0) with 1 mM $CaCl_2$. The reaction mixture was incubated at 20°C for 16 h and then stopped by addition of 0.2 volumes of formic acid. The products were dried and then either **(a)** not further treated or **(b)** digested with 0.05% Driselase in PyAW (containing 0.5% chlorobutanol), pH 4.7, at 37°C for 3 d. The TLCs were run in BAW 2:1:1 and stained with thymol.

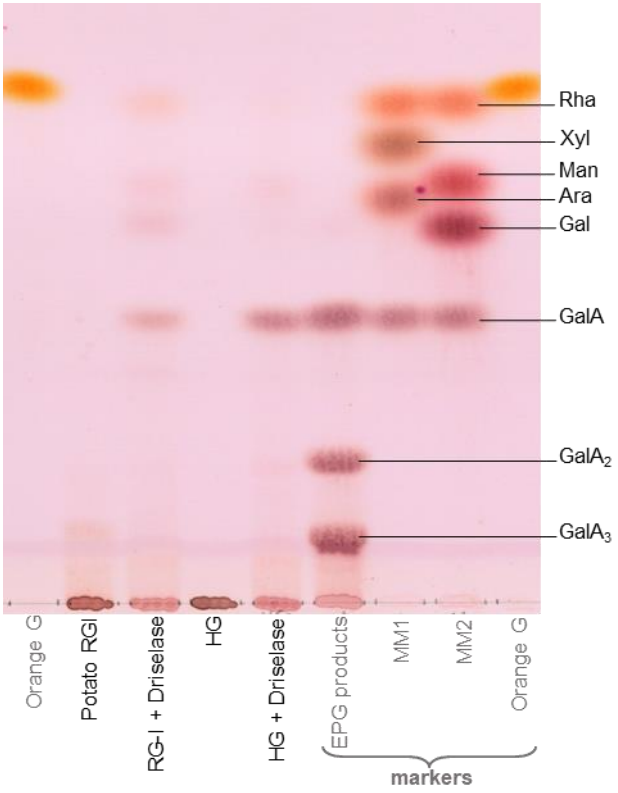

Fig. 3.30. Driselase digestion of commercial potato RG-I and HG. The RG-I/Driselase reaction mixture contained 1 mg/ml potato RG-I and 0.05% Driselase in in PyAW (containing 0.5% chlorobutanol), pH 4.7. The HG/Driselase reaction mixture contained 1 mg/ml HG and 0.05% Driselase in the same buffer. The reaction mixtures were incubated at 37°C for 3 d. The TLCs were run in BAW 2:1:1 and stained with thymol. MM1 and MM2 are marker mixtures containing the monosaccharides indicated.

The same experiment was repeated but with triple the amount of RGL and compared with RG-I hydrolase (RGH, also from Dr B. McCleary with no specifications). RGH should produce $[GalA\text{-}Rha]_n$ (perhaps in polymeric or oligomeric form) with no unsaturated products as it cleaves the RG-I by hydrolysis rather than β-elimination. After digestion of the RG-I with RGL or RGH, Driselase should release the smallest possible products and the difference between the products of each should be detected on TLC. The results (Fig. 3.31) showed spots of GalA, Gal and Rha in both products of RGL and RGH as expected. Two additional spots (in green rectangles) were detected from RGL products which could be the distinctive unsaturated products of

RGL. Both RGL and RGH preparations seemed to be contaminated with Ara and other sugars as shown on the TLC.

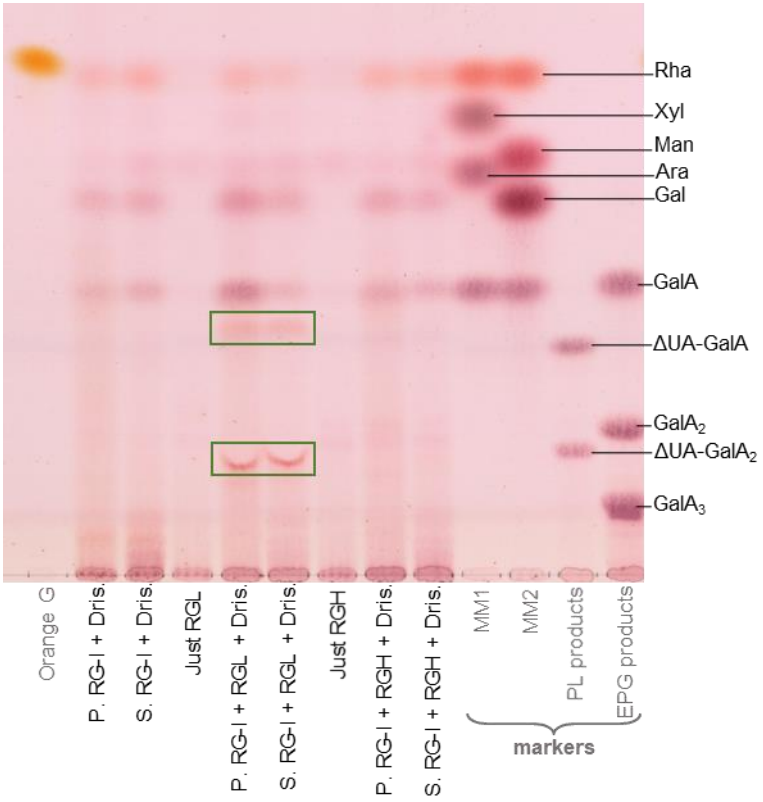

Fig. 3.31. Digestion of RG-I by RGL and RGH with subsequent Driselase treatment. The reaction mixtures contained RGL or RGH at 60µl (no specified concentration) (or neither) and 6.6 mg/ml RG-I (P: potato or S: soy) followed by Driselase digestion as in Fig. 3.30. The TLC was run in BAW 2:1:1 and stained with thymol. MM1 and MM2 are marker mixtures containing the monosaccharides indicated.

Buffers with pH 4–10 were tested to find the best conditions for RGL reaction with RG-I from potato. The RG-I from soy was excluded as it seemed to give less detectable products on TLC after Driselase digestion (Fig. 3.31). At pH 4 and 5, spots of GalA, Gal and Rha were detected in RGL products from potato RG-I even with no further digestion with Driselase suggesting that the RGL preparation was contaminated with other hydrolases which could release the Gal and Ara monomers from the side chains

of RG-I which is not what RGL is expected to do. These spots did not appear at higher pH values. In addition, unknown spots (black rectangles on TLC, Fig. 3.32a) were detected which migrated slower than GalA (probably of dimers or oligomers), formed mostly at pH 4 and 5 and not at higher pH values. Another two unknown spots (slower migrating than the previous two on TLC) were detected at all pH values (red rectangles on TLC, Fig. 3.32a) but predominantly at pH 6 and 7. Further digestion of these products with Driselase released more GalA, Gal and Rha in addition to Man (a common contaminant or autolysis product of Driselase) and probably xyl (a contaminant in potato RG-I). There was no obvious difference in the products of Driselase digestion at the different pH values tested. Three unknown products were produced at all pH values (labelled 1, 2 and 3 on Fig. 3.32b). Unknown 3 also appeared on the Driselase-only marker suggesting that it is a product of Driselase self-digestion rather than a product of RGL. The RG-I preparation itself seemed to be contaminated with some oligomers (appearing as a streak on the TLC plate).

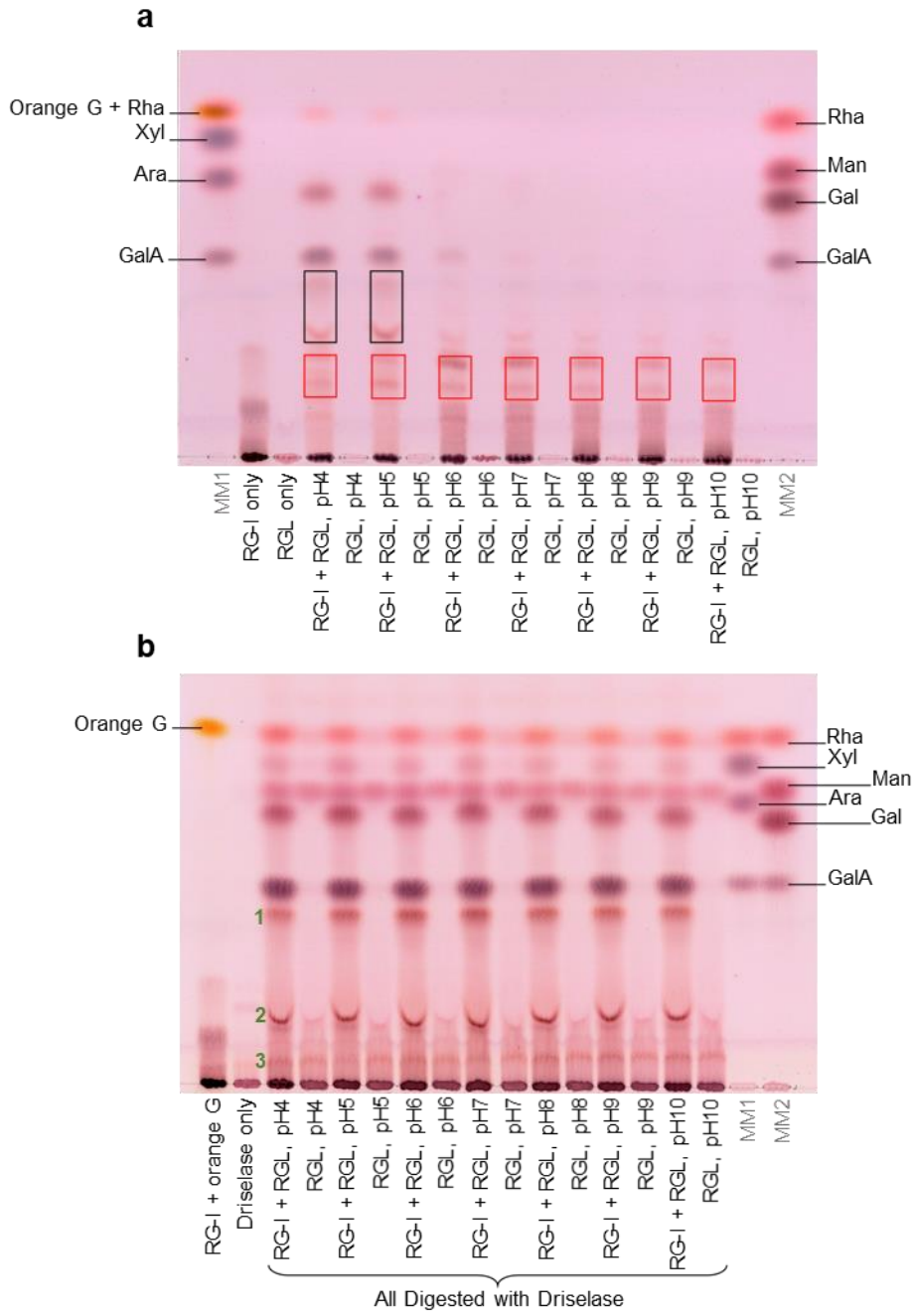

Fig. 3.32. RGL digestion of potato RG-I at various pH values. The RGL reaction mixture contained potato RGL at 200µl/ml (no specified concentration) and RG-I at 6.6 mg/ml in various pH buffers (refer to table 2.1) followed by Driselase digestion as in Fig. 3.30. (a) No Driselase; (b) RGL followed by Driselase. The TLCs were run in BAW 2:1:1 and stained with thymol. MM1 and MM2 are marker mixtures containing the monosaccharides indicated.

3.2.1.2. Digestion of potato RG-I with commercial RGL (from NZYtech) in vitro

As seen from the previous experiments, the RGL (of unknown source and properties) did not give any reliable results to be used as the basis of analysing the fruit endogenous RGL *in-vivo* products. A new stock of commercial RGL was bought (from NZYtech) and the experiments were repeated using the commercial enzyme on commercial potato RG-I (purified by dialysis and washing in 65% EtOH; see §2.2.6). Potato RG-I was digested with RGL under the conditions recommended by the supplier: pH 6 at 37°C (Laatu and Condemine, 2003). A volatile buffer (at pH 6) was used instead of the recommended buffer to avoid contaminating the products with high concentrations of salt (shown previously to interfere with the products' mobility on paper electrophoretograms, Fig. 3.15). After RGL digestion, products were digested with Driselase (2% un-purified Driselase) to get the smallest possible product. As in the usual procedure (see Section 2.4.5), products were then electrophoresed at pH 2 and then eluted from the paper electrophoretogram in fractions in 75% EtOH. TLC of the products (Fig. 3.33) showed the expected neutral sugars (Gal and Rha) in fractions 2–5. The acidic GalA was detected in fractions 5–9 as expected. Another acidic product was detected in fractions 11–14 which could potentially be the expected RGL product.

3.2.1.3. Mass spectrometry evidence of the proposed RGL product

The identity of the RGL product purified from preparative paper electrophoretogram and observed on TLC (Fig. 3.33) was confirmed by mass spectrometry which showed a peak at a mass of 667.17500 in positive mode (Fig. 3.34), corresponding to the

sodium adduct of the tetrasaccharide ΔUA-Rha-GalA-Rha ($C_{24}H_{36}O_{20}.Na^{1+}$). The simulated mass was 667.16921showing a mass error of 9 ppm.

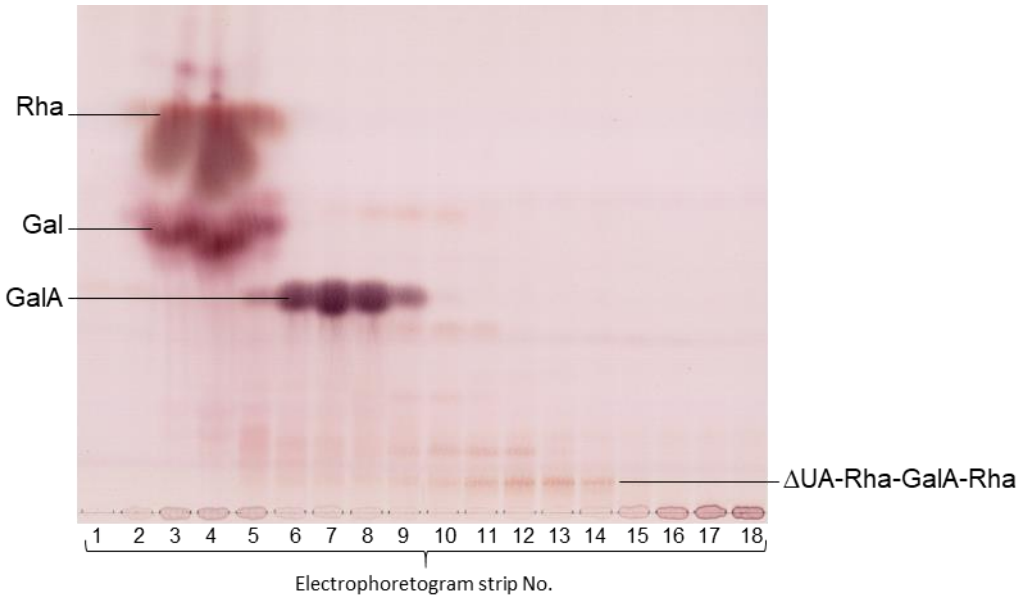

Fig. 3.33. Driselase digestion of commercial potato RG-I pre-treated with NZYtech RGL. The reaction mixture contained 2.9 mg/ml potato RG-I and 0.03 mg/ml commercial RGL in 14.7 mM lutidine buffer (pH6; §2.2.6) at 37°C for 16 h. The reaction was stopped by addition of 0.2 volumes of formic acid and products were dried for further digestion with Driselase as in Fig. 3.30. Products were then electrophoresed at pH2 and fractions were eluted in 75% EtOH and run by TLC as in Fig. 3.17).

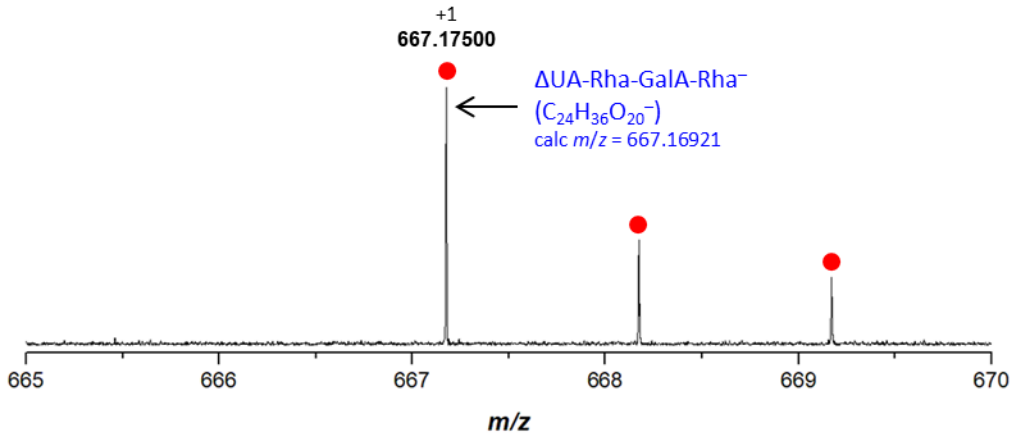

Fig. 3.34. Mass spectrometry of putative RGL products obtained by Driselase digestion of RGL/RG-I products. Positive-mode ESI FT-ICR mass spectrum (*m/z*) of sample from pooled fractions 11–14 (Fig. 3.33; purified from a preparative TLC). The *in-silico* isotope distribution is highlighted in red dots. The mass error is 9 ppm.

As a control, an experiment with potato RG-I digested with Driselase (with no prior RGL) was conducted to ensure that the 'RGL products' observed in Fig. 3.33 were a result of RGL action and not a result of Driselase. The regular procedure was to use 0.05% Driselase (the Driselase concentration which was used later to digest fruit cell walls) for RG-I digestion followed by electrophoresis. The products observed were Rha (fractions 3–5), Gal (fractions 3–5) and GalA (fractions 8–9) in addition to two unknown products (fractions 6–7 and 8–9) which could be oligosaccharides (e.g., Rha-GalA and GalA-Rha-GalA respectively) that Driselase failed to hydrolyse at this concentration (Fig. 3.35). The absence of any detectable products in the fractions 11–14 confirmed that the RGL products observed in Fig. 3.33 were a result of RGL digestion of RG-I and not from Driselase.

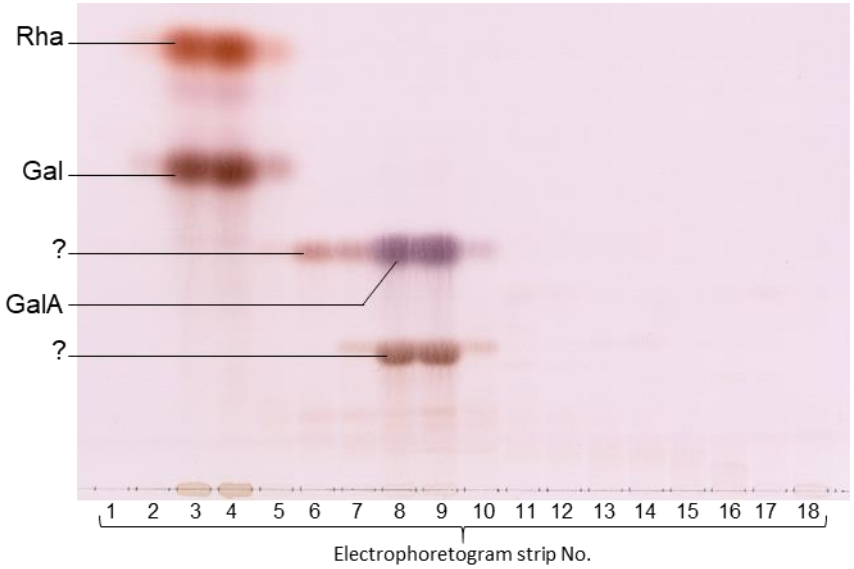

Fig. 3.35. Driselase digestion of commercial potato RG-I. Potato RG-I (2.9 mg/ml, purified by washing in 65% EtOH) and 0.05% Driselase in PyAW (containing 0.5% chlorobutanol), pH 4.7 were incubated at 37°C for 1 week. The reaction was stopped by 0.2 volumes of formic acid and products were electrophoresed at pH2. Fractions were eluted in 75% EtOH and run by TLC as in Fig. 3.17).

A higher Driselase concentration (2%, unpurified) was also tested. As expected, Rha and Gal in addition to Ara were detected in the neutral sugar zone (fractions 1–3) and GalA was detected in fractions 5–8 (Fig. 3.36). The unknown products observed previously in Fig. 3.34 (fractions 6–7 and 8–9) were not detected confirming that they were a result of RG-I/Driselase incomplete digestion. In the acidic sugars zone (fractions 11–14), RGL-like product (labelled X) was detected, superficially suggesting that Driselase contains detectable RGL activity. However, these products were also detected in the Driselase-only digests where no RG-I substrate was added, suggesting that either the unpurified Driselase was contaminated with these products or that they are a result of Driselase self-digestion.

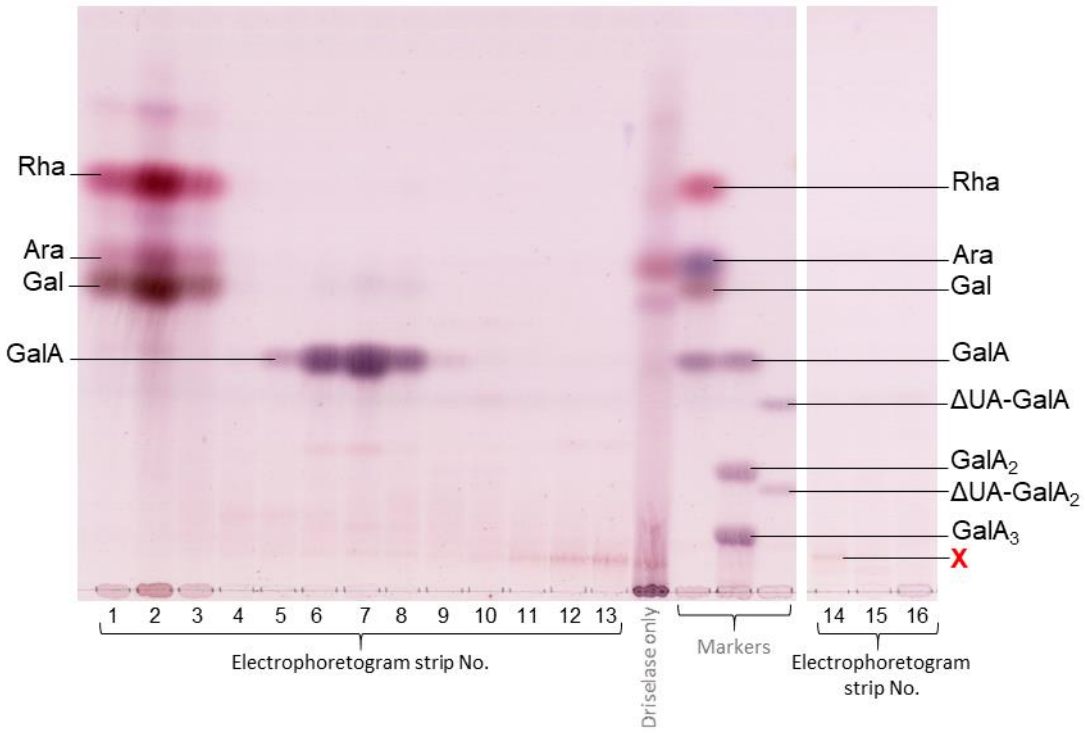

Fig. 3.36. Digestion of commercial potato RG-I by highly concentrated Driselase. Potato RG-I (2.9 mg/ml, purified by washing in 65% EtOH) and 2% unpurified Driselase in PyAW (containing 0.5% chlorobutanol), pH 4.7 was incubated at 37°C for 1 week. The reaction was stopped by addition of 0.2 volumes of formic acid and products were electrophoresed at pH2. Fractions were eluted in 75% EtOH and run by TLC as in Fig. 3.17).

As a confirmatory step, a sample of fraction 13 of the Driselase digestion products of potato RG-I and a sample of the crude (not electrophoresed) Driselase-only digest (Fig. 3.36) were analysed by mass spectrometry. The spectra (Fig 3.37a) showed no peak at the expected mass of the RGL tetramer product (ΔUA-Rha-GalA-Rha) or a bigger or smaller oligomer of it, confirming that Driselase lacks detectable RGL activity even at higher concentration. Although the product X co-migrated with the tetrameric RGL products by both paper electrophoresis and TLC, indicating the acidic nature of it, its identity remained unknown. The slow-migrating unknown spot in the Driselase-only sample (from Fig. 3.36) that lined up with the RGL-like product could be an unknown contamination or Driselase self-digestion product as no peak was observed at the proposed mass of RGL products (Fig. 3.37b).

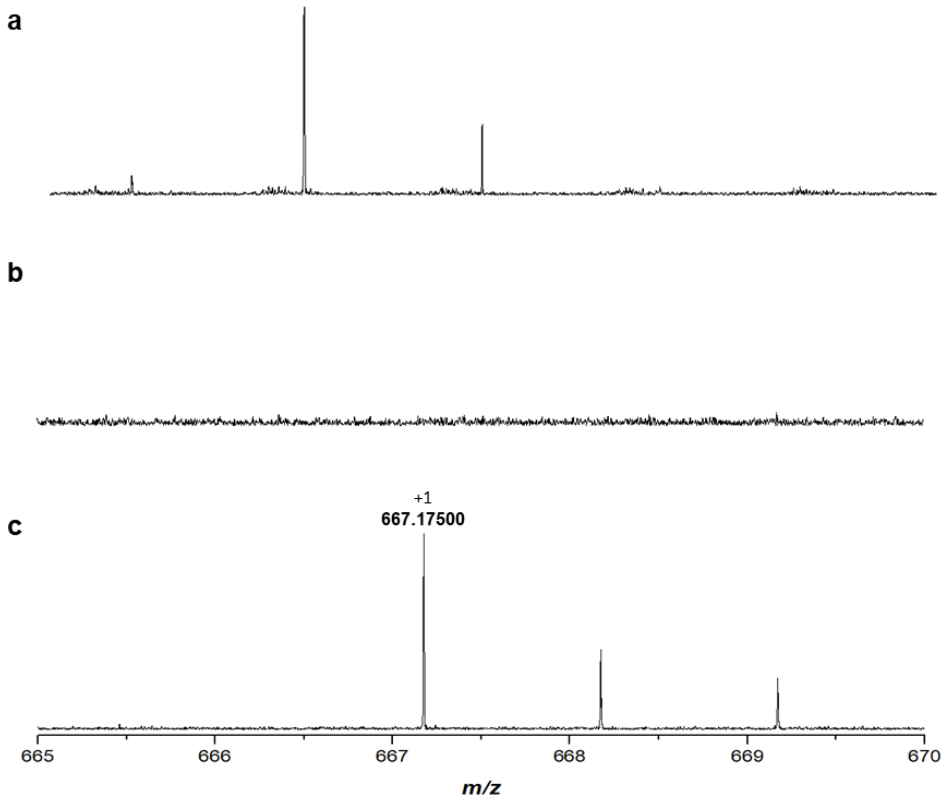

Fig. 3.37. Mass spectrometric evidence that Driselase lacks detectable RGL activity. Positive-mode ESI FT-ICR mass spectrum (*m*/*z*) of sample from: **(a)** Fraction 13 (Fig. 3.36). **(b)** Driselase-only digest (Fig. 3.36) after incubation at 37°C for 1 week. **(c)** Positive-mode ESI FT-ICR mass spectrum (*m*/*z*) of the authentic RGL tetrameric products (shown previously in Fig. 3.34) as a comparison with the spectra in (a) and (b).

3.3. PL and RGL action *in vivo*

3.3.1. Detection of PL and RGL products in ripe fruit cell walls

3.3.1.1. PL fingerprint in Driselase and EPG digestion products from date (Khalas cultivar) and rowan AIR

Using the knowledge gained from the *in-vitro* PL and RGL activity experiments, a protocol to detect PL and RGL action products *in vivo* was developed. Driselase digestion of de-esterified date fruit cell walls (AIR) would cleave any PL action products, even large products such as ΔUA-GalA$_{20}$ to release the smallest unsaturated products (ΔUA-GalA) plus free GalA. Driselase digestion would also cleave any RGL action products, even large ones such as those based on ΔUA-(Rha-GalA)$_{20}$ to release ΔUA-Rha-GalA-Rha, GalA, Rha, Gal and Ara. Paper electrophoresis was then used to separate the highly acidic ΔUA-GalA$_n$s and ΔUA-Rha-GalA-Rha from all other Driselase- or EPG-generated sugars. TLC then helped to resolve and visualise PL and RGL products, providing the evidence for PL and RGL action *in vivo*.

Paper electrophoresis (pH 2.0) of the products obtained by Driselase digestion of cell walls from ripe dates produced a heavy spot of neutral sugars, a heavy GalA spot, and a faster-migrating, UV-absorbing spot indicating the presence of highly acidic, unsaturated products (Fig. 3.38a left). The electrophoretogram was cut into transverse strips, eluates of which were analysed by TLC (Fig. 3.38a right). The neutral fractions (strips 4–6) gave a range of neutral sugars (including isoprimeverose, galactose, glucose, and rhamnose) which were further explored later (see section 3.3.2). Fractions 7–10, which had co-electrophoresed with GalA, were confirmed by TLC to contain predominantly the monosaccharide GalA. TLC of the highly anionic, UV-absorbing fractions (14–16), which had co-electrophoresed with the ΔUA-GalA$_n$, revealed

predominantly the dimer (ΔUA-GalA) previously shown in model experiments (Fig. 3.19b) to be the only unsaturated end-product of Driselase re-digestion of partial PL products. RGL products were detected in fractions 12–14, which made up the slowest-migrating part of the highly anionic products, revealed the tetramer ΔUA-Rha-GalA-Rha previously shown (Fig. 3.33) to be the unsaturated end-product of Driselase re-digestion of RGL products.

A molar ratio of about 1:20 of ΔUA-GalA:GalA was estimated by measuring their thymol-stained spots on TLC which indicates that one PL cleavage event occurred every 20 GalA units of HG (Fig. 3.38a). Estimating the ratio of ΔUA-Rha-GalA-Rha to total RG-I was a bit more challenging as it arises from the RG-I backbone (with repeating units of GalA and Rha) rather that the simple HG (with only GalA units). An estimate of this ratio was made by measuring the spot intensity density of ΔUA-Rha-GalA-Rha and Rha in the Driselase digests of fruit AIR (Table 3.2). Free rhamnose in the Driselase digest gave a reading of 89.8 arbitrary units. Then, since the RG-I backbone has a GalA:Rha ratio of ~1:1 (Yapo, 2011), the RG-I backbone can be estimated at a value of $2\times89.8 \approx 180$. The spot intensity density measured for ΔUA-Rha-GalA-Rha was ~9.3, which implies a value for ΔUA (25% of the tetrasaccharide) of $0.25\times9.3 \approx 2.3$, which means that in the RG-I backbone of 180 GalA + Rha units, 2 GalA units had been cleaved by RGL. This estimate is only approximate, and disregards the differences in molar colour-yield (on thymol staining) between ΔUA, GalA and Rha residues.

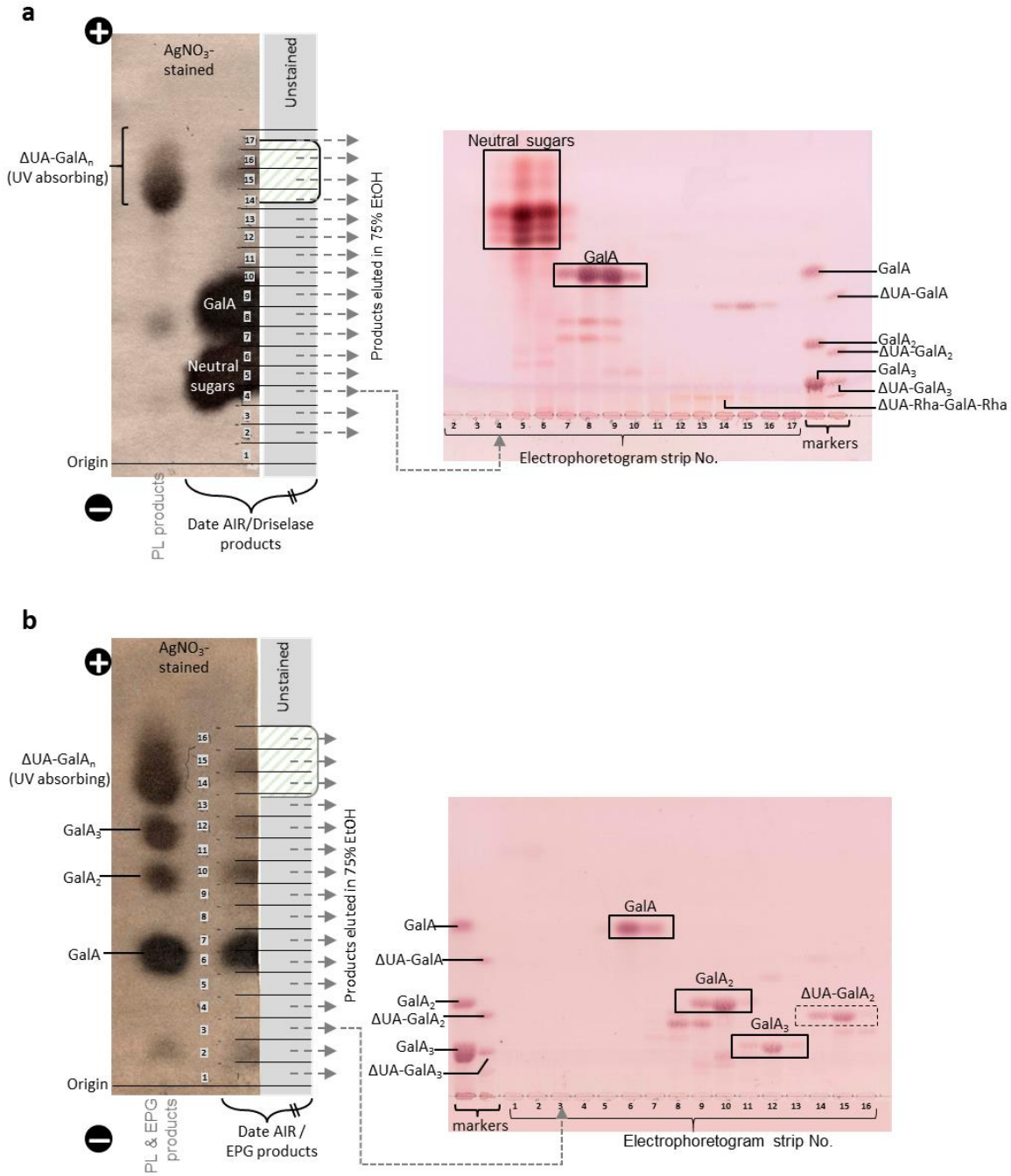

Fig. 3.38. Detecting pectate lyase and RG-I lyase fingerprints in digests of date (Khalas cultivar) fruit cell walls. (a) Driselase digestion. Date AIR (25 mg) was digested in 3 ml Driselase (0.05%) in pyridine/acetic acid/water (1:1:98 by vol., containing 0.5% chlorobutanol) at 37°C for 72 h. *Left:* The products were loaded as a 20-cm streak on Whatman No. 3 paper and electrophoresed at pH 2 (3 kV for 4 h). The left-hand fringe of the paper plus the markers were stained with $AgNO_3$, visualising the products. The major portion, only part of which is shown (in grey) was not stained; shading (green /////) indicates a UV-absorbing band. The whole unstained portion was cut into seventeen 1-cm strips and products were eluted. *Right:* Eluates from strips 2–17 were run by TLC in butan-1-ol/acetic acid/water (2:1:1) alongside marker mixtures, and stained with thymol. **(b)** EPG digestion. As (a), but digestion was with EPG (10 U/ml).

Table 3.2: Quantification of PL and RGL cleavage events detected by thymol staining of their products. The intensity density of the thymol-stained spots of ΔUA-GalA, GalA, ΔUA-Rha-GalA-Rha and Rha detected on TLC (Fig. 3.38a) was measured using ImageJ software*

Sample	Spot intensity density	Total intensity density
DUA-GalA	4.688 12.326 0.941	18.0
GalA	56.617 117.372 117.518 54.783	346
DUA-Rha-GalA-Rha	2.967 3.914 2.391	9.3
Rha	11.182 19.377 20.836 9.915 14.512 13.971	89.8

*Different numbers of rectangles were selected for ImageJ quantification, depending on (a) how many TLC tracks (2 or 3) contained the substance being measured and (b) whether the stained spot was covered by one or three standardised rectangles [the Rha spot was large because of the extra diffusion occurring as it travelled to near the top of the TLC plate, and was therefore estimated as the sum of two rectangles placed to cover the whole spot; the slow-migrating ΔUA-Rha-GalA-Rha spot was much narrower and was covered by a single rectangle].

Following the same procedure, Driselase digestion of ripe rowan berries' AIR produced the same range of products: a heavy spot of neutral sugars, a heavy GalA spot, and a faster-migrating, UV-absorbing spot of highly acidic, unsaturated products (Fig 3.39a, left). The eluates (analysed by TLC, Fig. 3.39a, right) from fractions 6–9 (co-electrophoresed with GalA) contained predominantly the monosaccharide GalA. Fractions 16–19, which co-electrophoresed with the ΔUA-GalA$_n$, revealed the dimer, ΔUA-GalA. Fractions 12–15, which made the slowest part of the highly anionic products revealed the tetramer ΔUA-Rha-GalA-Rha.

Further evidence that the ΔUA residue had been generated by the fruit *in vivo* (rather than artefactually by Driselase) came from a back-up study with commercial EPG, which lacks detectable PL activity (Fig. 3.19a). When Na_2CO_3-de-esterified fruit AIR from date and rowan berries was exhaustively digested with exogenous EPG, and the products were electrophoresed and fractions analysed by TLC, the major products were, as expected, three (saturated) hydrolysis products: GalA, $GalA_2$ and $GalA_3$ (Fig. 3.38b and 3.39b). In addition, a substantial spot of ΔUA-$GalA_2$ was detected in both species, electrophoresing with high mobility and running on TLC in the expected positions. A trace of ΔUA-GalA was detected in date. These observations confirm that endogenous PL had been acting *in vivo* on the pectin of live fruit.

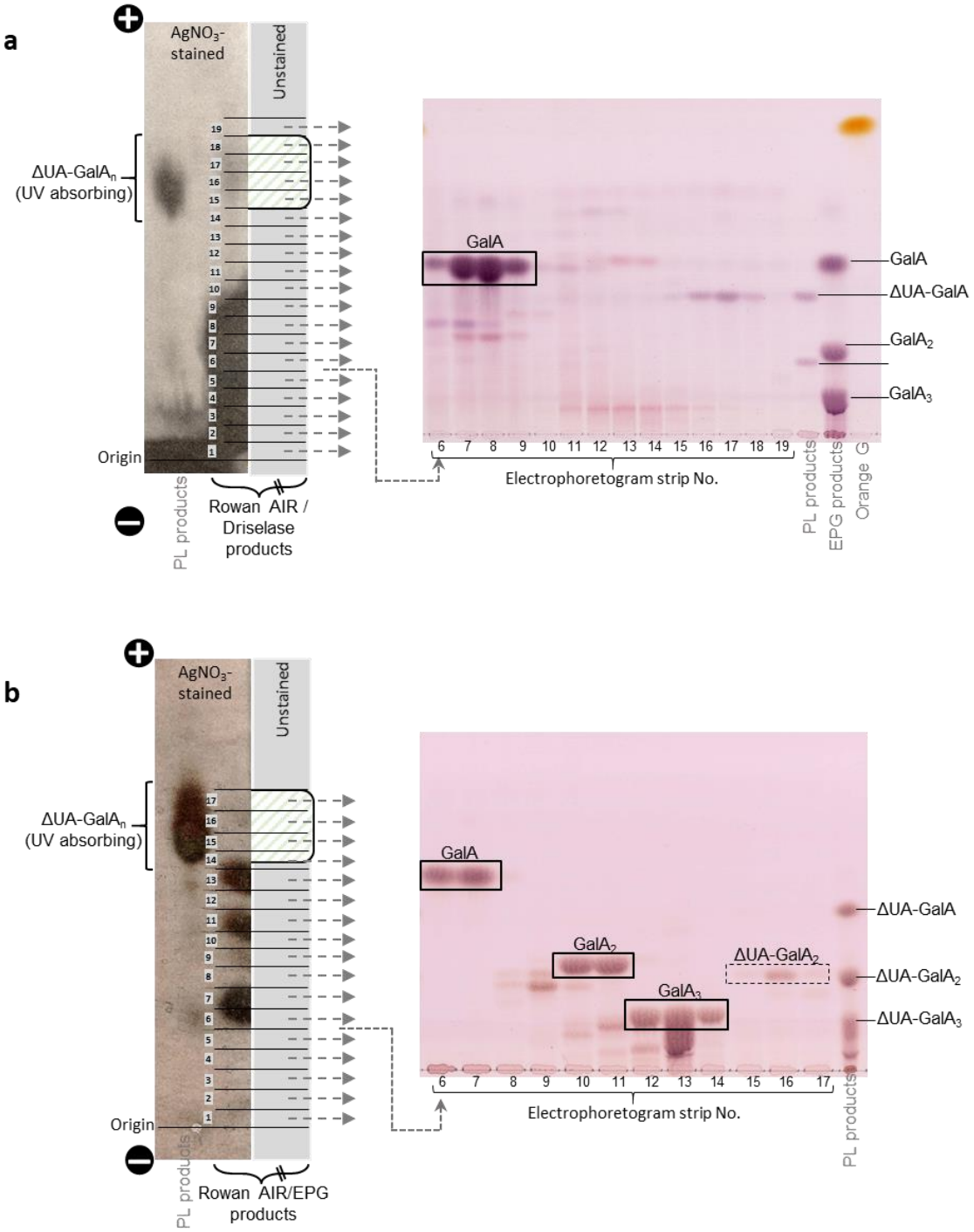

Fig. 3.39. Detecting pectate lyase and RG-I lyase fingerprints in digests of rowan berry fruit cell walls. (a) Rowan AIR (25 mg) was digested with Driselase and the products were run by HVPE, eluted and finally run by TLC as in Fig. 3.38. **(b)** As (a), but digestion was with EPG (10 U/ml).

3.3.1.2. The best solvent for eluting unsaturated oligosaccharides from paper electrophoretograms

For the best recovery of PL and RGL products from date fruit AIR after Driselase digestion and minimal contamination with the non-cellulosic polysaccharides traces of which are present in paper, water and various EtOH concentrations were tested as eluents. Water is known as a universal solvent for sugars and was used to elute the products from the preparative paper electrophoretogram in Fig. 3.38a which were then run by TLC and stained with thymol. However, thymol-stained spots appeared at the origin on the TLC indicating the presence of some polymeric sugars (probably from the paper itself) which are too big to migrate from the origin. To avoid eluting unwanted materials from the paper, various EtOH concentrations were tested as alternative eluents. Samples from the ΔUA-$GalA_n$ zone of a preparative PE of date AIR Driselase digestion products were eluted in H_2O and run by TLC as the usual process. After staining the TLC plate with thymol, spots appeared at the origin (Fig. 3.40a) as seen previously in Fig. 3.38a. Those samples were then treated with 75% EtOH to precipitate any polymers and another TLC was run and stained with thymol to visualize the intensity of the stain at the origin indicating the amount of polymers left on the solution. Polymer precipitation by 75% EtOH reduced the intensity of the thymol stain at the origin (Fig. 3.40b).

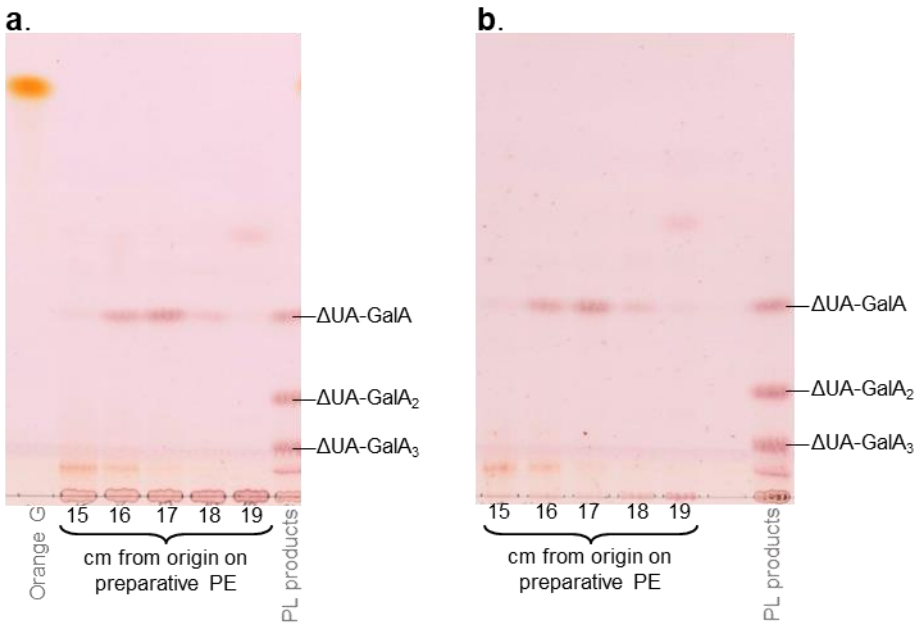

Fig. 3.40. Ethanol precipitation of unwanted polymers prior to TLC. Products from Driselase digestion of date AIR were run on a preparative paper electrophoretogram at pH 2, 3 kV for 4 h. **(a)** TLC of products eluted in water from 1-cm paper strips (unsaturated products zone, 15–19 cm from origin). **(b)** TLC of samples from supernatant from (a) incubated in 75% EtOH at 4°C for 16 h and centrifuged at 14500 *g* for 5 min. Both TLCs were run in BAW 2:1:1 and stained with thymol.

Instead of using H_2O as the eluent, a sequential elution from the same paper strips was done using various concentrations of EtOH (96, 85, 75, 65 and 55%) followed by H_2O to check the best concentration to use as eluent that would eluate all monomers and small oligomers and exclude polymers. Concentrated EtOH (96%) failed to elute anything from strips 16-19 (where ΔUA-GalA was expected to be found) of paper electrophoretograms of date AIR/Driselase products. However, spots of the ΔUA-GalA were detected when 75% EtOH was used (Fig. 3.41a). The 75% EtOH eluted almost all the ΔUA-GalA (detectable by thymol staining of TLC) and left no more to be eluted by the lower EtOH concentrations or even H_2O used after that (Fig. 3.41b). In addition, spots of carbohydrate polymers (or maybe big oligomers) showed up at the origin with reduced concentrations of EtOH, and with H_2O, indicating that those products were eluted by H_2O from the paper and not from the samples.

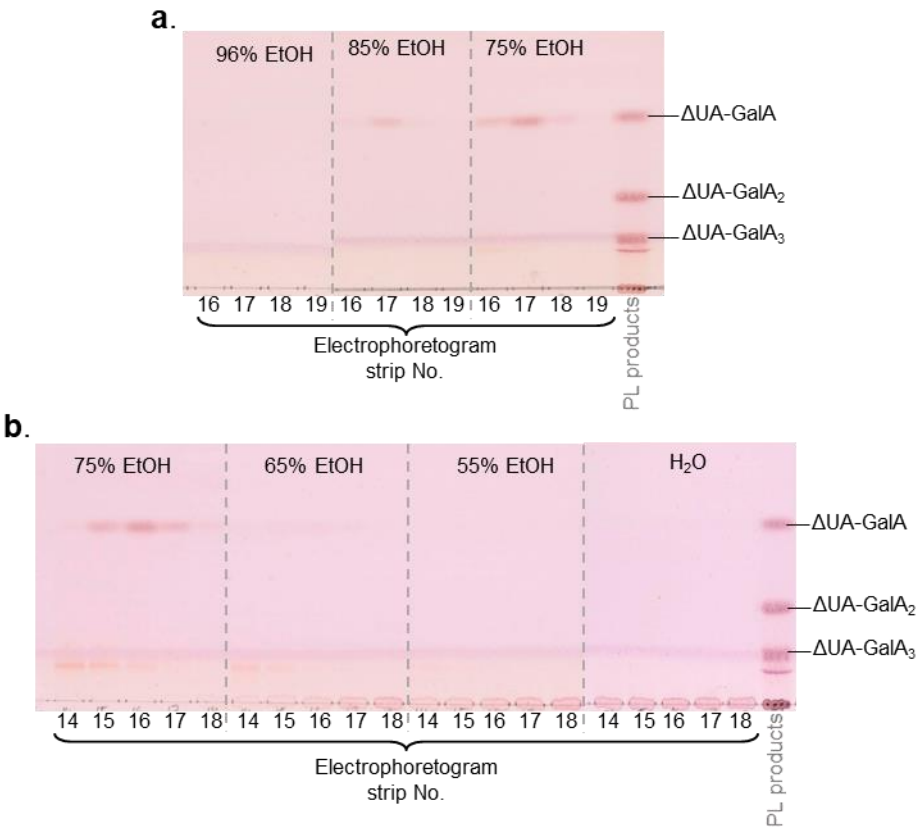

Fig. 3.41. Testing various ethanol concentrations as eluents for oligosaccharide products from preparative paper electrophoretograms. Products from Driselase digestion of date AIR were run by electrophoresis as in Fig. 3.40. **(a)** TLC of products eluted from the ΔUA-GalA$_n$ zone (fractions 16–17) first in 96%, then in 85% and finally in 75% EtOH. **(b)** TLC of products eluted from the ΔUA-GalA zone (from another paper, fractions 14–18) first in 75%, then in 65%, then in 55% EtOH and finally in H_2O. Both TLCs were run BAW 2:1:1 and stained with thymol.

3.3.1.3. Driselase efficiency in fruit AIR digestion

In the process of preparing AIR, fruits were homogenized and washed in 75% ethanol several times to get rid of all the monosaccharides and small oligosaccharides. The amount of EtOH-soluble sugars was monitored by TLC which showed reduced detectable spots after each wash, becoming undetectable in wash 4 (Fig. 3.42).

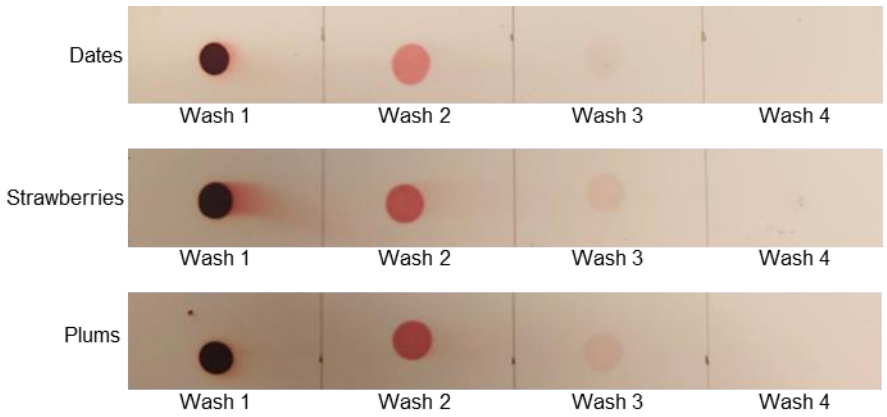

Fig. 3.42. Sugar content in the fruit ethanol washes in preparation of AIR. A sample of 2.5 µl of each of 4 washes of fruit homogenate with 75% EtOH was loaded on TLC, dried and stained with thymol.

The fresh fruit weight, AIR weight and the AIR weight remaining after Driselase digestion were recorded to study how much AIR could be prepared from certain starting fresh fruit weight at different stages of ripening and to study Driselase efficiency in digesting fruit cell walls.

Unripe fruits gave more AIR per gram fresh weight than ripe fruits (Fig. 3.43) which was expected because of cell wall degradation and solubilisation (and cell expansion in some species) as part of the ripening process (Gross and Wallner, 1979). The difference between the amounts of AIR generated from 1 g of fresh fruit varied between species as some fruits became softer and more juicy than others as they ripened. Mangos exhibited the highest difference between the amount of AIR obtained from 1 g of unripe and ripe fresh fruits.

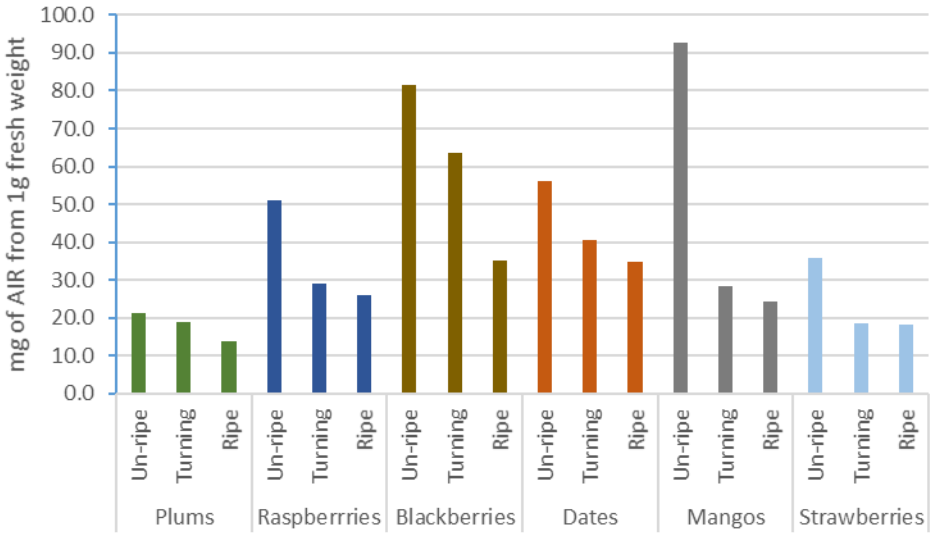

Fig. 3.43. Amount of AIR generated from 1 g fresh fruits at three ripening stages. Starting with 9 g of fresh fruits, the AIR was prepared as described in §2.9. The weight of the dry pellet was recorded. This experiment was conducted only once and may not be suitable for use as a reference.

Driselase digestion of these fruit AIR samples was conducted to look for PL and RGL action fingerprints. The ability of Driselase to hydrolyse the different samples was not always the same. The amount of AIR left undigested after Driselase (routinely used at 0.05%) reaction was recorded to study the efficiency of Driselase in hydrolysing fruit AIR. Throughout this experiment, the same batch of purified Driselase was used. Driselase efficiency could greatly be affected by specific modifications of polysaccharides. Almost 80% of strawberry AIR (un-ripe, turning and ripe) was digested by Driselase (Fig. 3.44). In mangos and raspberries, Driselase digested more of the AIR from ripe fruits than from the un-ripe ones. On the other hand, in dates and blackberries, Driselase digested more of the AIR from un-ripe fruits than the ripe ones. In plums, Driselase digested the AIR from ripe and the un-ripe fruits equally, but was less efficient with AIR from turning fruits.

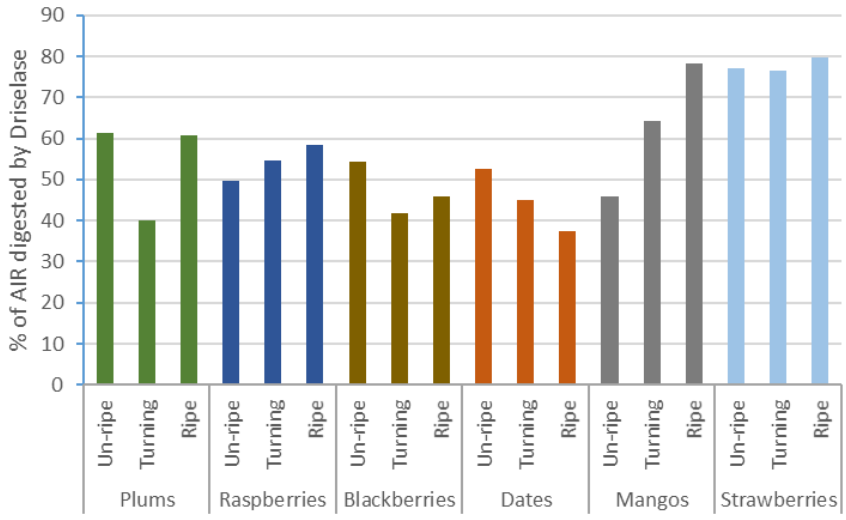

Fig. 3.44. Proportion of AIR (from fresh fruits at three ripening stages) Digested with Driselase. Driselase digestion was conducted on 30 mg of fruit AIR as described in §2.2.5 and the weight of the remaining insoluble residue was recorded after resuspension in water and drying in freeze-dryer. This experiment was conducted only once and may not be suitable for use as a reference.

3.3.1.4. Effects of using higher Driselase concentrations for AIR digestion

Using a 10 times higher concentration of Driselase for fruit AIR digestion seemed to cause a reduction in the amount of GalA produced. This was clear in Driselase digestion products of ripe cranberry and yew aril AIR visualized on TLC (Fig. 3.45). Products were electrophoresed at pH 2 and then eluted in 75% EtOH. The eluates were run in TLC and stained with thymol. The amount of GalA detected was quantified by pixel count (using Image J software), showing smaller amount in samples digested with the higher Driselase concentration in both species. In yew arils (Fig. 3.45c and d), using higher Driselase concentration also produced no detectable PL products which were detected (though very faint spots; in fractions 18–19) when 0.05% Driselase was used. The absence of PL products could be due to the use of non-de-esterified AIR in this experiment. RGL products were clearly detected in fractions 12–17 in both yew arils and cranberries in both cases. On the other hand, more unknown products which approximately co-electrophoresed with GalA were detected when

0.05% Driselase was used; these were absent in products obtained at higher Driselase concentration. These unknowns could be a result of failure of Driselase to complete its hydrolysis when used in lower concentrations as was observed with some batches of Driselase.

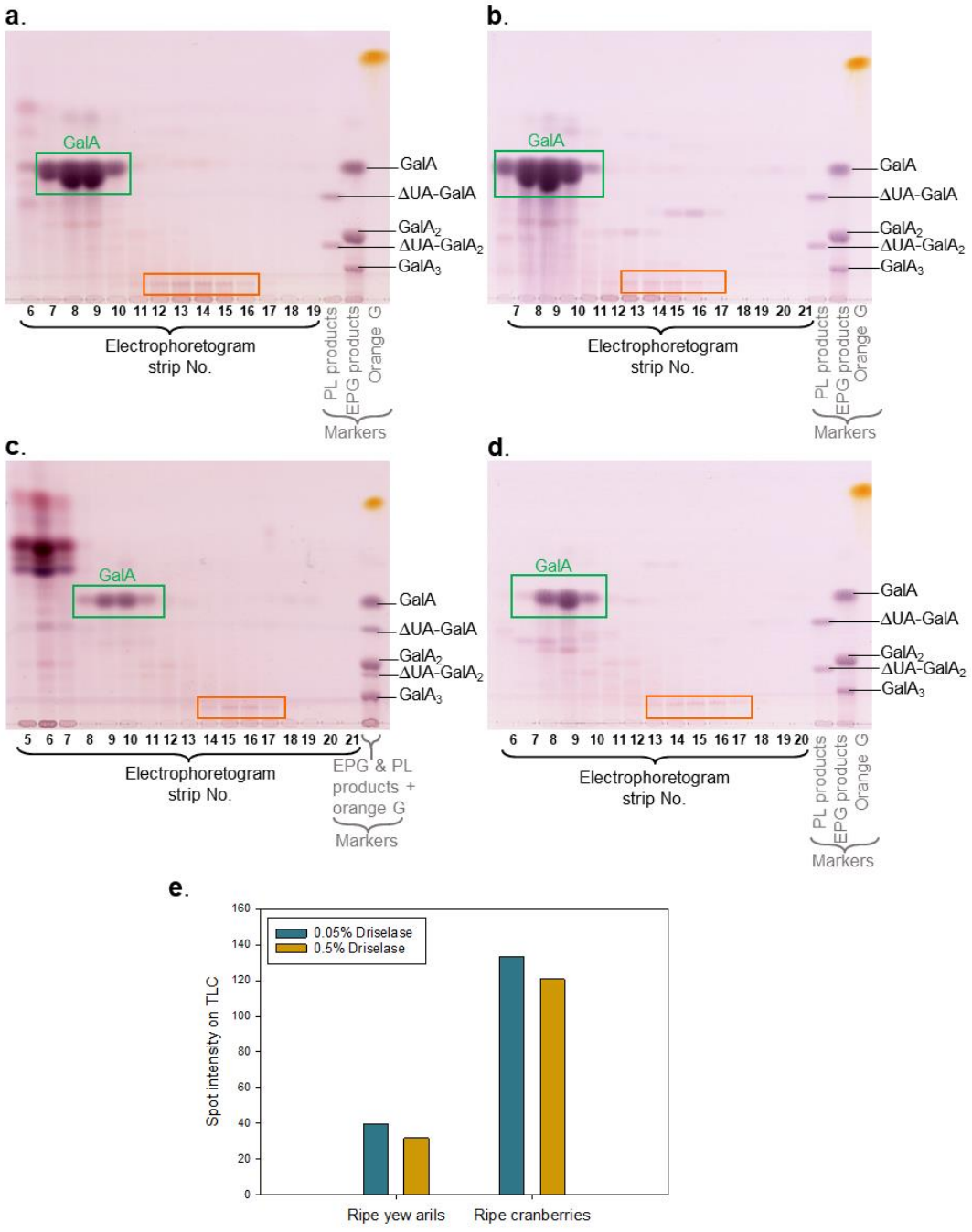

Fig. 3.45. Quantification of the amount of GalA generated from Driselase digestion of non-de-esterified ripe fruit cell walls. AIR (30 mg) was digested with 0.5% or 0.05% Driselase and products were electrophoresed at pH 2 and eluted in 75% EtOH as in Fig. 3.38. Eluates from the paper strips were run by TLC in BAW 2:1:1 alongside marker mixtures and stained with thymol. **(a)** Cranberry AIR digested with 0.5% Driselase. **(b)** Cranberry AIR digested with 0.05% Driselase. **(c)** Yew aril AIR digested with 0.5% Driselase. **(d)** Yew aril AIR digested with 0.05% Driselase. **(e)** GalA (µg) quantified from (a–d).

To study this phenomenon, various Driselase concentrations (from the same batch) were tested on HG and GalA. Driselase was expected to hydrolyse HG completely to GalA (Vreeburg *et al.* 2014; Airianah *et al.* 2016; also observed in Fig. 3.19a). Unfortunately, not all Driselase batches had the same efficiency. In addition, some Driselase batches had more self-digestion products than others. Acting on commercial HG, two purified Driselase stocks were tested (D1 and D2). Higher Driselase concentrations produced less GalA and more Driselase self-digestion products including mannose and rhamnose (Fig. 3.46). As the concentration of D1 and D2 was increased from 0.05 to 0.5%, the amount of detected GalA (estimated by pixel-counting in Image J; Vreeburg *et al.* 2014) decreased. However, this was not the case when 1% D1 and D2 were used. This might be due to oxidases present in the Driselase cocktail which could oxidize GalA to other products which could not be detected by thymol staining on TLC. It could also be just hidden or forming bigger products when in contact with Driselase self-digestion products making it less detectable in this method. Driselase self-digestion products were proved to be so by running Driselase only samples (no HG) as a marker along with the other products and markers. D1 seemed to yield more self-digestion products than D2 including an appreciable amount of GalA.

As D2 Driselase seemed to produce less by-products, it was used in the following experiments to test its effects on monomeric GalA. A decrease in the amount of GalA was detected by pixel-counting in Image J software with increasing Driselase concentration (Fig. 3.47). These results supported the hypothesis of GalA oxidation by Driselase.

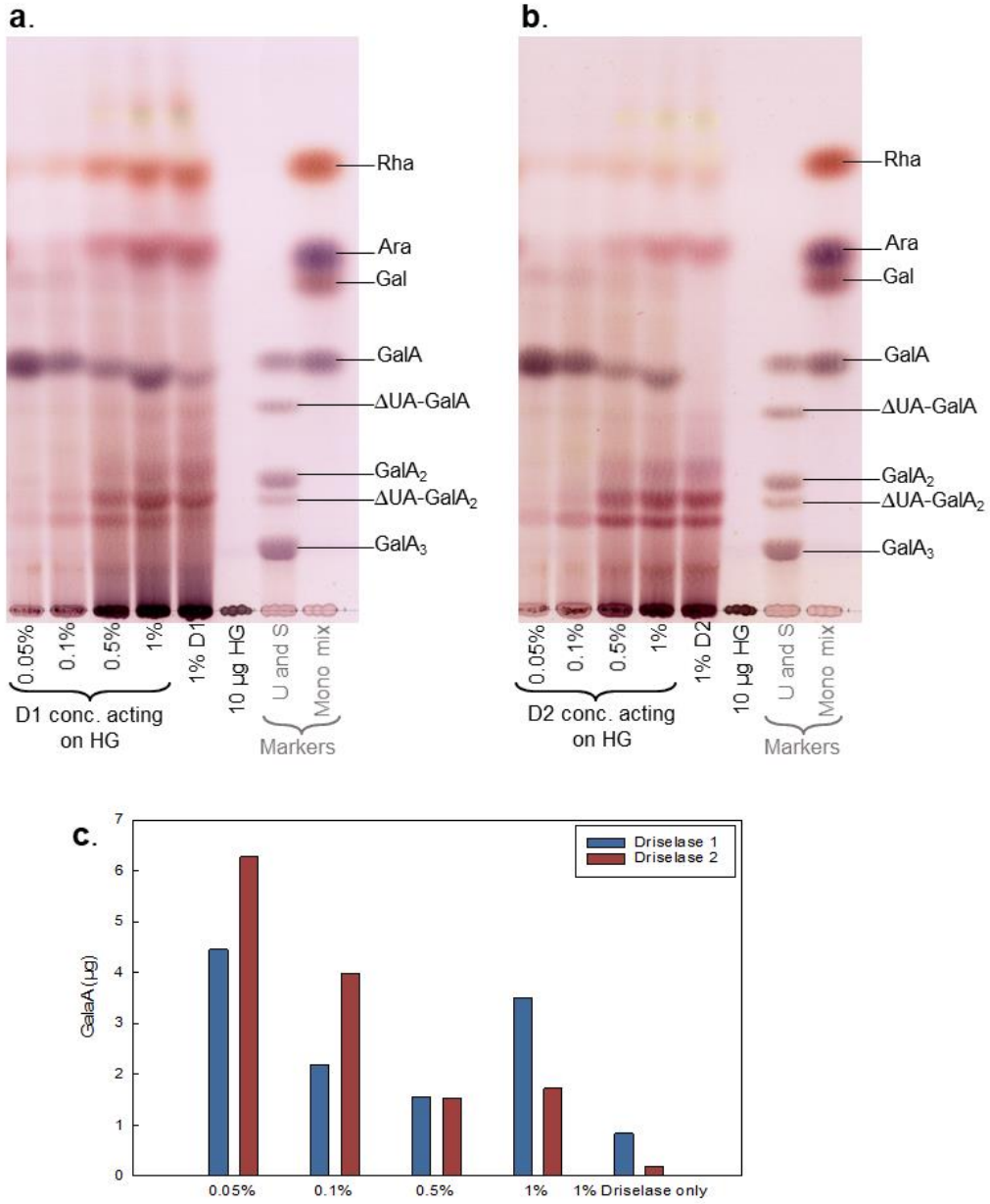

Fig. 3.46. Testing two Driselase stocks' activity on commercial HG. Reaction mixtures containing 25 µg HG and 200 µl of various Driselase concentrations (0.05–1%) were incubated at 37°C for 3 days. The reactions were stopped with 0.2 vol of formic acid. The products were dried in the SpeedVac, re-dissolved in H_2O, run by TLC in BAW 2:1:1 and stained with thymol. **(a)** Driselase stock 1 (D1) products. **(b)** Driselase stock 2 (D2) products. Markers were U, unsaturated oligogalacturonides; S, saturated oligogalacturonides; Mono mix, a mixture of Rha, Ara, Gal and GalA. **(c)** GalA (µg) quantified from the TLC spot of each product.

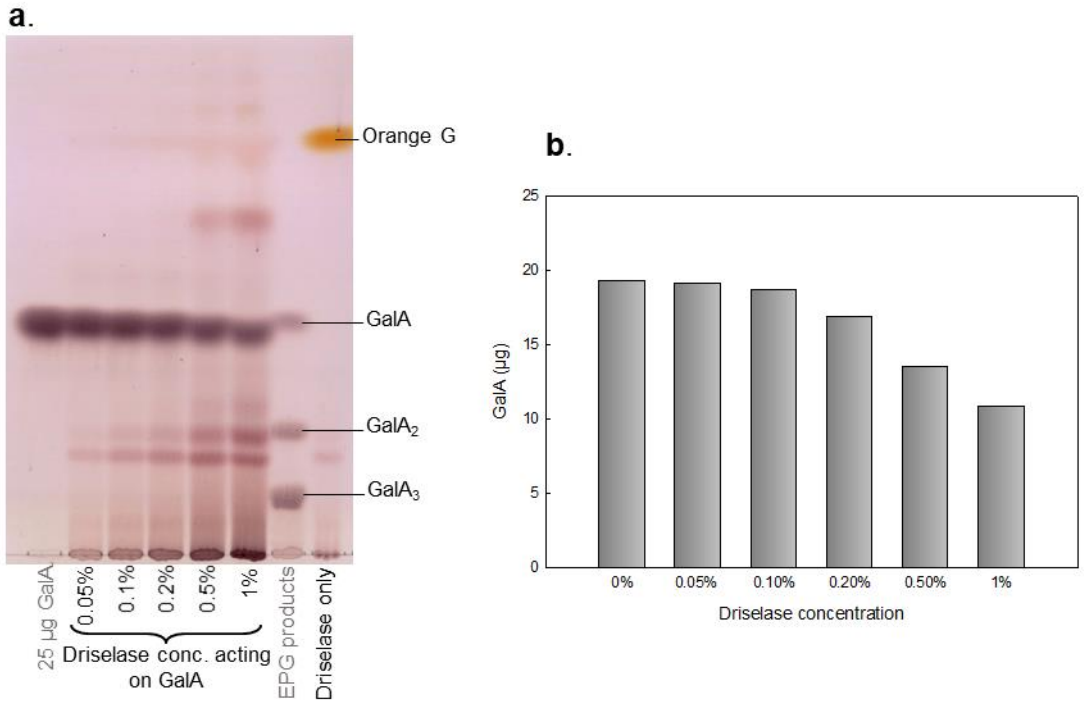

Fig. 3.47. Testing Driselase activity on commercial monomeric GalA. Reaction mixtures containing 25 µg GalA and 200 µl of various Driselase concentrations (0.05–1%) were incubated at 37°C for 3 days. The reactions were stopped with 0.2 vol of formic acid. The products were dried in SpeedVac, re-dissolved in H_2O, run by TLC in BAW 2:1:1 and stained with thymol. **(a)** TLC of the products. **(b)** GalA (µg) quantified from the TLC plate.

I attempted to solve the problem of GalA being oxidized by Driselase by using mercaptoethanol or sodium sulphite (Na_2SO_3) as antioxidants which could theoretically protect GalA. Mercaptoethanol (10 or 100 mM) was added to a HG/Driselase reaction mixture. More GalA was detected when 10 mM mercaptoethanol was used (Fig. 3.48a and b). Surprisingly, using 100 mM of it reduced the amount of detectable GalA as measured by thymol stain intensity (pixel) count. Mercaptoethanol was also used as 10 or 50 mM in reactions of Driselase with monomeric GalA but these concentrations produced no appreciable difference in the amount of GalA detected on the TLC plate (Fig. 3.48c and d).

As there was no clear-cut benefit of using mercaptoethanol to protect GalA from being oxidized by Driselase, Na_2SO_3 was tested as a possible treatment. As shown on the

TLC (Fig. 3.49), the effect of Na_2SO_3 treatment of GalA/Driselase digestion could not be evaluated as it interfered with the migration of GalA on the TLC plate even with Driselase added. The results from these tests were not conclusive as if Driselase really oxidize GalA or even if that could be stopped by anti-oxidizing agents such as mercaptoethanol and sodium sulphite.

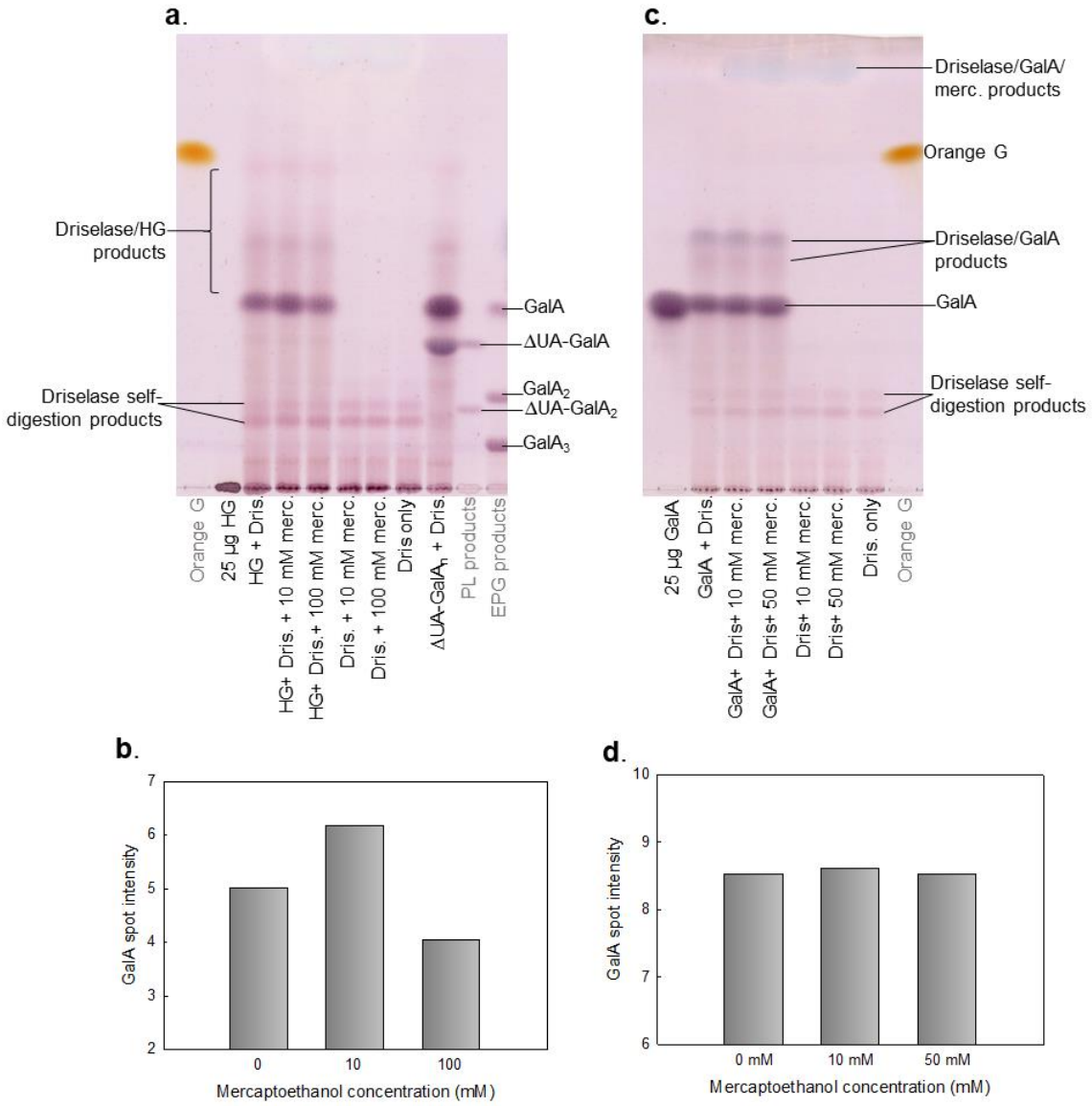

Fig. 3.48. Testing Driselase activity on commercial HG and GalA in presence of mercaptoethanol. Reaction mixtures contained 25 µg HG or GalA and 200 µl of 0.05% Driselase and were incubated at 37°C for 3 days. The reactions were stopped with 0.2 vol of formic acid. The products were dried in a SpeedVac, re-dissolved in H_2O, run by TLC in BAW 2:1:1 and stained with thymol. **(a)** TLC of the products from HG. **(b)** GalA (µg) quantified from the TLC plate in (a). **(c)** TLC of the products from GalA. **(d)** GalA (µg) quantified from the TLC plate in (c).

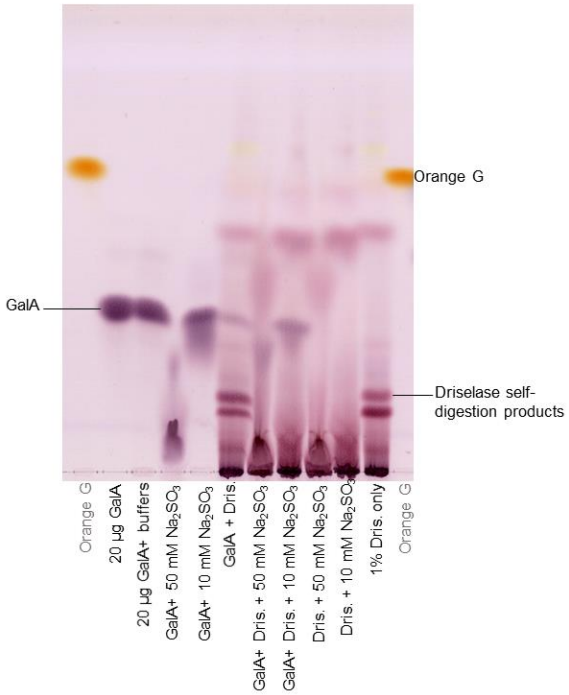

Fig. 3.49. Testing Driselase activity on commercial GalA in presence of sodium sulphite (Na_2SO_3). Reaction mixtures contained 20 µg GalA and 200 µl of 0.05% Driselase and were incubated at 37 °C for 3 days. The reactions were stopped with 0.2 vol of formic acid. The products were dried in SpeedVac, re-dissolved in H_2O, ran by TLC in BAW 2:1:1 and stained with thymol.

3.3.1.5. Testing un-purified stocks of Driselase on HG, RG-I and date AIR

To sort out the uncertainty about Driselase efficiency in digesting the fruit HG and RG-I and ripe date fruit AIR, a test of five available Driselase un-purified stocks was conducted. The reaction conditions were as before; however, since the Driselase stocks (numbered 1–5) were not purified, '2%' concentrations (some of which remained insoluble) were used instead of the 0.05%. The Driselase stocks 1, 2, 3 and 5 seemed to be best for digesting HG as more GalA was detected on TLC of the products (Fig. 3.50a). Dark spots at the origin were detected which could be of undigested HG or remnants from the un-purified Driselase as they seemed to be consistent in all the products. As GalA was the only expected product from HG, the other spots (including Man, Gal, Rha and probably some GalA) indicated the presence of contaminating

carbohydrates from the un-purified Driselase self-digestion. Acting on potato RG-I, all five Driselase stocks gave the expected products (GalA, Gal, Ara and Rha), probably contaminated with products from Driselase self-digestion (Fig. 3.50b). To decide on which of the tested Driselase stocks was the best, the amounts of GalA from each reaction with HG and RG-I and the contaminating Driselase self-digestion products were taken into consideration. Driselase 1 and Driselase 5 seemed to give most GalA and from RG-I while Driselase 5 had the least amount of self-digestion products (judged by the intensity of the Man spot). Not much difference between the products from date AIR was observed as it is hard to judge due to big amounts of other products (Fig. 3.50c). Samples of all five stock Driselase only were also run by TLC (Fig. 3.50d); however, the products observed were not reliable as the Driselase was not centrifuged (to discard the insoluble material) as done with the other experiments.

The products from Driselase 3 and 5 digestion of fruit AIR (from Fig. 3.50c) were electrophoresed at pH 2 to reveal the PL and RGL products and decide on which of them could be the most efficient Driselase stock. The samples were eluted from the paper electrophoretogram as done before and the fractions were analysed by TLC. In products from both Driselase 3 and 5, GalA was detected in fractions 6–8 (Fig. 3.51). The PL fingerprint (green rectangle, ΔUA-GalA) was detected in fractions 14–17. RGL fingerprint (orange rectangle) was detected in fractions 10–15. In addition, unexpected products which Driselase should have hydrolysed completely to their smallest units were detected: $GalA_2$ in fractions 10–12, $GalA_3$ in fractions 13–14 and $\Delta UA\text{-}GalA_2$ in fractions 16–17. Thus, the tested un-purified Driselase stocks still did not fully digest the date AIR (should give the products observed in Fig. 3.38a as the AIR sample was the same). However, since more RGL fingerprint and less other unexpected products were detected in Driselase 5 digest, it was recommended to be used for future experiments.

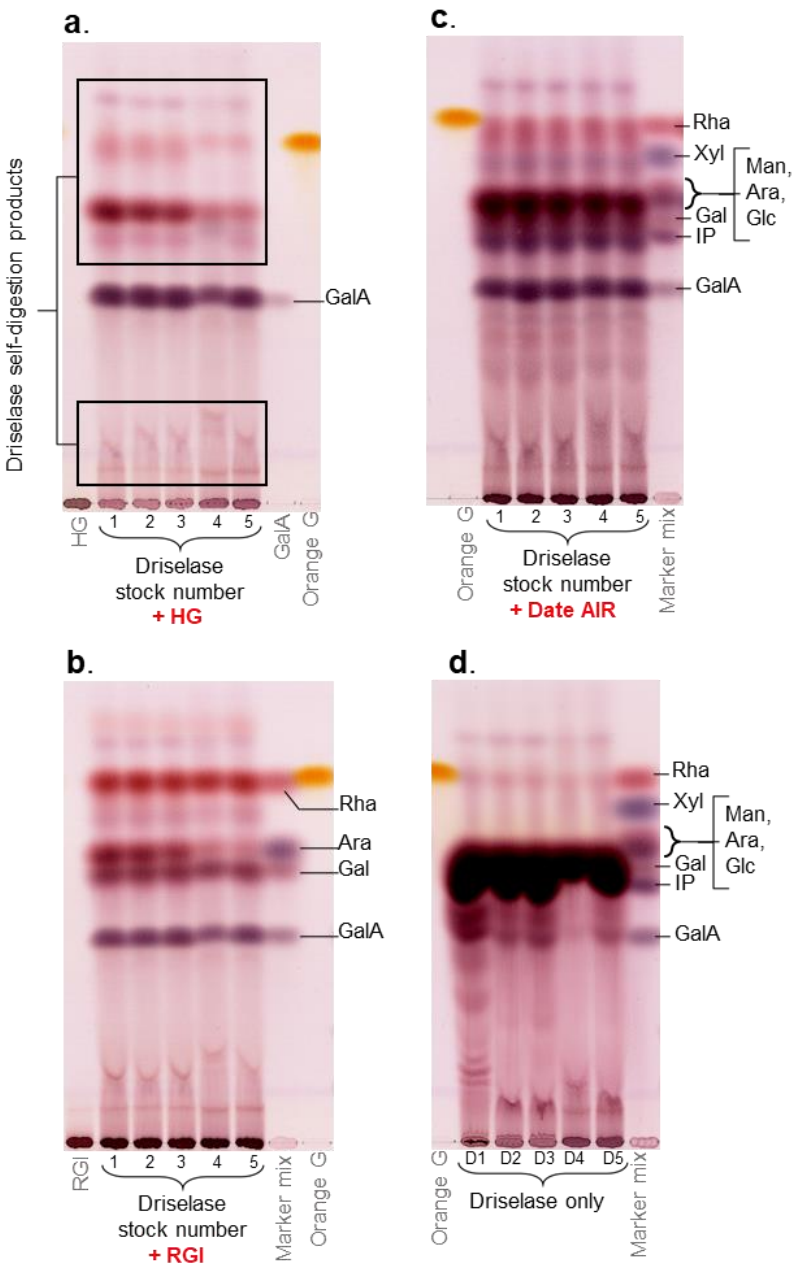

Fig. 3.50. Testing the activity of five un-purified Driselase stocks on HG, RG-I and date fruit AIR. Each Driselase stock was prepared as 2% suspension incubated on a wheel for 2 hours at 4 °C. The suspension was spun at 14500 g and the supernatant was used. The Driselase digestion of each of **(a)** HG (2.5 mg/ml), **(b)** potato RG-I (5 mg/ml) and **(c)** 25 mg/ml date AIR (**d**) Driselase only (2% suspension with no prior centrifugation) was conducted at 37°C for 3 days. 5 µl of digest was applied to the TLC.

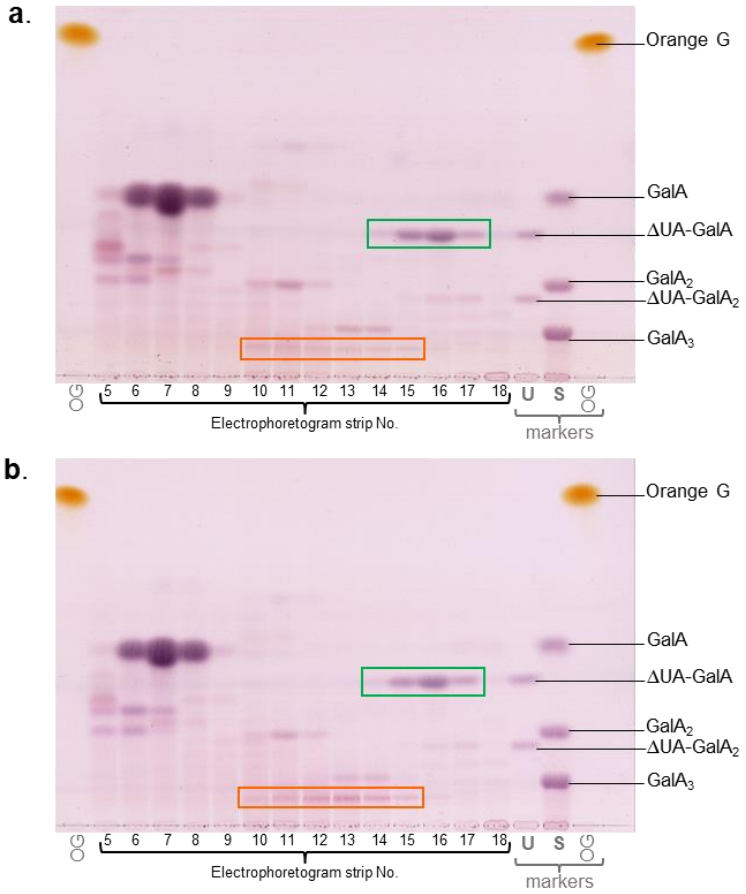

Fig. 3.51. Detecting pectate lyase and RG-I lyase fingerprints in products of digesting date fruit AIR with two un-purified Driselase stocks. Ripe date AIR (10 mg) was digested with Driselase and products were electrophoresed at pH 2 and eluted in 75% EtOH as in Fig. 3.38. Eluates from the paper strips were run by TLC in BAW 2:1:1 alongside marker mixtures and stained with thymol. **(a)** Products of Driselase 3. **(b)** Products of Driselase 5. Markers were U, unsaturated oligogalacturonides; S, saturated oligogalacturonides; OG, orange G.

3.3.1.6. PL and RGL fingerprint in Driselase digestion products from AIR of other ripe fruits

Using the methods developed for dates and rowan berries, i.e. Driselase digestion of de-esterified ripe fruit AIR followed by electrophoresis and TLC, fingerprints of the *in-vivo* actions of endogenous PL (ΔUA-GalA) and RGL (ΔUA-Rha-GalA-Rha) were obtained in ripe fruits of pear, apple, yew (arils; a gymnosperm), raspberry, mango, plum and blackberry, suggesting the widespread and important role of these enzymes throughout the plant kingdom. On the other hand, RGL products were detected in sea

buckthorn and cranberries but no evidence of PL action was found. These products were identified by paper electrophoresis and TLC by reference to markers obtained by *in-vitro* digestion of HG with PL or EPG (Fig. 3.52).

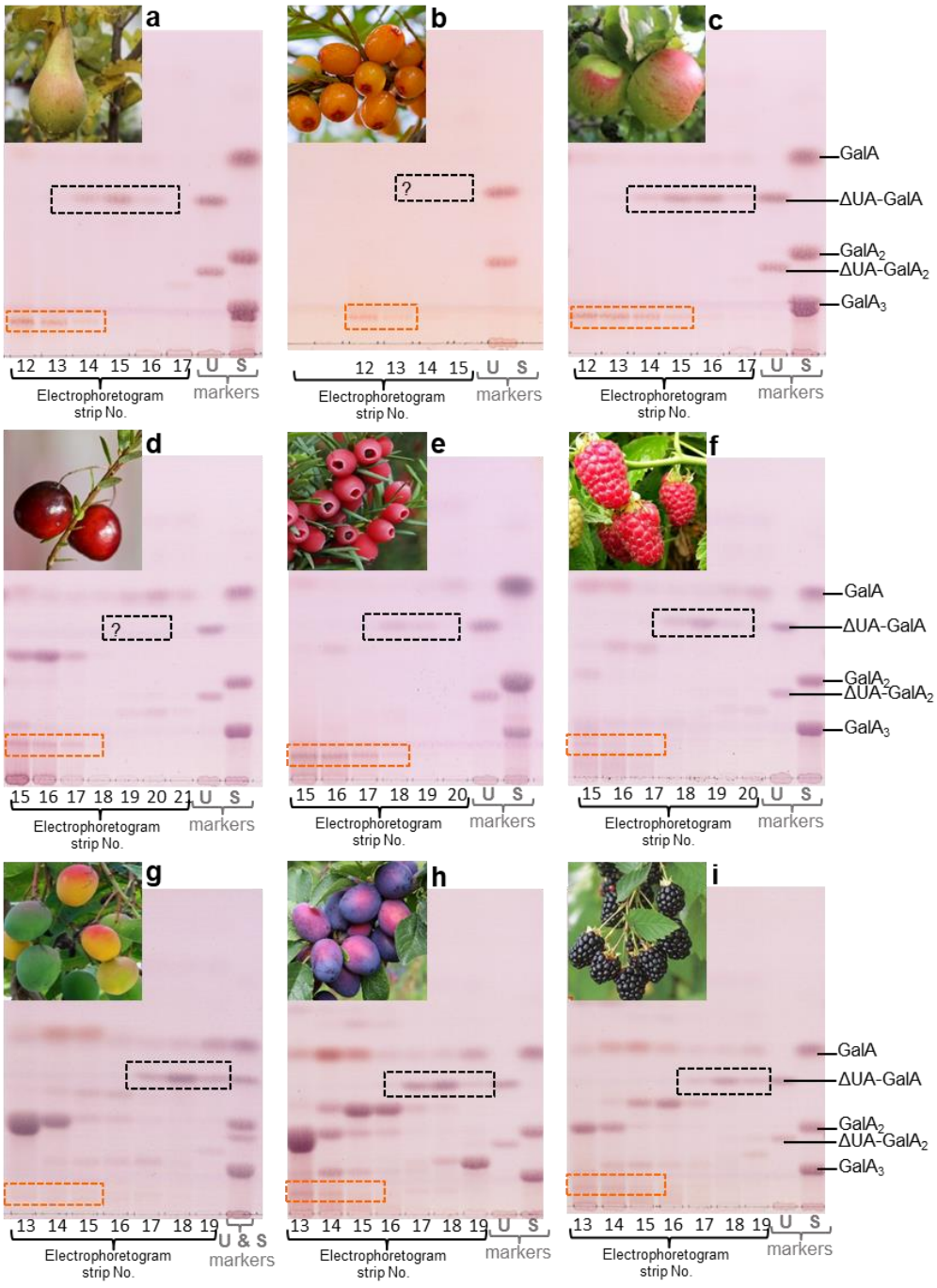

Fig. 3.52. Detecting pectate lyase and RG-I lyase fingerprints in Driselase digests of fruit cell walls of various species. AIR from the various fruit species were Driselase-digested and analysed as in Fig.3.38a. The electrophoretogram fractions expected to contain ΔUA-GalA$_n$s were subjected to TLC as before. TLCs of the PL and RGL products zone. In black dotted rectangles are PL products and in orange dotted rectangles are RGL products. **(a)** Pear. **(b)** Sea buckthorn. **(c)** Apple. **(d)** Cranberry. **(e)** Yew aril. **(f)** Raspberry. **(g)** Mango. **(h)** Plum. **(i)** Blackberry. TLCs were run in BAW 2:1:1 and stained with thymol. Markers were U, unsaturated oligogalacturonides; S, saturated oligogalacturonides.

3.3.1.7. PL fingerprint in Driselase digestion products from ripe mutant strawberries

Strawberries transformed with silenced PL gene were analysed for PL and RGL fingerprints. Three lines of strawberries were received from Malaga University, Spain, as part of a collaboration to analyse strawberries including wild type (C1) and 2 mutants (A14.1 and A39.1; Jiménez-Bermúdez *et al.* 2002) for PL and RGL fingerprints. The mutant strawberries were transformed by *Agrobacterium tumefaciens* LBA4404 strain carrying a plasmid with the strawberry PL gene (*njjs25*) in the antisense orientation (*pJLC32a*). According to Jiménez-Bermúdez et al. (2002), PL gene expression in the transformed fruits was less than 30% of the control. These mutants were initially constructed to study PL gene expression and its effect on fruit softening. The antisense inhibition of PL gene expression was accompanied by increased fruit firmness, indicating a role for PL in fruit softening. Decreased PL protein levels were also reported, indicating that PL gene expression was not completely blocked. The incompleteness in blocking gene expression is often observed with antisense lines.

The strawberries were de-achened and freeze-dried to ensure safe transportation from Spain. The AIR was prepared and digested with Driselase as done before with date and other fruits. After eluting the fractions from preparative electrophoretogram and running by TLC to visualize the products, all mutant (A14.1 and A39.1) and wild-type (C1) strains showed evidence of PL and RGL *in-vivo* attack.

No ΔUA-GalA$_n$s were detected when C1 was digested with 0.5% Driselase without prior de-esterification with alkali (10X higher Driselase concentration than usually used); however, RGL products (typically the tetramer ΔUA-Rha-GalA-Rha) were detected as expected in fractions 13–17 (Fig. 3.53a). GalA was detected mainly in fractions 8–11 as expected. However, additional GalA was observed in the rest of the

fractions suggesting that it was made after electrophoresis (maybe by hydrolysis of the unsaturated PL products) as it is known from experience that GalA cannot migrate that fast on electrophoretograms under these conditions. A trace of $GalA_2$ was also detected suggesting that Driselase failed to hydrolyse it fully to GalA. Issues with Driselase are discussed later as this was observed in other experiments as well. In addition to that, some unknown spots were observed in fractions 14–16 which did not line up with any of the markers.

The same experiment was repeated with 0.05% Driselase (the routinely used concentration) and interestingly the PL fingerprint showed up in the expected region in fractions 18–20 but as a trimer (ΔUA-$GalA_2$) instead of the expected dimer (Fig. 3.53b). This could be explained as Driselase failure to hydrolyse it completely to ΔUA-GalA. Supporting this explanation, $GalA_2$ was detected in fractions 12–13 which was not expected to be present after Driselase digestion. RGL products were detected as expected in fractions 12–13, usually slightly slower migrating than PL products (making the bottom part of the unsaturated products smear) on electrophoretograms. The unknown (observed in Fig. 3.53a) was detected again in fractions 14–16 suggesting its consistency. Another unknown spot was detected in fractions 18–20 co-electrophoresing with PL products, but slightly slower migrating on TLC which is further explored and discussed later.

Another repeat of the experiment was done with de-esterified AIR and 0.05% Driselase from a different batch. The dimeric PL product (ΔUA-GalA) was detected in fractions 16–18 as well as a trace of ΔUA-$GalA_2$ (Fig. 3.53c). RGL products were not clear (very faint smear in fractions 10–15). A large amount of $GalA_2$ was detected in fractions 11–14. All these observations suggest that Driselase failed to complete its

job. The same unknowns were detected again confirming their consistency in strawberries.

The same range of products was detected in the mutant strains (A14.1 and A39.1). Three experiments were conducted using each of the mutant strains as done with the wild type (C1). With 0.5% Driselase and no prior de-esterification of AIR, RGL products were detected but not PL products (Fig. 3.54a and 3.55a). With 0.05% Driselase and no prior de-esterification, RGL products, a trace of trimeric PL products, $GalA_2$ and the two unknowns were detected in both A14.1 (Fig. 3.54b) and A39.1 (Fig. 3.55b) strains. With 0.05% Driselase and pre-de-esterified AIR, dimeric PL products (ΔUA-GalA), $GalA_2$ and the two unknowns were detected in both A14.1 (Fig. 3.54c) and A39.1 (Fig. 3.55c) strains while RGL products were not clear.

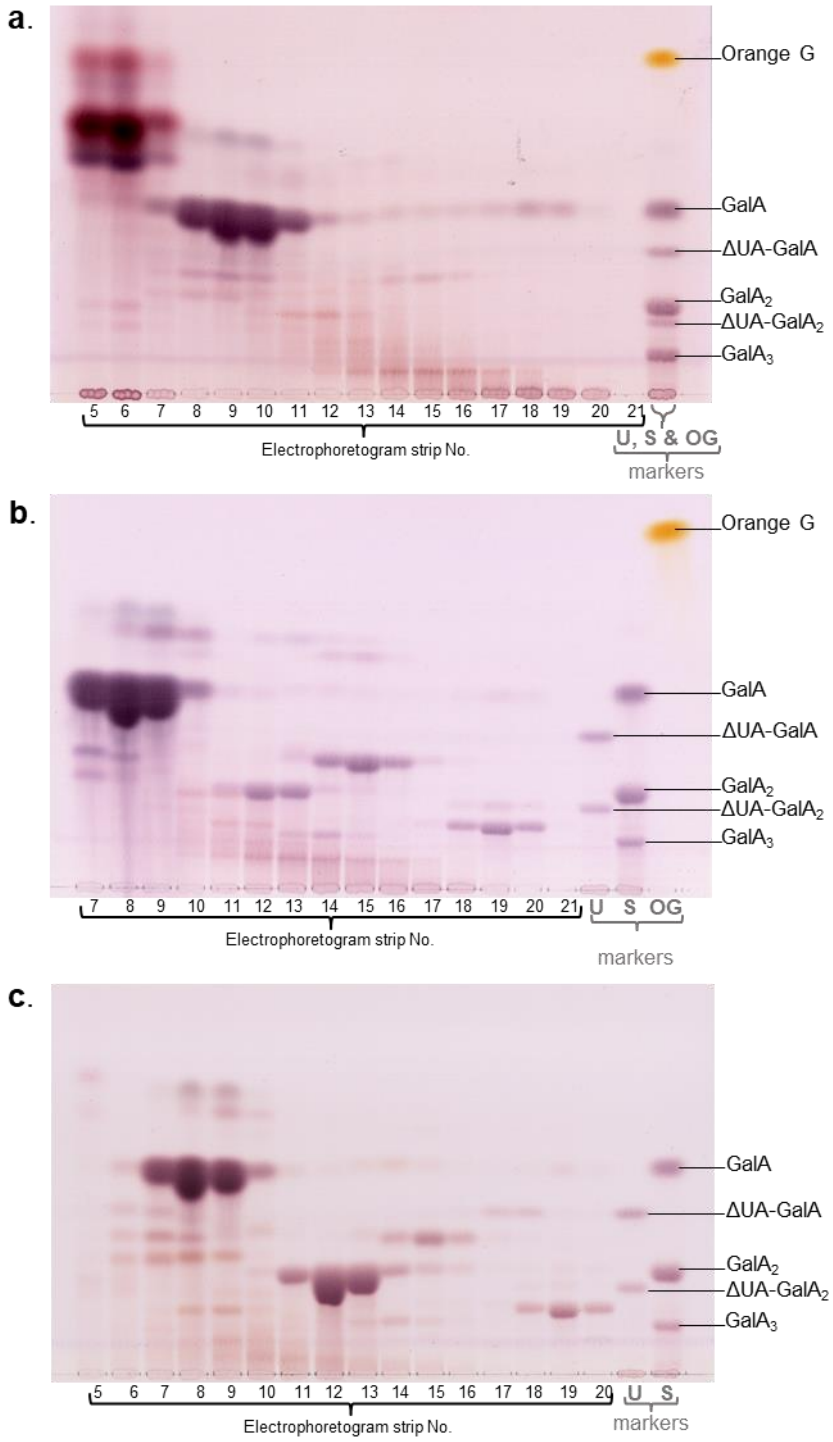

Fig. 3.53. Detecting pectate lyase and RG-I lyase fingerprints in digests of wild-type strawberry fruit cell walls. Strawberry (wild type C1.1) AIR (30 mg) was digested with Driselase (specified concentrations) and products were electrophoresed at pH 2 and eluted in 75% EtOH as in Fig. 3.38. Eluates from the paper strips were run by TLC in BAW 2:1:1 alongside marker mixtures and stained with thymol. **(a)** Non-de-esterified AIR digested with 0.5% Driselase. **(b)** non-de-esterified AIR digested with 0.05% Driselase. **(c)** De-esterified AIR digested with 0.05% Driselase. Markers were U, unsaturated oligogalacturonides; S, saturated oligogalacturonides.

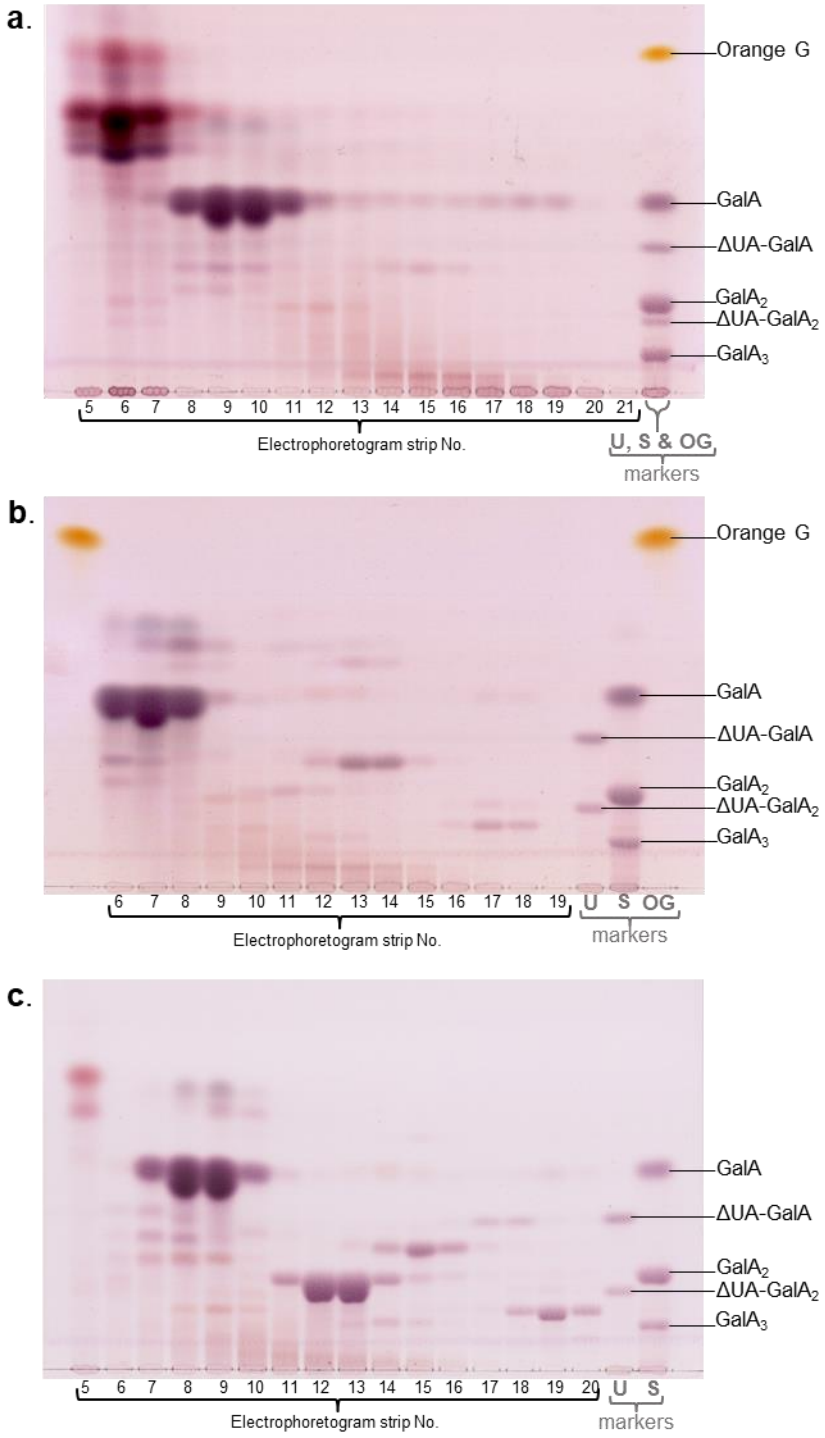

Fig. 3.54. Detecting pectate lyase and RG-I lyase fingerprints in digests of mutant strawberry (A14.1) fruit cell walls. Treatments and other details as in Fig. 3.53. **(a)** Non-de-esterified AIR digested with 0.5% Driselase. **(b)** non-de-esterified AIR digested with 0.05% Driselase. **(c)** De-esterified AIR digested with 0.05% Driselase.

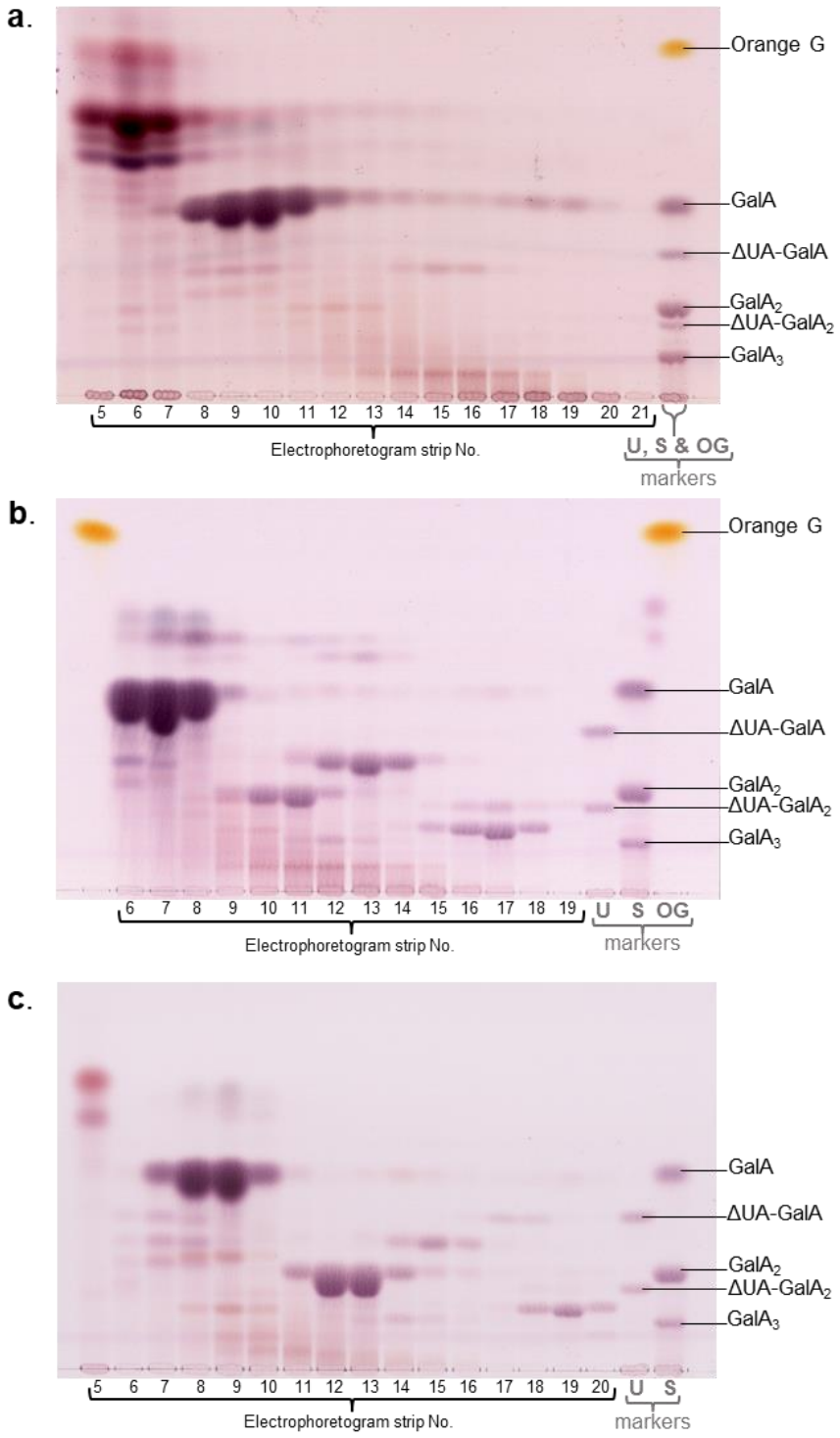

Fig. 3.55. Detecting pectate lyase and RG-I lyase fingerprints in digests of mutant strawberry (A39.1) fruit cell walls. Treatments and other details as in Fig. 3.53. **(a)** Non-de-esterified AIR digested with 0.5% Driselase. **(b)** non-de-esterified AIR digested with 0.05% Driselase. **(c)** De-esterified AIR digested with 0.05% Driselase.

3.3.1.8. Looking for PL and RGL products in the EtOH-soluble sugar fractions of ripe fruits

The AIR (alcohol-insoluble residue) is composed of cell wall polysaccharides that do not dissolve in ethanol. In the process of preparing it, fruits were homogenized and washed in 75% ethanol several times to get rid of all the monosaccharides and small oligosaccharides. The first ethanolic wash from dates, wild type and mutant strawberries, pear, plums, apples, yew arils, cranberries, sea buckthorn and rowan berries was kept for analysis to look for any unsaturated products that may have resulted from PL or RGL (most probably *exo* enzymes) action *in vivo*. A preparative HVPE (3 kV for 4 h) of concentrated fractions was conducted and samples were eluted from the expected unsaturated products zone according to the markers. The eluates were then analysed by TLC. No sign of PL or RGL products was detected in dates, wild type and mutant strawberries, plums, apples, cranberries, sea buckthorn and rowan berries (Fig. 3.56). Interestingly, the dimeric PL product (ΔUA-GalA) was detected in pear in fractions 13–14 in addition to some unknown acidic products. In yew arils, a faint band closely aligned with the marker ΔUA-GalA was also detected in fraction 20; however, judging from the band colour, it did not seem to be ΔUA-GalA. The probable presence of the PL fingerprint as a small soluble dimer in pears suggested the presence of *exo*-PL action, which would cleave one dimeric unit (ΔUA-GalA) at a time from the terminus (probably non-reducing) of HG. The absence of small, unsaturated products in all the other tested fruits suggested that only *endo*-PL and -RGL were acting *in vivo* in these species.

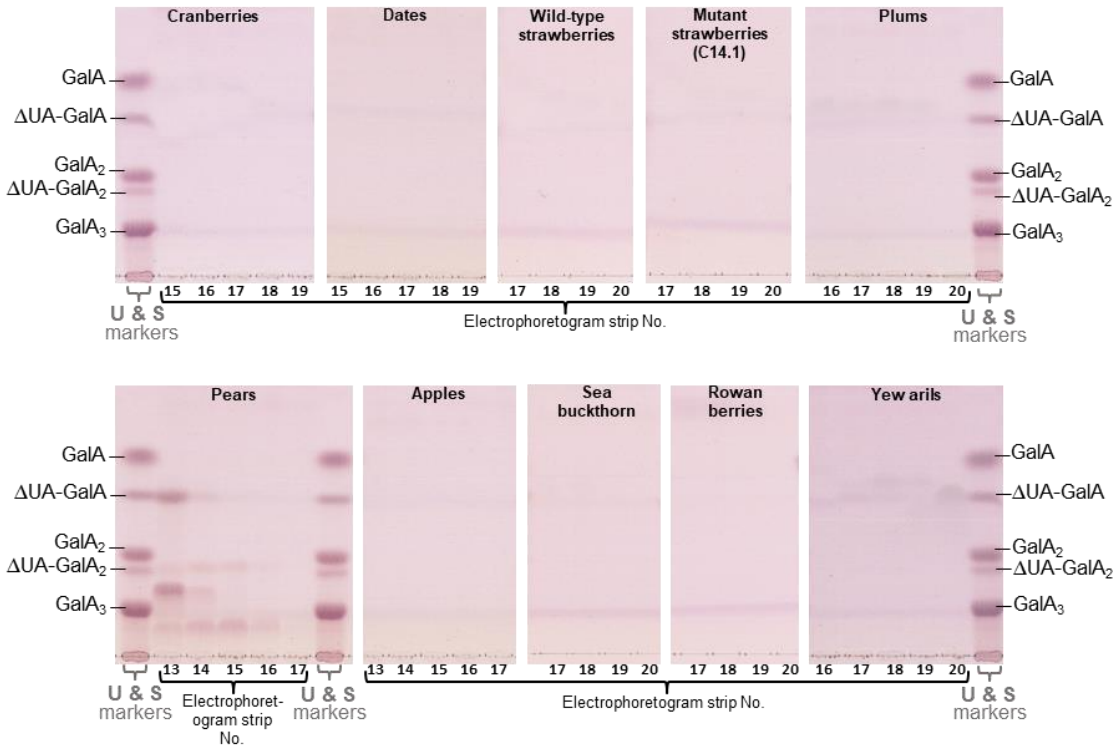

Fig. 3.56. Detecting PL and RGL fingerprints in ethanol-soluble fruit extracts. A sample of 10 ml of the first wash of fruit-EtOH homogenate was dried in a SpeedVac and re-dissolved in 1 ml H_2O. A preparative paper electrophoretogram was run as in Fig. 3.38. Samples were eluted from the expected unsaturated product zone guided by the markers (e.g. ΔUA-GalA). The specified fractions were then applied to TLC plates alongside markers, run in BAW 2:1:1, and stained with thymol. Markers were U, unsaturated oligogalacturonides; S, saturated oligogalacturonides.

3.3.2. Neutral sugar composition of fruit cell walls at three stages of ripening

3.3.2.1. Neutral sugars released by Driselase digestion of fruit AIR

Along with the acidic sugars released from fruit cell walls as a result of the digestion with Driselase, neutral sugars were also released. The migration of neutral sugars on paper electrophoretograms was minimal due to their neutral charges. They were eluted from the zones around the line of origin in 75% ethanol and run on TLC using EPAW (6:3:1:1) solvent which is known for resolving neutral monosaccharides, disaccharides and small oligosaccharides. The neutral sugar samples from fruit AIR hydrolysates

were run in triplicate (2.0, 1.0 and 0.5 µl). Along with the neutral sugars from the different fruits, a range of six loadings of markers were run as references for identification and quantification (Fig. 3.57 and 3.58).

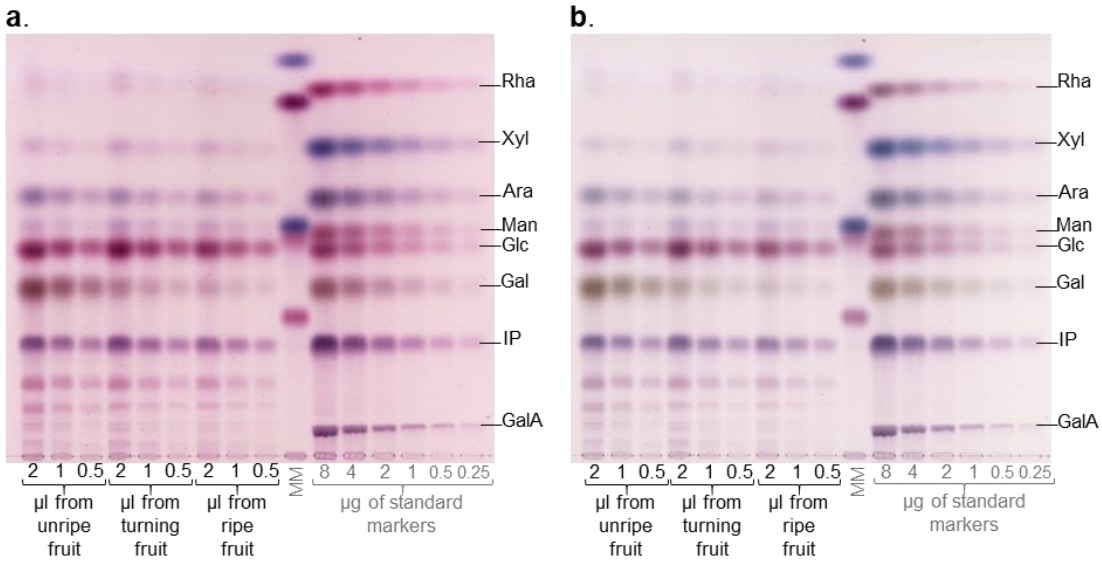

Fig. 3.57. Neutral sugars detected in date AIR Driselase digestion products. Date AIR (30 mg) was digested with Driselase and products were electrophoresed at pH 2 and eluted in 75% EtOH as in Fig. 3.38. **(a)** Eluates from the neutral sugar zone (around the line of origin) were run at three dilutions by TLC in EPAW (6:3:1:1) representing the Driselase hydrolysate of 0.05, 0.1 and 0.2 mg AIR along with a serial dilution of a standard marker mixture. The TLC was stained with thymol. **(b)** Rescan of the plate in (a) after 1 h incubation on the bench. IP refers to isoprimeverose; MM, sucrose, fructose, xylobiose, 3-*O*-methylglucose and 2-*O*-methylxylose (bottom to top).

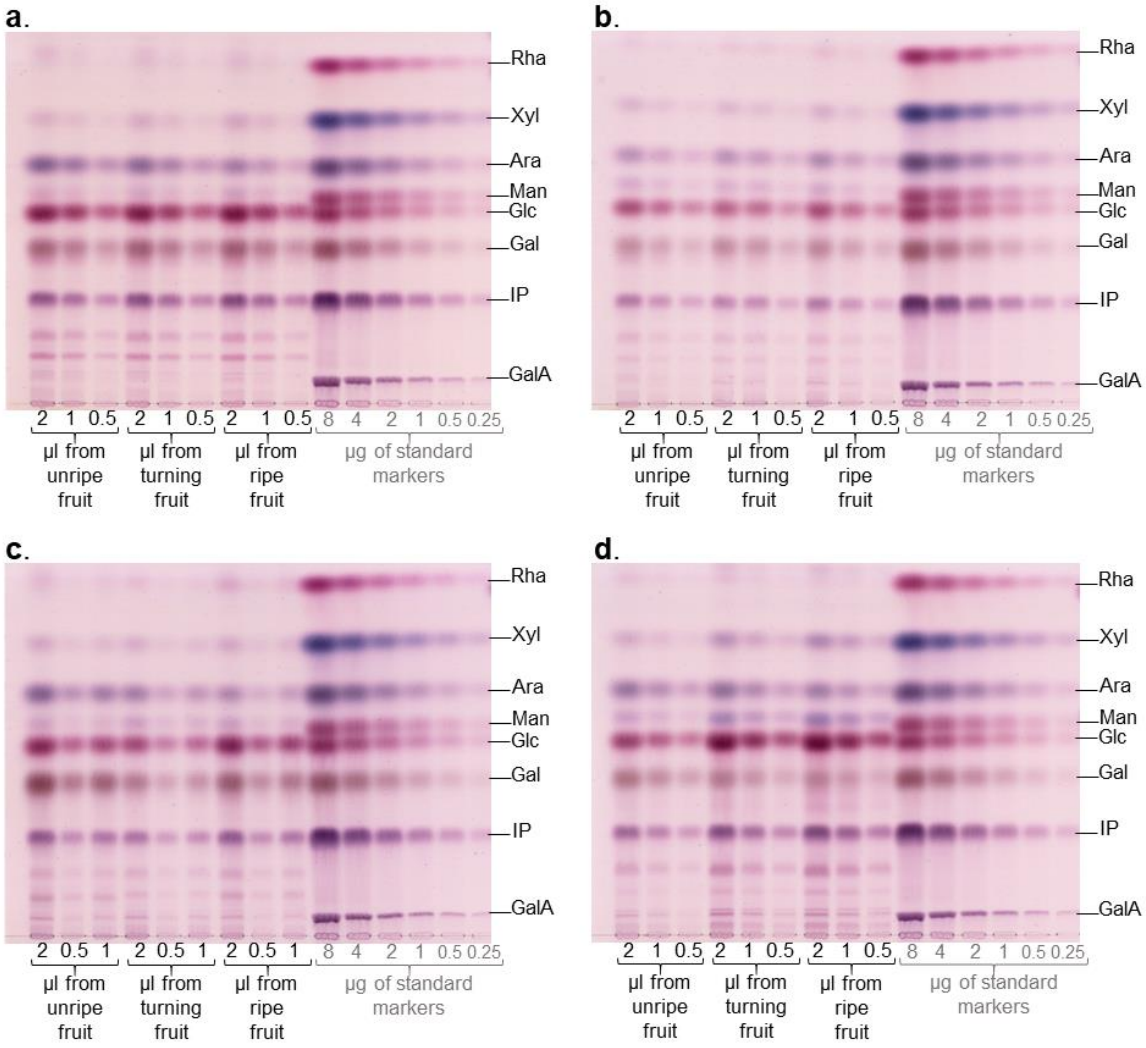

Fig. 3.58. Neutral sugars detected in Driselase digestion products of AIR from strawberry, blackberry, plum and mango. AIR (30 mg) from each fruit was digested with Driselase and products were electrophoresed at pH2 and eluted in 75% EtOH as in Fig. 3.38. Eluates from the neutral sugar zone (around the line of origin) were run by TLC in EPAW (6:3:1:1; 2 ascents) as in Fig. 3.57a along with a serial dilution of a standard marker mixture. The 4 TLC plates from **(a)** strawberry, **(b)** blackberry, **(c)** plum and **(d)** mango were stained with thymol.

For each of the markers, a standard curve of the spot intensity density (read by ImageJ software) was created to help estimate the concentration of the neutral sugars from the fruit samples at the three ripening stages (un-ripe, turning and ripe). A separate standard curve of each marker from each of the five TLC plates was created to avoid any possible errors resulting from any difference in staining between plates (shown here only for date (Fig. 3.59). An average standard curve of the spot intensity of each of the markers was created, showing the inter-plate standard error which seemed to be negligible (Fig. 3.60)

The same range of neutral sugars was detected in all the tested fruits. These were isoprimeverose (the diagnostic unit of xyloglucan composed of xylose and glucose), galactose (mainly from side chains of RG-I and xyloglucan), glucose (mainly from cellulose, xyloglucan and possibly starch and callose), arabinose (mainly from side chains of RG-I and arabinoxylan), xylose (mainly from xylan and possibly xylogalacturonan) and rhamnose (from the RG-I backbone). Mannose was not resolved from xylobiose but stained a different colour with thymol. A few other unknown sugars, slower migrating on TLC than isoprimeverose indicating that they could be di- or trisaccharides, were also detected. Arabinogalactan proteins (AGPs), which are composed of 90% carbohydrates, could also contribute to the total sugar content of fruit cell walls (especially arabinose and galactose); however, it has been established that Driselase cannot digest AGPs (Leszczuk *et al.* 2020).

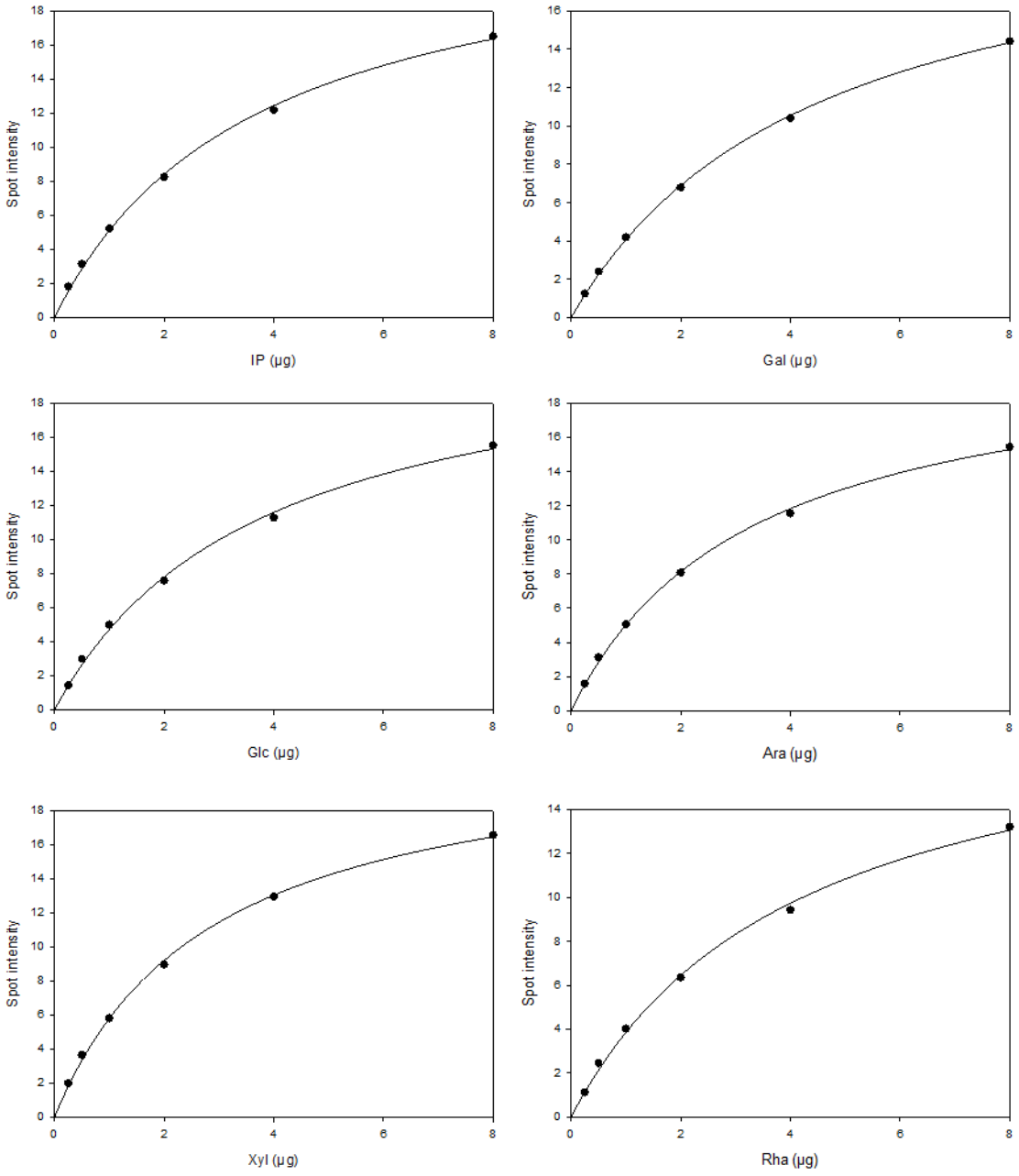

Fig. 3.59. Standard curves of each of the markers obtained from TLC spot intensity relative to their concentrations. The standard curves were obtained from the serial dilutions of the markers from Fig. 3.57a. The spot intensity densities were recorded using Image J software as described in §2.13.

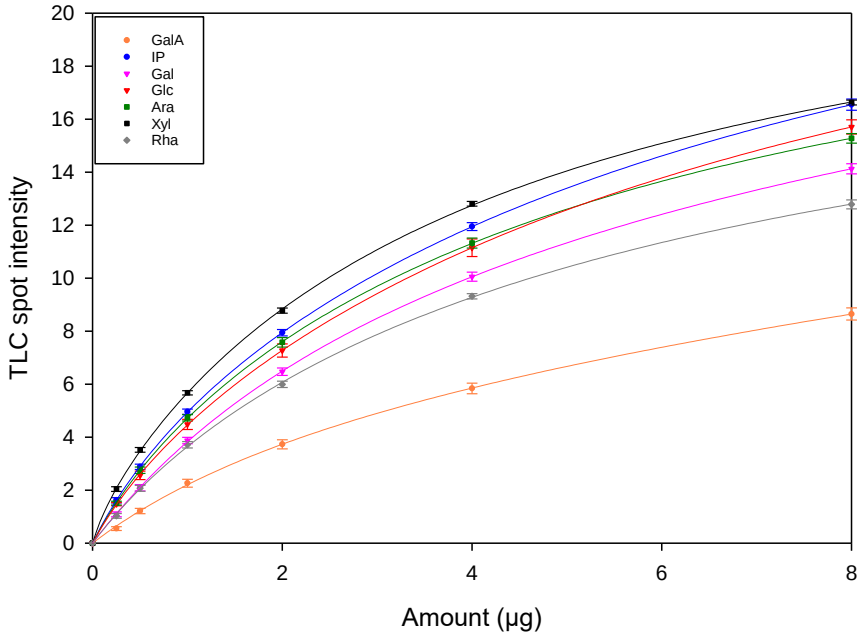

Fig. 3.60. Average standard curves of the markers from five TLC plates. The standard curves (single-rectangular hyperbola) were obtained from the average serial dilutions of each of the markers from five TLC plates (Fig. 3.57a and 3.58). The spot intensity densities were recorded using Image J software as described in §2.13. Error bars are of standard error; n=5.

In date, there was a significant decrease in the concentration of galactose and glucose detected (per unit dry weight of AIR) from un-ripe to ripe fruits (Fig. 3.61). A significant decrease of galactose was also detected in plum. Loss of galactose was a general trend in all the tested fruits (except strawberry and blackberry); the strawberry result agrees with the data of Gross and Sams (1984). Loss of arabinose was also observed in the tested fruits (significant in strawberry; not conclusive in mango) except blackberry, agreeing with Gross and Sams (1984). A slight increase in the concentration of rhamnose and xylose was observed in all the tested fruits using these methods although generally very low. The low concentration of xylose could be explained by partially being part of isoprimeverose and xylobiose, appreciable concentrations of which were detected in all the fruits (Fig. 3.61).

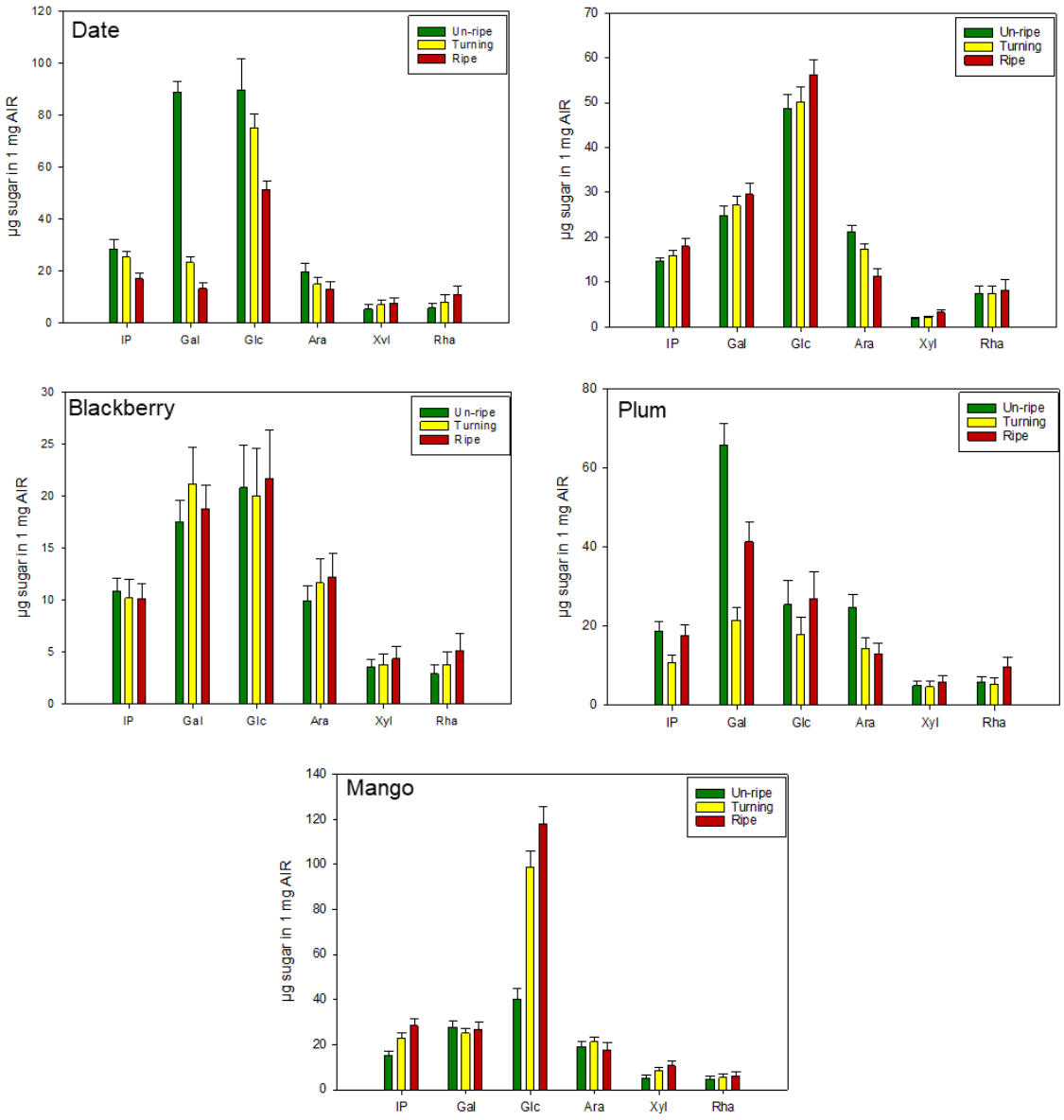

Fig. 3.61. The concentration of neutral sugar residues detected in Driselase/AIR digestion products of various fruits. The concentration of each sugar detected on the TLCs (Fig. 3.57 and 3.58) was estimated from the standard curves of the known markers (e.g. Fig. 3.59) and expressed as µg per mg AIR. Error bars are for standard error; n=3.

A loss in the total concentration of Driselase-releasable neutral sugars was observed in date during ripening while an increase was observed in mango. The total concentration of neutral sugars was similar in the different ripening stages of strawberry, blackberry and plum (Fig. 3.62). Although this was expected for plum, a loss of 30% and 17% of the neutral sugar concentration of strawberry and blackberry

was reported (Gross and Sams, 1984). The discrepancy in the results was due to the difference in the methods used to extract and quantify these sugars. It should be admitted that Driselase digestion of fruit AIR may not release all the monosaccharides as shown previously (refer to section 3.3.1.3), which explains the missing sugar weight obtained from the total of 1 mg AIR used in the experiment (Fig. 3.62). However, Driselase digestion was the best way to release the unsaturated PL and RGL products, which were the main objective of this project.

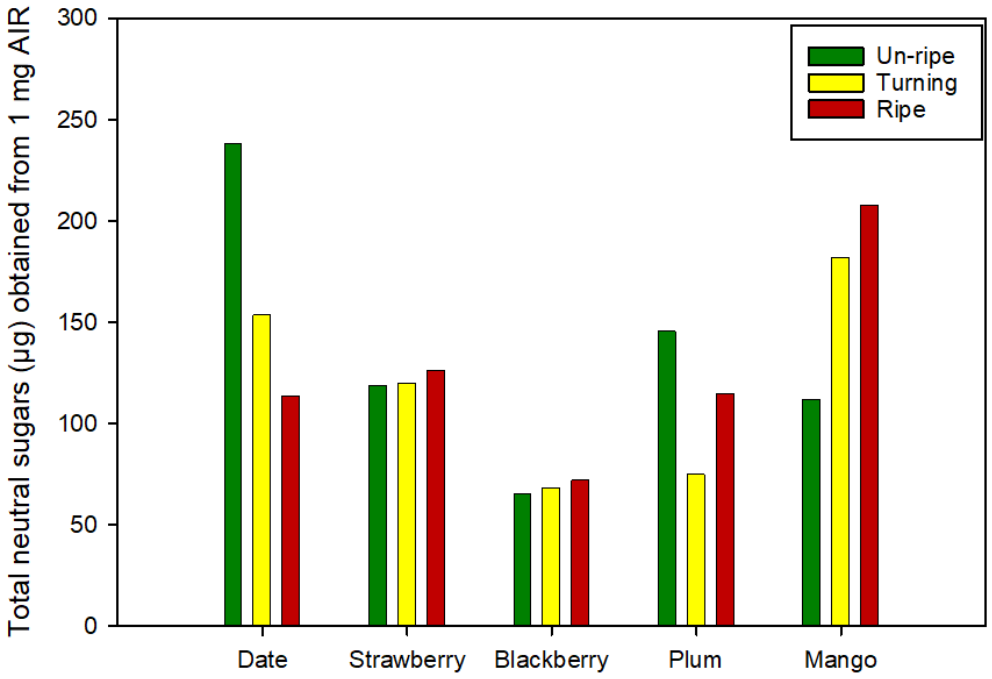

Fig. 3.62. Total concentration of neutral sugars detected in Driselase/AIR digestion products of various fruits. The total concentration of sugars was calculated as the sum of the concentration of all the sugars previously quantified in Fig. 3.61.

3.3.2.2. Neutral and acidic sugars released by TFA hydrolysis of AIR

Driselase hydrolysis of fruit AIR was not the best method to release the neutral sugars and quantify their concentrations since a maximum of only 25% of the released sugars were recovered (Fig. 3.62), some of which were in dimeric and oligomeric forms. A

better method for this purpose is TFA hydrolysis which could potentially hydrolyse all cell wall polysaccharides except cellulose (Gross and Sams, 1984).

Fruit AIR (10 mg) of date, strawberry, blackberry, plum and mango at the three stages of ripening were hydrolysed with 2 M TFA. Of the total AIR dry weight used, TFA solubilised up to 70% (Fig. 3.63). The TFA/AIR hydrolysates were run in triplicate (2.0 µl each) by TLC in EPAW (6:3:1:1) in addition to six loadings of markers (Fig. 3.64) as was done earlier with Driselase/AIR hydrolysates (§3.3.2.1).

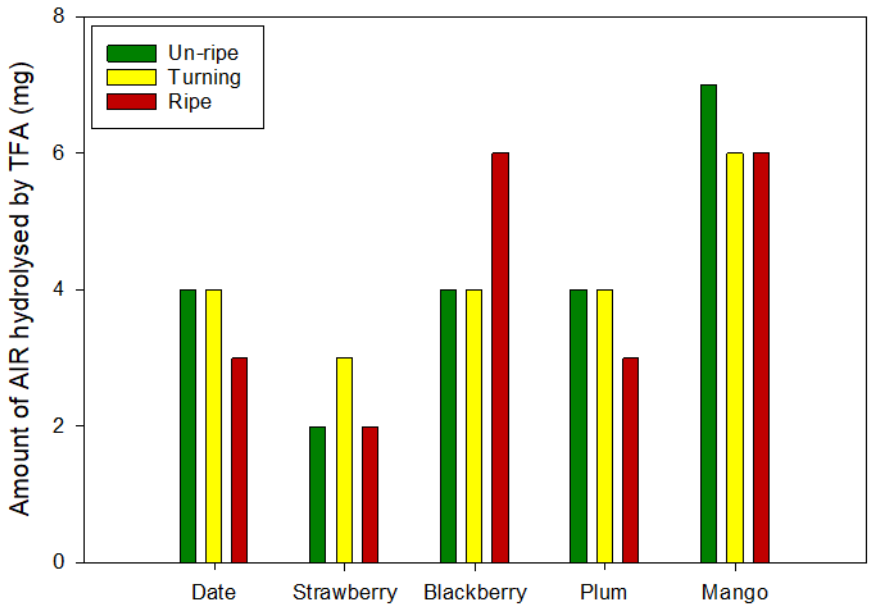

Fig. 3.63. Proportion of AIR (from fresh fruits at three ripening stages) hydrolysed with TFA. Driselase digestion was conducted on 10 mg of fruit AIR as described in §2.2.5 and the weight of the remaining insoluble residue was recorded after resuspension in water and drying in freeze-dryer.

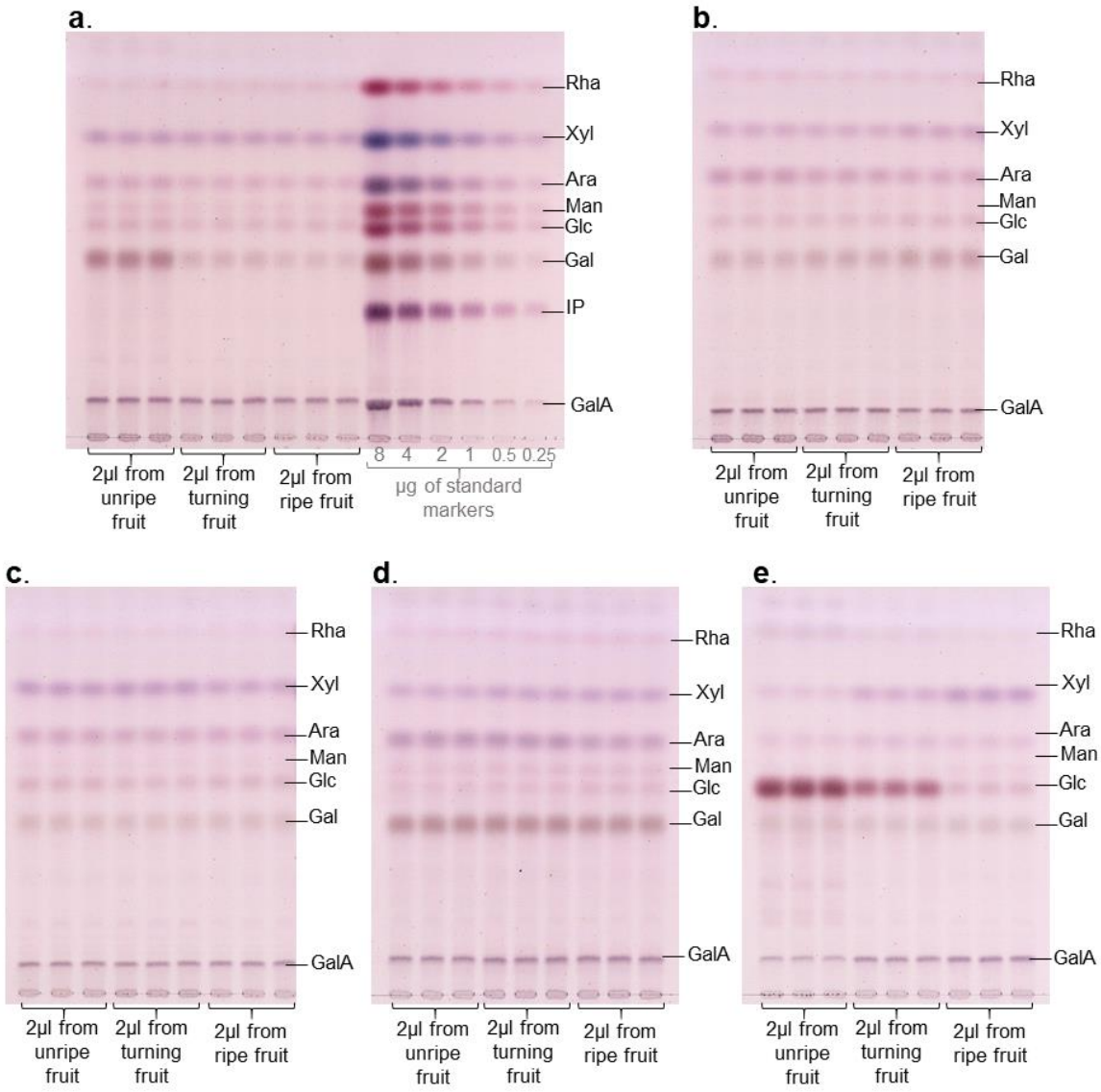

Fig. 3.64. Neutral and acidic sugars detected in TFA hydrolysis products of fruit AIR. AIR (10 mg) from each fruit was hydrolysed with 2 M TFA at 120℃ for 1 h. The products were centrifuged at 14500 g for 1 min and 0.5 ml of the supernatant was collected, dried and re-dissolved in 1 ml H_2O. Products (2 µl of each) were run by TLC in EPAW (6:3:1:1; 2 ascents) as in Fig. 3.58 along with a serial dilution of a standard marker mixture (shown only on date TLC (a). The 5 TLC plates from **(a)** date, **(b)** strawberry, **(c)** blackberry, **(d)** plum and **(e)** mango were stained with thymol.

As done before (§3.3.2.1), a standard curve of the spot intensity density (read by Image J software) for each of the markers was created to estimate the concentration of the sugars from the fruit samples at the three ripening stages (un-ripe, turning and ripe). An average standard curve of each of the markers was created, showing the inter-plate standard error which seemed to be negligible (Fig. 3.65).

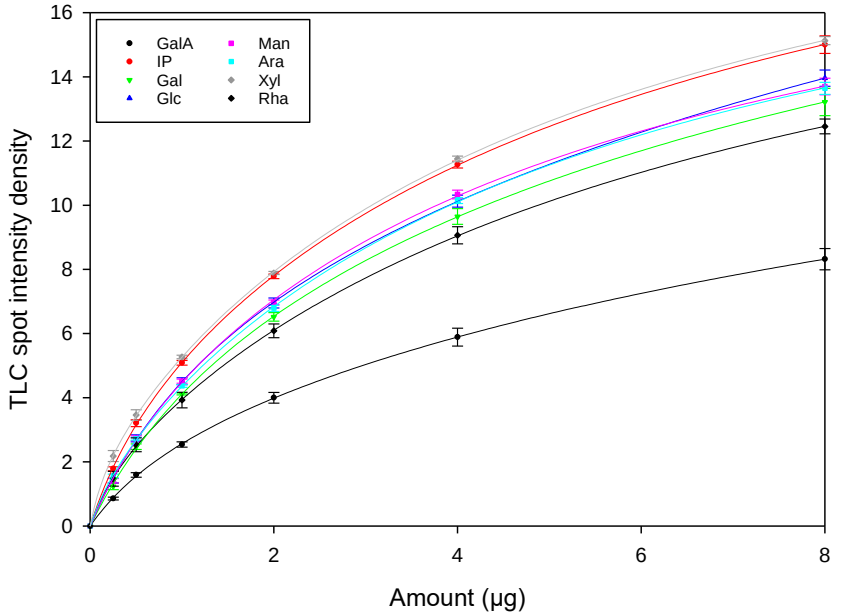

Fig. 3.65. Average standard curves of the markers from three TLC plates. The standard curves (single-rectangular hyperbola) were obtained from the average serial dilutions of each of the markers from 3 TLC plates (Fig. 3.64a, b and c; shown only for a). The spot intensity densities were recorded using Image J software as described in §2.13. Error bars are of standard error; n=3.

Loss of GalA concentration was observed in date, strawberry and blackberry with ripening (Fig. 3.66). A significant loss of galactose was observed in date. Loss of galactose was a general trend in all the tested fruits except strawberry. Loss of arabinose was also observed in the tested fruits, agreeing with Gross and Sams (1984). A slight increase in the concentration of xylose was observed in strawberry, plum and mango. The concentration of rhamnose slightly decreased in blackberry and mango and stayed about constant in the other fruits. The concentration of rhamnose was generally low indicating the low amount of RG-I within fruit cell walls compared to HG. Loss of mannose was observed in date and strawberry and no difference in the other fruits. In mango, a significant loss of glucose was observed (Fig. 3.66), which could be due to loss of starch reported with ripening (Bello-Pérez *et al.* 2007). AGPs might also contribute to the total sugars released by TFA from the fruit AIR (especially arabinose and galactose). The contribution of AGPs to the total sugar content may not

be significant as cell walls are not rich in AGPs (Cosgrove and Jarvis 2012) and the difference in the total arabinose and galactose quantified from fruit AIR by Driselase and TFA digestion was not very big.

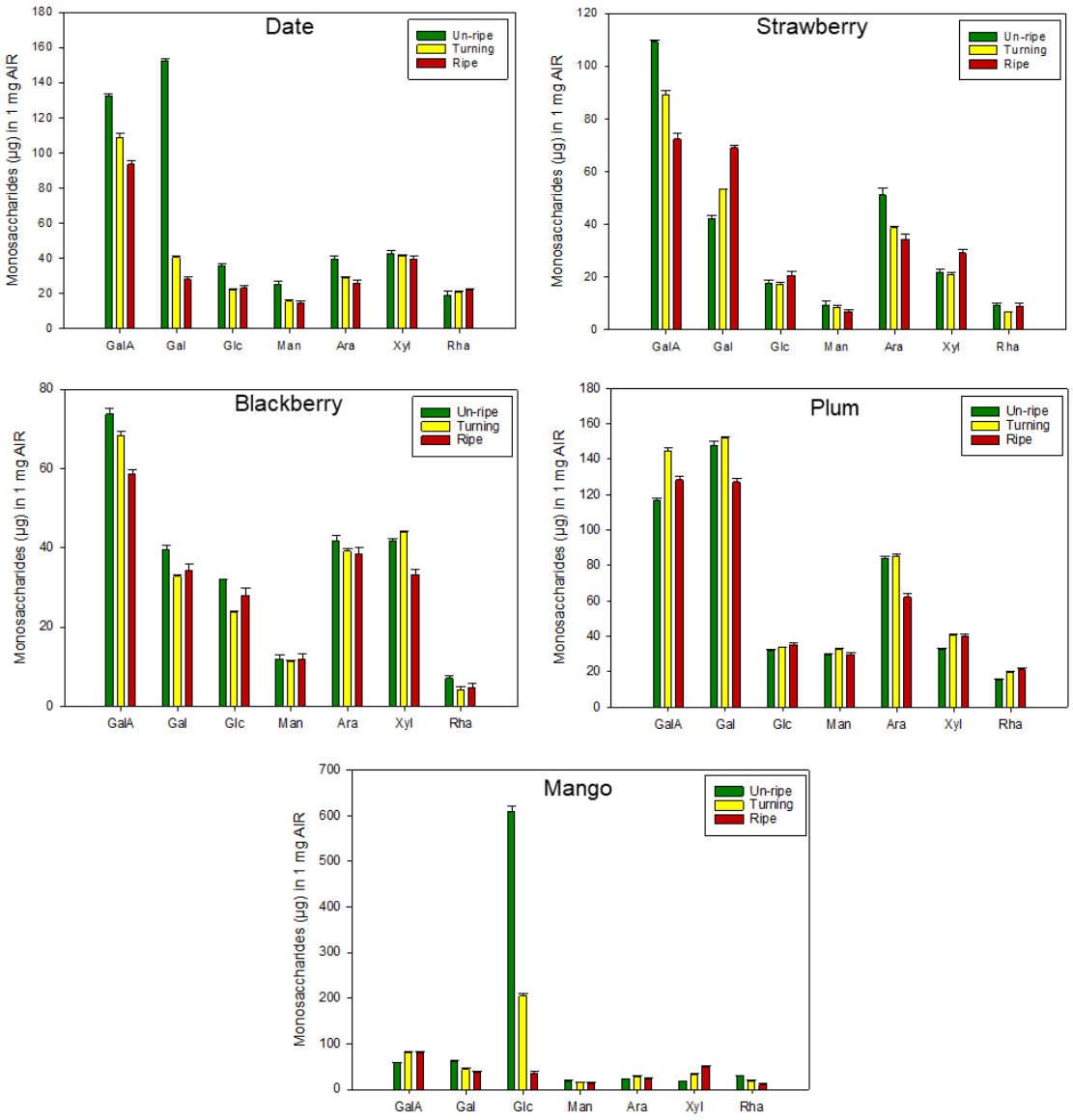

Fig. 3.66. The concentration of sugar residues detected in TFA/AIR hydrolysates of various fruits. The concentration of each sugar detected on the TLCs (Fig. 3.64) was estimated from the standard curves of the known markers (e.g. Fig. 3.59) and expressed as µg per mg AIR. Error bars are for standard error; n=3.

The total sugar concentration in fruit AIR released by TFA hydrolyses was more than the sugar released by Driselase (as expected; Fig. 3.67). The difference in the sugar concentration between unripe and ripe fruits was more pronounced in date and mango, while remained approximately constant in the other tested fruits.

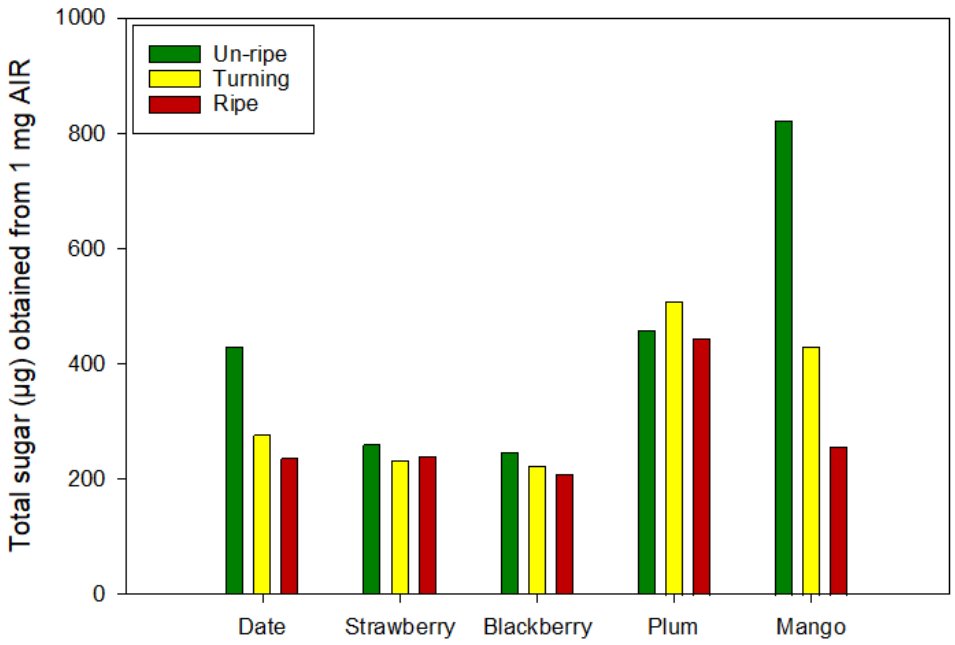

Fig. 3.67. Total concentration of sugars detected in TFA/AIR hydrolysates of various fruits. The total concentration of sugars was calculated as the sum of the concentration of all the sugars previously quantified in Fig. 3.61.

The total solubilised sugars and the insoluble residue after treatments with Driselase or TFA should add up to 100% or slightly more (keeping in mind adding H_2O molecules to the mass as a result of the hydrolysis); however, there was some unexplained loss in some fruits as summarized in table 3.3. The quantification of sugars in this experiment was limited as the AIR samples were prepared only once (n=1).

Table 3.3. The total sugar recovered (either as soluble or insoluble residue) after AIR treatment with Driselase or TFA.

		Driselase			TFA		
Fruit	Stage of ripening	% Solubilized and quantified sugars	% Insoluble residue	% Total sugar recovered from 1 mg AIR	% Solubilized and quantified sugars	% Insoluble residue	% Total sugar recovered from 1 mg AIR
Date	Unripe	24	47	71	43	60	103
	Turning	15	55	70	28	60	88
	Ripe	11	63	74	24	70	94
Strawberry	Unripe	12	23	35	26	80	106
	Turning	12	24	36	23	70	93
	Ripe	13	20	33	24	80	104
Blackberry	Unripe	7	46	53	25	60	85
	Turning	7	58	65	22	60	82
	Ripe	7	54	61	21	40	61
Plum	Unripe	15	39	54	46	60	106
	Turning	8	60	68	51	60	111
	Ripe	11	39	50	44	70	114
Mango	Unripe	11	54	65	82	30	112
	Turning	18	36	54	43	40	83
	Ripe	21	22	43	26	40	66

3.3.3. PL and RGL fingerprints in fruit cell walls at different stages of ripening

3.3.3.1. Softness measurements of fruits at three ripening stages

Fruits of various species at three ripening stages (un-ripe, turning and ripe) were picked freshly and their firmness was checked by measuring the compression force (in Newton) required to cause 20% deformation without real penetration of the fruits. There was a significant difference ($p<0.05$) in the fruit firmness between the three stages of each fruit species shown in Fig. 3.68, agreeing with previous reports of date

(Serrano *et al.* 2001), mango, strawberry (Airianah *et al.* 2016), raspberry (Vicente *et al.* 2007) and blackberry (Zhang *et al.* 2019).

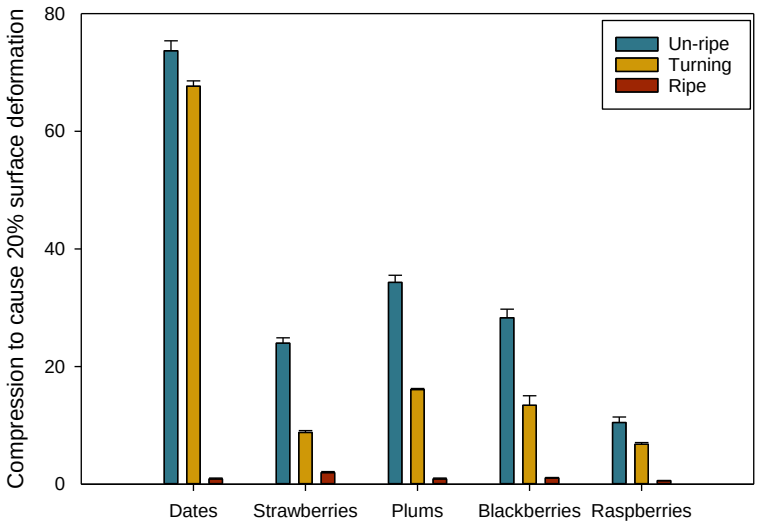

Fig. 3.68. Firmness measurements of fruits at three ripening stages. Fruits were randomly picked from 3 groups of three ripening stages (unripe, turning and ripe). Firmness was measured as the force (N) required to cause 20% surface deformation (reduction in fruit radius). Error bars are of standard error; n=3.

3.3.3.2. PL and RGL fingerprints in pre-de-esterified strawberries and date (Hilali cultivar) AIR at different stages of ripening

Fruit AIR pre-de-esterified by 0.2 M Na_2CO_3 was digested with 0.05% Driselase. Products were electrophoresed at pH 2, 3 kV for 4 h. Samples were then eluted from the paper electrophoretogram in 75% EtOH and run on TLC in BAW (2:1:1) followed by thymol staining to visualize the products. This standard procedure was used with samples of un-ripe, turning and ripe strawberries and date (Hilali cultivar). There was no difference in the range of products detected at the different stages of ripening. PL fingerprint was detected in all three stages of both strawberries and dates indicating that PL enzyme act early in fruit development.

In strawberries, a PL fingerprint (mainly the expected ΔUA-GalA) was detected in fractions 15–18 in all three stages of ripening as visualized on TLC (Fig. 3.69). Faint spots of the trimer ΔUA-$GalA_2$ were detected in fractions 17–19, indicating incomplete Driselase digestion. Three unknown spots were detected (also seen previously in mutant strawberries) in fractions 11–13, 13–15 and 17–19 which indicates highly acidic products (because they migrated further away than GalA on the electrophoretogram). The unknowns in fractions 13–15 and 17–19 did not line up with any of the markers; however, the unknown at fractions 11–13 line up nicely with $GalA_2$ (its identity was confirmed later by MS, section3.3.3.4) on TLC despite the fact that it was expected to be completely hydrolysed to GalA by Driselase. The three unknowns could be intermediate products which Driselase failed to fully hydrolyse to their final products. These unknowns were further investigated in section 3.3.3.4. Major spots of GalA were detected in fractions 6–10 as expected in all three stages. However, minor spots of GalA were detected in almost all the other fractions which was not expected to be the case because GalA is less acidic than ΔUA-GalA and would never migrate the same distance on electrophoresis. The only explanation for that is the degradation of some of the products to GalA after electrophoresis and before TLC. The unknowns could be the source of that. Unfortunately, RGL products were not detected in any of the three stages of ripening. That could not be true as RGL products had been detected in strawberries previously (Fig.3.53) and the only reason for not detecting them here would be that Driselase failed to release them either due to certain modification that made them not accessible to Driselase or that this particular batch of Driselase just failed to do its job.

In dates, the same range of products as in strawberries was detected (Fig. 3.70). The PL fingerprint (ΔUA-GalA) was detected in fractions 19–21 as expected (co-electrophoresing with the marker) in all three stages of ripening. RGL products were not detected, contradicting the previous results (Fig. 3.38) and confirming that the unknown spots (which had not been detected in date previously) were a result of Driselase incomplete digestion. No $GalA_2$ or the other acidic unknowns were detected in ripe date except one in fractions 17–18 which migrated slower than ΔUA-GalA on both PE and TLC. The intensity of the unknown spots was less in ripe fruit/Driselase digestion products (as observed on the TLCs of both strawberries and dates) than the other two stages, suggesting that the accessibility of these products to Driselase is better than in earlier stages of ripening.

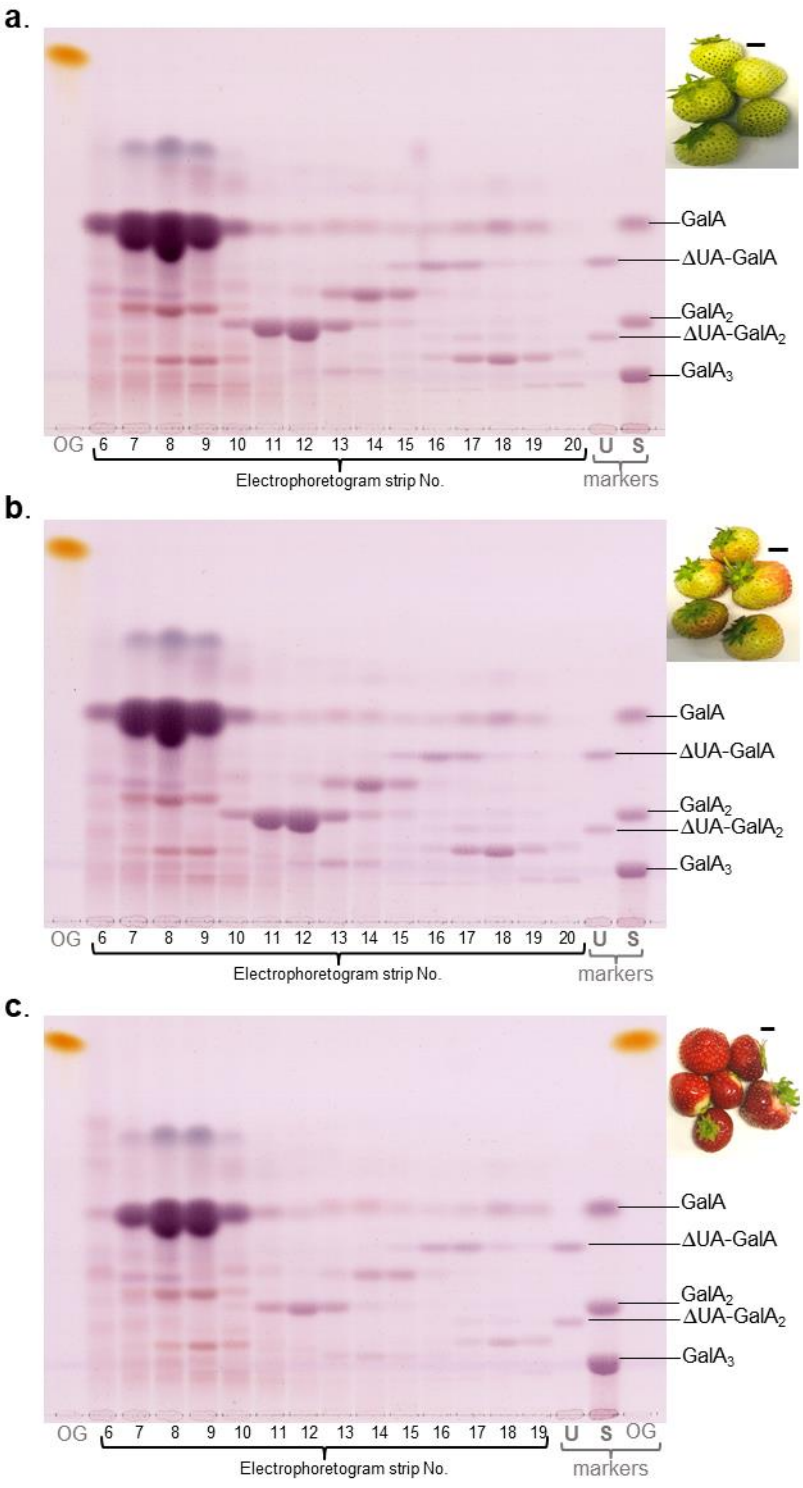

Fig. 3.69. Detecting pectate lyase and RG-I lyase fingerprints in digests of pre-de-esterified strawberry fruit cell walls. Strawberry AIR (30 mg, de-esterified with 0.2 M Na_2CO_3) was digested with 0.05% Driselase and products were electrophoresed at pH 2 and eluted in 75% EtOH as in Fig. 3.38. Eluates from the paper strips were run by TLC in BAW 2:1:1 alongside marker mixtures and stained with thymol. **(a)** Unripe strawberry **(b)** Turning strawberry. **(c)** Ripe strawberry. Markers were U, unsaturated oligogalacturonides; S, saturated oligogalacturonides; OG, orange G. Scale bar= 1 cm.

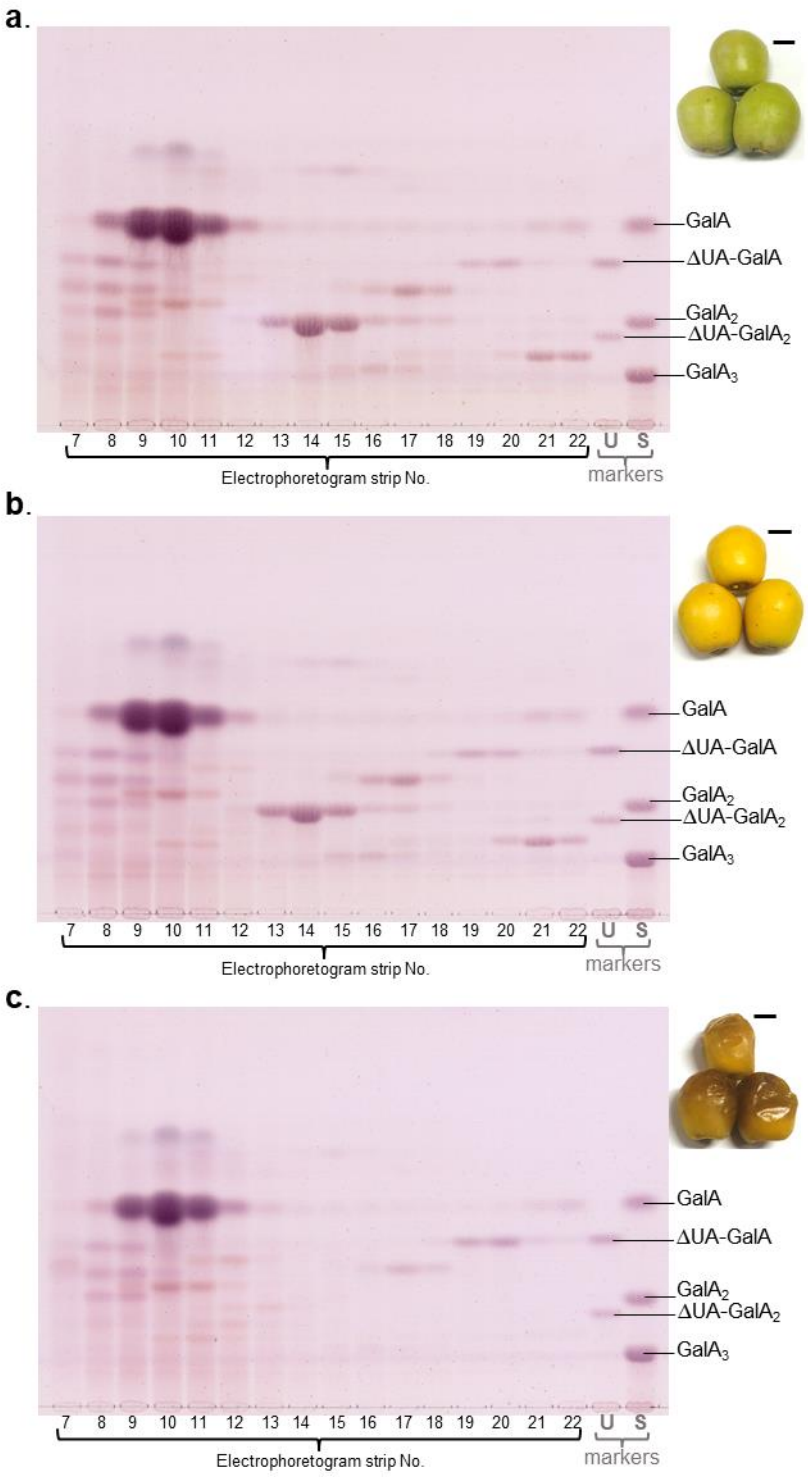

Fig. 3.70. Detecting pectate lyase and RG-I lyase fingerprints in digests of pre-de-esterified date (Hilali variant) fruit cell walls. Date AIR was digested and products were analysed as in Fig. **3**.69. **(a)** Unripe date **(b)** Turning date. **(c)** Ripe date. Markers were U, unsaturated oligogalacturonides; S, saturated oligogalacturonides. Scale bar= 1 cm.

3.3.3.3. PL and RGL fingerprints in post-de-esterified fruit AIR

The AIR of other fruits at the three stages (unripe, turning and ripe) of ripening of strawberry, date (new harvest of Khalas cultivar), blackberry, plum and mango was prepared with no pre-de-esterification treatment as the Driselase was thought to have PME activity which would cleave any methyl-ester group allowing the hydrolysis of the polymers. Samples of fruit AIR were digested with Driselase and were ready for preparative HVPE as done before. However, a step back to de-esterification was taken as a precaution in case some polysaccharides could be esterified not only with methyl-ester groups but also acetyl-ester groups that Driselase would not be able to cleave as Driselase has no acetyl esterase activity. Therefore, for this set of samples, the AIR/Driselase digests were dried and re-dissolved in 75% EtOH in which all monomers and small oligomers came into solution. The supernatant was then collected, de-esterified in 0.2 M Na_2CO_3 and digested again 0.05% Driselase. The same standard procedure was then followed and the products were analysed by TLC.

In strawberry, major GalA spots were detected in fractions 8–12 (Fig.3.71). Both PL and RGL fingerprints (ΔUA-$GalA_2$ and ΔUA-Rha-GalA-Rha respectively) were detected on TLC of all three stages of ripening. The PL product was the trimeric form (ΔUA-$GalA_2$) instead of the expected dimer, indicating failure of Driselase to complete its digestion. The ΔUA-$GalA_2$ was detected in fractions 19–22 of all three ripening stages. The RGL products were detected in fractions 13–17 as expected, running slightly slower than PL products on electrophoresis and slightly slower that $GalA_3$ on TLC. $GalA_2$ was also detected in fractions 13–15 (present due to Driselase incomplete digestion). In addition, the two unknowns (in fractions 15–18 and 19–21) were detected that had been observed previously in strawberry (Fig. 3.69) and date (Fig. 3.70) confirming their consistency (also due to Driselase incomplete digestion).

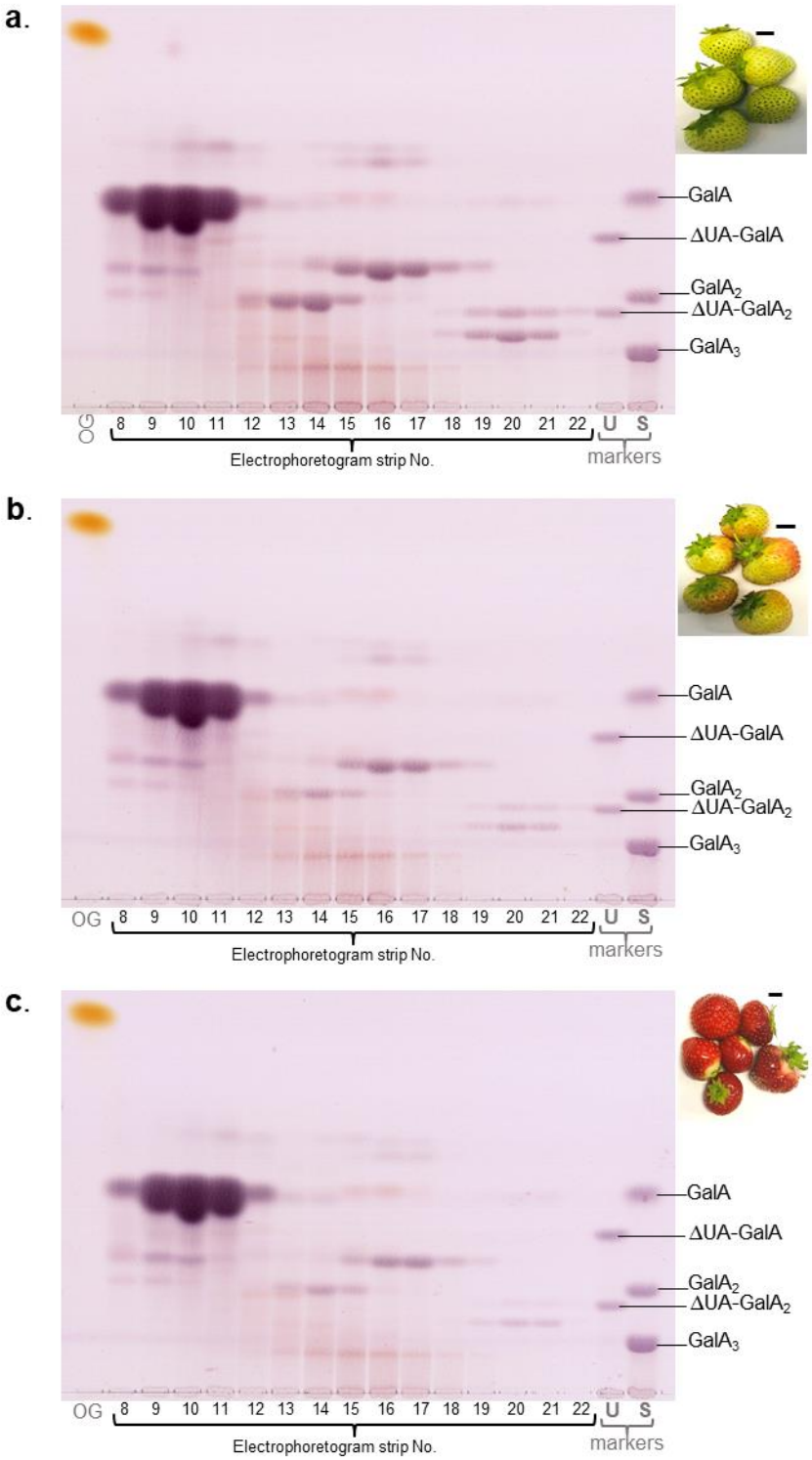

Fig. 3.71. Detecting pectate lyase and RG-I lyase fingerprints in digests of post-de-esterified strawberry fruit cell walls. Fruit AIR was digested with 0.05% Driselase. Products were dried and re-dissolved in 75% EtOH and incubated at 4 °C for 16 h. The supernatant was then collected, de-esterified in 0.2 M Na2CO3 and neutralized with acetic acid. Products were then dried and digested again 0.05% Driselase. Products were electrophoresed at pH 2 and eluted in 75% EtOH as in Fig. 3.38. Eluates from the paper strips were run by TLC in BAW 2:1:1 alongside marker mixtures and stained with thymol. **(a)** Unripe fruit. **(b)** Turning fruit. **(c)** Ripe fruit. Markers were U, unsaturated oligogalacturonides; S, saturated oligogalacturonides; OG, orange G. Scale bar= 1 cm.

In unripe and turning dates (Fig. 3.72a and b), the same range of products was observed as in strawberries. Major GalA spots were detected in fractions 6–9. The PL products were detected in the trimeric form in fractions 17–18. The RGL products were detected in fractions 11–15 which appeared to extend to fraction 18. That could not be true based on previous experience of the electrophoresis, but could actually be a different product which was more acidic than RGL products and co-migrated with them on TLC. $GalA_2$ was detected in fractions 11–12 and the two unknowns in fractions 12–16 and 17–18. On the other hand, in ripe dates (Fig. 3.72c), Driselase digestion seemed to be more efficient. The PL products were detected in both dimeric and trimeric forms in fractions 15–17 and 17–18 respectively. No $GalA_2$ was detected, however GalA (other than the expected major spots in fractions 6–9) was detected instead (in fractions 11–14) indicating that it could have been produced after electrophoresis. The two unknowns were detected in fractions 12–16 and 17–18 as in un-ripe and turning stages.

In blackberries, a similar range of products was detected in the three ripening stages (Fig. 3.73). Major GalA spots were detected in fractions 7–9. A very low amount of dimeric PL product was detected in fractions 15–17 (more in ripe than in earlier stages). The RGL products were detected in fractions 11–13 as expected. Only one of the two unknowns seen previously in strawberries and dates was detected in fractions 12–15. In addition, 3 more acidic unknowns were detected in fractions 11–15, one of which co-migrated with GalA on TLC.

In plums, the three stages exhibited the same range of products; however, the spot intensities on TLC of turning fruit were less than those of un-ripe and ripe fruits (Fig. 3.74). GalA major spots were detected in fractions 7–10. PL products were detected in both dimeric and trimeric forms in fractions 16–18 and 18–20, respectively. RGL products were detected in fractions 12–17. $GalA_2$ was detected in fractions 12–13. The

two unknowns seen previously in strawberries, dates and blackberries were detected in fractions 13–17 and 17–20, respectively.

In mangos, GalA major spots were detected in fractions 8–11 in samples from all three ripening stages (Fig. 3.75). Very little (not clearly seen spots) PL products were detected in unripe mangos; however, the dimer ΔUA-GalA appeared as faint spots in turning and ripe mangos in fractions 17–19. RGL products were detected in fractions 13–16 in un-ripe fruit, but were barely seen in turning and ripe fruits. No $GalA_2$ or any of the unknowns seen previously in other fruit species were detected in un-ripe mangos. However, they appeared in fractions 13–14 and 15–17 in turning fruit. In ripe mangos, $GalA_2$ was detected in fractions 13–14 and one of the unknowns in fractions 15–17 as in turning mangos in addition to another common unknown in fractions 19–20.

Table 3.4 summarizes the products (GalA and PL and RGL products) detected on the TLCs of all the tested fruits with a qualitative indication of their spot intensities.

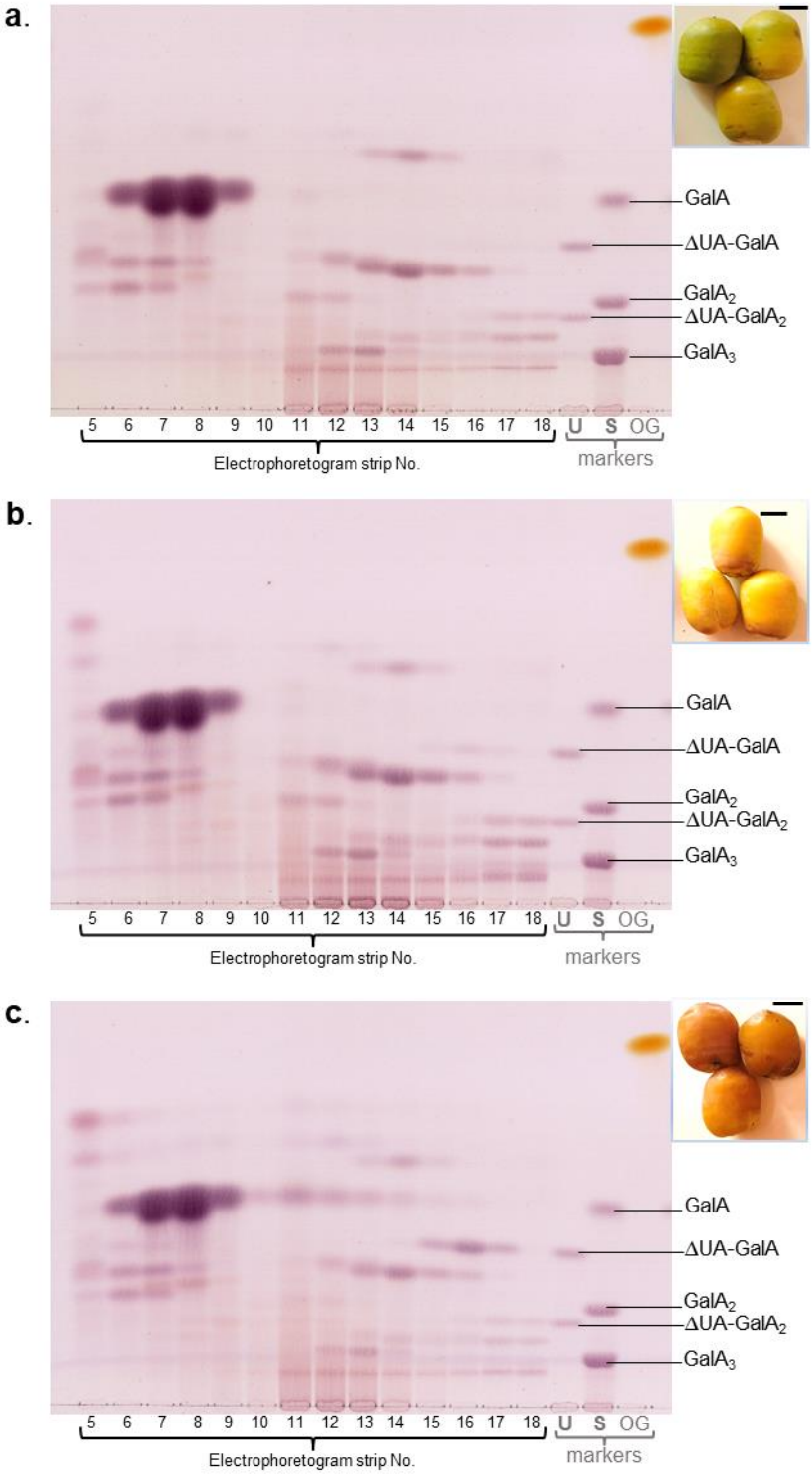

Fig. 3.72. Detecting pectate lyase and RG-I lyase fingerprints in digests of post-de-esterified date (khalas cultivar) fruit cell walls. Fruit AIR was de-esterified and digested with Driselase and products were electrophoresed and applied to TLC as in Fig. 3.71. **(a)** Unripe fruit. **(b)** Turning fruit. **(c)** Ripe fruit. Markers were U, unsaturated oligogalacturonides; S, saturated oligogalacturonides; OG, orange G. Scale bar= 1 cm.

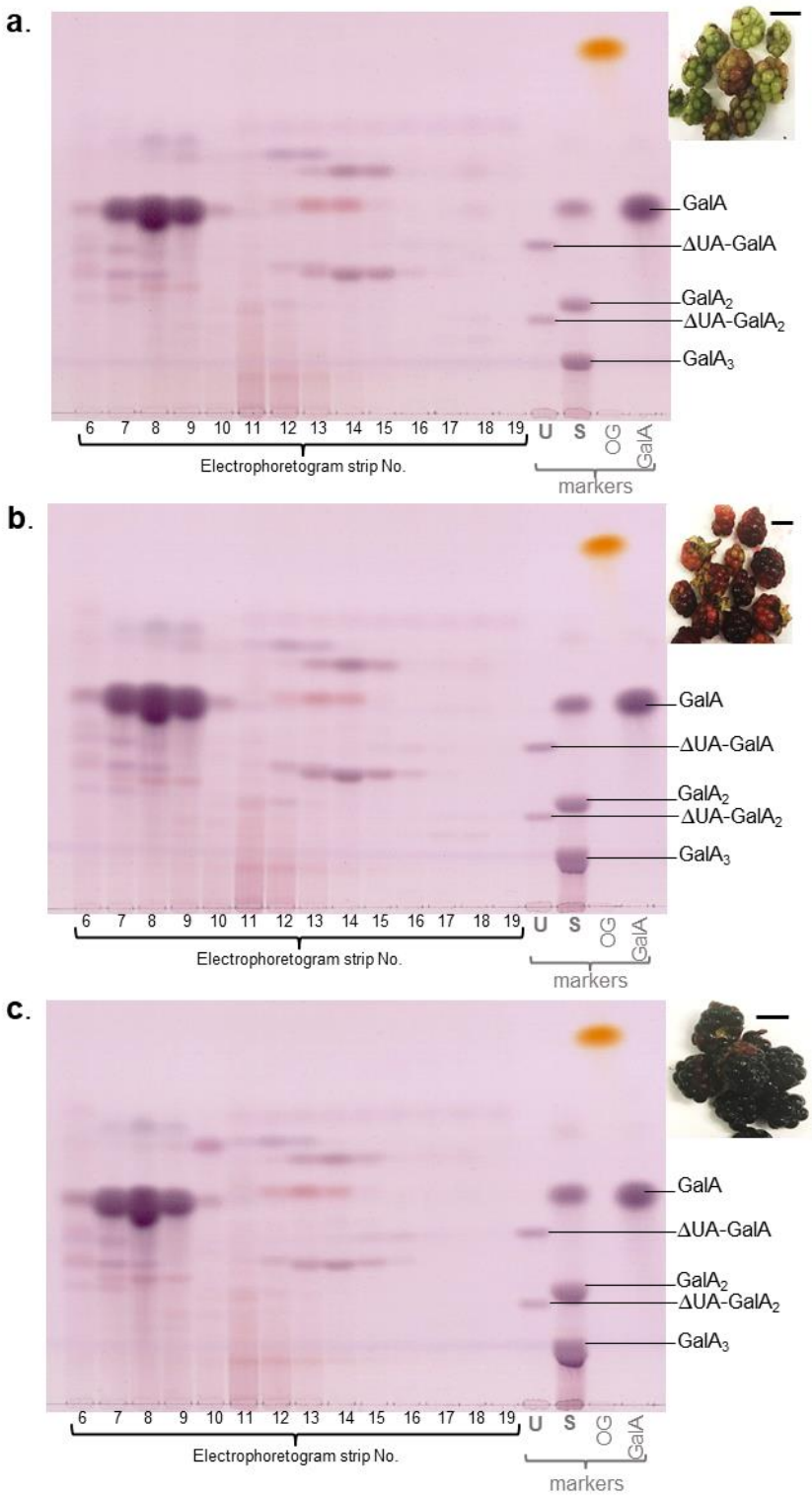

Fig. 3.73. Detecting pectate lyase and RG-I lyase fingerprints in digests of post-de-esterified blackberry fruit cell walls. Fruit AIR was de-esterified and digested with Driselase and products were electrophoresed and applied to TLC as in Fig. 3.71. **(a)** Unripe fruit. **(b)** Turning fruit. **(c)** Ripe fruit. Markers were U, unsaturated oligogalacturonides; S, saturated oligogalacturonides; OG, orange G; GalA. Scale bar= 1 cm.

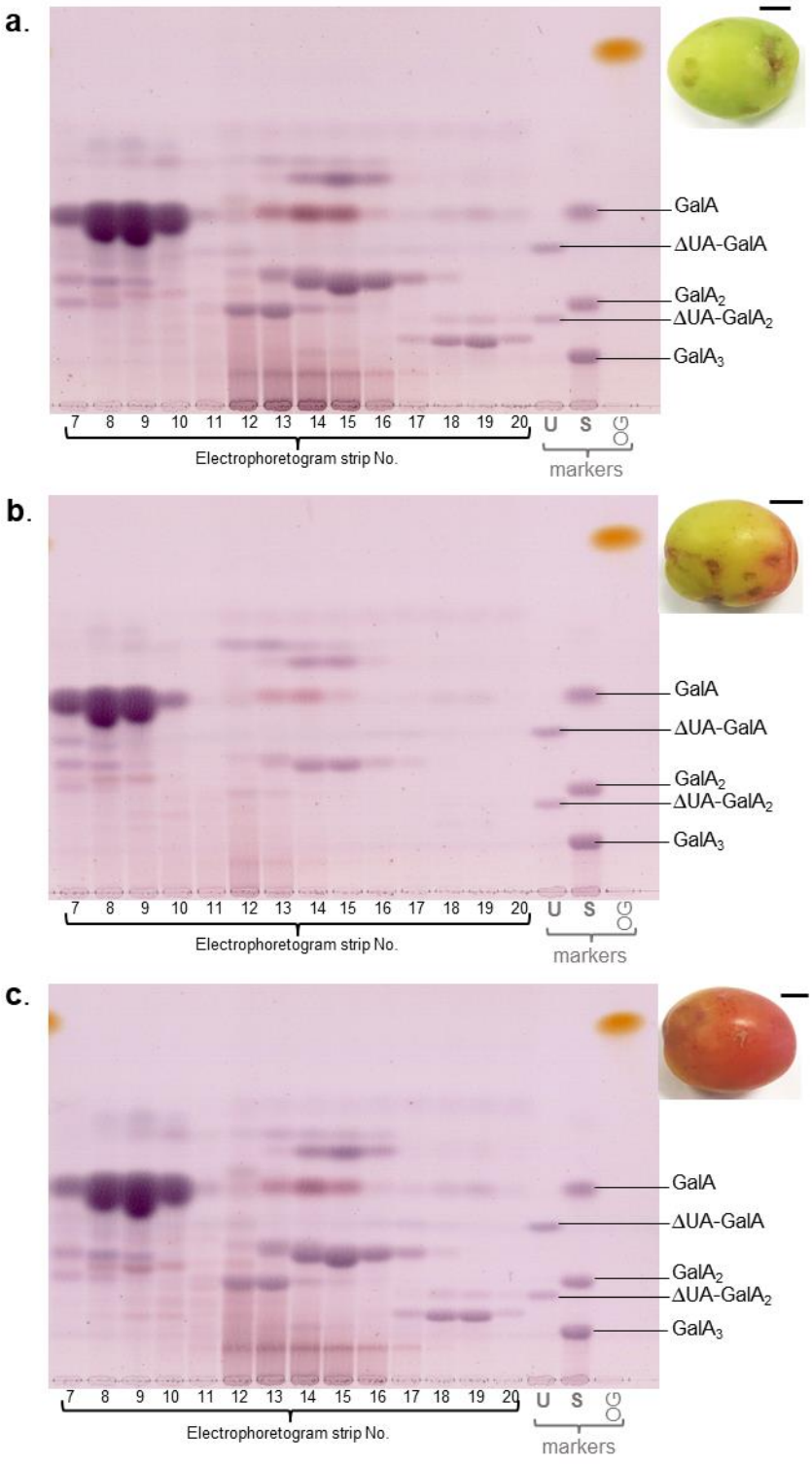

Fig. 3.74. Detecting pectate lyase and RG-I lyase fingerprints in digests of post-de-esterified plum fruit cell walls. Fruit AIR was de-esterified and digested with Driselase and products were electrophoresed and applied to TLC as in Fig. 3.71. **(a)** Unripe fruit. **(b)** Turning fruit. **(c)** Ripe fruit. Markers were U, unsaturated oligogalacturonides; S, saturated oligogalacturonides; OG, orange G. Scale bar= 1 cm.

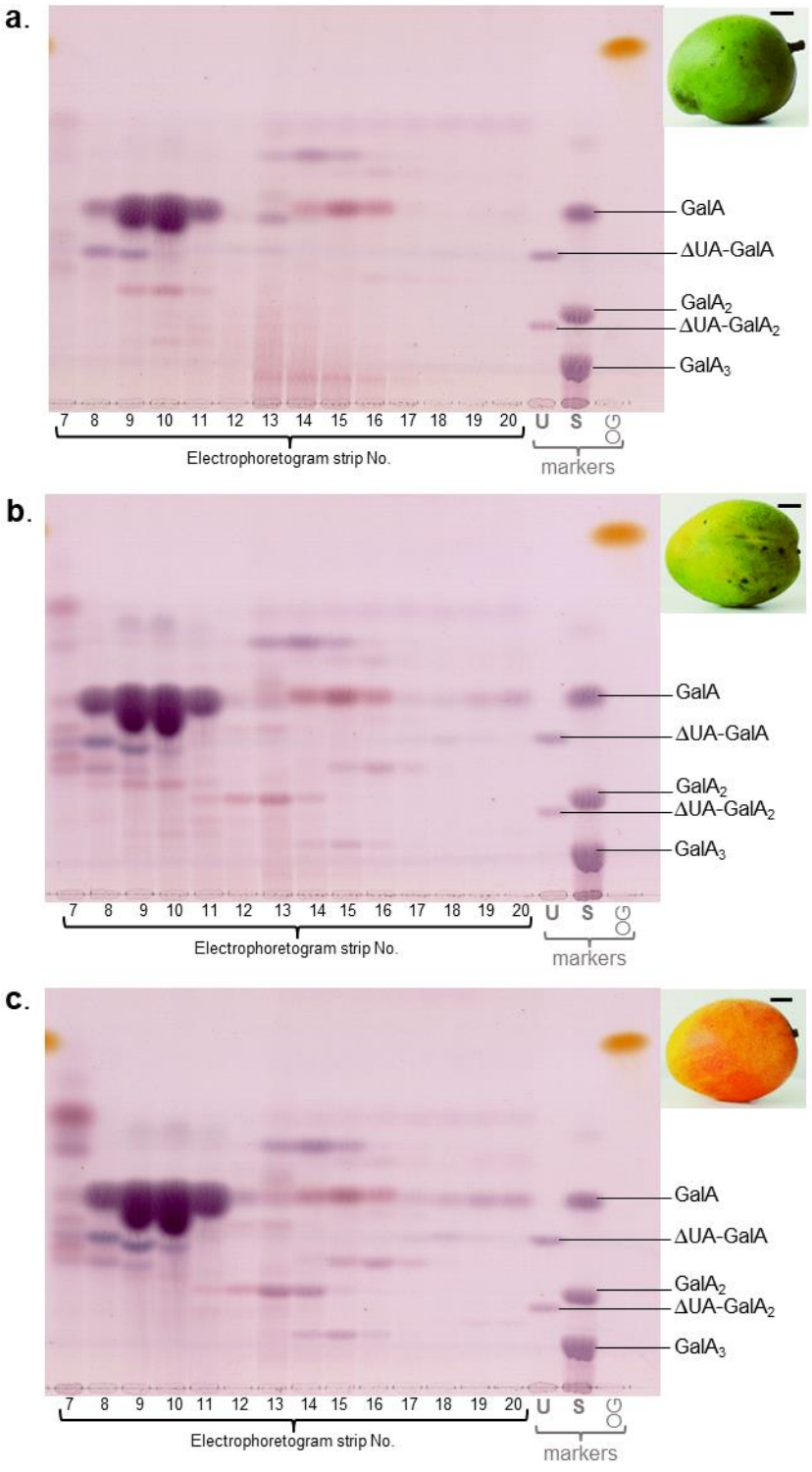

Fig. 3.75. Detecting pectate lyase and RG-I lyase fingerprints in digests of post-de-esterified mango fruit cell walls. Fruit AIR was de-esterified and digested with Driselase and products were electrophoresed and applied to TLC as in Fig. 3.71. **(a)** Unripe fruit. **(b)** Turning fruit. **(c)** Ripe fruit. Markers were U, unsaturated oligogalacturonides; S, saturated oligogalacturonides; OG, orange G. Scale bar= 1 cm.

Table 3.4. Summary of the main products detected on the TLC plates of the fruits (Fig. 3.71–3.75) with indication of their spot intensities.

		GalA		PL products		RGL products
Fruit	Stage	Monomer	Dimer	Dimer	Trimer	Tetramer
Date	Unripe	++++	++		++	+++
	Turning	++++	++	+	++	+++
	Ripe	++++		+++	+	++
Strawberry	Unripe	+++++	+++		+++	+++
	Turning	+++++	++		++	+++
	Ripe	+++++	++		+	+++
Blackberry	Unripe	++++		+		++
	Turning	++++		+		++
	Ripe	++++		+		++
Plum	Unripe	+++++	+++	+	++	+++
	Turning	+++++	+++	+		+
	Ripe	+++++	+++	+	++	+++
Mango	Unripe	++++		+		++
	Turning	+++++		+		+
	Ripe	+++++	++	+		+

3.3.3.4. Characterisation of the unknown anionic products of Driselase digestion

Some unknown acidic products that appeared on TLCs of fruit-AIR/Driselase digestion products were further investigated to identify their composition. They were absent in ripe date and rowan and other fruits which had been digested with an old purified stock of Driselase (refer to Fig. 3.38 and 3.39). However, they were observed in almost all the fruits studied at three ripening stages in which a different stock of purified Driselase was used (Figs. 3.71–3.75). Therefore, these unknowns might actually be intermediates that the new batch of Driselase failed to fully hydrolyse to their smallest units. Although the samples had been previously de-esterified, it was

also necessary to check by de-esterifying these unknowns again to make sure that Driselase would surely be able to hydrolyse them. Preparative TLCs of the unknowns from strawberry and date were run and samples of each were eluted as a pure stock. The four major unknowns were labelled 1–4 according to their position on paper electrophoretograms; less to more acidic. Unknown 1 (a) was closest to GalA on the electrophoretogram and co-migrated with $GalA_2$ on TLC. Its position on both electrophoretogram and TLC agreed with the expected $GalA_2$ spot seen in AIR/EPG products (Fig. 3.38b). Unknown 2 (b) ran faster that unknown 1 on the electrophoretogram (i.e. had a higher charge:mass ratio) and ran between ΔUA-GalA and $GalA_2$ on TLC. Unknown 3 (c) ran further than Unknowns 1 and 2 on the electrophoretogram and co-migrated with ΔUA-$GalA_2$ on TLC (its probable identity). Unknown 4 (d) electrophoresed with ΔUA-$GalA_n$s and ran between ΔUA-$GalA_2$ and $GalA_3$ on TLC.

TFA hydrolysis of the unknowns from dates (Fig.3.70b) and strawberry (Fig. 3.53b) was done to study their monomeric sugar composition. All of them showed a major spot of GalA only (Fig.3.76). Therefore, these unknowns might just be $GalA_{(n)}$ or ΔUA-$GalA_{(n)}$ modified with certain non-sugar molecules. A spot of galactose was detected in samples with TFA indicating a contamination (very faint in the TFA-only marker due to smaller loading).

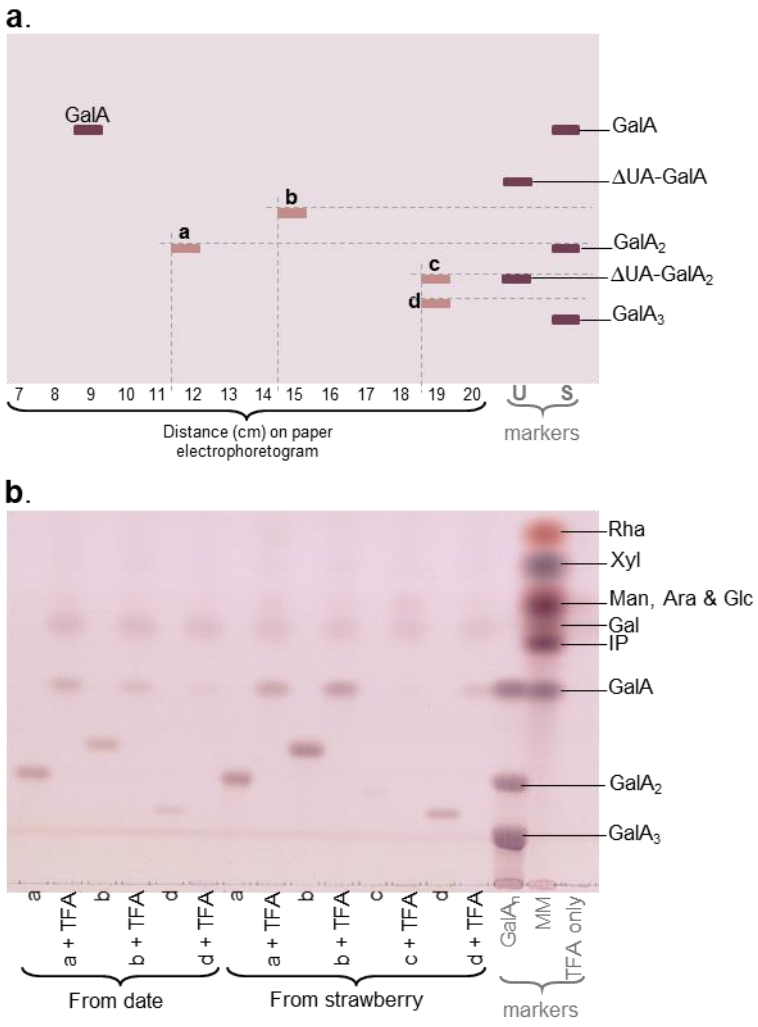

Fig. 3.76. TFA hydrolysis of four unknowns from date and strawberry fruit AIR/Driselase products. A sample of each of unknown products a–d from date and strawberry was dried in the SpeedVac and hydrolysed in 2 M TFA at 120°C for 1 h. The products were then dried, re-dissolved in H_2O and applied to TLC. **(a)** A schematic diagram of the original approximate location of the samples a–d on TLC. **(b)** TLC of TFA hydrolysed samples a–d. TLC solvent was BAW 2:1:1. Markers were $GalA_n$ from EPG products; MM, marker mixture (components as labelled); TFA.

Another experiment to characterise the unknowns from strawberry was done by treating them with NaOH as a way to de-esterify them in case previous de-esterification with Na_2CO_3 and Driselase digestion had not been completely successful. This step was then followed by Driselase digestion giving it the opportunity to completely hydrolyse them. Treatment of the unknowns with NaOH did not change their mobility on TLC which indicated that de-esterification was not the issue.

Driselase digestion of all the unknowns with or without NaOH pre-treatment revealed GalA as the only product detectable by thymol staining on TLC (Fig. 3.77). These results suggested that those unknowns were actually intermediates consisting of GalA which Driselase had failed to hydrolyse the first time. Some of the GalA might have been lost due to oxidation during the Driselase treatment (discussed in section 3.3.1.4). The Driselase-only marker showed all the Driselase self-digestion products contaminating the other products released from the unknown compounds.

The mass of the unknown a from strawberry (obtained from Fig. 3.53c) was checked by mass spectrometry. Negative-mode MS of sample a gave a mass of 369.06596 (Fig. 3.78a) and the positive-mode MS gave a mass of 393.06355 (representing $GalA_2$,Na^+; Fig. 3.78b) confirming that the unknown a was $GalA_2$ which actually agreed with the TLC in which the unknown a migrated the same distance as the marker $GalA_2$.

The unknown c was assumed to be ΔUA-$GalA_2$ as it co-electrophoresed and co-migrated with the marker ΔUA-$GalA_2$ on TLC. The identity of unknowns b and d remained unknown as the MS spectra (not included) did not reveal any clear-cut information.

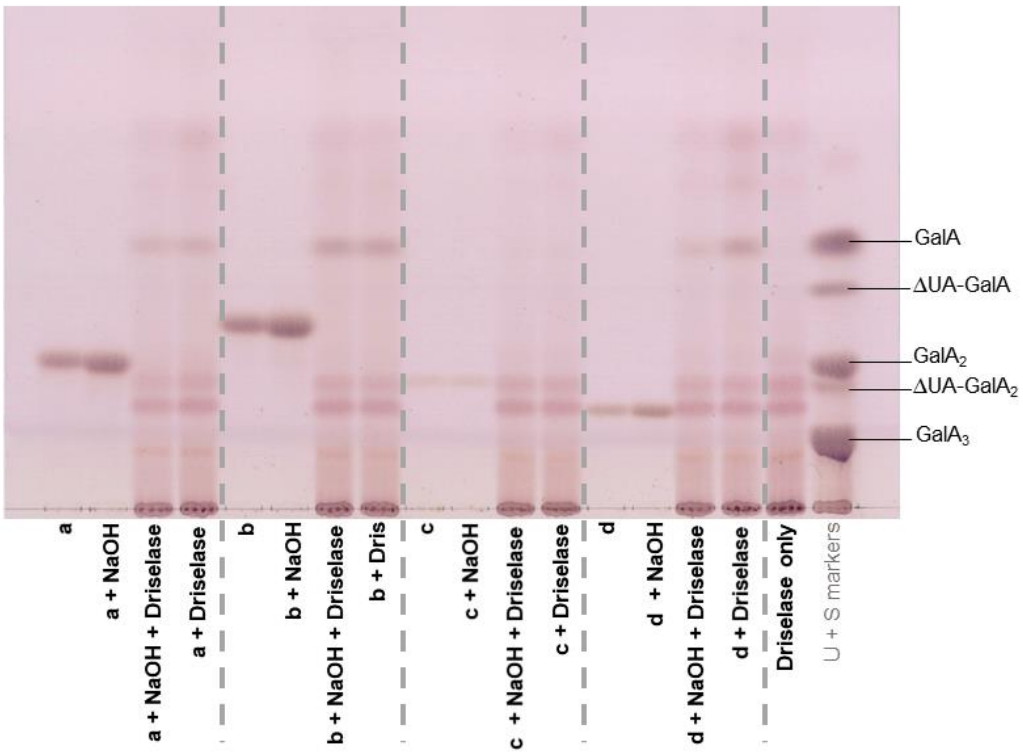

Fig. 3.77. Alkali and Driselase treatments of four unknowns from strawberry fruit AIR/Driselase products. A sample of each of unknown products a–d and divided into two portions. One portion was digested with 0.05% Driselase and the other was treated with 10 mM NaOH at 20°C for 30 min. The products of NaOH treatment were neutralized with acetic acid, dried in SpeedVac. All products were analysed by TLC and stained with thymol. TLC solvent BAW 2:1:1. Markers were U, unsaturated oligogalacturonides; S, saturated oligogalacturonides.

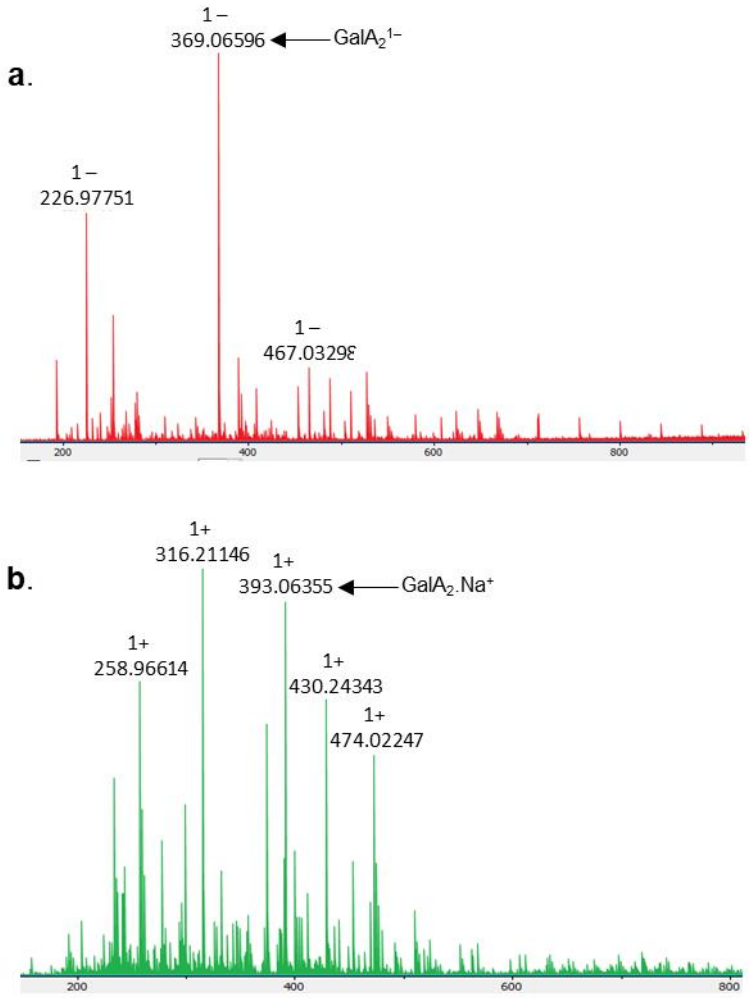

Fig. 3.78. Mass spectra of unknown a from strawberry. A pure sample of unknown a was obtained from a preparative TLC of the product from fractions 11–13 (Fig. 3.53c). **(a)** Negative-mode ESI FT-ICR mass spectrum. **(b)** Positive-mode ESI FT-ICR mass spectrum.

3.3.3.5 Mass spectrometric confirmation of in-vivo PL and RGL action product's identity

Driselase digestion products of de-esterified date AIR were resolved by high-voltage paper electrophoresis as in Fig. 3.38a. The PL products (ΔUA-GalA) fraction was then analysed by negative-mode electrospray-ionisation FT-ICR mass spectrometry (MS). The simulated *m/z* of the ΔUA-GalA anion is 351.05690 based on its formula of $C_{12}H_{15}O_{12}^-$. Experimentally, molecular-ion negative-mode MS measured the *m/z* at

351.05677, i.e. the value expected with 0.37 ppm error (Fig. 3.79a), agreeing with the mass of the ΔUA-GalA obtained from *in-vitro* digestion of commercial HG with commercial PL (Fig. 3.27). CID fragmentation of the ion observed at *m/z* 351.05629 resulted several fragments that further supported the proposed structure (Fig. 3.79b). An NMR spectrum could not be generated as it would have required a larger amount of pure sample than was available.

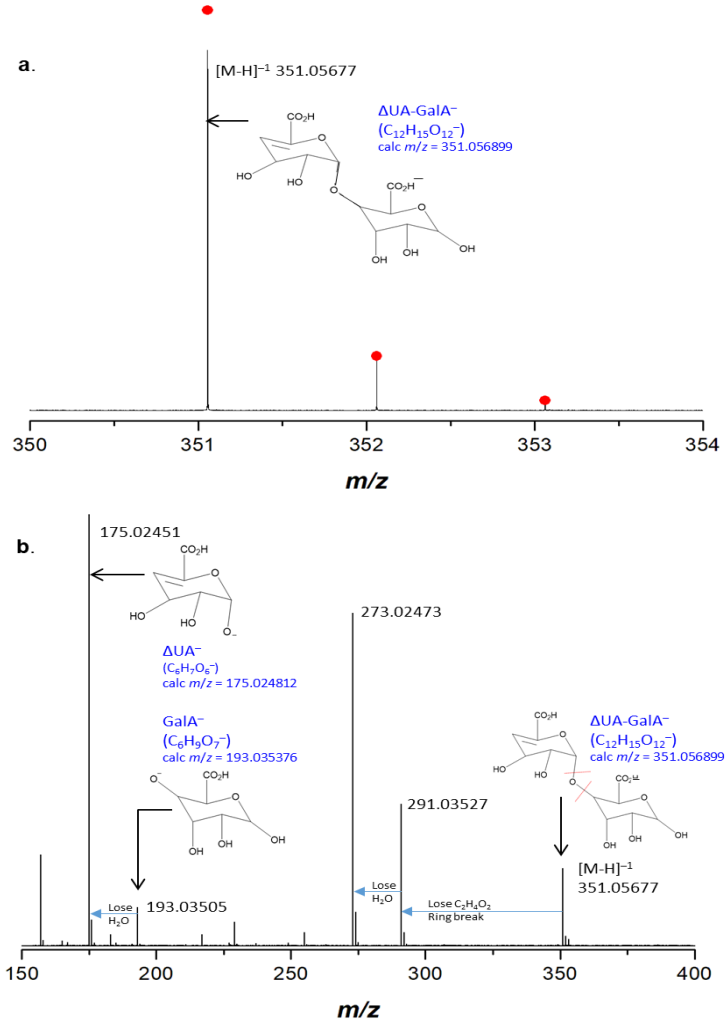

Fig. 3.79. Mass spectrometry of putative ΔUA-GalA obtained by Driselase digestion of de-esterified date fruit cell walls. (a) Negative-mode ESI FT-ICR mass spectrum. The *in-silico* simulated isotope distribution due to naturally occurring ^{13}C is highlighted (red dots). **(b)** Negative-mode ESI FT-ICR CID fragmentation mass spectrum of the species modelled in (a). Observed *m/z* values are labelled in black; proposed identities and their calculated *m/z* values are in blue. The mass error of the parent ion (ΔUA-GalA⁻), observed *vs.* theoretical, is 370 ppb.

The RGL products (ΔUA-Rha-GalA-Rha) fraction was also analysed by negative-mode electrospray-ionisation FT-ICR mass spectrometry (MS). The simulated *m/z* of the ΔUA-Rha-GalA-Rha anion is 643.17272 based on its formula of $C_{24}H_{36}O_{20}^{-}$. Experimentally, molecular-ion negative-mode MS measured the *m/z* at 643.17922, i.e. the value expected with 0.37 ppm error (Fig. 3.80a), agreeing with the mass of the ΔUA-Rha-GalA-Rha obtained from *in-vitro* digestion of commercial RG-I with commercial RGL (Fig. 3.34). Peaks for bigger oligomers of RGL products (ΔUA-Rha-GalA-Rha-GalA-Rha and ΔUA-Rha-GalA-Rha-GalA-Rha-GalA-Rha) were also detected (Fig. 3.80b); however, it was suggested that these products were non-covalent resulted from fragmentation and re-bonding of the predominant tetramer (ΔUA-Rha-GalA-Rha). The lepidimoic acid detected in the sample (peak at 321.08565) was suggested to be a break-down product from the predominant tetramer. These findings suggested that the oligomers of RGL products were always terminated by Rha at the non-reducing end rather than GalA, which was also observed by Schols *et al.* (1990).

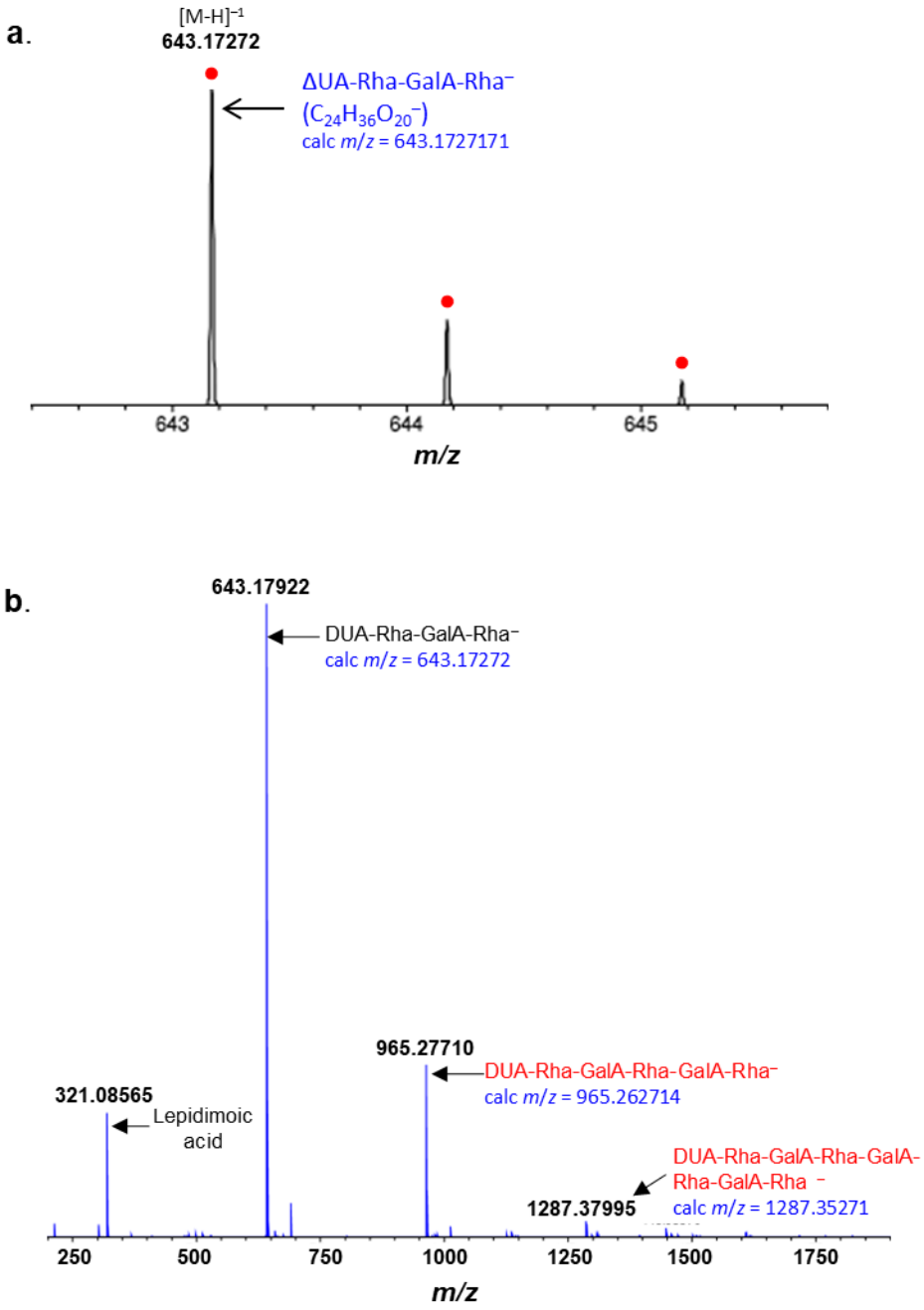

Fig. 3.80. Mass spectrometry of putative ΔUA-Rha-GalA-Rha obtained by Driselase digestion of de-esterified ripe apple fruit cell walls. (a) Negative-mode ESI FT-ICR mass spectrum. The *in-silico* simulated isotope distribution due to naturally occurring ^{13}C is highlighted (red dots). **(b)** Negative-mode ESI FT-ICR mass spectrum of the species modelled in (a). Observed *m/z* values are labelled in black; proposed identities and their calculated *m/z* values are in blue. Peaks highlighted in red are probably non-covalent complexes.

3.3.3.6. Quantification of PL products in fruit cell walls at three ripening stages

Driselase digestion of HG (even when pre-digested by EPG) is expected to give only GalA, whereas Driselase digestion of PL-pre-treated HG yields in addition one unsaturated dimer, ΔUA-GalA, for every PL cleavage event, from the new non-reducing terminus (Fig. 3.19b). Thus, the ΔUA-GalA:GalA ratio approximately indicates the number of PL-catalysed cuts per unit chain-length of HG. In ripe dates (Fig. 3.38a), the ΔUA-GalA:GalA ratio was estimated by pixel-counting in Photoshop (Vreeburg *et al.* 2014) to be ~1:20, mol/mol, suggesting that roughly 1 glycosidic bond in 20 of the endogenous HG domains had been cleaved by *in-vivo* PL action in dates (Al Hinai *et al.* 2021). This approximation neglects the GalA generated by Driselase digestion of fruit RG-I domains, but remains a reasonable approximation — it can be assumed that the GalA arising from RG-I is equal to the small amount of total Rha, which has been measured; see § 3.3.2.

In the study of PL and RGL action *in vivo* at three ripening stages of date, strawberry, blackberry, plum and mango, a different batch of Driselase was used which failed to fully hydrolyse $GalA_2$ and $\Delta UA\text{-}GalA_2$ to GalA and ΔUA-GalA respectively (shown in Fig. 3.71–3.75). This made the quantification of PL products more challenging. In addition, $\Delta UA\text{-}GalA_n$ markers with known concentrations were not available to calibrate a standard curve. To overcome the latter difficulty, the amount of ΔUA-GalA and the ΔUA-GalO generated by its reduction with $NaBH_4$ was quantified relative to a standard curve of known GalA quantities. The galactonic acid (GalO) moiety of the product is known to be unstainable by thymol. Therefore, the spot slightly slower migrating than ΔUA-GalA detected on the TLC corresponded to ΔUA-GalO (Fig. 3.81) confirming that the ΔUA moiety of PL products was detectable on TLC by thymol staining. Curiously, ΔUA-GalA migrated faster than ΔUA-GalO, whereas

ΔUA-GalA$_3$ ran slightly slower than ΔUA-GalA$_2$-GalO. It was estimated that a quantity of ΔUA-GalA staining as 3.0 µg GalA-equivalents contained 1.3 µg GalA-equivalents of ΔUA (GalO does not stain with thymol). Therefore, GalA contributed 1.7 µg of the total amount of ΔUA-GalA loaded on the TLC and stained with thymol. Hence, data for a ΔUA-GalA standard curve of a serial dilutions of GalA were fitted to a single rectangular hyperbola with the equation of y= a × x/(b+x) (Fig. 3.82). The same method was used to estimate the amount of GalA cleaved by PL from the GalA-equivalent amount of ΔUA-GalA$_2$ (Table 3.5). Likewise, ΔUA-GalA-GalO generated from ΔUA-GalA$_2$ counted for about 1 µg while ΔUA-GalA$_2$ counted for 1.5 µg; therefore, the cleaved GalA counted for 0.5 µg and GalA$_2$ counted for 1 µg.

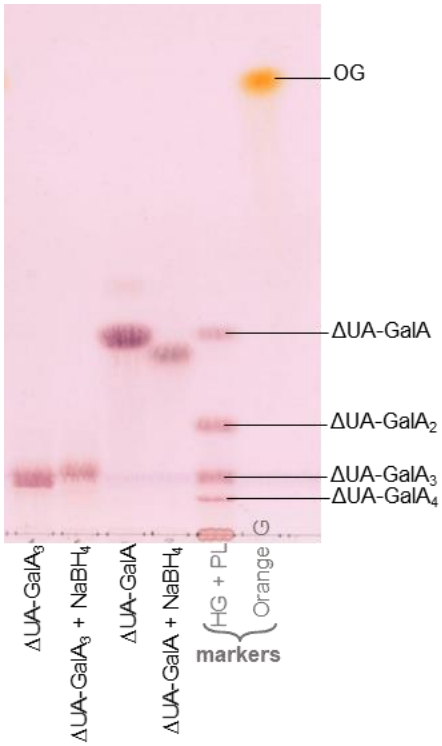

Fig. 3.81. TLC of PL products (particularly ΔUA-GalA$_2$ and ΔUA-GalA) oxidised by NaBH$_4$ treatment. ΔUA-GalA$_2$ and ΔUA-GalA were purified from preparative PC of PL products (prepared as in Fig. 3.3). ΔUA-GalA$_2$ and ΔUA-GalA were incubated with 0.5% NaBH$_4$ in 1 M NH$_4$OH at 20 °C for 16 h. The products were neutralized with acetic acid and run by TLC in BAW (2:1:1). The TLC plate was stained with thymol.

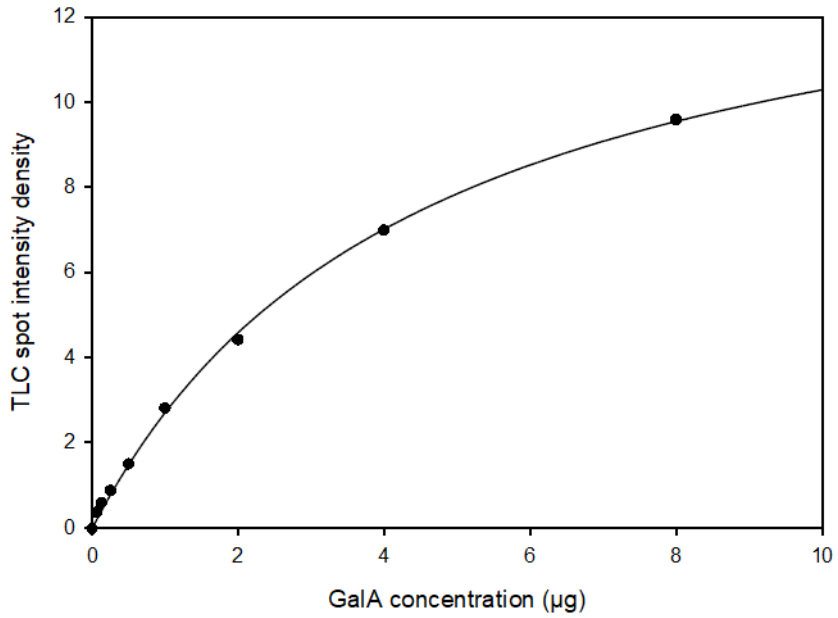

Fig.3.82. Standard curve of GalA. A single rectangular hyperbola standard curve of various GalA quantities used to estimate the amount of GalA and GalA-equivalent ΔUA in fruit cell walls.

Table 3.5. Staining of ΔUA-GalA$_n$ on a TLC plate before and after reduction of the reducing terminal GalA to GalO (with NaBH$_4$). The µg 'GalA-equivalent' values are based on thymol staining of a GalA dilution series (Fig. 3.81).

Initial sample	Treatment	Product loaded on TLC	Intensity Density*	GalA-equivalents of ΔUA + GalA (µg)	Hence µg actual GalA in initial sample	Hence µg GalA-eq of ΔUA	Hence µg GalA-equiv of ΔUA that would be generated by PL from 1 µg GalA
ΔUA-GalA	–	ΔUA-GalA	5.974	3.000 (=D+U)	U=3.0–1.3= 1.7	D=3.0–1.7= 1.3	1.30/1.70= 0.765
ΔUA-GalA	NaBH$_4$	ΔUA-GalO**	3.351	1.300 (=D)			
ΔUA-GalA$_2$	–	ΔUA-GalA$_2$	3.779	1.526 (=D+2U)	U=1.526–0.982 = 0.544	D=1.526–1.088 = 0.438	0.438/0.544= 0.805
ΔUA-GalA$_2$	NaBH$_4$	ΔUA-GalA-GalO	2.673	0.982 (=D+U)			

*See section 2.12 for details. **GalO moiety is unstainable by thymol. D = ΔUA; U = GalA.

Based on ΔUA-GalA → ΔUA-GalO, 1 µg PL-cleaved GalA → 0.765 µg (GalA-eq) ΔUA.

Based on ΔUA-GalA2 → ΔUA-GalA-GalO, 1 µg PL- cleaved GalA → 0.805 µg (GalA-eq) ΔUA.

Average estimate: 1 µg PL-cleaved GalA → 0.785 µg (GalA-eq) ΔUA.

These values were used to understand the contribution of each of the GalA, $GalA_2$ and the ΔUA moieties of the PL products detected on thymol-stained TLCs from the different fruits at the three ripening stages. Another standard curve (with broader range of GalA quantities; Fig. 3.83) was used to estimate the exact amount of these products based on the data acquired from Table 3.5. The best fit curve was a double rectangular hyperbola ($y= (a \times x/b+x) + (c \times x/d+x)$).

Less total GalA (mg) was detected (per 30 mg AIR) in ripe date, strawberry and plum than in the unripe fruit AIR. However, more GalA was detected in ripe blackberry and much more in ripe mango than the un-ripe fruits (Fig. 3.84). The total GalA was measured by quantification of thymol-stained GalA spots on TLCs, which was run once for each sample due to the very long time of sample processing resulting in limited statistics. The total amount of GalA could highly be affected by the presence of other polysaccharides at early stages of development, which then diminish with ripening. For instance, unripe mango is known to be transiently very rich in starch (Bello-Pérez *et al.* 2007), which makes the percentage of pectin in AIR much less than in ripe mango even if there is no loss of pectin per fruit.

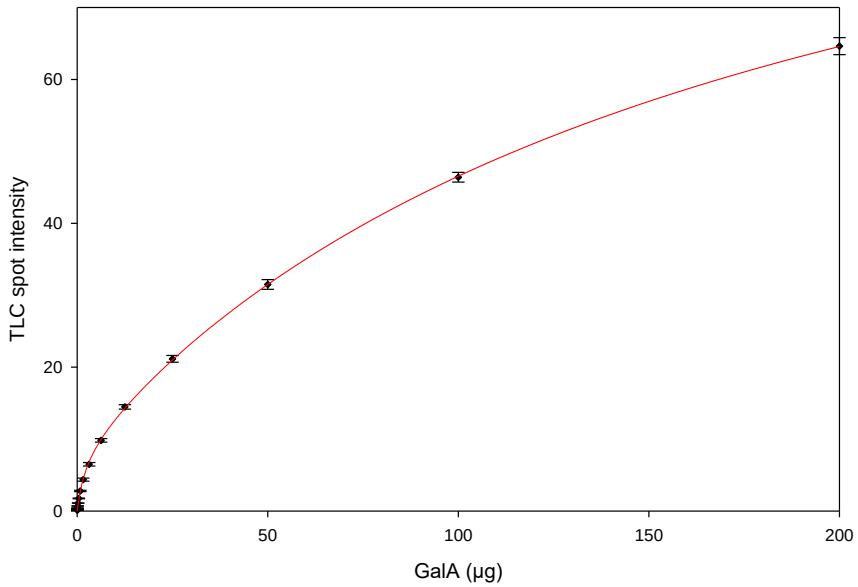

Fig. 3.83. A standard curve of GalA spot intensity density on TLC at various quantities. This standard curve was obtained from reading the GalA spot intensity densities of a range of GalA quantities from four different TLC plates. The TLCs were run in BAW 2:1:1 and stained with thymol. The spot intensity densities were read by Image J software. Error bars are of standard error; n=4.

The percentage of GalA cleaved by endogenous PL action increased in date, blackberry and plum and decreased in strawberry and mango throughout ripening (Fig. 3.85). However, it remained less than 1% in all cases, indicating that although PL action started early during ripening, it was a rather infrequent event. The differences in the trend of increasing or decreasing percentage of detected PL action events could highly be affected by the fruit species and the stability of the unsaturated products *in vivo* throughout the ripening process as this has never been tested or reported before.

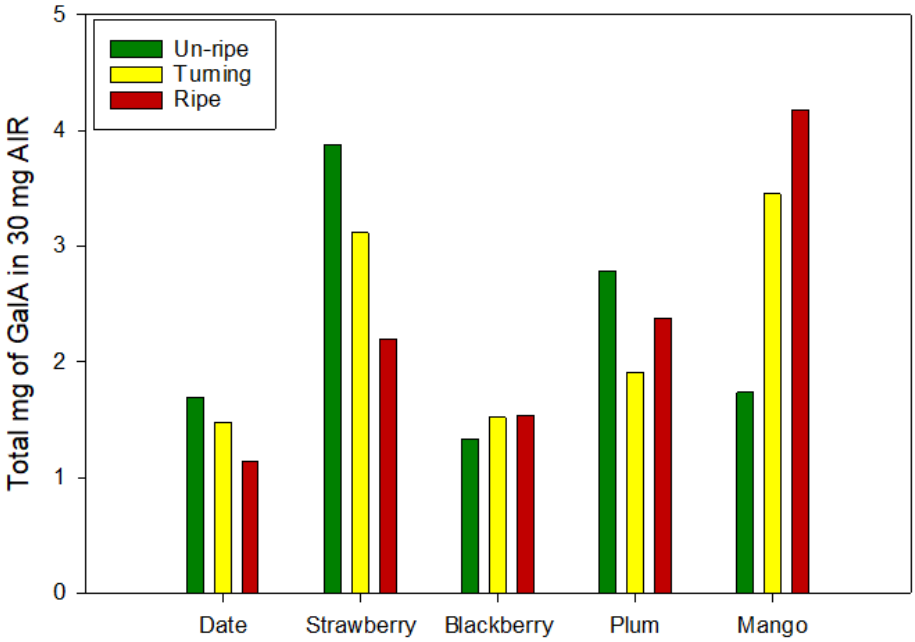

Fig. 3.84. Total GalA (mg) detected in AIR/Driselase hydrolysate of different fruits at different ripening stages. The total amount of GalA (mg) was estimated by reading the spot intensity density on the TLCs (Fig. 3.71–3.75) using Image J software relative to the standard curve of GalA (Fig. 3.83).

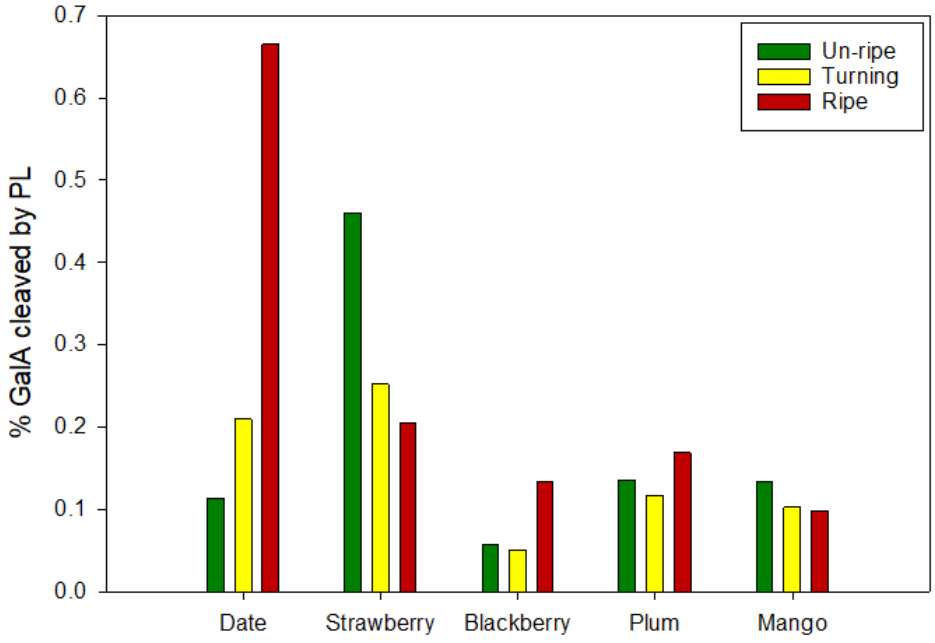

Fig. 3.85. Percentage of PL cleavage events in different fruits at different ripening stages. The percentage of PL cleavage events was estimated by measuring the total ΔUA content relative to GalA detected in AIR/Driselase hydrolysates by TLC (Figs. 3.71–3.75) using ImageJ software relative to the standard curve of GalA (Fig. 3.83).

Chapter 4

Discussion

4.1. *In-vitro* PL, EPG and RGL activities: standardizing the methods

4.1.1. PL and EPG activities on de-esterified HG in vitro

Acting on de-esterified HG, EPG causes endo-hydrolysis producing new saturated non reducing termini and new standard reducing termini while PL cleaves HG by a β-elimination reaction (non-hydrolytically) producing new unsaturated non-reducing termini (ΔUA; described by Fuchs (1965) and Nasuno and Starr (1967)) and new standard reducing termini (Fig. 1.10). These enzymes (commercial) were tested to understand their behaviour, standardize the reaction conditions and produce markers of their products with different sizes.

Different chromatography techniques were tested to separate the unique unsaturated PL product from the saturated EPG product as both were expected to be present (in addition to many other products) in ripening fruits. Paper electrophoresis at pH 2.0 effectively gave a group separation of saturated from unsaturated oligogalacturonides. PL products ran faster than EPG products at pH 2 owing to the low pK_a of the ΔUA residue (Fig. 3.4a), allowing the isolation of pure stocks of the unsaturated products. TLC resolved PL products, especially ΔUA-GalA and ΔUA-$GalA_2$ very well from each other and from GalA and $GalA_2$ (EPG products) on the F254 TLC plates (Fig. 3.2a).

It was essential to test the stability of PL products under different pH and chemical treatments to avoid losing them when starting the work with natural fruit samples. Working with fresh fruit samples required preparation of alcohol-insoluble residue (AIR) as the source of fruit pectic polysaccharides. In the process of AIR preparation, various concentrations of ethanol were required which have been tested and showed no harm to PL products (Fig. 3.11). In order for AIR to be digested with EPG (to

release the smallest products) *in vitro*, all methyl ester groups must be removed, which can be achieved by chemical treatment with NaOH (Xu *et al.* 2011) or Na_2CO_3 (Dong *et al.* 2018). The PL products were observed to be sensitive to NaOH (Fig. 3.13). The PL products were confidently stable when treated with up to 0.2 M Na_2CO_3 (Fig. 3.14) which was proposed to be give a high enough pH for pectin de-esterification as a much lower concentration (0.05 M) was previously tested by Wakabayashi *et al.* (2003) and caused a 70% decrease in the level of pectin-methylesters.

4.1.2. EPG and Driselase digest large PL products to smaller products

It was proposed that PL will cleave fruit pectin (in mid chain) only partially and the products will remain in the polymeric form (Fuchs 1965; Al Hinai *et al.* 2021) which will be hard to isolate with the methods used in this project, so further digestion of these large PL products was required. Both EPG and Driselase were good candidates for this purpose as they both can cleave HG pectic domains (Dumville and Fry 2000; Airianah *et al.* 2016). Applying EPG to large PL products (from brief digestion of commercial HG with commercial PL) gave a mixture of the unsaturated trimer (ΔUA-$GalA_2$), the unsaturated dimer (ΔUA-GalA), GalA, $GalA_2$ and $GalA_3$ as the smallest products detected by TLC (Fig. 3.17). Applying Driselase to the large PL products gave the unsaturated dimer (ΔUA-GalA) and GalA as the smallest products detected by TLC (Fig. 3.18; demonstrated in Fig. 4.1a). These results gave Driselase priority for use to release the smallest PL products from fruit AIR. In addition, Driselase was checked to have no pectate lyase activity of its own and to be unable to cleave the dimer (ΔUA-GalA) to its monomers (Fig. 3.19).

4.1.3. RGL activity on RG-I in vitro

Acting on RG-I, RGL cleaves the α-(1,4) glycosidic bond between Rha and GalA by β-elimination, creating a double bond between C4 and C5 in the GalA residue (making the unsaturated ΔUA) at the new non-reducing terminus. Following RGL (commercial) digestion of commercial potato RG-I, Driselase digestion released the tetramer (ΔUA-Rha-GalA-Rha) as the smallest product, which was detected on TLC (Fig. 3.33; demonstrated in Fig. 4.1b) and confirmed by mass spectrometry (Fig. 3.34). The tetrameric product of RGL was previously reported by Schols *et al.* (1990) as a result of apple RG-I digestion to the limit degradation products with microbial RGL (from *Aspergillus aculeatus*) and by Azadi *et al.* (1995) as a result of sycamore RG-I digestion with microbial RGL (from *Aspergillus aculeatus*; previously described by Kofod *et al.* (1994)). It was also confirmed (by TLC and mass spectrometry; Fig. 3.35 and 3.37) that Driselase lacks RGL activity, suggesting its suitability to be used to release RGL products from fruit AIR.

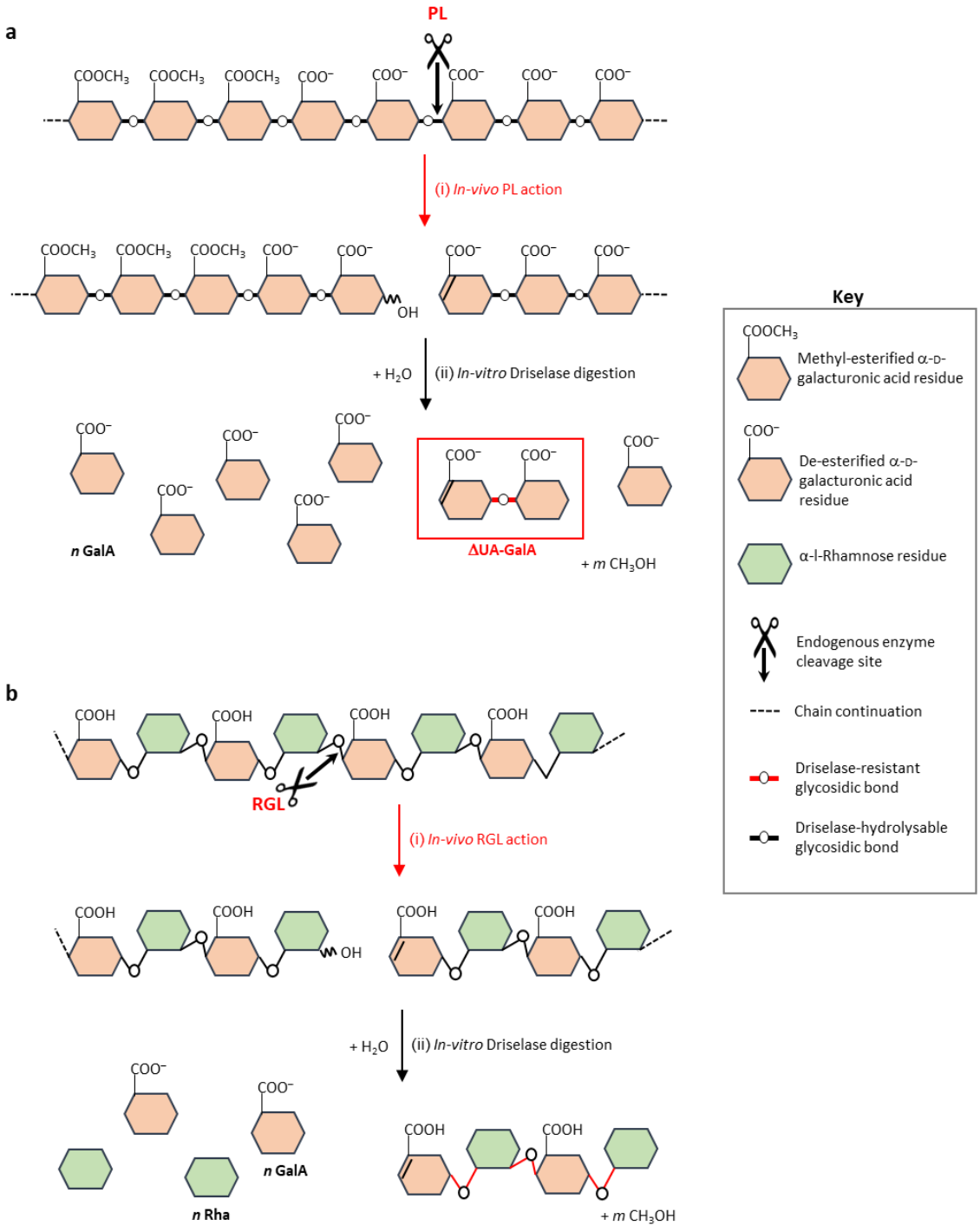

Fig. 4.1. PL and RGL action on HG and RG-I, respectively, followed by Driselase digestion. (a) PL attacking the α-(1,4) glycosidic bond between de-esterified GalA residues of HG, producing a new reducing terminus and a new unsaturated non-reducing terminus (ΔUA) terminus by β-elimination. Digestion of PL products with Driselase cleaves the remaining methyl ester groups and the whole chain of HG to monomeric GalA plus the dimer, ΔUA–GalA (the unique PL action fingerprint) by its combination of hydrolysing enzymes including PME, EPG and galacturonidase. **(b)** RGL attacking the α-(1,4) glycosidic bond between rhamnose and galacturonic acid of the RG-I backbone by β-elimination producing a new rhamnose reducing terminus and a new unsaturated non-reducing (ΔUA) terminus. Digestion of RGL products with Driselase cleaves the whole chain of RG-I to GalA and Rha monomers (and galactose and arabinose from the side-chains; not shown) plus the tetramer, ΔUA–Rha–GalA–Rha, the unique RGL action fingerprint. RG-I side chains (not shown) are cleaved by Driselase to their monomers (Gal and Ara).

4.2. Wall polysaccharide degradation in fruit: enzyme action contrasted with enzyme activity, gene transcription and protein synthesis

During fruit softening in many species, cell wall composition changes have been reported, especially in pectin domains, mostly presumed to be due to the actions of polysaccharide-modifying enzymes, although additional non-enzymic wall degradation mechanisms can occur (Brummell *et al.* 1999; Dumville and Fry 2003;Vreeburg *et al.* 2014; Airianah *et al.* 2016). Attention has focused on endo-enzymes, since these cleave polysaccharide molecules in mid-chain, potentially having a greater effect on wall mechanics than exo-enzymes, which only remove single monosaccharide (or in a few cases disaccharide) residues. The two endo-enzyme activities that can cleave HG are EPG and PL. While initially reported absent (Besford and Hobson 1972), and later somewhat side-lined, PL is becoming a focus of renewed interest (Marin-Rodriguez *et al.* 2002; Santiago-Doménech *et al.* 2008; Wang *et al.* 2018; Moya-León *et al.* 2019; Uluisik and Seymour 2020). Modification of RG-I by RGL (also an endo-enzyme) was also of interest to scientists recently as evidence of its role in fruit softening was reported (Molina-Hidalgo *et al.* 2013; Dautt-Castro *et al.* 2015; Ochoa-Jiménez *et al.* 2018; Méndez-Yañez *et al.* 2020). This project focused on the action of PL and RGL in various fruit species at various stages of ripening.

A ripening-related increase in extractable PL activity, assayed *in vitro*, was reported in many fruits including tomato (Uluisik *et al.* 2016), banana (Marín-Rodríguez *et al.* 2003) and strawberry (Zhou *et al.* 2016). However, *in-vitro* enzyme activity does not confirm action as there could be restrictions on substrate accessibility, presence of certain inhibitors and/or non-optimum action conditions *in vivo*.

RGL is a less well-studied enzyme in relation to fruit softening than PL. Expression of RGL genes was reported in strawberry (Molina-Hidalgo *et al.* 2013) and mango (Dautt-Castro *et al.* 2015). An increase in extractable RGL activity was reported in

Chilean strawberry fruits (Méndez-Yañez *et al.* 2020) and tomato (Ochoa-Jiménez *et al.* 2018). In tomato, the RGL gene expression profile did not correlate with the measured extractable enzyme activity, confirming that gene expression is not necessarily a proof of enzyme *in-vivo* action.

Although gene expression and extractable enzyme activity can suggest that a given enzyme-catalysed reaction could possibly occur during a physiological process such as ripening, the demonstration of *in-vivo* action of the enzyme remains a gold standard that is difficult to achieve. By quantifying the *in-vivo* action products of an enzyme, all transcriptional, post-transcriptional and post-translational modifications are taken in account, together with the regulation of enzyme activity by local cellular environments. In addition to providing a more biologically relevant proof of the *in-vivo* occurrence of polysaccharide modifications, determination of *in-vivo* enzyme action also circumvents problems associated with possible enzyme denaturation during extraction.

4.3. A strategy for detecting products of PL and RGL action

PL action in fruit *in vivo* would be unlikely to digest the HG to products anything like as small as ΔUA-GalA or ΔUA-$GalA_2$, which were easily resolved by the methods used in this project. On the contrary, products of (partial) PL action in fruit would mainly be present in polymeric form (alcohol-insoluble polysaccharides in AIR), making them difficult to isolate and characterise. In a similar manner, RGL action in fruit *in vivo* would be unlikely to digest the RG-I to products as small as the tetrasaccharide ΔUA-Rha-GalA-Rha. Therefore, further *in-vitro* hydrolysis of the fruit AIR was performed with Driselase to release small and well-defined products.

Driselase (rather than EPG) was recommended for routine analysis of *in-vivo* PL action products because (a) Driselase gave a single unsaturated product (ΔUA-GalA) whereas EPG gave a mixture of ΔUA-$GalA_2$ and ΔUA-GalA; (b) EPG gives three saturated oligogalacturonides in addition to the unsaturated ones, whereas the only saturated acidic product of Driselase is the monomer, GalA; and (c) EPG requires the AIR to be pre-saponified, e.g. with Na_2CO_3, removing methylester groups, whereas Driselase contains esterases which can remove the methylester groups of homogalacturonan; (d) Driselase gives one RGL unsaturated product (ΔUA-Rha-GalA-Rha), which can clearly be resolved from PL products by TLC, whereas EPG does not hydrolyse RG-I. Although some batches of Driselase failed to fully hydrolyse PL (and probably RGL) products to their smallest expected products, it remained the best tool to release them from cell walls while preserving the unsaturated fingerprint (ΔUA) and giving obviously different fingerprints for each of PL and RGL.

The acidic (low pK_a; ΔUA-containing) products of PL and RGL were separated by preparative paper electrophoresis at pH 2.0 from all other detectable products (e.g. Fig. 3.38a). The PL and RGL products were eluted from the paper electrophoretograms and resolved successfully by TLC and gave samples pure enough to prove their identity using TLC mass spectrometry and NMR spectroscopy.

4.4. PL and RGL action in ripening fruits

4.4.1. The first evidence of PL and RGL action in ripe fruits

The PL action fingerprint (ΔUA-GalA) was obtained by Driselase digestion of ripe date fruit AIR and documented by electrophoresis and TLC. The mass of the putative ΔUA-GalA isolated from date fruits was confirmed by mass spectrometry (Fig. 3.79) and found to be identical to that of the product obtained *in vitro* by digestion of commercial HG by commercial PL (Fig. 3.27). The identity of the PL 'fingerprint' compound was further confirmed chromatographically and electrophoretically (Fig. 3.38).

PL action products were successfully detected by the same strategy in ripe rowan berry, apple, pear, raspberry, blackberry and plum (all dicots of the family Rosaceae), as well as mango (Anacardiaceae) and yew (a gymnosperm of the family Taxaceae), confirming that fruit PL action is taxonomically widespread (Fig. 3.52). It is interesting that this contributor to fruit softening was observed both in true fruits (the monocot date and dicot rowan) and in the fleshy parts of false fruits (apple and pear). Another proposed *in-vivo* contributor to fruit softening — apoplastic hydroxyl radicals — was found in true fruits but not false fruits (Airianah *et al.* 2016).

PL products were not detected in ripe cranberry (Ericaceae) and sea buckthorn (Elaeagnaceae; not detected on TLC, Fig. 3.52). It was reported that cranberry has high levels of HG (Andreani *et al.* 2021) and extractable activity of EPG was reported (Arakji and Yang 1969), but no data were found about PL in this fruit. Sea buckthorn cell walls were reported to be rich in GalA residues (Farzaliyev *et al.* 2022); however, no data about EPG or PL genes expression or enzyme activities were found.

The PL products were also detected in mutant strawberries expressing an antisense PL gene (reported to result in firmer fruits and less protein levels than the control; Jiménez-Bermúdez *et al.* 2002) with no significant difference in their concentration from the control line tested (Fig. 3.53c, 3.54c 3.55c), suggesting the presence of more than one gene encoding PL in strawberries with the same effect on cleaving HG creating the unique fingerprint (ΔUA-GalA). In addition, although the methods used in this project have successfully been used to detect low concentrations of PL and RGL fingerprints, their accuracy in quantification of moderate changes in gene expression (therefore enzyme action) in antisense lines may be limited and requires further assessment.

The RGL action fingerprint (ΔUA-Rha-GalA-Rha) was also obtained by Driselase digestion of ripe date fruit AIR and documented by electrophoresis and TLC. RGL products overlapped with PL products on paper electrophoresis, but were resolved clearly on TLC as they have a slightly lower mobility on electrophoresis than PL products and run much slower on TLC owing to their larger size (Fig. 3.38; Fry 2000; Abari *et al.* 2021; Zheng *et al.* 2021). The mass of the putative ΔUA-Rha-GalA-Rha isolated from apple fruits was confirmed by mass spectrometry (Fig. 3.80) and found to match that of the product obtained *in vitro* by digestion of commercial RG-I by commercial RGL (Fig. 3.34).

The RGL action products were also successfully detected in ripe rowan berry, apple, pear, raspberry, blackberry and plum (all dicots of the family Rosaceae), as well as mango (Anacardiaceae) and yew (a gymnosperm) in addition to cranberry (Ericaceae) and sea buckthorn (Elaeagnaceae) where PL action products were absent.

4.4.2. Quantification of PL and RGL action products and other sugars at three stages of fruit ripening

PL and RGL action products were also detected in earlier ripening stages in date, strawberry, blackberry, plum and mango (Fig. 3.71–3.75), i.e. in fruit that had not fully softened. Quantification of PL products was quite challenging as Driselase (new batch) failed to release the expected dimer (ΔUA-GalA) as the only fingerprint in this experiment; instead, the trimer (ΔUA-$GalA_2$) was also detected. $GalA_2$ was also detected, indicating incomplete digestion of fruit AIR by this Driselase. There was no commercial marker available for ΔUA-GalA or ΔUA-$GalA_2$; therefore, quantification was achieved by finding the contribution of each residue to the total thymol stain on TLC, which was then converted to µg using a standard curve of GalA (§3.3.3.6) and adjusted to the fact that ΔUA has a different molar colour yield than GalA. In ripe date, it was estimated that of every 20 GalA units in HG, one had been cleaved by PL. Although this approximation neglects the GalA generated by Driselase digestion of fruit RG-I domains, it remains reasonable as the GalA arising from RG-I is expected to be equal to the small the amount of total Rha, which has been measured and found to be low compared to Driselase-released GalA (see § 3.3.2).

The quantification of RGL products was even more challenging as its backbone is made of repeating units of a disaccharide (GalA-Rha) additionally decorated with Gal and Ara side chains, unlike the HG which is made of GalA residues only. An estimate of RGL cleavage events per RG-I chain was made by measuring the relative spot ‘intensity densities’ (in ImageJ) of the thymol-stained ΔUA-Rha-GalA-Rha and Rha in the Driselase digests of ripe date AIR detected on TLC (Fig. 3.38a). Using this method, it was estimated that, per 90 backbone residues (GalA + Rha) in RG-I, one GalA units had been cleaved by RGL. This estimate is only approximate, and it

disregards the differences in molar colour-yield (on thymol staining) between ΔUA, GalA and Rha residues.

4.4.3. Sugar content of fruit cell walls at three ripening stages

Along with PL and RGL fingerprints, Driselase released (but not effectively) numerous neutral sugars in addition to GalA, which were identified and quantified in this project. Driselase may not be the best way to release and quantify all the sugar residues in the cell walls because: (a) it failed to completely hydrolyse the treated AIR (Fig. 3.44), (b) there are some Driselase-resistant bonds (including the glycosidic bonds in isoprimeverose (Popper and Fry 2005; Kim *et al.* 2020) and the glycosidic bonds close to the ΔUA residue in PL and RGL products (Al Hinai *et al.* 2021) and acetyl-ester groups; (Ishii 1997; Perrone *et al.* 2002).

During fruit ripening, loss of neutral sugars from polysaccharide side chains is commonly observed (Gross and Sams 1984). The decrease in the concentration of GalA (per mg AIR) released by Driselase from unripe to ripe fruit (observed in date, strawberry and plum, Fig. 3.84) was expected as more pectin gets depolymerised with ripening. However, the concentration of GalA detected may not be conclusive as it was always measured as per a certain weight of AIR. For instance, GalA concentration detected in mango (Fig. 3.66 and 3.84) increased from unripe to ripe fruit, which could be misleading as it was reported that molecular weight of pectin (therefore GalA concentration) in mango decreased with ripening (Bello-Pérez *et al.* 2007). Unripe mango is known to be rich in starch (Bello-Pérez *et al.* 2007) which would have contributed a big proportion of polysaccharides per mg of AIR, therefore reducing the pectic proportion. With ripening, starch is hydrolysed to small sugars such as glucose

(Derese *et al.* 2017), which explains the decrease in glucose concentration detected (Fig. 3.66), so the proportion of starch per mg AIR decreased and the proportion of pectin increased. In addition, the *in-vivo* depolymerisation of pectin might not be complete and the end products could still be in polymeric form, making slight or even no difference in the total GalA content (released by Driselase) per mg AIR. This was previously reported in some other fruits including tomato, avocado (Huber and O'Donoghue 1993) and peach (Dawson *et al.* 1992; Brummell *et al.* 2004) where progressive pectin depolymerisation was evident by loss in high molecular weight polymers and generation of smaller products (Brummell 2006).

Acid hydrolysis of fruit AIR could be more reliable for quantification of sugar residues as it cleaves all the polysaccharides (except cellulose; Fry 2011) to their monomers. Negligible amounts of unknown oligomeric sugars were detected on TLCs (Fig. 3.64) in addition to the monosaccharides and the insoluble residue, which was thought to be mainly cellulose (Fry 2011). On the other hand, Driselase digestion resulted in appreciable amounts of oligomers including isoprimeverose, xylobiose and other unknown products as detected by TLCs (Fig. 3.57 and 3.58). The general trend of GalA loss was observed (except form mango, due to the presence of high starch content as discussed earlier). The difference in the concentration of GalA (and the other sugars) released by Driselase and TFA reflected the efficiency of each method in hydrolysing the AIR.

Loss of polymeric galactose and/or arabinose is a remarkable feature of fruit softening (Gross and Sams 1984; Redgwell *et al.* 1997; Brummell 2006; Goulao and Oliveira 2008). In this project, loss of polysaccharide-associated arabinose and galactose residues was observed in all the tested fruits (from unripe to ripe fruit) except strawberry where a significant increase in galactose residues was observed. These

results did not agree with a previous report where arabinose and galactose residues (per gram of cell wall material) increased in plum (Redgwell *et al.* 1997).

The concentration of rhamnose residues was generally low in cell walls of the tested fruits (Fig. 3.61 and 3.66), indicating a low total RG-I content (as the main source of rhamnose). The concentration of RG-II in fruit is very low (Atmodjo *et al.* 2013; Wang *et al.* 2018). The RG-I backbone consists of repeating units of GalA-Rha (Ridley *et al.* 2001; Yapo 2011), so a minor concentration of GalA (approximately equal to the concentration of Rha) arose from RG-I and the remaining majority of the GalA concentration arose from HG. The concentration of the various sugar residues in fruit cell walls may vary depending on fruit species (and even fruit variety), and extraction and quantification methods.

The low concentration of Rha (per mg of AIR; approximately indicating the total RG-I content) and the relatively high GalA concentration (indicating the total pectin content) detected in fruit cell walls predict that HG is more 'in control' of fruit softening than is rhamnogalacturonan, supported by reports of HG making up to 60% of fruit cell wall pectin (Caffall and Mohnen 2009; Atmodjo *et al.* 2013). In addition, mutant Arabidopsis plants with 50% less HG were reported to be more flexible and their HG was more rigid than RG-I (Ralet *et al.* 2008). This might seem to suggest that regulation of the gene expression and enzyme action of HG-modifying enzymes would have more effect on fruit softening than that of RG-I-modifying enzymes. However, increased fruit firmness as a result of silencing RGL genes was reported in strawberry (Molina-Hidalgo *et al.* 2013; Moya-León *et al.* 2019).

4.5. Conclusions

The fruit primary cell wall undergoes various biochemical changes during ripening such as depolymerisation of its polysaccharides. Plants express numerous 'wall-related' genes, generating mRNAs which, if translated, would encode proteins whose *in-silico* predicted enzymic activities suggest that they may be able to re-model the cell wall. In some cases, plant cell walls have been shown to contain the corresponding encoded proteins which, when extracted, exhibit *in-vitro* activity on wall-related polysaccharides. However, in many cases, it remains to be proven that these enzymes exert *in-vivo* action, actually re-modelling the walls of living plant cells. This important question has often been neglected. In this project, methods were developed to demonstrate that PL and RGL exhibit *in-vivo* actions in several fruits. Such actions, cleaving the backbone of the pectic HG and RG-I domains, occur at the right time and in the right place to play a role in fruit softening. The methods presented open the way to wider documentation of PL and RGL actions, e.g. in fruits of other species and in non-fruit tissues that also express PL genes, complementing the evidence for *in-vivo* non-enzymic cleavage of polysaccharides by hydroxyl radicals (Airianah *et al.* 2016).

The unique fingerprints of PL and RGL actions (ΔUA-GalA and ΔUA-Rha-GalA-Rha) were created *in vitro* using commercial substrates and commercial enzymes to help understand their properties and test the methods before applying them to fruit samples. The identity of these fingerprints was confirmed by mass spectrometry and NMR spectrometry.

This project demonstrated that PL and RGL exhibit actions not only in ripe fruits, but also in earlier stages even when no signs of ripening (no change in colour or softness) were seen. These results suggest that the early action of PL and RGL contributes in an important way to pectin solubilisation, making it more accessible to other pectin-

degrading enzymes such as EPG (Wang *et al.* 2018). The PL and RGL *in-vivo* actions fingerprints were released by Driselase digestion of AIR and were resolved electrophoretically (by HVPE at pH 2) and chromatographically (by TLC and thymol staining). These fingerprints were successfully detected at three ripening stages (unripe, turning and ripe) in date, strawberry, blackberry, plum and mango in addition to several other species (at the ripe stage) including a gymnosperm (yew), suggesting that these enzymes' actions are taxonomically widespread.

Overall, this project demonstrated the first evidence for PL and RGL action *in vivo*, supporting the studies on their contribution to fruit softening, which have always been assumed (but never confirmed) by their gene expression and extractable activities. The methods developed in this project could be used to detect PL and RGL action products in other plant tissues where such evidence could be important to understand certain plant developmental processes such as pollen grain development (Rogers *et al.* 1992; Medina-Escobar *et al.* 1997; Jiang *et al.* 2014) and abscission zones (Agustí *et al.* 2008; Lashbrook and Cai 2008; Merelo *et al.* 2017) where PL gene expression was reported.

The results obtained in this project added to our knowledge about fruit softening confirming the contribution of PL and RGL action. The work done could be used as a base for further experiments on the role of PL and RGL on fruit softening, including genetic engineering of fruits with controlled softening and longer shelf-life via manipulating PL and RGL genes. The effect of such approaches on the fruits' nutritional values, fruit size and other aspects of fruit production needs to be addressed. Other (probably more sensitive) methods of isolating the unique PL and RGL fingerprints, such as HPLC, or creating specific antibodies to detect and localize these fingerprints *in vivo* could also be explored.

References

Abari HA, Amini Rourani H, Ghasemi SM, Kim H, Kim YG. **2021**. Investigation of antioxidant and anticancer activities of unsaturated oligo-galacturonic acids produced by pectinase of Streptomyces hydrogenans YAM1. *Scientific Reports* **11**: 1–9.

Abeles FB, Takeda F. **1990**. Cellulase activity and ethylene in ripening strawberry and apple fruits. *Scientia Horticulturae* **42**: 269–275.

Abu-Sarra AF, Abu-Goukh AA. **1992**. Changes in pectinesterase, polygalacturonase and cellulase activity during mango fruit ripening. *Journal of Horticultural Science* **67**: 561–568.

Agustí J, Merelo P, Cercós M, Tadeo FR, Talón M. **2008**. Ethylene-induced differential gene expression during abscission of citrus leaves. *Journal of Experimental Botany* **59**: 2717–2733.

Ahmed IA, Ahmed AWK, Robinson RK. **1995**. Chemical composition of date varieties as influenced by the stage of ripening. *Food Chemistry* **54**: 305–309.

Airianah OB, Vreeburg RAM, Fry SC. **2016**. Pectic polysaccharides are attacked by hydroxyl radicals in ripening fruit: evidence from a fluorescent fingerprinting method. *Annals of botany* **117**: 441–455.

Albersheim P, Neukom H, Deuel H. **1960**. Über die Bildung von ungesättigten Abbauprodukten durch ein pektinabbauendes Enzym. *Helvetica Chimica Acta* **43**: 1422–1426.

Al Hinai TZS, Vreeburg RA, Mackay LC, Murray L, Sadler IH, Fry SC. **2021**. Fruit softening: evidence for pectate lyase action in vivo in date (*Phoenix dactylifera*) and rosaceous fruit cell walls. *Annals of Botany* **128**: 511–525.

Andreani ES, Karboune S, Liu L. **2021**. Structural characterization of pectic polysaccharides in the cell wall of stevens variety cranberry using highly specific pectin-hydrolyzing enzymes. *Polymers* **13**: 1842–1856.

Arakji OA, Yang HY. **1969**. Identification and characterization of the pectic enzymes of the McFarlin cranberry. *Journal of Food Science* **34**: 340–342.

Asif MH, Nath P. **2005**. Expression of multiple forms of polygalacturonase gene during ripening in banana fruit. *Plant Physiology and Biochemistry* **43**: 177–184.

Atkinson RG, Sutherland PW, Johnston SL, Gunaseelan K, Hallett IC, Mitra D, Brummell DA, Schröder R, Johnston JW, Schaffer RJ. 2012. Down-regulation of polygalacturonase1 alters firmness, tensile strength and water loss in apple (*Malus* × *domestica*) fruit. *BMC Plant Biology* **12**: 129–142.

Atmodjo MA, Hao Z, Mohnen D. **2013**. Evolving views of pectin biosynthesis. *Annual Review of Plant Biology* **64**: 747–779.

Azadi P, O' Neill MA, Bergmann C, Darvill AG, Albersheim P. **1995**. The backbone of the pectic polysaccharide rhamnogalacturonan I is cleaved by an endohydrolase and an endolyase. *Glycobiology* **5**: 783–789.

Barry CS, Giovannoni JJ. **2007**. Ethylene and fruit ripening. *Journal of Plant Growth Regulation* **26**: 143–159.

Bartley IM. **1978**. Exo-polygalacturonase of apple. *Phytochemistry* **17**: 213–216.

Bello-Pérez LA, García-Suárez F, Agama-Acevedo E. (2007). Mango carbohydrates. *Food* **1**: 36–40.

Benítez-Burraco A, Blanco-Portales R, Redondo-Nevado J, Bellido ML, Moyano E, Caballero JL, Muñoz-Blanco J. 2003. Cloning and characterization of two ripening-related strawberry (*Fragaria* × *ananassa* cv. Chandler) pectate lyase genes. *Journal of Experimental Botany* **54**: 633–645.

Besford RT, Hobson GE. **1972**. Pectic enzymes associated with the softening of tomato fruit. *Phytochemistry* **11**: 2201–2205.

Brummell DA. **2006**. Cell wall disassembly in ripening fruit. *Functional Plant Biology* **33**: 103–119.

Brummell DA, Cin VD, Lurie S, Crisosto CH, Labavitch JM. **2004**. Cell wall metabolism during the development of chilling injury in cold-stored peach fruit: Association of mealiness with arrested disassembly of cell wall pectins. *Journal of Experimental Botany* **55**: 2041–2052.

Brummell DA, Harpster MH. **2001**. Cell wall metabolism in fruit softening and quality and its manipulation in transgenic plants. *Plant Molecular Biology* **47**: 311–339.

Brummell DA, Harpster MH, Civello PM, Palys JM, Bennett AB, Dunsmuir P. **1999**. Modification of expansin protein abundance in tomato fruit alters softening and cell wall polymer metabolism during ripening. *The Plant Cell* **11**: 2203–2216.

Caffall KH, Mohnen D. **2009**. The structure, function, and biosynthesis of plant cell wall pectic polysaccharides. *Carbohydrate Research* **344**: 1879–1900.

Cárdenas FDFR, Suárez YR, Rangel RMC, Garcia VL, Aguilera KLG, Martínez NM, Folter SD. 2017. Effect of constitutive miR164 expression on plant morphology and fruit development in Arabidopsis and tomato. *Agronomy* **7**: 1–14.

Castillejo C, De La Fuente JI, Iannetta P, Botella MÁ, Valpuesta V. **2004**. Pectin esterase gene family in strawberry fruit: Study of FaPE1, a ripening-specific isoform. *Journal of Experimental Botany* **55**: 909–918.

Chattopadhyay DP, Patel BH. **2016**. Synthesis, characterization and application of nano cellulose for enhanced performance of textiles. *Journal of Textile Science & Engineering* **6**: 248–256.

Chea S, Yu DJ, Park J, Oh HD, Chung SW, Lee HJ. **2019**. Fruit softening correlates with enzymatic and compositional changes in fruit cell wall during ripening in 'Bluecrop' highbush blueberries. *Scientia Horticulturae* **245**: 163–170.

Chen G, Hackett R, Walker D, Taylor A, Lin Z, Grierson D. **2004**. Identification of a specific isoform of tomato lipoxygenase (*TomloxC*) involved in the generation of fatty acid-derived flavor compounds. *Plant Physiology* **136**: 2641–2651.

Cheng G, Duan X, Shi J, Lu W, Luo Y, Jiang W, Jiang Y. 2008. Effects of reactive oxygen species on cellular wall disassembly of banana fruit during ripening. *Food Chemistry* **109**: 319–324.

Chourasia A, Sane VA, Nath P. **2006**. Differential expression of pectate lyase during ethylene-induced postharvest softening of mango (*Mangifera indica* var. Dashehari). *Physiologia Plantarum* **128**: 546–555.

Chormova D, Messenger DJ, Fry SC. 2014. Boron bridging of rhamnogalacturonan-II, monitored by gel electrophoresis, occurs during polysaccharide synthesis and secretion but not post-secretion. *Plant Journal* **77**: 534–546.

Collmer A, Keen NT. **1986**. The role of pectic enzymes in plant pathogenesis. *Annual Review of Phytopathology* **24**: 383–409.

Cosgrove DJ. 2018. Nanoscale structure, mechanics and growth of epidermal cell walls. *Current Opinion in Plant Biology* **46**: 77–86.

Cosgrove DJ, Jarvis MC. 2012. Comparative structure and biomechanics of plant primary and secondary cell walls. *Frontiers in Plant Science* **3**: 1–6.

Dardick C, Callahan AM. **2014**. Evolution of the fruit endocarp: Molecular mechanisms underlying adaptations in seed protection and dispersal strategies. *Frontiers in Plant Science* **5**: 1–10.

Dautt-Castro M, Ochoa-Leyva A, Contreras-Vergara CA, Pacheco-Sanchez MA, Casas-Flores S, Sanchez-Flores A, Kuhn DN, Islas-Osuna MA. 2015. Mango (*Mangifera indica L.*) cv. Kent fruit mesocarp *de novo* transcriptome assembly identifies gene families important for ripening. *Frontiers in Plant Science* **6**: 1–12.

Dawson DM, Melton LD, Watkins CB. **1992**. Cell Wall Changes in Nectarines (*Prunus persica*) . *Plant Physiology* **100**: 1203–1210.

Derese S, Guantai EM, Souaibou Y, Kuete V. 2017. *Mangifera indica* L. (Anacardiaceae). In: Medicinal spices and vegetables from Africa (Kuete V, ed). *Academic Press*, pp. 451–483.

Deshpande AB, Anamika K, Jha V, Chidley HG, Pranjali S. **2017**. Transcriptional transitions in Alphonso mango (*Mangifera indica L.*) during fruit development and ripening explain its distinct aroma and shelf life characteristics. *Scientific Reports* **7**: 1–19.

Dommguez-Puigjaner E, Lop IL, Vendrell M, Prat S. **1997**. A cDNA clone highly expressed in ripe banana fruit shows homology to pectate lyases. *Plant Physiology* **114**: 1071–1076.

Dong Y, Zhang S, Wang Y. **2018**. Compositional changes in cell wall polyuronides and enzyme activities associated with melting/mealy textural property during ripening following long-term storage of ‘Comice’ and ‘d’Anjou’ pears. *Postharvest Biology and Technology* **135**: 131–140.

Dorokhov YL, Sheshukova EV, Komarova TV. 2018. Methanol in plant life. *Frontiers in Plant Science* **871**: 1–6.

Duan X, Zhang H, Zhang D, Sheng J, Lin H, Jiang Y. **2011**. Role of hydroxyl radical in modification of cell wall polysaccharides and aril breakdown during senescence of harvested longan fruit. *Food Chemistry* **128**: 203–207.

Dumville JC, Fry SC. **2000**. Uronic acid-containing oligosaccharins: Their biosynthesis, degradation and signalling roles in non-diseased plant tissues. *Plant Physiology and Biochemistry* **38**: 125–140.

Dumville JC, Fry SC. **2003**. Solubilisation of tomato fruit pectins by ascorbate: A possible non-enzymic mechanism of fruit softening. *Planta* **217**: 951–961.

Duran-Flores D, Heil M. **2016**. Sources of specificity in plant damaged-self recognition. *Current Opinion in Plant Biology* **32**: 77–87.

El Arem A, Flamini G, Behija SE, Manel I, Nesrine Z, Ali F, Mohamed H, Noureddine HA, Lotf A. 2011. Chemical and aroma volatile compositions of date palm (*Phoenix dactylifera L.*) fruits at three maturation stages. *Food Chemistry* **127**: 1744–1754.

Farzaliyev EB, Golubev VN, Hafizov GK. **2022**. Structure and properties of pectin substances of wild sea buckthorn (*Hippophae rhamnoides* L.) growing in Azerbaijan. *BIO Web of Conferences* **01028**: 0–5.

Figueroa CR, Pimentel P, Gaete-Eastman C, Moya M, Herrera R, Caligari PDS, Moya-León MA. 2008. Softening rate of the Chilean strawberry (*Fragaria chiloensis*) fruit reflects the expression of polygalacturonase and pectate lyase genes. *Postharvest Biology and Technology* **49**: 210–220.

Figueroa CR, Rosli HG, Civello PM, Martínez GA, Herrera R, Moya-León MA. **2010**. Changes in cell wall polysaccharides and cell wall degrading enzymes during ripening of *Fragaria chiloensis* and *Fragaria ×ananassa* fruits. *Scientia Horticulturae* **124**: 454–462.

Fry SC. 2000. The growing plant cell wall: chemical and metabolic analysis. *Caldwell, NJ: Blackburn Press*.

Fry SC. **2004**. Primary cell wall metabolism: Tracking the careers of wall polymers in living plant cells. *New Phytologist* **161**: 641–675.

Fry SC. 2011. Cell wall polysaccharide composition and covalent crosslinking: In: *Annual plant reviews: plant polysaccharides, biosynthesis and bioengineering* (Ulvskov P, ed). *Oxford Wiley-Blackwell*, pp 1–42.

Fry SC. 2017. Plant cell wall polymers. In: Biofuels and Bioenergy (Love J, ed). *John Wiley & Sons*, pp. 59–87.

Fry SC. 2020. High-voltage paper electrophoresis (HVPE). In: (Popper ZA, ed) The Plant Cell Wall. Methods and Protocols (Methods in Molecular Biology), vol. 2149. *Humana Press, Totowa, NJ*, pp 01-31.

Fry SC, Mohler KE, Nesselrode BHWA, Franková L. **2008**. Mixed-linkage β-glucan: Xyloglucan endotransglucosylase, a novel wall-remodelling enzyme from Equisetum (horsetails) and charophytic algae. *The Plant Journal* **55**: 240–252.

Fry SC, Smith RC, Renwick KF, Martin DJ, Hodge SK, Matthews KJ. **1992**. Xyloglucan endotransglycosylase, a new wall-loosening enzyme activity from plants. *Biochemical Journal* **282**: 821–828.

Fuchs A. **1965**. The trans-eliminative breakdown of Na-polygalacturonate by *Pseudomonas fluorescens*. *Antonie van Leeuwenhoek* **31**: 323–340.

Giovannoni JJ, Dellapenna D, Bennett AB, Fischer RL. **1989**. Expression of a chimeric polygalacturonase gene in transgenic *rin* (Ripening Inhibitor) tomato fruit results in polyuronide degradation but not fruit softening. *The Plant Cell* **1**: 53–63.

Given NK, Venis MA, Gierson D. **1988**. Hormonal regulation of ripening in the strawberry, a non-climacteric fruit. *Planta* **174**: 402–406.

Goulao LF, Oliveira CM. **2008**. Cell wall modifications during fruit ripening: when a fruit is not the fruit. *Trends in Food Science and Technology* **19**: 4–25.

Goulao LF, Santos J, de Sousa I, Oliveira CM. **2007**. Patterns of enzymatic activity of cell wall-modifying enzymes during growth and ripening of apples. *Postharvest Biology and Technology* **43**: 307–318.

Gribaa A, Dardelle F, Lehner A, Rihouey C, Burel C, Ferchichi A, Driouich A, Mollet J. 2013. Effect of water deficit on the cell wall of the date palm (*Phoenix dactylifera* "Deglet nour", Arecales) fruit during development. *Plant Cell and Environment* **36**: 1056–1070.

Griffiths HR, Lunec J. 1996. Investigating the effects of oxygen free radicals on carbohydrates in biological systems. In: (Punchard NA, Kelly FJ, ed) Free radicals: A practical approach. *Oxford: IRL Press*, pp.185–200.

Gross KC. **1982**. A rapid and sensitive spectrophotometric method for assaying polygalacturonase using 2-cyanoacetamide. *HortScience* **17**: 933–934.

Gross KC, Sams CE. **1984**. Changes in cell wall neutral sugar composition during fruit ripening: a species survey. *Phytochemistry* **23**: 2457–2461.

Gross KC, Wallner SJ. 1979. Degradation of cell wall polysaccharides during tomato fruit ripening. *Plant Physiology* **63**: 117–120.

Gwanpua SG, Verlinden BE, Hertog MLATM, Nicolai BM, Hendrickx M, Geeraerd A. **2016**. Slow softening of Kanzi apples (*Malus* × *domestica L.*) is associated with preservation of pectin integrity in middle lamella. *Food Chemistry* **211**: 883–891.

Harb J, Gapper NE, Giovannoni JJ, Watkins CB. **2012**. Molecular analysis of softening and ethylene synthesis and signaling pathways in a non-softening apple cultivar, "Honeycrisp" and a rapidly softening cultivar, "McIntosh". *Postharvest Biology and Technology* **64**: 94–103.

Harholt J, Suttangkakul A, Scheller HV. **2010**. Biosynthesis of pectin. *Plant Physiology* **153**: 384–395.

Harker FR, Sutherland PW. **1993**. Physiological changes associated with fruit ripening and the development of mealy texture during storage of nectarines. *Postharvest Biology and Technology* **2**: 269–277.

Hasegawa S, Smolensky DC. **1971**. A research note cellulase in dates and its role in fruit softening. *Journal of Food Science* **36**: 966–967.

Hirschberg J. **2001**. Carotenoid biosynthesis in flowering plants. *Current Opinion in Plant Biology* **4**: 210–218.

Hobson GE. **1968**. Cellulase activity during the maturation and ripening of tomato fruit. *Journal of Food Science* **33**: 588–592.

Huber DJ, O'Donoghue EM. **1993**. Polyuronides in avocado (Persea americana) and tomato (*Lycopersicon esculentum*) fruits exhibit markedly different patterns of molecular weight downshifts during ripening. *Plant Physiology* **102**: 473–480.

Iqbal A, Miller JG, Murray L, Sadler IH, Fry SC. **2016**. The pectic disaccharides lepidimoic acid and β-d-xylopyranosyl-(1→3)-d-galacturonic acid occur in cress-seed exudate but lack allelochemical activity. *Annals of Botany* **117**: 607–623.

Ishii T. **1997**. *O*-acetylated oligosaccharides from pectins of potato tuber cell walls. *Plant Physiology* **113**: 1265–1272.

Ishii T, Matsunaga T, Pellerin P, O'Neill MA, Darvill A, Albersheim P. **1999**. The plant cell wall polysaccharide rhamnogalacturonan II self-assembles into a covalently cross-linked dimer. *Journal of Biological Chemistry* **274**: 13098–13104.

Jarvis MC, Briggs SPH, Knox JP. **2003**. Intercellular adhesion and cell separation in plants. *Plant, Cell and Environment* **26**: 977–989.

Jiang J, Yao L, Yu Y, Lv M, Miao Y, Cao J. **2014**. Pectate lyase-like10 is associated with pollen wall development in *Brassica campestris*. *Journal of Integrative Plant Biology* **56**: 1095–1105.

Jiménez-Bermúdez S, Redondo-Nevado J, Muñoz-Blanco J, Caballero JL, López-Aranda JM, Valpuesta V, Pliego-Alfaro F, Quesada MA, Mercado JA. 2002. Manipulation of strawberry fruit softening by antisense expression of a pectate lyase gene 1. *Plant Physiology* **128**: 751–759.

Keegstra K. **2010**. Plant cell walls. *Plant Physiology* **154**: 483–486.

Kim SJ, Chandrasekar B, Rea AC, Danhof L, Zemelis-Durfee S, Thrower N, Shepard ZS, Pauly M, Brandizzi F. 2020. The synthesis of xyloglucan, an abundant plant cell wall polysaccharide, requires CSLC function. *Proceedings of the National Academy of Sciences of the United States of America* **117**: 20316–20324.

Kobayashi M, Matoh T, Azuma JI. **1996**. Two chains of rhamnogalacturonan II are cross-linked by borate-diol ester bonds in higher plant cell walls. *Plant Physiology* **110**: 1017–1020.

Koch JL, Nevins DJ. **1989**. Tomato fruit cell wall. *Plant Physiology* **91**: 816–822.

Kofod LV, Kauppinen S, Christgau S, Andersen LN, Heldt-Hansen HP, Dörreich K, Dalbøge H. 1994. Cloning and characterization of two structurally and functionally divergent rhamnogalacturonases from *Aspergillus aculeatus*. *Journal of Biological Chemistry* **269**: 29182–29189.

Kohn R, Kovác P. 1978. Dissociation constants of D-galacturonic and D-glucuronic acid and their *O*-methyl derivatives. *Chemicke Zvesti* **32**: 478–485.

Laatu, M. and Condemine, G. 2003. Rhamnogalacturonate lyase rhiE is secreted by the out system in Erwinia chrysanthemi. *J. Bacteriol.*, **185**, 1642–1649.

Lacan D, Baccou JC. **1998**. High levels of antioxidant enzymes correlate with delayed senescence in nonnetted muskmelon fruits. *Planta* **204**: 377–382.

Lashbrook CC, Cai S. **2008**. Cell wall remodeling in Arabidopsis stamen abscission zones: Temporal aspects of control inferred from transcriptional profiling. *Plant Signaling and Behavior* **3**: 733–736.

Lee CW, Wu MC, Lee BH, Jiang CM, Chang HM. **2003**. Changes in molecular weight of transacylated pectin catalyzed by tomato and citrus pectinesterases as determined by gel permeation chromatography. *Journal of Agricultural and Food Chemistry* **51**: 5455–5461.

Lenucci M, Piro G, Miller JG, Dalessandro G, Fry SC. **2005**. Do polyamines contribute to plant cell wall assembly by forming amide bonds with pectins? *Phytochemistry* **66**: 2581–2594.

Lerouxel O, Cavalier DM, Liepman AH, Keegstra K. **2006**. Biosynthesis of plant cell wall polysaccharides - a complex process. *Current Opinion in Plant Biology* **9**: 621–630.

Leszczuk A, Kalaitzis P, Blazakis KN, Zdunek A. 2020. The role of arabinogalactan proteins (AGPs) in fruit ripening: a review. *Horticulture Research* **7:** 176.

Limberg G, Körner R, Buchholt HC, Christensen TMIE, Roepstorff P, Mikkelsen JD. **2000**. Analysis of different de-esterification mechanisms for pectin by enzymatic fingerprinting using endopectin lyase and endopolygalacturonase II from *A. Niger*. *Carbohydrate Research* **327**: 293–307.

Loix C, Huybrechts M, Vangronsveld J, Gielen M, Keunen E, Cuypers A. **2017**. Reciprocal interactions between cadmium-induced cell wall responses and oxidative stress in plants. *Frontiers in Plant Science* **8**: 1–19.

Manning K, Tör M, Poole M, Hong Y, Thompson AJ, King GJ, Giovannoni JJ, Seymour GB. 2006. A naturally occurring epigenetic mutation in a gene encoding an SBP-box transcription factor inhibits tomato fruit ripening. *Nature Genetics* **38**: 948–952.

Manzocco L, Dri A, Quarta B. **2009**. Inactivation of pectic lyases by light exposure in model systems and fresh-cut apple. *Innovative Food Science and Emerging Technologies* **10**: 500–505.

Marin-Rodriguez MC, Orchard J, Seymour GB. **2002**. Pectate lyases, cell wall degradation and fruit softening. *Journal of Experimental Botany* **53**: 2115–2119.

Marín-Rodríguez MC, Smith DL, Manning K, Orchard J, Seymour GB. **2003**. Pectate lyase gene expression and enzyme activity in ripening banana fruit. *Plant Molecular Biology* **51**: 851–857.

Mauseth JD. 2009. Botany: An introduction to plant biology. *Jones and Bartlett Publishers, Replika press*, pp 188-211.

McDonough MA, Kadirvelraj R, Harris P, Poulsen JCN, Larsen S. **2004**. Rhamnogalacturonan lyase reveals a unique three-domain modular structure for polysaccharide lyase family 4. *FEBS Letters* **565**: 188–194.

McKie VA, Vinoken JP, Voragen AGJ, Van Den Broek LAM, Stimson E, Gilbert HJ. **2001**. A new family of rhamnogalacturonan lyases contains an enzyme that binds to cellulose. *Biochemical Journal* **355**: 167–177.

McQueen-Mason SJ, Cosgrove DJ. **1995**. Expansin mode of action on cell walls: Analysis of wall hydrolysis, stress relaxation, and binding. *Plant Physiology* **107**: 87–100.

Medina-Escobar N, Cárdenas J, Moyano E, Caballero JL, Muñoz-Blanco J. **1997**. Cloning, molecular characterization and expression pattern of a strawberry ripening-specific cDNA with sequence homology to pectate lyase from higher plants. *Plant Molecular Biology* **34**: 867–877.

Méndez-Yañez A, González M, Carrasco-Orellana C, Herrera R, Moya-León MA. **2020**. Isolation of a rhamnogalacturonan lyase expressed during ripening of the Chilean strawberry fruit and its biochemical characterization. *Plant Physiology and Biochemistry* **146**: 411–419.

Merchante C, Vallarino JG, Osorio S, Aragüez I, Villarreal N, Ariza MT, Martínez GA, Medina-Escobar N, Civello MP, Fernie AR, Botella MA, Valpuesta V. 2013. Ethylene is involved in strawberry fruit ripening in an organ-specific manner. *Journal of Experimental Botany* **64**: 4421–4439.

Merelo P, Agustí J, Arbona V, Costa ML, Estornell LH, Gómez-Cadenas A, Coimbra S, Gómez MD, Pérez-Amador MA, Domingo C, Talón M, Tadeo FR. 2017. Cell wall remodeling in abscission zone cells during ethylene-promoted fruit abscission in citrus. *Frontiers in Plant Science* **8**.

Miedes E, Lorences EP. **2009**. Xyloglucan endotransglucosylase/hydrolases (XTHs) during tomato fruit growth and ripening. *Journal of Plant Physiology* **166**: 489–498.

Mohnen D. **2008**. Pectin structure and biosynthesis. *Current Opinion in Plant Biology* **11**: 266–277.

Molina-Hidalgo FJ, Franco AR, Villatoro C, Medina-Puche L, Mercado JA, Hidalgo MA, Monfort A, Caballero JL, Muñoz-Blanco J, Blanco-Portales R. 2013. The strawberry (*Fragaria×ananassa*) fruit-specific rhamnogalacturonate lyase 1 (*FaRGLyase1*) gene encodes an enzyme involved in the degradation of cell-wall middle lamellae. *Journal of Experimental Botany* **64**: 1471–1483.

Mouille G, Ralet MC, Cavelier C, Eland C, Effroy D, Hématy K, McCartney L, Truong HN, Gaudon V, Thibault JF, Marchant A, Höfte H. 2007. Homogalacturonan synthesis in Arabidopsis thaliana requires a Golgi-localized protein with a putative methyltransferase domain. *The Plant Journal* **50**: 605–614.

Moya-León MA, Mattus-Araya E, Herrera R. **2019**. Molecular events occurring during softening of strawberry fruit. *Frontiers in Plant Science* **10**: 615.

Naran R, Pierce ML, Mort AJ. **2007**. Detection and identification of rhamnogalacturonan lyase activity in intercellular spaces of expanding cotton cotyledons. *Plant Journal* **50**: 95–107.

Nasuno S, Starr MP. **1967**. Polygalacturonic acid trans-eliminase of *Xanthomonas campestris*. *The Biochemical journal* **104**: 178–185.

Nguyen-Phan TC, Fry SC. 2019. Functional and chemical characterization of XAF: A heat-stable plant polymer that activates xyloglucan endotransglucosylase/hydrolase (XTH). *Annals of Botany* **124**: 131–148.

Nishitani K. **1997**. The role of endoxyloglucan transferase in the organization of plant cell walls. *International Review of Cytology* **173**: 157–206.

Nunan KJ, Davies C, Robinson SP, Fincher GB. 2001. Expression patterns of cell wall-modifying enzymes during grape berry development. *Planta* **214**: 257–264.

Ochoa-Jiménez VA, Berumen-Varela G, Burgara-Estrella A, Orozco-Avitiaa JA, Ojeda-Contrerasa ÁJ, Trillo-Hernándeza EA, Rivera-Domínguezc M, Troncoso-Rojasa R, Báez-Sañudoa R, Datsenkad T, Handad AK, Tiznado-Hernándeza ME. 2018. Functional analysis of tomato rhamnogalacturonan lyase gene *Solyc11g011300* during fruit development and ripening. *Journal of Plant Physiology* **231**: 31–40.

Ochoa-Jiménez VA, Berumen-Varela G, Fernández-Valle R, Martín-Ernesto, Hernández T. **2018**. Rhamnogalacturonan lyase: A pectin modification enzyme of higher plants. *Emirates Journal of Food and Agriculture* **30**: 910–917.

Orr G, Brady C. **1993**. Relationship of endopolygalacturonase activity to fruit softening in a freestone peach. *Postharvest Biology and Technology* **3**: 121–130.

Paniagua C, Blanco-Portales R, Barceló-Muñoz M, García-Gago JA, Waldron KW, Quesada MA, Muñoz-Blanco J, Mercado JA. 2016. Antisense down-regulation of the strawberry β-galactosidase gene *FaβGal4* increases cell wall galactose levels and reduces fruit softening. *Journal of Experimental Botany* **67**: 619–631.

Paniagua C, Posé S, Morris VJ, Kirby AR, Quesada MA, Mercado JA. **2014**. Fruit softening and pectin disassembly: An overview of nanostructural pectin modifications assessed by atomic force microscopy. *Annals of Botany* **114**: 1375–1383.

Paniagua C, Santiago-Doménech N, Kirby AR, Gunning AP, Morris VJ, Quesada MA, Matas AJ, Mercado JA. 2017. Structural changes in cell wall pectins during strawberry fruit development. *Plant Physiology and Biochemistry* **118**: 55–63.

Perrone P, Hewage CM, Thomson AR, Bailey K, Sadler IH, Fry SC. **2002**. Patterns of methyl and *O*-acetyl esterification in spinach pectins: New complexity. *Phytochemistry* **60**: 67–77.

Phan TD, Bo W, West G, Lycett GW, Tucker GA. **2007**. Silencing of the major salt-dependent isoform of pectinesterase in tomato alters fruit softening. *Plant Physiology* **144**: 1960–1967.

Popper ZA, Fry SC. **2005**. Widespread occurrence of a covalent linkage between xyloglucan and acidic polysaccharides in suspension-cultured angiosperm cells. *Annals of Botany* **96**: 91–99.

Posé S, Kirby AR, Paniagua C, Waldron KW, Morris VJ, Quesada MA, Mercado JA. 2015. The nanostructural characterization of strawberry pectins in pectate lyase or polygalacturonase silenced fruits elucidates their role in softening. *Carbohydrate Polymers* **132**: 134–145.

Posé S, García-Gago JA, Santiago-Doménech N, Pliego-Alfaro F, Quesada MA, Mercado JA. 2011. Strawberry fruit softening : Role of cell wall disassembly and its manipulation in transgenic plants. *Genes, Genomes and Genomics* **5**: 40-48.

Pua E, Ong C, Liu P, Liu J. **2001**. Isolation and expression of two pectate lyase genes during fruit ripening of banana (*Musa acuminata*). *Physiologia Plantarum* **113**: 92–99.

Quesada MA, Blanco-Portales R, Posé S, García-Gago JA, Jiménez-Bermúdez S, Muñoz-Serrano A, Caballero JL, Pliego-Alfaro F, Mercado JA, Muñoz-Blanco J. 2009. Antisense down-regulation of the FaPG1 gene reveals an unexpected central role for polygalacturonase in strawberry fruit softening. *Plant Physiology* **150**: 1022–1032.

Ralet MC, Crépeau MJ, Lefèbvre J, Mouille G, Höfte H, Thibault JF. **2008**. Reduced number of homogalacturonan domains in pectins of an Arabidopsis mutant enhances the flexibility of the polymer. *Biomacromolecules* **9**: 1454–1460.

Rastegar S, Rahemi M, Baghizadeh A, Gholami M. **2012**. Enzyme activity and biochemical changes of three date palm cultivars with different softening pattern during ripening. *Food Chemistry* **134**: 1279–1286.

Reca IB, Lionetti V, Camardella L, D'Avino R, Giardina T, Cervone F, Bellincampi D. 2012. A functional pectin methylesterase inhibitor protein (*SolyPMEI*) is expressed during tomato fruit ripening and interacts with PME-1. *Plant Molecular Biology* **79**: 429–442.

Redgwell RJ, Fischer M, Kendal E, MacRae EA. **1997**. Galactose loss and fruit ripening: High-molecular-weight arabinogalactans in the pectic polysaccharides of fruit cell walls. *Planta* **203**: 174–181.

Ridley BL, O'Neill MA, Mohnen D. **2001**. Pectins: Structure, biosynthesis, and oligogalacturonide-related signaling. *Phytochemistry* **57**: 929–967.

Rogers HJ, Harvey A, Lonsdale DM. **1992**. Isolation and characterization of a tobacco gene with homology to pectate lyase which is specifically expressed during microsporogenesis. *Plant Molecular Biology* **20**: 493–502.

Rose JKC, Bennett AB. **1999**. Cooperative disassembly of the cellulose-xyloglucan network of plant cell walls: Parallels between cell expansion and fruit ripening. *Trends in Plant Science* **4**: 176–183.

Rose JKC, Braam J, Fry SC, Nishitani K. 2002. The XTH family of enzymes involved in xyloglucan endotransglucosylation and endohydrolysis: Current perspectives and a new unifying nomenclature. *Plant and Cell Physiology* **43**: 1421–1435.

Rosli HG, Civello PM, Martínez GA. **2009**. α-l-Arabinofuranosidase from strawberry fruit: Cloning of three cDNAs, characterization of their expression and analysis of enzymatic activity in cultivars with contrasting firmness. *Plant Physiology and Biochemistry* **47**: 272–281.

Saladié M, Rose JKC, Cosgrove DJ, Catalá C. **2006**. Characterization of a new xyloglucan endotransglucosylase/hydrolase (XTH) from ripening tomato fruit and implications for the diverse modes of enzymic action. *Plant Journal* **47**: 282–295.

Santiago-Doménech N, Jiménez-Bemúdez S, Matas AJ, Rose JKC, Muñoz-Blanco J, Mercado JA, Quesada MA. 2008. Antisense inhibition of a pectate lyase gene supports a role for pectin depolymerization in strawberry fruit softening. *Journal of Experimental Botany* **59**: 2769–2779.

Scheller HV, Ulvskov P. **2010**. Hemicelluloses. *Annual Review of Plant Biology* **61**: 263–289.

Schols HA, Geraeds CCJM, Searle-van Leeuwen MF, Kormelink FJM, Voragen AGJ. **1990**. Rhamnogalacturonase: a novel enzyme that degrades the hairy regions of pectins. *Carbohydrate Research* **206**: 105–115.

Sénéchal F, Wattier C, Rustérucci C, Pelloux J. **2014**. Homogalacturonan-modifying enzymes: Structure, expression, and roles in plants. *Journal of Experimental Botany* **65**: 5125–5160.

Serrano M, Pretel MT, Botella MA, Amorós A. 2001. Physicochemical changes during date ripening related to ethylene production. *Food Science and Technology International* **7**: 31–36.

Seymour GB, Colquhoun IJ, Dupont MS, Parsley KR, Selvendran RR. **1990**. Composition and structural features of cell wall polysaccharides from tomato fruits. *Phytochemistry* **29**: 725–731.

Seymour GB, Gross KC. 1996. Cell wall disassembly and fruit softening. *Postharvest News and Information* **7**: 45–52.

Shaligram NS, Singhal RS. **2010**. Surfactin -a review on biosynthesis, fermentation, purification and applications. *Food Technology and Biotechnology* **48**: 119–134.

Smith DL, Abbott JA, Gross KC. **2002**. Down-regulation of tomato β-Galactosidase 4 results in decreased fruit softening. *Plant Physiology* **129**: 1755–1762.

Smith DL, Gross KC. **2000**. A family of at least seven β-galactosidase genes is expressed during tomato fruit development. *Plant Physiology* **123**: 1173–1183.

Smith CJS, Watson CF, Morris PC, Bird CR, Seymour GB, Gray JE, Arnold C, Tucker GA, Schuch W, Harding S, Grierson D. 1990. Inheritance and effect on ripening of antisense polygalacturonase genes in transgenic tomatoes. *Plant Molecular Biology* **14**: 369–379.

Sørensen SO, Pauly M, Bush M, Skjøt M, McCann MC, Borkhardt B. 2000. Pectin engineering: Modification of potato pectin by *in vivo* expression of an endo-1,4-β-D-galactanase. *Proceedings of the National Academy of Sciences of the United States of America* **97**: 7639–7644.

Sozzi GO, Greve LC, Prody GA, Labavitch JM. **2002**. Gibberellic acid, synthetic auxins, and ethylene differentially modulate α-L-Arabinofuranosidase activities in antisense 1-aminocyclopropane-1-carboxylic acid synthase tomato pericarp discs. *Plant Physiology* **129**: 1330–1340.

Sun JH, Luo JJ, Tian L, Li CL, Xing Y, Shen YY. **2013**. New evidence for the role of ethylene in strawberry fruit ripening. *Journal of Plant Growth Regulation* **32**: 461–470.

Takizawa A, Hyodo H, Wada K, Ishii T, Satoh S, Iwai H. **2014**. Regulatory specialization of xyloglucan (XG) and glucuronoarabinoxylan (gax) in pericarp cell walls during fruit ripening in tomato (*Solanum lycopersicum*). *PLoS ONE* **9**: 3–10.

Tateishi A. **2008**. β-Galactosidase and α-L-arabinofuranosidase in cell wall modification related with fruit development and softening. *Journal of the Japanese Society for Horticultural Science* **77**: 329–340.

Tateishi A, Inoue H, Shiba H, Yamaki S. **2001**. Molecular cloning of β-galactosidase from Japanese pear (*Pyrus pyrifolia*) and its gene expression with fruit ripening. *Plant and Cell Physiology* **42**: 492–498.

Tieman DM, Harriman RW, Ramamohan G, Handa AK. **1992**. An antisense pectin methylesterase gene alters pectin chemistry and soluble solids in tomato fruit. *The Plant cell* **4**: 667–679.

Tieman D, Taylor M, Schauer N, Fernie AR, Hanson AD, Klee HJ. **2006**. Tomato aromatic amino acid decarboxylases participate in synthesis of the flavor volatiles 2-phenylethanol and 2-phenylacetaldehyde. *Proceedings of the National Academy of Sciences of the United States of America* **103**: 8287–8292.

Trainotti L, Spinello R, Piovan A, Spolaore S, Casadoro G. **2001**. β-Galactosidases with a lectin-like domain are expressed in strawberry. *Journal of Experimental Botany* **52**: 1635–1645.

Tucker GA, Grierson D. **1982**. Synthesis of polygalacturonase during tomato fruit ripening. *Planta* **155**: 64–67.

Uluisik S, Chapman NH, Smith R, Poole M, Adams G, Gillis RB, Besong TMD, Sheldon J, Stiegelmeyer S, Perez L, Samsulrizal N, Wang D, Fisk ID, Yang N, Baxter C, Rickett D, Fray R, Blanco-Ulate B, Powell ALT, Harding SE, Craigon J, Rose JKC, Fich EA, Sun L, Domozych DS, Fraser PD, Tucker GA, Grierson D, Seymour GB. 2016. Genetic improvement of tomato by targeted control of fruit softening. *Nature Biotechnology* **34**: 950–952.

Uluisik S, Seymour GB. **2020**. Pectate lyases: Their role in plants and importance in fruit ripening. *Food Chemistry* **309**: 125559.

Vicente AR, Ortugno C, Powell ALT, Greve LC, Labavitch JM. 2007. Temporal sequence of cell wall disassembly events in developing fruits. 1. Analysis of raspberry (*Rubus idaeus*). *Journal of Agricultural and Food Chemistry* **55**, 4119–4124.

Vicente AR, Saladie M, Rose JK, Labavitch JM. **2007**. The linkage between cell wall metabolism and fruit softening: looking to the future. *Journal of the Science of Food and Agriculture* **1243**: 1237–1243.

Villarreal NM, Martínez GA, Civello PM. **2009**. Influence of plant growth regulators on polygalacturonase expression in strawberry fruit. *Plant Science* **176**: 749–757.

Villarreal NM, Rosli HG, Martínez GA, Civello PM. **2008**. Polygalacturonase activity and expression of related genes during ripening of strawberry cultivars with contrasting fruit firmness. *Postharvest Biology and Technology* **47**: 141–150.

Vogel J. **2008**. Unique aspects of the grass cell wall. *Current Opinion in Plant Biology* **11**: 301–307.

Vogler H, Felekis D, Nelson B, Grossniklaus U. **2015**. Measuring the mechanical properties of plant cell walls. *Plants* **4**: 167–182.

Vreeburg RAM, Airianah OB, Fry SC. **2014**. Fingerprinting of hydroxyl radical-attacked polysaccharides by *N*-isopropyl-2-aminoacridone labelling. *Biochemical Journal* **463**: 225–237.

Vreeburg RAM, Fry SC. 2005. Reactive oxygen species in cell walls. In: Anti-oxidants and Reactive Oxygen Species in Plants (Smirnoff N, ed). *Blackwell, Oxford*, pp. 215–249.

De Vries RP, Visser J. **2001**. Aspergillus enzymes involved in degradation of plant cell wall polysaccharides . *Microbiology and Molecular Biology Reviews* **65**: 497–522.

Wakabayashi K, Hoson T, Huber DJ. **2003**. Methyl de-esterification as a major factor regulating the extent of pectin depolymerization during fruit ripening: A comparison of the action of avocado (*Persea americana*) and tomato (*Lycopersicon esculentum*) polygalacturonases. *Journal of Plant Physiology* **160**: 667–673.

Wang D, Yeats TH, Uluisik S, Rose JKC, Seymour GB. **2018**. Fruit Softening: revisiting the role of pectin. *Trends in Plant Science* **23**: 302–310.

Wu MC, Chen YW, Hwang JY, Lee BH, Chang HM. **2004**. Transacylation of citrus pectin as catalyzed by pectinesterase from tendril shoots of chayote [*Sechium edule* (Jacq.) Swartz]. *Food Research International* **37**: 759–765.

Wu Q, Szakács-Dobozi M, Hemmat M, Hrazdina G. **1993**. Endopolygalacturonase in apples (*Malus domestica*) and its expression during fruit ripening. *Plant Physiology* **102**: 219–225.

Xu C, Zhao L, Pan X, Šamaj J. **2011**. Developmental localization and methylesterification of pectin epitopes during somatic embryogenesis of banana (*Musa spp.* AAA). *PLoS ONE* **6**.

Xue C, Guan SC, Chen JQ, Wen CJ, Cai JF, Chen X. **2020**. Genome wide identification and functional characterization of strawberry pectin methylesterases related to fruit softening. *BMC Plant Biology* **20**: 1–17.

Yang L, Huang W, Xiong F, Xian Z, Su D, Ren M, Li Z. 2017. Silencing of *SlPL*, which encodes a pectate lyase in tomato, confers enhanced fruit firmness, prolonged shelf-life and reduced susceptibility to grey mould. *Plant Biotechnology Journal* **15**: 1544–1555.

Yang Y, Yu Y, Liang Y, Anderson CT, Cao J. **2018**. A profusion of molecular scissors for pectins: classification, expression, and functions of plant polygalacturonases. *Frontiers in Plant Science* **9**: 1–16.

Yapo BM. **2011**. Rhamnogalacturonan-I: A structurally puzzling and functionally versatile polysaccharide from plant cell walls and mucilages. *Polymer Reviews* **51**: 391–413.

Yapo BM, Lerouge P, Thibault JF, Ralet MC. **2007**. Pectins from citrus peel cell walls contain homogalacturonans homogenous with respect to molar mass, rhamnogalacturonan I and rhamnogalacturonan II. *Carbohydrate Polymers* **69**: 426–435.

Youssef SM, Jiménez-Bermúdez S, Bellido ML, Martín-Pizarro C, Barceló M, Abdal-Aziz SA, , Caballero JL, López-Aranda JM, Pliego-Alfaro F, Muñoz J, Quesada MA, Mercado JA. 2009. Fruit yield and quality of strawberry plants transformed with a fruit specific strawberry pectate lyase gene. *Scientia Horticulturae* **119**: 120–125.

Zhang C, Xiong Z, Yang H, Wu W. 2019. Changes in pericarp morphology, physiology and cell wall composition account for flesh firmness during the ripening of blackberry (*Rubus spp*.) fruit. *Scientia Horticulturae* **250**: 59–68.

Zhang WW, Zhao SQ, Zhang LC, Xing Y, Jia WS. **2020**. Changes in the cell wall during fruit development and ripening in *Fragaria vesca*. *Plant Physiology and Biochemistry* **154**: 54–65.